Vascular Endothelial Growth Factor (VEGF) and Semaphorin 3A (Sema3A) signaling for vascularized bone grafts

Inauguraldissertation

Zur

Erlangung der Würde eines Doktors der Philosophie

vorgelegt der

Philosophisch-Naturwissenschaftlichen Fakultät

der Universität Basel

von

Andrea Grosso

von Italien

Basel (Schweiz), 2021

Genehmigt von der Philosophisch-Naturwissenschaftlichen Fakultät

auf Antrag von

Prof. Dr. Markus Affolter

PD. Dr. Andrea Banfi

Prof. Dr. Ivan Martin

Basel, 02 März 2021

Prof. Dr. Marcel Mayor

Dekan der Philosophisch-Naturwissenschaftilchen Fakultät

Table of contents

Chapter 1

1. Bone tissue biology

1.1 Bone tissue structure and function

Bone is a hard, highly vascularized mineralized connective tissue that exerts important functions in the body such as locomotion, support, protection of soft tissues, mineral storage, metabolic and endocrine functions and it contains the bone marrow which is the primary site of hematopoiesis. Despite its inert appearance, bone it's a dynamic organ that is continuously renewed and remodeled throughout the life of vertebrate organisms thus allowing the skeleton to respond to changes in its mechanical environment, to different loading and to damages, in order to maintain an optimal balance between function and shape.

Bone tissue is classified in two different categories: cortical and cancellous bone, with each of them characterized by different structure, morphology and function. Cortical or compact bone is a dense tissue which composes the outer layer (cortex) of bones and it is covered by periosteum on its outer surface and by the endosteum on the inner one. It makes up 80% of total skeletal tissue mass and it has high density and low porosity. These features allow cortical bone to contribute to the mechanical role of bone. It is located primarily in mechanically demanding regions, such as the shafts of long bones. Cancellous (or trabecular) bone is light and less dense than cortical bone and it has a porous, honeycomb-like structure, named trabeculae, enclosing large spaces with a spongy appearance that contain the bone marrow. It makes up about 20% of the skeleton, providing structural support and flexibility. It is found in areas that are not subject to great mechanical stress, such as at the ends of long bones, near joints and inside the vertebrae [1] (Fig. 1A).

Bone extracellular matrix consists of organic and inorganic components and provides mechanical strength and stability to the skeleton, as well as serves as a scaffold for bone

formation, cell attachment as deposit for minerals. The organic phase of the bone matrix is mainly composed by a network of interlinked type I collagen fibers, with trace amounts of types III and V and FACIT collagens during stages of bone formation [2]. Collagen accounts for 90-95% of the organic components of the bone matrix and it consists of strands of repeating units of tropocollagen molecules, which are long rigid molecules consisting of two α-1 chains and one α-2 chain with a distinct motif bounded together in a right-handed triple helix [3] (Fig. 1B).

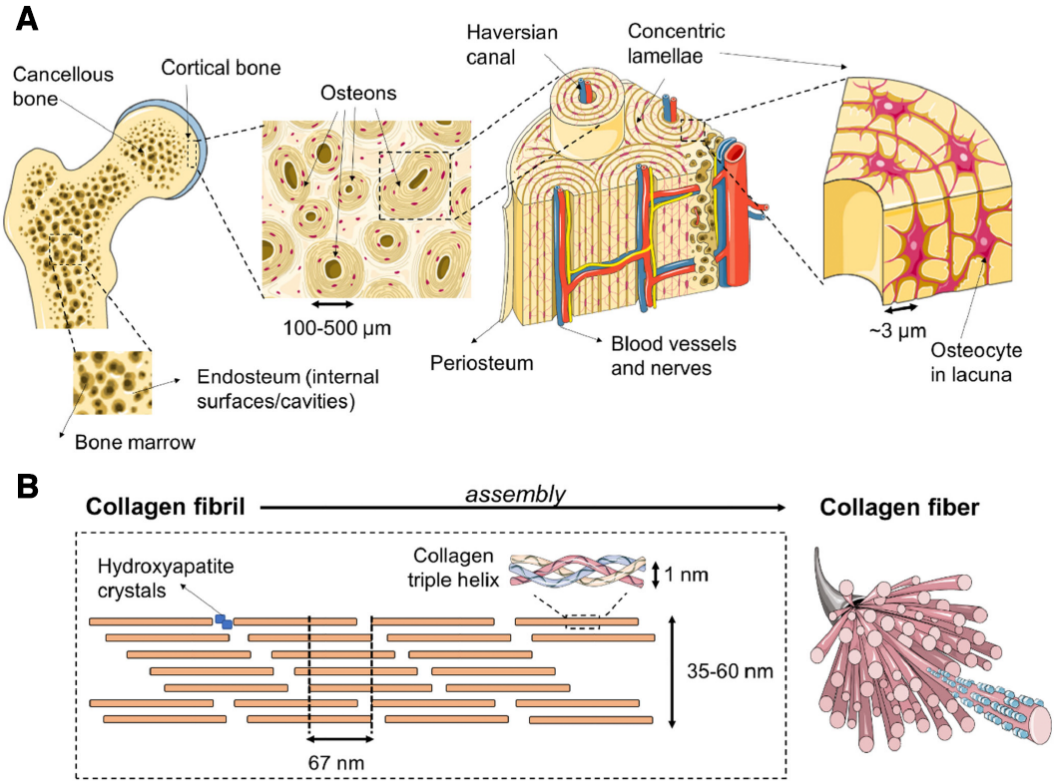

Figure 1. *(A) Bone structure: cancellous and cortical bone. Bone marrow lies in the cavities of cancellous bone, which are lined by the endosteum structure. Tightly packed osteons integrate cortical tissue, which is covered by the periosteum membrane. Osteons are formed by Harversian canals, which contain blood vessels and nerve tissue, surrounded by concentric lamellae. Osteocytes reside in the osteon inside lacuna structures. (B) Bone tissue is constituted at the nanometric scale by collagen fibers that comprise assembled collagen triple helix structures that give rise to the collagen fibril, with a characteristic periodic spacing of 67 nm, and gaps of 40 nm where the mineral component of bone is located. Reproduced from [4].*

Collagen is organized in a hierarchical manner and arranged in a directional manner corresponding to cellular orientation. Collagen fibers are highly cross-linked in physiological condition, which makes the bone matrix insoluble, except during bone remodeling [5, 6].

The other component of the organic part of bone extracellular matrix are non-collagenous proteins produced by bone cells. Among them Bone Sialoprotein (BSP), osteopontin (OPN), ostenectin (ON), fibronectin (FN), proteoglycans and matrix metalloproteins (MMPs) are the most characterized [7]. Even if they represent a minor and quantitatively variable portion of the organic components of the calcified matrices they play a major role in inducing and regulating the mineralization process [8, 9] Moreover, bone matrix also contains numerous growth factors, including bone morphogenic proteins (BMPs), transforming growth factor-beta (TGFβ) superfamily, fibroblast growth factors (FGFs), platelet-derived growth factors (PDGFs), colony stimulating factors (CSFs). These proteins and many more play key roles in cell proliferation, differentiation, cross-talk, and are crucial during bone development and bone repair, and in maintaining bone homeostasis during adult life [10-12].

The inorganic component within the bone matrix consists predominantly of phosphate and calcium ions and a minor quantity of bicarbonate, fluorite, sodium, potassium, citrate, magnesium, carbonate, fluorite, zinc, barium and strontium. Calcium and phosphate are organized in nanosized crystals which have composition and structure similar to the synthetic hydroxyapatite (HA) mineral. Differently from HA, which as a chemical formula of $Ca_{10}(PO_4)_6(OH)_2$, bone mineral incorporates substantial carbonate CO_3, and it is characterized by small and poorly crystalline units. Bone-apatite has to be consider a carbon-substitute apatite that is insoluble enough to provide stability, yet sufficiently reactive to allow continuous resorption and deposit during the process of remodeling [13, 14].

Bone is formed mainly by three types of cells: osteoblasts, osteocytes and osteoclasts that are respectively responsible for production, maintenance, and resorption of bone. These cells types are highly specialized and differentiated, and they have lost the capacity to proliferate. Bone tissue is continuously remodeled and the high demand of new cells is met by less differentiated cells, referred as osteogenic progenitors, which are responsible to generate mature bone cells.

Osteoblasts are cuboidal cells located on the interface of newly synthetized bone where bone is actively formed. Osteoblasts stem from two distinct embryonic germ layers and they form different bones in the skeleton: 1) craniofacial bones and the clavicle are formed by osteoblasts directly derived from condensation of mesenchymal progenitors that originates from the neural ectoderm, without intermediate stages through a process termed intramembranous ossification [15, 16]; 2) the remaining part of the skeleton is built by cells of mesoderm origin and by endochondral ossification, where osteoblasts differentiate from an intermediate class of perichondral cells [17, 18] or directly from hypertrophic chondrocytes [19-21].

Osteoblast lineage cells, including osteoprogenitors, osteoblasts, and osteocytes, derive from mesenchymal progenitor cells commonly referred to as mesenchymal stromal cells (MSCs). MSCs from bone marrow, periosteum, and other sources are capable of differentiating along the osteoblastic, chondrogenic, adipogenic, and/or myogenic cell lineages *in vitro* using inductive cell culture conditions [22]. The lineage commitment of MSCs to osteoblast is spatially and temporally determined by the expression of specific genes. The expressions of Runt-related transcription factors 2 (Runx2), Distal-less homeobox5 (Dlx5), and osterix (Osx) are crucial for osteoblast differentiation. Runx2 is a master regulator of osteoblast differentiation. Indeed, $Runx2^{-/-}$ mice show complete lack of both

intramembranous and endochondral ossification due to the absence of osteoblast differentiation [23-25].

Runx2 upregulates genes such as Col1A1, ALP, BSP and OCN and initiates osteoblast maturation. Once osteoblast progenitors start to express Runx2 and Col1A1 a proliferation phase is initiated. In this phase, osteoblast progenitors show alkaline phosphatase (ALP) activity, and are considered pre-osteoblasts. The transition of pre-osteoblasts to mature osteoblasts is characterized by an increase in the expression of Osx and in the secretion of bone matrix proteins such as osteocalcin (OCN), BSP I/II, and type I collagen [1]. Some of the cells ultimately undergo apoptosis or become bone lining cells, while another subset of osteoblasts becomes embedded in the bone matrix and further differentiates to osteocytes, expressing dentin matrix protein 1 (Dmp1) and sclerostin (Sost) [25].

Osteocytes are the most abundant cell population of mammalian bones, making up 90-95% of the adult bone cells. Despite many studies, the processes of how osteoblasts are buried within the matrix and how osteocytes are formed are still largely unclear. How osteoblasts transform into osteocytes is dependent on the mode of ossification (intramembranous or endochondral), the type of bone (woven or lamellar), the location, the species and on the age/gender of the individual [26]. The transition from osteoblast to osteocyte results in profound changes in morphology, including the reorganization of the actin cytoskeleton that leads to a distinctive dendritic shape and a decrease in cell size [27]. During osteocyte maturation many of the previously expressed osteoblast markers, such as OCN, BSPII, type I collagen and ALP are downregulated and osteocyte markers, as Dmp1 and Sost start to be highly expressed [28]. Osteocytes are located in the lacunae and they are interconnected to neighboring osteocytes and cells at the bone surface through adherent junctions made of cadherins and gap junctions made of connexins (Cx) [29]. Recent evidences

have been demonstrated that osteocytes can directly control and regulate the differentiation and activity of both osteoclasts and osteoblasts [30].

Osteoclasts are multinucleated giant cells that differentiate from myeloid precursors that are fundamental for bone homeostasis. They are responsible for bone resorption in physiological and pathological conditions; indeed, any unbalance between bone formation and bone resorption cause bone abnormalities such as osteopetrosis and osteoporosis. Osteoclasts originate from mononuclear cells of the hematopoietic stem cells lineage under the influence of several factors like macrophage colony stimulating factor (M-CSF) and receptor activator of NF-kB ligand (RANKL) produced by osteoblasts and/or osteocytes [31]. M-CSF binds to its receptor (cFMS) present on osteoclast precursors and stimulates their proliferation and inhibits their apoptosis. RANKL is a crucial factor for osteoclastogenesis and is expressed by osteoblasts, osteocytes, and stromal cells. When it binds to its receptor RANK in osteoclast precursors, osteoclast formation is induced. On the other hand, another factor called osteoprotegerin (OPG), which is produced by a wide range of cells including osteoblasts and stromal cells, binds to RANKL, preventing the RANK/RANKL interaction and, consequently, inhibiting the osteoclastogenesis. Thus, the RANKL/RANK/OPG system is a key mediator of osteoclastogenesis [1, 31, 32]. The initial event in bone degradation is the attachment of osteoclasts to the target matrix. Once attached to bone, the cell generates an isolated extracellular microenvironment between itself and the bone surface. Bone demineralization involves acidification of the isolated extracellular microenvironment, a process mediated by a vacuolar H^+–adenosine triphosphatase (H^+-ATPase) in the cell's ruffled membrane. The result of these ion transporting events is secretion of HCl into the resorptive microenvironment, prompting a pH of ∼4.5. This acidic milieu first mobilizes bone mineral; subsequently, the demineralized organic component of bone is degraded by a lysosomal

protease, cathepsin K and metalloproteinases (MMPs). The products of bone degradation are endocytosed by the osteoclast and transported to and released at the cell's antiresorptive surface [33].

1.2 Bone tissue development

In mammals, during embryogenesis, bone tissue is formed via two different processes. Intramembranous bone formation produces many of the craniofacial bones directly from mesenchymal condensations. In contrast, endochondral ossification, the principal process responsible for forming the majority of the mammalian skeleton, generates bone via a cartilage intermediate, and it is also the main process through which bone heal after fracture. Neural crest cells from the dorsal margins of the closing neural tube migrate into the anterior region of the skull, giving rise to dentin of teeth and the connective tissue and some of the bones and cartilages of the face and anterior skull. Prechordal mesodermal cells produce cartilages and bones in the posterior part of the skull. Paraxial mesoderm (somites) is the cellular source of the axial skeleton, whereas lateral plate mesodermal cells form the appendicular skeleton. The initiation of skeletogenesis starts with migration of mesenchymal cells, which express paired-related homeobox 1 (Prx1), derived from these embryonic lineages to the sites of the future bones. Here they form condensations of high cellular density that outline the shape and size of the future bones.

1.2.1 Endochondral bone formation

During endochondral ossification $Prx1^{+}$ mesenchymal progenitors from the lateral plate mesoderm proliferate and populate the emerging limb bud (Fig. 2a). Cells at the center of the mesenchymal condensation express Col2a1 and enter in chondrogenic differentiation program, and start secrete type II collagen and aggrecan (Fig. 2b). These cells express a characteristic genetic program driven by the transcription factors Sox9, FGFs, Prx1, and Indian hedgehog (Ihh) [34]. The cartilage enlarges through chondrocyte proliferation and matrix production. Chondrocytes start forming a polarized structure comprising primarily three different chondrocyte layers. The periarticular layer near the end of the cartilage comprises round, non-column-forming chondrocytes with a moderate proliferation rate. Some periarticular chondrocytes form the joint surface, while others differentiate into flat, column-forming proliferating chondrocytes that proliferate vigorously (Fig. 2d). Chondrocytes in the center of the cartilage template stop proliferating and enlarge becoming hypertrophic (Fig. 2b and 2c) [35]. Central hypertrophic chondrocytes upregulate Col10a1 and start producing high level of type X collagen, and fibronectin preparing the matrix for calcification. Around the same time that chondrocyte hypertrophy occurs, osteoblast precursors first appear in the surrounding region termed the perichondrium (Fig. 2c).

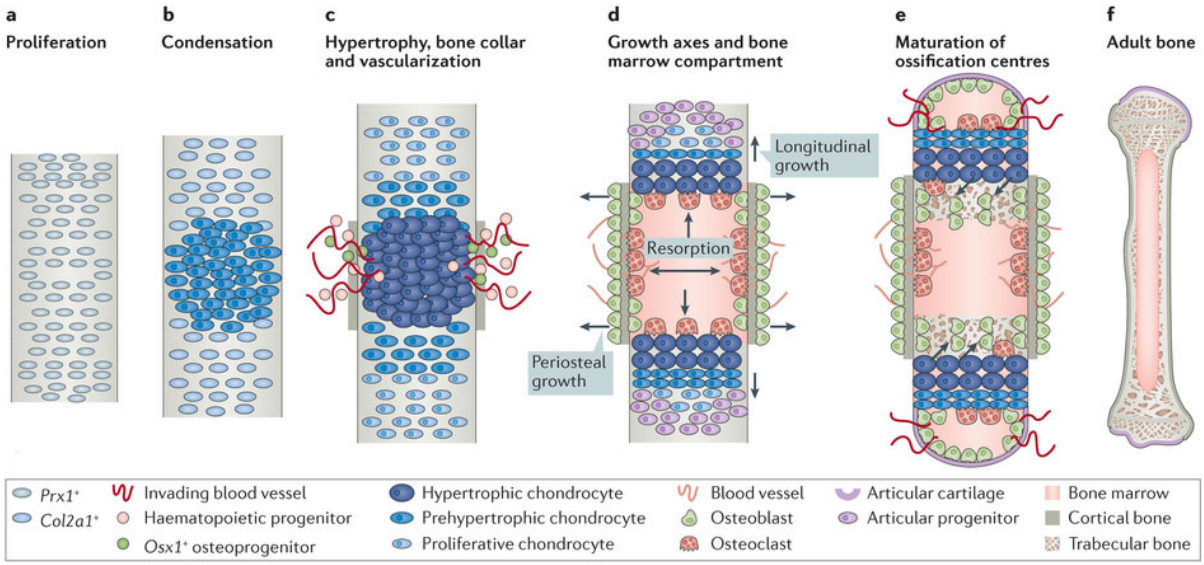

Figure 2. *Longitudinal views of key steps of endochondral bone formation during development of mouse limbs (a) Prx1⁺ progenitors proliferate and populate the future limb; (b) Cells in the center of the template, condensate and differentiate to chondrocytes expressing Col2a1; (c) Central chondrocytes stop proliferating, become hypertrophic and express Col10a1. This event is followed by matrix deposition, vascular invasion and recruitment of hematopoietic progenitors and Osx1⁺ osteoprogenitors; (d) Osteoclasts resorb the cartilage template, blood vessels enlarge, osteoprogenitors differentiate into osteoblasts and two growth plates are established; (e) Within the remodeled cartilage template, bone-forming osteoblasts are derived from Osx1⁺ cells arriving with the invading vasculature, as well as hypertrophic Col10a1⁺ chondrocytes that transdifferentiate as they exit the growth plate into the marrow cavity. As bones grow in length and width, a second wave of vascularization forms the secondary ossification centers; (f) mature endochondral bone. Reproduced from [36].*

The calcification of the extracellular matrix prevents nutrients from reaching the chondrocytes and causes them to undergo apoptosis. The resulting cell death creates voids in the cartilage template and allows blood vessels to invade. Blood vessels further enlarge the spaces, which eventually combine and become the medullary cavity. This is followed by invasion of osteoblast progenitors (Osx⁺ cells), osteoclasts and hematopoietic cells from the perichondrium into the hypertrophic cartilage (Fig. 2c) [36]. The hypertrophic cartilage is resorbed (Fig. 2d), the incoming osteoblast progenitors differentiate into trabecular bone-forming osteoblasts, and hematopoietic and endothelial cells form the bone marrow, which

becomes the primary ossification center. Osteoblast progenitors in the perichondrium differentiate into osteoblasts that deposit cortical bone around the cartilage template. As the fetus grows, the primary ossification center expands and secondary ossification centers form in one or both ends of the developing bone (Fig. 2e). This results in the development of epiphyseal cartilage growth-plate, responsible for the longitudinal growth of bones. Within growth plates, chondrocytes are organized into structural and functional zones, which display distinct gene expression patterns. Small and relatively inactive cells are located in the reserve zone close to the secondary ossification center, whereas proliferating chondrocytes are present in the adjacent proliferative zone. These cells undergo clonal expansion and align themselves into columns parallel to the direction of longitudinal growth [18]. The process of endochondral ossification is largely recapitulated during the healing of large and unstable fractures. This involves generation of fibrocartilage and soft callus at the center of the fracture site that undergo endochondral bone formation. During fracture healing osteoprogenitors cells positive for Prx1 are present in the periosteum and differentiate into chondrocytes in a similar way as during bone development [37]. Bone healing processes are addressed in detail in paragraph 1.6.

1.2.2 Intramembranous bone formation

Intramembranous ossification is the direct conversion of mesenchymal tissue into bone that generates the flat bones of the skull and the lateral clavicles. Mesenchymal stem cells initially proliferate and condensate in dense cluster and subsequentially undergo differentiation into osteoblast with an associated morphological change from spindle-shaped to columnar. Osteoblasts deposit the extracellular matrix called osteoid tissue, which is mainly composed of type I collagen fibrils and is able to bind calcium. Finally, the osteoid

tissue mineralizes to form rudimentary bone tissue with mature osteocytes in the middle and active osteoblasts at the osteogenic front [38]. These bones constantly grow by new osteogenic differentiation and the deposition of new bone material at their margins. As during endochondral bone formation, angiogenesis plays a crucial role also in intramembranous ossification. Compared to endochondral ossification, intramembranous ossification and intramembranous angiogenesis are poorly understood. However, just like long bones, flat bones are highly vascularized, and intramembranous angiogenesis appears to occur similarly to endochondral vascularization [39] (Fig. 3).

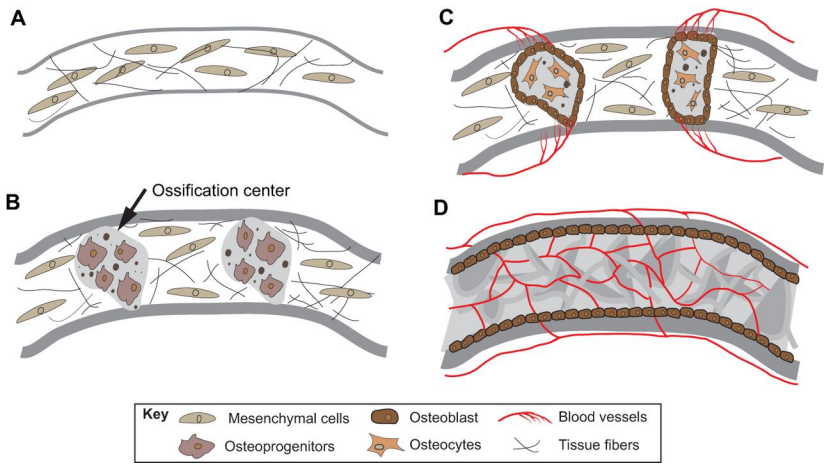

Figure 3. *Intramembranous ossification and angiogenesis. (A) Mesenchymal cells condensate to form sponge-like structures and differentiate into osteoprogenitors and osteoblast; (B) These cells secrete ECM and form ossification centers, and ultimate differentiate into osteocytes; (C) Matrix proteins and pro-angiogenic factors generated by the ossification centers attract blood vessels; (D) The subsequent vascularization of the developing flat bone promotes osteogenesis. Reproduced from [39].*

During development, intramembranous bones do not fuse but remain separated by specialized structures, the sutures [40]. Sutures allow spatial separation of the bones during growth and they need to remain in an unossified state, yet allow new bone to be formed at the edges of the overlapping bone fronts. This process relies on the production of sufficient new bone cells to be recruited into the bone fronts, while ensuring that the cells remaining in

the suture remain undifferentiated. Once sutures are formed, a second phase of development occurs, in which rapid growth of the cranial bone takes place via the regulated proliferation and differentiation of osteoprogenitor at the periphery of each bone field, which is called the osteogenic front. While the sutures are developing, the growing and expanding bone fronts both invade and recruit the intervening mesenchymal tissue into the advancing edges of the bone fronts. In this process, the mesenchyme is separated with an outer ectoperiosteal layer and an inner dura mater by the intervening bones [41]. At birth, the flat bones of the skull are rather widely separated by the sutures. These open spaces, the fontanelles, allow a considerable amount of deformation of the skull at birth, a fact which is important in allowing the relatively large head to pass through the birth canal. After birth, apposition of bone along the edges of the fontanelles eliminates these open spaces fairly quickly, but the bones remain separated by a thin periosteum line suture for many years, eventually fusing in adult life.

The cellular origin and transcriptional regulation of osteoblasts differentiation during intramembranous bone formation is still poorly understood. It has been recently shown the Runx2 play a crucial role in this process [42]. In this study was shown that Runx2 deficiency in $Prx1^{+}$ progenitors resulted in defective intramembranous ossification and that Runx2 was heterogeneously expressed in Prx1-GFP^{+} cells located at the intrasutural mesenchyme in the calvaria of transgenic mice expressing GFP under the control of the Prx1 promoter. The authors suggested that osteoblast differentiation in the calvaria begins from double-positive cells for Prx1 and stem cell antigen-1 (Sca1) ($Prx1^{+}Sca1^{+}$ cells). These cells mature into $Runx2^{+}Osx^{+}Prx1^{-}Sca1^{-}$ osteoblast precursor, which eventually form mature osteoblast. Moreover, Runx2 deficiency in Osx^{+} cells resulted in severe defects in intramembranous ossification

1.3 Bone remodeling

Bone is highly dynamic tissue that undergoes remodeling throughout life. Remodeling is a physiological process due to the activity of osteoblasts and osteoclasts, and it is fundamental to maintain bone homeostasis and repair microfractures. In normal conditions bone resorption and bone deposition are perfectly balanced so that old and damaged bone is continuously replaced by new tissue. The remodeling cycle starts with an initiation phase, which consists of bone resorption by osteoclasts, followed by a transition phase (or reversal) and conclude by a phase of bone deposition by osteoblasts. These two cells type closely collaborate in what is called a basic multicellular unit (BMU). In the initiation phase, mechanical loading and microdamage are sensed by osteocytes, which stimulate the recruitment of osteoclasts precursors by releasing RANKL, M-CSF and ligands for immunoglobulin receptors. In the subsequent transition phase, osteoprogenitors migrate to the resorbed sites and differentiate into osteoblast. This phase is controlled by many coupling factors, including BMPs, Wnts, parathyroid hormone, prostaglandins, insulin-like growth factors (IGFs), TGF-β1, FGFs and angiogenic factors. Many of these factors are stored in the bone matrix and released during bone resorption [11]. Recent evidences showed the involvement of another category of molecules called semaphorins. During the initial phase, osteoblast differentiation is inhibited by semaphorin 4D (Sema4D), released by osteoclasts, in order to allow a complete resorption of the bone. The binding of Sema4D to its receptor Plexin-B1 on osteoblasts inhibits IGF-1 pathway that is essential for osteoblast differentiation [43]. Conversely, during the phase of bone deposition, osteoblasts prevent the generation of additional sites of bone resorption by inhibiting osteoclasts differentiation. Osteoblasts

produce and release semaphorin 3A (Sema3A) which inhibits osteoclast differentiation and migration, and at the same time stimulate bone formation [44, 45] (Fig. 4).

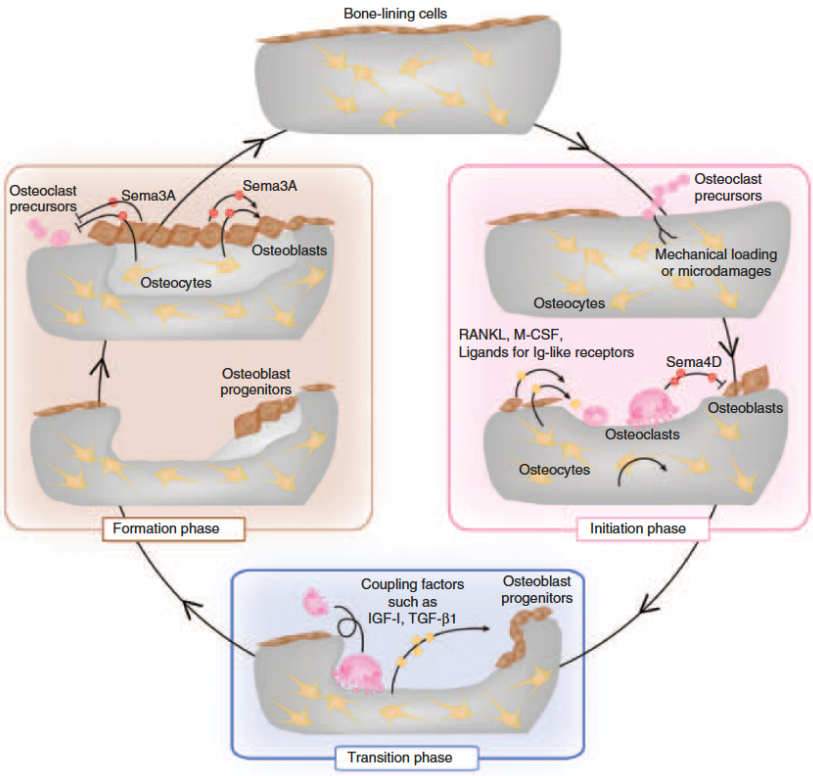

Figure 4. *The bone remodeling cycle and its phases. Osteoclastogenesis is stimulated by the RANKL, macrophage colony-stimulating factor (M-CSF) and ligands for immunoglobulin-like receptors, which are produced by osteoblast lineage cells including osteocytes, and bone resorption starts. Osteoclasts inhibit bone formation during bone resorption through the expression of Sema4D. In the transition phase, classical coupling factors, including IGF-I and TGF-β1, stimulate the migration of osteoprogenitors to the resorbed sites and promote differentiation into osteoblasts. In the bone formation phase, osteoblasts replenish the resorbed area with new bone. Sema3A, which is produced by osteoblast lineage cells, inhibits osteoclastogenesis and simultaneously promotes bone formation in this phase. Reproduced from [45].*

In addition, it has been shown that ephrinB2/ephrinB4 pathway is involved in the ending the resorption phase and in inducing osteoblast differentiation. EphrinB2 is expressed on the osteoclasts membrane and binds to eprhineB4 expressed on osteoblast. The ephrinB2/ephrinB4 binding transduces bidirectional signals, which promote osteoblast differentiation, whereas the reverse signaling (ephrinB4/ephrinB2) inhibits

osteoclastogenesis [46]. Besides osteoclasts and osteoblasts, it has been demonstrated that osteocytes play key roles during bone remodeling. Osteocyte apoptosis may indirectly stimulate osteoclastogenesis by inducing stromal/osteoblastic cells to secrete RANKL. In addition, osteocytes can directly produce and potentially secrete RANKL. Mature osteocytes embedded in the matrix selectively secrete sclerostin, the product of the Sost gene, which antagonizes several members of the BMP family of proteins and also binds to LRP5/LRP6 preventing canonical Wnt signaling and inhibiting of bone formation. During the phase of bone formation Sost is downregulated leading to an increase in Wnt signaling and subsequent bone deposition [47].

1.4 Bone marrow

The bone marrow (BM) is a highly vascularized tissue which is found in the central cavities of axial and long bones. It consists of hematopoietic tissue islands and adipose cells surrounded by vascular sinuses interspersed within a meshwork of trabecular bone. The bone marrow is the major hematopoietic organ, and a primary lymphoid tissue, responsible for the production of erythrocytes, granulocytes, monocytes, lymphocytes and platelets. Macroscopically the bone marrow can be red or yellow, depending on whether it consists of mainly hematopoietic (and therefore, red-colored) tissue or fatty (and therefore a yellow-colored) tissue. Both types of bone marrow are highly vascularized, being enriched with numerous blood vessels and capillaries. Red marrow is found mainly in the flat bones, such as the hip bone, sternum bone, skull, ribs, vertebrae, and shoulder blades, as well as in the metaphyseal and epiphyseal ends of the long bones, such as the femur, tibia, and humerus, where the bone is cancellous or spongy. Yellow marrow is found in the hollow interior of the diaphyseal portion or the shaft of long bones. During aging the red marrow is replaced by

yellow marrow. However, the yellow marrow can revert to red if there is increased demand for red blood cells, such as in instances of blood loss.

Blood vessels localized in the BM cavity orchestrate the process of hematopoiesis, and provide the Hematopoietic Stem Cells (HSCs) with the necessary niche. Although it is currently commonly accepted that HSCs are localized in the vicinity of bone blood vessels (both arteries and veins), a specific location of their niche has been unclear and controversial so far. It has been recently reported that, in mouse, 85% of HSC are placed within 10-30μm of a sinusoidal blood vessel and that most HSCs, both dividing and non-dividing, are distant from arterioles, transition zone vessels, and bone surfaces [48].On the other hand, others reported that quiescent HSCs associate specifically with the small arterioles distributed within the endosteal bone marrow [49]. More recently, Kusumbe et al. [50] showed that HSCs are frequently detected in close proximity of a specific subtype of capillaries and arterioles in the endosteal region. Recent improvements with bone imaging methods provided insights into the localization of HSCs within the bone marrow where they frequently localize close to blood vessels. Endothelial cells maintain and regulate the HSC niche by releasing numerous angiocrine factors, such as stem cell factor (SCF), interleukins (ILs) and chemokines like CXCL12 [51] (Fig. 5).

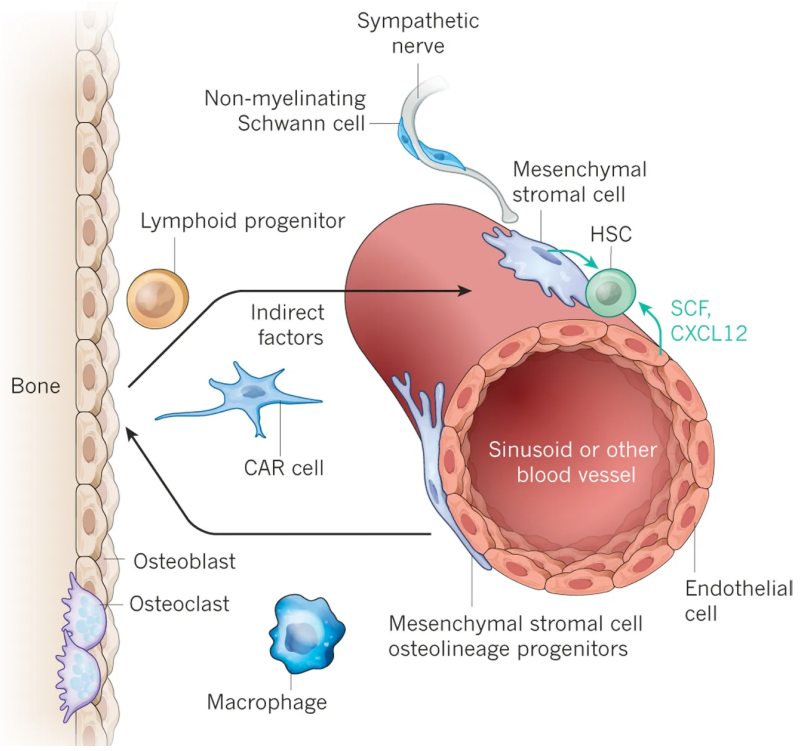

Figure 5. *The bone marrow hematopoietic niche. HSC are found associated to sinusoids, where mesenchymal stromal cells and endothelial cells promote their maintenance by producing SCF, CXCL12 and other coupling factors. Skeletal progenitors are also located in close proximity of blood vessels. Reproduced from [52].*

The post-natal BM has traditionally been seen as an organ composed of two main systems rooted in distinct lineages: the hematopoietic tissue and the associated supporting stroma, that is poor in collagen and essentially made of network of cells. The predominant types of blood vessel in the bone marrow are large-caliber, venous vessels called sinusoids. Cell trafficking in and out of the bone marrow takes place across the endothelial wall of sinusoids. Slow blood flow in sinusoids facilitates adherence and extravasation of blood-borne cells. Their outer abluminal, surface is covered with stromal cells called adventitial reticular cells (ARCs) for their position and morphology. These cells express alkaline phosphatase, low-affinity nerve growth factor receptor (CD271), vascular cell adhesion molecule-1 (CD106), the melanoma cell adhesion molecule (CD146), endoglin (CD105), α-smooth muscle actin and CD10 [53]. Even though the identification of these markers was proven in many works during

the last decades, ARC markers are dynamically expressed *in vivo* and no marker yet identifies all ARCs at all times. ARCs share their anatomical location (directly beneath the endothelial layer) with pericytes in other tissues, although BM sinusoids are not the same as capillaries in other tissues. ARCs also express markers otherwise expressed in pericytes of other tissues, such as in skeletal muscle and myocardium [53-55]. ARCs have been identified as self-renewing, multipotent progenitors for skeletal lineages (cartilage, bone, marrow adipocytes, fibroblasts). These progenitors (skeletal stem cells, SSCs) secure a reservoir of bone-forming cells for bone growth during development and bone remodeling. BM stromal cells (BMSCs), including SSCs, also shape and regulate the local microvascular network, regulate differentiation of osteoclasts, and establish and maintain the hematopoietic microenvironment necessary for growth and blood cell maturation (Fig. 5). In addition, they might be essential for retaining long-term self-renewing HSCs (niche function) [56]. All the extra-skeletal tissues and organs in which MSC have been found (e.g. muscle, placenta, adipose tissue) are developmentally distinct from skeletal lineages, do not contribute to skeletal development or postnatal physiology, do not display skeletogenic properties assayable *in vivo* and are not generated by skeletal progenitors found in the BM [57].

1.5 Mesenchymal stem cells

The term mesenchymal stem cell (MSC) was introduced for the first time in 1991 by Arnold Caplan to describe a class of cells from human and mammalian bone marrow, and periosteum, that could be isolated and expanded in culture while maintaining the *in vitro* capacity to be induced to form a variety of mesodermal phenotypes and tissues [58]. The first indication that cells in the BM had the ability to generate bone dates back in 1968, when Tavassoli and Crosby clearly stablished proof of an inherent osteogenic potential associated

with the BM [59]. However, these experiments were conducted with entire fragments of bone-free BM, the precise identity of any cell functioning as a progenitor of differentiated bone cells (and therefore of nonhematopoietic, mesenchymal cells) could not be delineated. It was in the early seventies that Friedenstein and coworkers demonstrated that the osteogenic potential, as revealed by heterotopic transplantation of BM cells, was associated with a minor subpopulation of BM cells [60, 61]. These cells were distinguishable from the majority of hematopoietic cells by their rapid adherence to tissue culture plastic and by the fibroblast-like appearance of their progeny in culture, pointing to their origin from the stromal compartment of BM.

Two opposing description of MSCs exist at this time in cell biology. The first one refers to MSCs as post-natal, self-renewing, and multipotent stem cells giving rise to all skeletal tissues. When explanted in culture, these progenitors generate a clonal progeny of transplantable stromal cells. Upon in vivo transplantation, these stromal populations generate miniature chimeric replicas of bone as an organ (an organoid), which include bone and bone marrow stroma of donor origin, as well as host-derived hematopoietic tissue and blood vessels within a marrow cavity. The single cell that initiates a clonal population in culture, which in turn can establish a complete organoid in vivo (including secondarily transplantable stromal cells), is a stem cell, and it is multipotent and self-renewing [55, 62].The second alternative description states that MSC are not necessarily either stem cells or mesenchymal, but rather Multipotent Stromal Cells [63], Mesenchymal Stomal Cells [64] or Medicinal Signaling Cells [65]. Despite the different terminologies it is becoming broadly accepted in the community that the term “Mesenchymal Stem Cell”, and in particular the “stem” part, should be abandoned [57, 66].Moreover, MSC cultures are characterized by strong heterogeneity and regardless of the mode of isolation and selection employed, and even if the culture is initiated by a single

cell, cultures initiated by explanted MSCs do not meet rigorous criteria that would allow them to be defined as cultures of stem cells, no matter how uniform their antigenic profile. Thus, culturing of stromal cells cannot be mistaken for, or referred to as, the expansion of stem cells [53].

Although clarifying the nature of MSC is difficult, it is possible to affirm the BM stroma hosts self-renewing, multipotent progenitors for skeletal lineages that can be defined as Skeletal Stem or Skeletal Progenitor Cells (SSCs) [57].

1.5.1 Characteristic of MSCs

Skeletal progenitors can be isolated on the base of surface marker expression (although no unique markers have been identified yet) or by establishing clonal adherent cultures. However, these cultures of stromal cells contain heterogeneous mixtures of cells with indeterminate potencies and promiscuous contribution to many overlapping lineages, such as bone, cartilage, fat, muscle, fibroblast, endothelial cells, and stroma. Likely, these cells represent a population comprised of multiple types of distinct stem cells rather than a uniform purified skeletal stem cell [67].

Several markers have been found to characterized MSC *in vitro*: they express CD105, CD49a, CD73, CD90, CD146 and STRO-1 and they lack the expression of haemopoietic markers, such as CD45, CD34, CD13, CD11b, CD79a, CD19 [63, 68]. On the basis of immune-localization several studies identified skeletal progenitors in association with blood vessels in different tissues [54, 69], and some stromal cell populations have further been described to be pericytes [55, 70]. In contrast, it has also been shown that skeletal progenitors in bone are enriched in and around the avascular regions of the hypertrophic growth plates, though they have also been found in the periosteum as well as fracture calluses [71]. It is, therefore,

possible that MSCs are either comprised of more committed progenitor populations descending from SSCs settling in sinusoidal regions or contain a multipotent pericyte-like stem cell giving rise to more restricted progenitor cell types itself [72]. The description of SSCs have been extended by single and combinatorial use of surface marker/genetic labeling, transplantation assays, and *in vivo* lineage tracing. This has led to the discovery of multiple SSC populations in the growth plate, the endosteal and perisinusoidal bone marrow space, or the perichondrium. However, the description of these cell populations is often incomplete or redundant leaving contradictory results. A potential explanation can be found in the complex and plastic nature of bone tissues and might be vested in technical limitations or an indication for the presence of an everchanging network of multiple subtypes of SSCs orchestrating skeletal homeostasis and repair [72].

At a clonal level, MSCs display different phenotypes: fibroblastic elongated cells, large flattened cells and thin star-shaped cells. When plated at low density they form colonies (fibroblastic colony forming units, CFU-f) of different diameter size, indicating heterogeneity in terms of morphology and proliferation capacity. It has been shown that several growth factors, including EGF (epidermal growth factor), PDGF and FGF-2 are able to increase the MSCs proliferative potential [73]. FGF-2 expanded MSCs maintain unaltered their original elongated phenotype for a longer time. It was shown that expression of osteogenic differentiation markers was reduced in the presence of FGF-2. Moreover, Bianchi et al. showed that FGF-2 may select for a population of earlier progenitors. In fact, assessment of telomere length, medium switch experiments, and a decrease in the number of the initial colonies indicated that FGF-2 supported the survival of a subpopulation with increased proliferation and differentiation potential [74].

1.5.2 MSC based therapy for bone regeneration

MSCs play a key role in fracture repair by differentiating into bone-forming osteoblast and cartilage-forming chondrocytes. Several signaling pathways, including BMP, Wnt, and Notch signaling, regulate MSC proliferation and differentiation. MSCs can be harvested, cultivated, and delivered to promote bone healing. Whether isolated and purified, MSCs participate directly in the healing process or indirectly influence healing is not well defined [75]. Tissue engineering and regenerative medicine (TERM) strategies combine scaffolds, growth-factors (e.g. BMP-2), and MSCs to improve bone repair and regeneration. Most *in vitro* and many *in vivo* studies have suggested that MSCs have the potential to promote osteogenesis [76, 77]. How MSCs home to the injury site has not been clarified yet. Many chemo-attractant molecules released at the site of injury have been shown to be essential for MSC recruitment, such as stromal cell-derived factor 1 (SDF-1), macrophage inflammatory protein 1α (MIP-1α) and monocytes chemotactic protein 1 (MCP-1) [78]. However, despite the long-lasting therapeutic efficacy of MSCs in many *in vivo* models (such as bone and cartilage repairing, cardiovascular and neurological diseases), the incidence of MSCs engraftment remained very low. These data suggested that the general therapeutic effects of MSCs might be due their ability to modulate the host microenvironment and host progenitor cells rather than directly participating to the healing process.

Transplanted adult MSCs were shown to mediate regeneration of tissues by releasing paracrine signals and this inspired the definition of these cells as “site-regulated, multidrug dispensaries, or injury drugstores” [65]. For example, it has been shown that primary MSCs cultured in the presence of FGF-2 *in vitro*, have the potential to induce host regenerative response *in vivo* [79]. Recent studies started to identified the specific components present in

the MSC conditioned medium that could be responsible for the activation of endogenous repair processes. Recent studies indicated that the cross-talk between MSCs and cells of the innate immunity could be carried out by secreted extracellular vesicles (EVs). In particular, EVs isolated from the conditioned medium of MSC harvested under both normoxic and hypoxic culture conditions acted as mediators of the dynamic interplay between MSCs and cells of the innate immunity both *in vitro* and *in vivo* in a mouse model of skeletal muscle regeneration. In particular, EVs effectively triggered the macrophage proliferation and polarization from an M1 to an M2 phenotype [80]. Generally, the basic mechanisms of MSCs action on bone regeneration and repairing can be summarized in: replacing damaged cells by proliferation and differentiation; modulation of the immune system; secretion of factors that induce tissue repair; recruitment of endogenous MSCs or progenitor cells to the injury site; possible transfer of vesicular components containing mRNA, miRNA and proteins [81]. Although MSCs were studied because of their differentiation capacity, there is now accumulating evidences suggesting that immunomodulatory and paracrine actions predominantly contribute to their therapeutic efficacy. Some molecules such as VEGF, BMP-2 and MCP-1 play essential roles in the mechanism of MSCs induce tissue regeneration.

1.6 Bone healing

Bone has the unique and intrinsic ability to heal tissue damage without the formation of scar tissue. In physiological conditions and for small defects bone can regenerate and restore its characteristics and function with high efficiency. This tremendous regenerative capacity depends on the fact that fracture repair in the adult closely resembles bone development, as it recapitulates many of the key molecular pathways during fetal life. The precise series of ordered events required to produce new bone are modulated by systemic and local factors,

and disruption of these orderly events may cause healing problems. Thus, a clear understanding of the sequence of events and their regulation is needed to promote healing and to avoid complications [82].

Facture healing, the most common form of bone repair, is a multistage process that involves complex and well-orchestrated steps, namely, inflammation phase, soft callus phase, cartilage turnover (replacement by bony callus) phase and bone remodeling phase [83]. Depending on the stability of fracture fixation and supply of blood vessels, endochondral or intramembranous ossification occurs at the facture sites. Instability or lack of blood supply may lead to endochondral bone formation during the repair, while a stable facture or fracture rich in vasculature results in intramembranous ossification [84]. However, most of the fractures heal mainly by endochondral ossification with limited contribution of intramembranous ossification. In addition, a third type of ossification called transchondroid bone formation has been proposed in a model of distraction osteogenesis. During transchondroid ossification, chondrocyte-like cells induced by mechanical strains form chondroid bone, which is gradually transformed to bone [85].

Following a trauma, disruption of the local vascular system results in blood clotting and hematoma formation, which consists of cells from both peripheral and intramedullary blood, as well as bone marrow cells. The injury initiates an inflammatory response which is necessary for the healing to progress. The response causes the hematoma to coagulate in between and around the fracture ends, and within the medulla forming a template for callus formation. Cells within the hematoma are crucial for the initiation of the inflammation phase. The initial proinflammatory response involves secretion of tumor necrosis factor-α (TNF-α), interleukin-1 (IL-1), IL-6, IL-11 and IL-18 [83]. These factors further recruit inflammatory cells and promote angiogenesis. As a consequence of the vascular trauma, the fracture site becomes hypoxic

and osteocytes are deprived of nutrition supply and undergo apoptosis. The formation of necrotic tissue triggers the recruitment of leukocytes and macrophages to the region. Macrophages phagocyte the necrotic tissue and release signaling factors, such as BMPs (BMP-2, BMP-5 and BMP-7), bFGF, TGFβ, PDGF, IGF and VEGF. These factors orchestrate crucial events such as recruitment, proliferation and differentiation of osteoprogenitor cells and MSCs (Fig. 6).

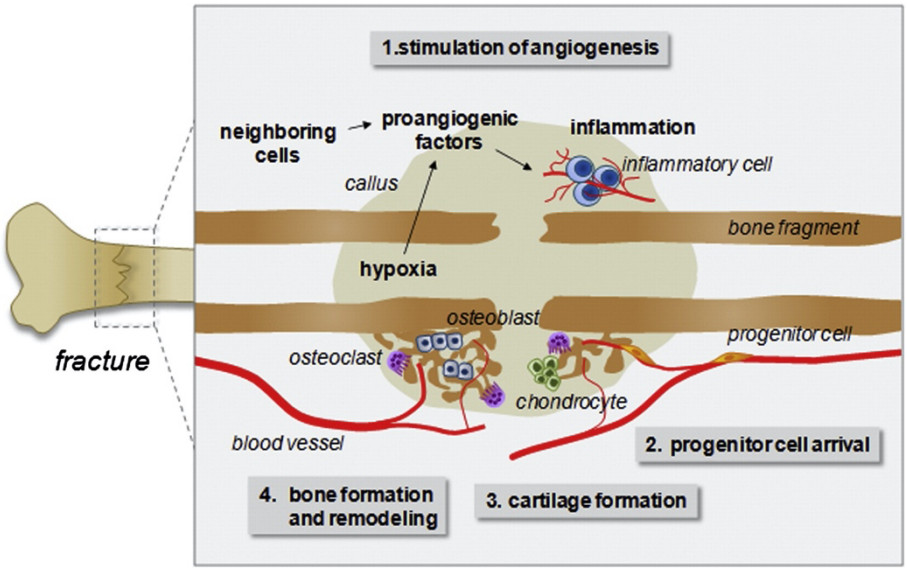

Figure 6. *The angiogenic response during normal fracture healing. Activation of the hypoxia signaling pathway stimulates the production of VEGF and PlGF by several cell types present at the fracture site. In addition, early blood vessel formation supports the invasion of inflammatory cells which actively contribute to the fracture healing process and produce proangiogenic cytokines. During the formation of the soft and hard callus, the vascular system also mediates the progenitors migration to the fracture site and promote bone regeneration by supplying oxygen, nutrients and ions necessary for mineralization. Reproduced from [86].*

Depending on their relative distance to the blood vessels, these progenitor cells either differentiate into chondrocytes, which deposit a collagenous matrix that is later replaced by bone, or they directly maturate into bone-forming osteoblasts. Indeed, chondrocytes are located furthest away from the blood vessels [87], possibly because their metabolism is adapted to survive and function in a poorly vascularized environment. In contrast, differentiation of osteoprogenitors to mature osteoblasts during intramembranous bone

repair depends more on oxidative metabolism and thus requires a constant substantial supply of nutrients from neighboring blood vessels [88]. The cartilage callus is subsequently replaced by bone tissue in a process resembling endochondral ossification. In the final phase of fracture repair, the healing bone undergoes remodeling together with the restoration of the vascular supply to the normal state. Bone repair requires the mobilization of stem cells to allow deposition of mineralized matrix at the injury site. Two major sources for these stem cells are the periosteum and the bone marrow, although other sources are also possible. Lineage-tracing experiments indicate that two distinct types of stem cells, periosteal stem cells and MSCs differentially participate in bone repair; cells from the periosteum are the source of chondrocytes and osteoblasts, whereas cells from the bone marrow undergo osteoblast differentiation. Therefore, periosteal stem cells are likely to retain the capability to regenerate a growth plate after fracture, at least in early life. Interestingly, during the postnatal period, Prx1 expression becomes confined to the periosteum in the cambium layer, immediately outside the osteoblasts lining the bone surface [89]. Prx1 periosteal cells differentiate into chondrocytes and osteoblast in the fracture callus suggesting the possibility that Prx1-expressing cells in the periosteum include stem cells retaining characteristics similar to those of limb bud mesenchymal cells during early morphogenesis [34].

2. VEGF family, receptors and signaling

2.1 VEGF family

Vascular Endothelial Growth Factors (VEGF) are the most important growth factors for the regulation of vascular development and angiogenesis, both in physiological and in pathological conditions. Since bone is a highly vascularized organ and angiogenesis plays an important role in osteogenesis, VEGF also influences skeletal development and postnatal bone repair [85]. In mammals, the VEGF family comprises five members: VEGF-A, placenta growth factor (PGF), VEGF-B, VEGF-C and VEGF-D. VEGF-A, as now on referred as VEGF, is the most abundant form and plays crucial role in proliferation, migration and activation of endothelial cells as well as in promotion of permeability of blood vessels [90]. VEGF-C and -D are important for lymphangiogenesis [91, 92] and VEGF-B has a role in embryonic angiogenesis [93, 94]. Two other non-mammalian proteins have been included in the VEGF family: the parapoxvirus VEGF-E and the snake venom VEGF-F [95].

The VEGF gene is organized as eight exons separated by seven introns (Fig. 7A). Depending on alternative splicing, VEGF mRNA is translated into four major isoforms ($VEGF_{121}$, $VEGF_{165}$, $VEGF_{189}$, $VEGF_{206}$), having respectively 121, 165, 189 and 206 amino acids, after signal sequence cleavage. In mouse, instead, VEGF isoforms have one amino acid less compared to the human ones ($VEGF_{120}$, $VEGF_{164}$, $VEGF_{188}$, $VEGF_{205}$).

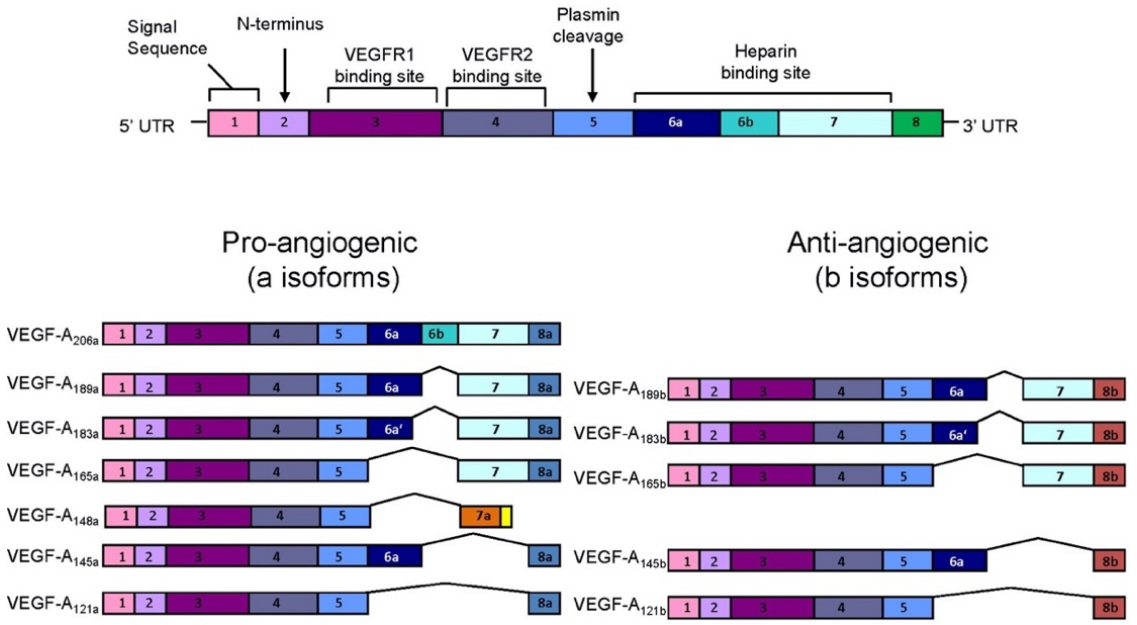

Figure 7. *(A) Vegfa mRNA exons composition. (B) Pro-angiogenic VEGF-A splicing isoforms. (C) Anti-angiogenic VEGF-A isoforms. Adapted from [96].*

VEGF is a heparin-binding homodimeric glycoprotein and its isoforms differ in their affinity for the extracellular matrix (ECM) [97]. $VEGF_{121}$ is an acidic polypeptide that does not bind to the ECM and can diffuse freely. $VEGF_{189}$ and $VEGF_{206}$ are highly basic and bind to heparin with high affinity and they are almost completely sequestered by the ECM. $VEGF_{165}$ has intermediary properties, as it is secreted but a significant fraction remains bound to the cell surface and ECM. The ECM-bound isoforms may be released in a diffusible form by plasmin cleavage at the C terminus, which generates a bioactive fragment [90]. Studies in transgenic models expressing only one of the major VEGF isoforms showed that their specific ability to bind ECM is critical for proper vascular morphogenesis. $VEGF_{120}$, which does not bind ECM, induces vascular networks with reduced branching and abnormally enlarged diameters, $VEGF_{188}$, which binds ECM strongly, causes opposite defects, with ectopic branching and reduced capillary size, whereas $VEGF_{164}$, which binds ECM with intermediate affinity, is the only isoform capable of inducing physiologically patterned vasculature [98].

2.3 VEGF receptors

VEGF molecules bind to three distinct tyrosine kinase receptors in mammals: VEGFR-1 (Flt-1) and VEGFR-2 (Flk-1), which can also exist as soluble forms, named sVEGFR-1 and sVEGFR-2 respectively, and VEGFR- 3 (Flt-3). Ligand binding leads to receptor dimerization, which is followed by autophosphorylation of the intracellular kinase domain and subsequent initiation of the signal transduction cascade. Depending on the ligand, both homodimeric and heterodimeric receptor complexes can be formed. Furthermore, the three VEGF-Receptors are also able to interact with co-receptors of the neuropilin family (neuropilin-1, NRP1 and neuropilin-2, NRP2), macromolecules like heparan sulfate and proteoglycans (syndecan and glypican), non-VEGF-binding auxiliary proteins like vascular endothelial cadherin (VE-cadherin), integrins, ephrin-B2, and protein tyrosine phosphatase [99]. VEGFR-1, which can also bind to VEGF-B, is the receptor with the highest affinity for VEGF-A, but it displays only weak tyrosine phosphorylation activity. As a consequence, the interaction of VEGFR-1 with the ligand does not start the signal transduction cascade efficiently, and VEGFR-1 may rather act as both a decoy receptor by sequestering VEGF-A and as a modulator of the activity of VEGFR-2 homodimers. VEGFR-2 is able to bind to VEGF-A with an affinity 10-fold lower than that of VEGFR-1, but it is the main mediator of VEGF-A activity in endothelial cell differentiation, proliferation, migration, angiogenesis and vessel permeabilization (Fig. 8) [100].

2.4 VEGF signaling pathway

VEGFR signaling is tightly regulated at numerous different levels, including receptor expression levels, the availability and affinities for binding of its different ligands, the presence of VEGF-binding co-receptors, non-VEGF binding auxiliary proteins and inactivating tyrosine phosphatases, the rate of receptor cellular uptake, degradation and speed of recycling. VEGFR endocytosis and trafficking regulate the specificity as well as the duration and amplitude of the signaling output. Once they are in the cytoplasm, VEGFRs are either transported to lysosomes for degradation or recycled back to the membrane via fast or slow recycling pathways [101].

The canonical (classical VEGF ligands) and non-canonical (non-VEGF ligands) activation of VEGFR2 trigger intracellular pathways that are crucial to endothelial biology and regulate cell survival, migration, proliferation and blood vessels permeability. These include the phospholipase Cγ (PLCγ)-ERK1/2 pathway, which has a central role during vascular development and in adult arteriogenesis; the PI3K–AKT–mTOR pathway, which is crucial for cell survival, regulation of vasomotion and regulation of barrier function; and SRC and small GTPases, which are involved in cell shape, cell migration and polarization, as well as regulation of endothelial junctions and the vascular barrier function (Fig. 8) [101, 102].

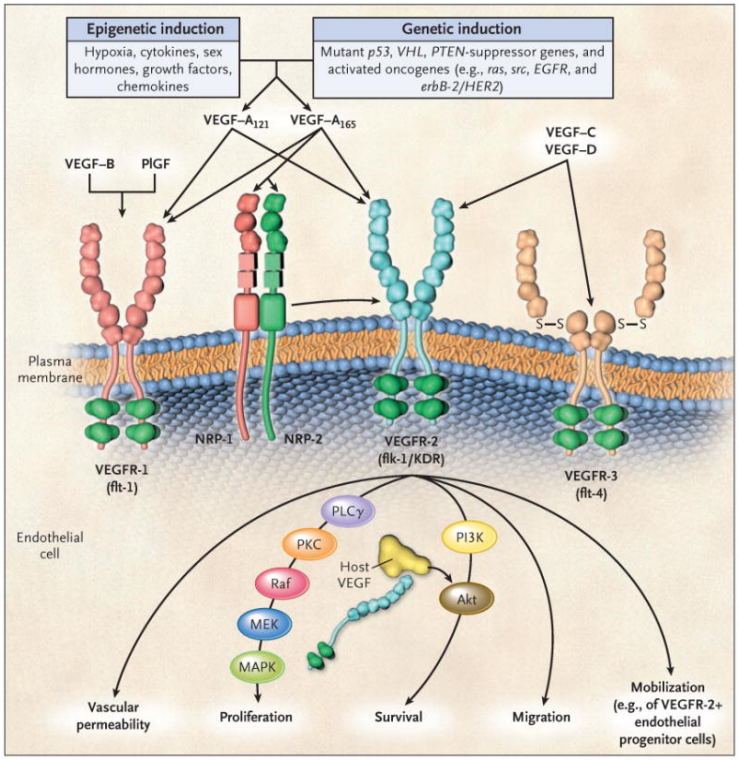

Figure 8. *VEGF receptors and their downstream pathways. The diffusible isoforms of VEGF, including $VEGF_{121}$ and $VEGF_{165}$, signal through VEGFR2, the major VEGF signaling receptor for angiogenesis. The binding of VEGF to VEGFR2 leads to a cascade of different signaling pathways. Binding of ligands causes dimerization of the receptor, followed by intracellular activation of the PLCγ– PKC–Raf kinase–MEK–MAPK pathway and subsequent initiation of DNA synthesis and cell growth, whereas activation of PI3K–Akt pathway leads to increased endothelial-cell survival. Activation of Src can lead to actin cytoskeletal changes and induction of cell migration. Reproduced from [103]*

In contrast to VEGF signaling in endothelial cells that has been widely studied, VEGF signaling in osteoblasts remains less well known. The levels of VEGFR expression in osteoblastic cells depend on animal species and methods used for cell isolation. Osteoblast-derived VEGF usually acts in a paracrine manner on adjacent endothelial cells via binding to VEGF receptors to regulate endothelial migration, proliferation and vessel permeability. In addition to endothelial cells, VEGF receptors are also expressed and functional in other cells types, including pericytes and osteoclasts [104]. However, expression of VEGF receptors in osteoblasts is quite variable, particularly in mice, making paracrine/autocrine effects of

osteoblast-derived VEGF on osteoblasts difficult to study. Expression of VEGF and its receptors in differentiating osteoblasts has been detected in cultured cells [105], and *in vivo* by in situ hybridization [106]. In some studies, it has been shown that migration, proliferation and differentiation of the osteoblastic cells could be stimulated by recombinant VEGF (rVEGF) [107]. It has also been shown that *in vitro*, in murine osteoblastic MC3T3 cells, VEGF promoted alkaline phosphatase and osteocalcin expression [108]. In other studies, primary murine mesenchymal progenitors and osteoblasts failed to respond to rVEGF [85, 109]. However, mice with conditional deletion of Vegfr1 or Vegfr2 in osteoblastic cells exhibited reduced bone density two weeks after birth, and their bone marrow had reduced numbers of osteoprogenitors [109]. These findings suggest that both VEGFR1 and VEGFR2 are regulators of skeletal development [104]. VEGF has also been found to directly affect activation of osteoclast precursor differentiation through binding to VEGFR-2 [110], and VEGF overexpression was shown to cause bone resorption by excessive osteoclast recruitment [111].

3. Angiogenesis

Angiogenesis is the growth or expansion of micro-vascular capillary networks from preexisting ones and is driven by ischemia and hypoxia. However, hypoxia-induced angiogenesis alone is not sufficient to restore physiological blood flow after an ischemic event. In fact, capillaries are responsible for the metabolic exchanges between blood and tissue, but feeding arteries are required to supply sufficient blood flow to satisfy the tissue needs. In contrast, arteriogenesis is the formation of mature, functional arteries through the functional remodeling of pre-existing and little-perfused interconnecting arterioles after an occlusion of large conductance arteries, thereby bypassing the block and restoring blood flow to ischemic tissue downstream [100]. Angiogenesis is a complex process in which the growth of normal, stable, and functional vessels is critically dependent on the coordinated interplay in space and time of different cell types and growth factors [112].

3.1 Cellular mechanisms: sprouting/intussusception

The growth of new blood vessels can occur in two different, but complementary, ways: sprouting and intussusception (or splitting angiogenesis). Sprouting is the best characterized mode of vascular growth, and it consists in the invasion of avascular tissues by new vessels guided by gradients of growth factors, e.g. during embryonic development. Instead, in intussusceptive angiogenesis new blood vessels originate from the expansion and remodeling of pre-exiting vascular networks, both in development and in post-natal life [113, 114]. Initiation of sprouting requires the functional specification of endothelial cells into either tip or stalk cells. Tip cells do not proliferate and they extend filopodia through which they can sense VEGF gradients, and migrate towards the VEGF source, thereby guiding the nascent sprout. Stalk cells, which instead proliferate just behind the tip, form the body of the sprout

and start the process of lumen formation (Fig. 9A). This phenotype specialization is transient and reversible, depending on the balance between pro-angiogenic factors, such as VEGF and Jagged-1 (JAG-1), and suppressors of endothelial proliferation such as delta-like ligand 4 (Dll4)-Notch activity [115]. Physiological patterning of sprouting vessels requires a balanced formation of tip and stalk cells, which is finely regulated by Notch signaling. In fact, tip cells increase expression of the Dll4 in response to VEGF signaling. This activates Notch1 in adjacent cells, instructing them in turn to downregulate VEGFR2 and Dll4 and acquire the stalk phenotype [116]. Once endothelial cells are assembled in tubular structures (morphogenesis phase), pericytes, recruited by PDGF-BB, released by the activated endothelium, associate with the newly formed vessels (maturation phase). Pericytes provide many regulatory signals, such as TGF-β1, Angiopoietin 1 (Ang1) and EphrinB2, leading to endothelial quiescence and new vessel survival independently of further angiogenic stimulation (stabilization phase) [98] (Fig. 9C).

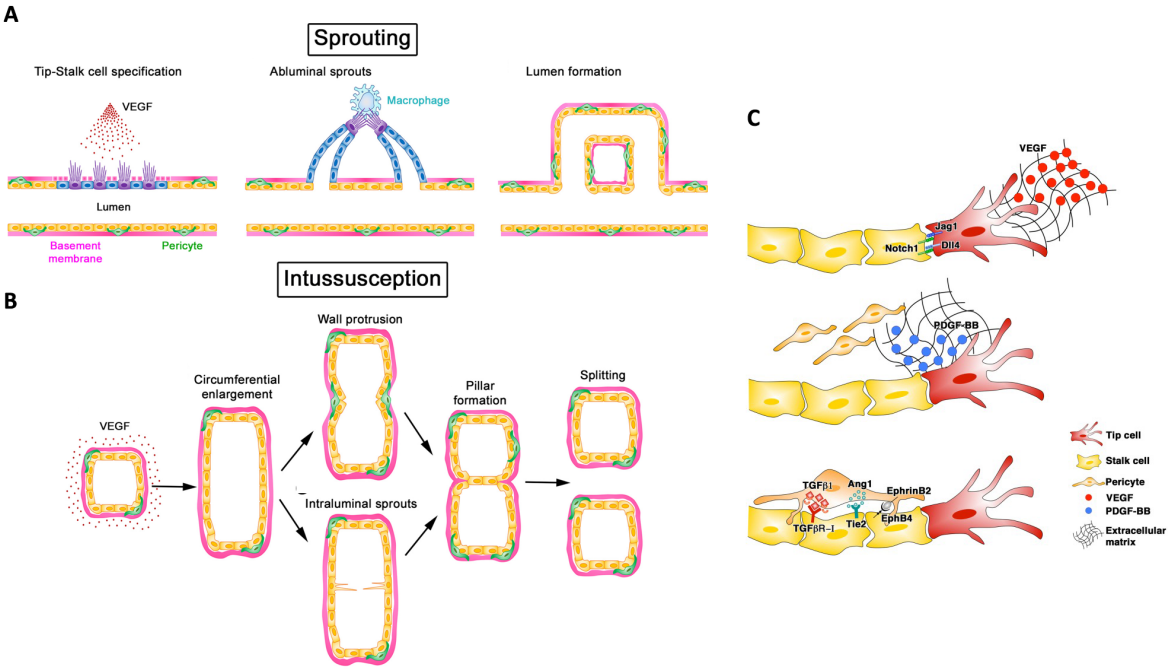

Figure 9. *(A, C) Sprouting and (B) Intussusception: two alternative ways of angiogenesis. (A,C) Sprouting angiogenesis implies the functional specification of endothelial tip cells , which migrate towards the VEGF*

gradient source, and stalk cells , which proliferate behind the tip, forming ab-luminal sprouts that fuse together and generate new vessels. (B) In the absence of a gradient, all endothelial cells respond to VEGF by assuming a stalk phenotype without tip cells. The subsequent proliferation without migration leads to circumferential enlargement of vessels without sprouting followed by formation of intra-luminal endothelial pillars which fuse together and cause longitudinal splitting into two new vessels. Adapted from [117](A,B) and [98](C).

In contrast, in intussusception morphogenic events take place inside the lumen rather than towards the ab-luminal side of vessels. Trans-luminal tissue pillars form either through a zone of contact between the endothelial cells of opposite capillary walls, with subsequent reorganization of the endothelial junctions and invasion of the pillar core by myofibroblasts, or through the extension and fusion of intraluminal protrusions exclusively made of endothelial cells (intraluminal sprouting). Subsequently, transluminal tissue pillars align along the length of the preexisting vessel, progressively fuse together and divide the affected vascular segment longitudinally into new, individual vascular structures (Fig. 9B). It is not completely clear what determines whether VEGF induces sprouting or splitting angiogenesis. However, recent reports showed that VEGF over-expression, at the doses required to induce functional benefit and to restore tissue perfusion after ischemia in the therapeutic target tissue of skeletal muscle, induces angiogenesis intussusception rather than sprouting [118]. Therapeutic doses of VEGF may saturate the very limited amount of extracellular matrix between muscle fibers, and the lack of a concentration gradient may cause endothelium to acquire an all-stalk phenotype, leading to proliferation without migration and therefore circumferential enlargement rather than sprouting (Gianni-Barrera et al, unpublished data).

3.4 Therapeutic angiogenesis

Therapeutic angiogenesis aims at restoring blood flow to ischemic tissues by the generation of new vessels. This strategy targets the treatment of ischemic diseases, where endogenous tissue itself is insufficiently perfused, and may improve the rapid vascularization of tissue-engineered grafts, where *in vitro*-generated new tissue is transplanted to repair tissue lost through damage or surgery [98]. Blood vessels are critical in developmental, adult physiology and in tissue regeneration since they bring oxygen, nutrients, cells and signals. Without sufficient blood supply, tissues and organs cannot maintain regular activities. On the other hand, induction of neovasculature provides a potential strategy to treat many ischemic illnesses, especially cardiovascular diseases, including coronary and peripheral arterial diseases. Therapeutic angiogenesis has also been suggested for management of fracture healing in acute injuries, non-unions, and distraction osteogenesis. Various growth factors in the angiogenic cascade, including VEGF, FGF, and PDGF, are potential targets for upregulation and direct administration [119]. Additionally, other suggested therapies to improve angiogenesis include enhancement of HIF signaling, blockade of angiogenesis inhibitors, delivery of endothelial progenitor cells and others. Therapeutic options and strategies to improve bone regeneration and vascularization in bone grafts are addressed in paragraph 7.

4. Coupling of angiogenesis and osteogenesis

Bone regeneration entails a complex series of biological events, with the interplay of different cell types and the orchestration of several intracellular and extracellular signaling pathways. Bone health requires vascular control since blood vessels are key regulators for bone homeostasis, both providing nutrients and minerals and serving as structural templates for bone development [119]. In the bone marrow, the vasculature also provides a niche environment for HSCs regulating their quiescence and mobilization. HSCs and progenitors have been found in the proximity of small arterioles and specialized sinusoids [49], where different cell types, including endothelial cells, pericytes, stromal progenitors and sympathetic neuronal cells, contribute to the maintenance of HSCs self-renewal. In addition to these well-known functions, blood vessels have been recently ascribed a so-called angiocrine function [120], providing paracrine signals that coordinate growth, differentiation, and regeneration of different tissues, including bone, where they can promote osteogenesis [121]. Therefore, angiogenesis and vascular cells can affect biological processes in the bone/marrow organ at several different levels [122]. Osteogenesis and angiogenesis are intimately coupled. The coupling consists of a complex molecular cross-talk among cells involved in both processes. Importantly, such angiocrine functions of the endothelium are not confined to a few specialized settings but appear to represent a fundamental principle controlling many aspects of developmental and regenerative tissue growth.

4.1 Bone vascular architecture

As in other organs, vasculature in bone shows a typical hierarchical organization. Typical long bones, such as the femur and tibia, are supplied by several arteries and arterioles, which are classified based on their region of blood supply. The central artery, also called nutrient

artery, enters bone through a foramen and branches into a number of smaller arteries and arterioles to supply maximum regions of adult bone. It sustains high blood pressure to reach distant locations, usually terminating into capillaries present in the metaphysis and endosteum. There is a central large vein that receives blood from capillaries present in various regions and drains deoxygenated blood and nutrient waste from bone. Periosteal arteries supply the outer surface of bone and are connected to Haversian arteries present in the cortical region through Volkmann's arteries. Haversian arteries run parallel to the longitudinal axis of the long bone in the cortex while shorter Volkmann's arteries run perpendicularly to the long bone axis. Haversian arteries eventually converge into metaphyseal capillaries to deliver blood into the medullary region. In contrast, blood supply from epiphyseal arteries does not have a route to enter the medullary region of long bones, thus maintaining a separate blood circulation in the epiphysis region. Epiphyseal arteries enter the bone from a heavy network of periarticular vascular plexus present near the ends of long bones. The veins draining the epiphyseal blood are relatively smaller compared to the vein present in the medullary region [123].

Bone vasculature is mainly formed by angiogenesis. During endochondral bone formation of murine long bones blood vessels start to invade the cartilage template at embryonic day (E) 13.5 to 14.5, and vascular growth is largely completed in adolescent and young adult animals [124]. Hypertrophic chondrocyte, located in the future primary ossification center, secrete pro-angiogenic factors that stimulate angiogenesis; recruited osteoprogenitors are also a source of pro-angiogenic factors. Later on, blood vessels invade the hypertrophic template and form an initial vascular network, which is accompanied by ossification processes. The release of signals by maturing and hypertrophic growth plate chondrocytes at the two ends of the developing long bone further promotes vessel growth and ossification

along the longitudinal axis, which leads to the extension of the growing skeletal element. This also involves the formation of distinguishable metaphyseal and diaphyseal capillary networks [125]. Later in development, vessels invade the epiphyseal chondrocytes at the two distal ends of the long bone and thereby initiate secondary ossification center formation [39]. Bones formed by intramembranous ossification are also highly vascularized and vascularization occurs in a similar fashion to that seen during endochondral angiogenesis, which suggests that similar molecular mechanisms are involved [126].

Based on marker expression and functional characteristics, two subtypes of bone capillaries can be distinguished in long bones: H and L [125]. Type H capillaries express high levels of CD31 (or PECAM1) and the sialoglycoprotein endomucin (EMCN) ($CD31^{hi}$ $EMCN^{hi}$). They are found in the metaphysis in close proximity of the avascular growth plate, and they are organized as vessel columns that are interconnected at their distal end in proximity to the growth plate (Fig. 10B). These vessels, as well as the endosteal type H capillaries that are proximal to compact bone, are closely associated with perivascular osterix (or SP7) expressing osteoprogenitor cells (Fig. 10C). By contrast, type L vessels express lower levels of CD31 and EMCN ($CD31^{lo}$ $EMCN^{lo}$) and they form the dense, highly branched capillary network in the bone marrow cavity of the diaphysis (Fig. 10C). Sinusoidal type L capillaries, which are surrounded by densely packed hematopoietic cells, connect to the large central vein. Interestingly, arteries and distal arterioles do not deliver blood directly into type L sinusoidal capillaries, but instead arteries exclusively connect to type H vessels in the metaphysis and endosteum (Fig. 10B) [125]. Blood flows through arteries into type H capillaries, enters the type L sinusoidal network at the interface between the metaphysis and diaphysis, and is finally drained into the large central vein. As a consequence, distinct metabolic environments can

be detected in postnatal long bone: the diaphysis is highly hypoxic due to the lack of direct arterial supply, whereas the metaphysis is comparably more and well oxygenated [125, 127].

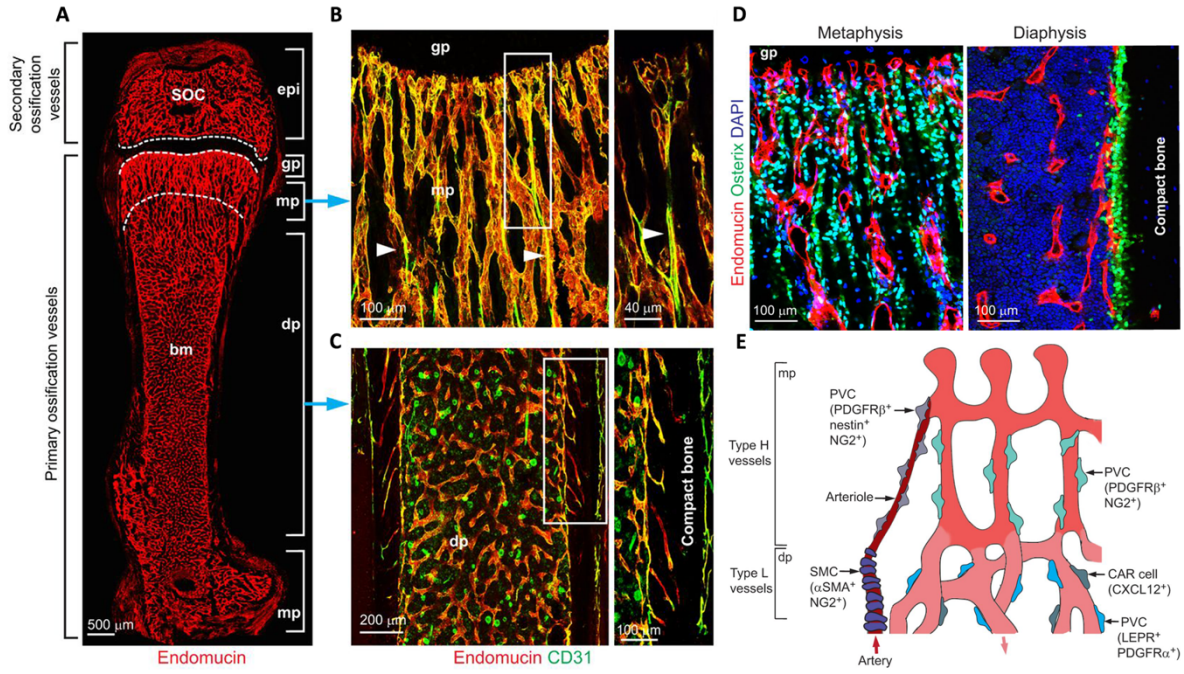

Figure 10. *Architecture of the long bone vasculature. (A) Confocal image of endomucin (EMCN, in red)-immunostained endothelium in a 100 µm thick section of P21 murine femur; (B) In the metaphysis, type H vessels (CD31^{hi}EMCN^{hi}) exhibit a columnar organization and arterial connections (arrowheads); (C) In the diaphysis, highly branched sinuoidal type L capillaries (CD31^{lo}EMCN^{lo}) are found; these connect to endosteal type H vessels in the proximity of compact bone; (D) Osterix-positive osteoprogenitors (marked by green nuclear staining) associate with type H capillaries found in the metaphysis (left panel) and with endosteal type H vessels found in the proximity of compact bone in the diaphysis (right panel) but not with diaphyseal type L vessels found in the bone marrow cavity (right panel), gp =growth plate; (E) Perivascular cells associated with blood vessels in the bone. Larger arteries within bone are covered by smooth muscle cells (SMCs) that are αSMA^{+}NG2^{+}. Distal arterioles, which connect to type H capillaries, are surrounded by perivascular cells (PVCs) expressing nestin, PDGFRβ^{+} and NG2. PDGFRβ^{+}NG2^{+} PVCs are also found around type H vessel columns. By contrast, two types of PVCs LEPR^{+} PDGFRα^{+} mesenchymal cells and CXCL12-abundant reticular (CAR) cells are found on sinusoidal type L vessels. Red arrows indicate the direction of blood flow. Adapted from [39].*

Type H vessels, in mice, are mostly present during development and they gradually disappear during the first 4 weeks of age [128]. It has been recently shown that at E16.5 during development, type H cells are rare and another separate subset of endothelial cells is

mainly present. This endothelial subpopulation, named type E, is also characterized by high expression of CD31 and EMCN, but rapidly declined postnatally. Characteristic features of type E endothelial cells are their strong association with Osx^+ cells and capacity to promote osteogenesis. Moreover, type E endothelium can give rise to type H endothelium and both subtypes can differentiate into type L and arterial endothelial cells during postnatal development [128].

The bone vasculature is associated with several different kind of perivascular cells (Fig. 10E). Type L vessels are surrounded by leptin receptor (LERPR) positive cells and CXCL12-abundant reticular (CAR) cells, that have important roles in the regulation of hematopoiesis by secreting angiocrine signal such as stem cell factors (SCF), CXCL12 and angiopoietin [129]. LEPR positive cells have been described to have the capability to differentiate into the mesenchymal lineage cells (bone, cartilage, adipocytes) and they express platelet derived growth factor receptor α (PDGFRα) and are negative for the pericyte markers PDGFRβ and neural/glial antigen 2 (NG2) [130]. Arteries are covered by smooth muscle cells positive for alpha smooth muscle active (αSMA), NG2 and Nestin and they can differentiate into different mesenchymal lineages [50]. PDGFRβ and NG2 positive perivascular cells surround H type capillaries and they are regulated by PDGFB secreted from the endothelium [50]. Interestingly, a new population of vessel associated osteoclasts (VAOs) has been found to be closely in contact with type H vessels [131]. To be distinguished from bone-associated osteoclasts (BAOs), VAOs are predominant in early developing bones and are located in close contact with the type H vessels in proximity of the growth plate (Fig. 10A). Surprisingly, the research team found that VAOs are not directly involved in resorbing processes but sustain type H vessels elongation and activity. Instead, H endothelium secrete metalloproteases (Mmp2, Mmp9 and Mmp14) that mediate cartilage resorption [131].

4.2 Role of angiocrine and coupling signals in bone homeostasis

To date, several factors have been described to regulate both blood vessels formation and osteogenesis. Osteoclasts, osteoblasts, chondrocytes secrete factors that induce proliferation of endothelial cells, vessel formation and stabilization, such as PDGF-BB, VEGF, and SLIT3 (Fig. 11).

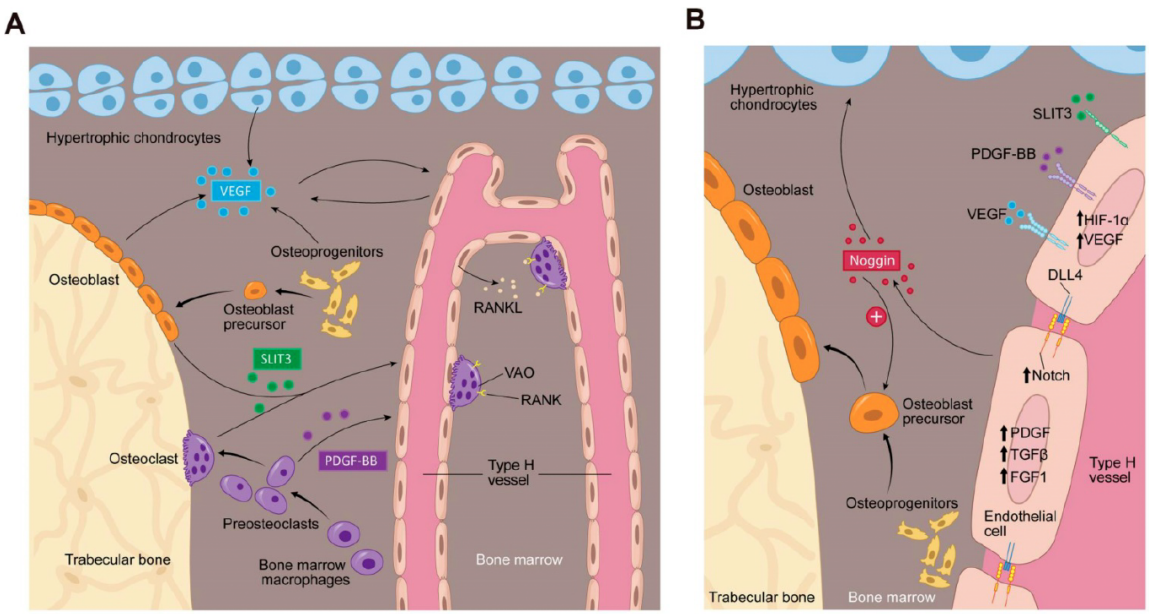

Figure 11. *Bone marrow microenvironment paracrine signaling coupling angiogenesis and osteogenesis. (A) Multiple cells secrete factors into the bone marrow microenvironment to support type H vessel formation. Hypertrophic chondrocytes, osteoblast lineage cells and ECs can secrete VEGF. Mature osteoblasts and osteoclasts secrete SLIT3. Preosteoclasts secrete PDGF-BB. VEGF, SLIT3, and PDGF-BB promote type H vessels formation. Type H ECs express RANKL and support VAOs through a RANKL–RANK signaling mechanism to facilitate cartilage resorption and bone formation. VAOs also promote anastomoses of type H vessels. (B) During hypoxia, type H ECs increase HIF-1α expression, which triggers the expression of genes controlling angiogenesis, such as VEGF. VEGF binds its receptor on ECs to stimulate blood vessel growth. PDGF-BB and SLIT3 also bind to their respective receptors on ECs, which can further enhance EC VEGF expression and promote EC migration, tube formation, and branching. The increase in blood flow can stimulate Notch signaling within the EC. Endothelial Notch/Dll4 signaling stimulates Noggin production. Noggin stimulates differentiation of perivascular osteoprogenitor cells, facilitates chondrocyte hypertrophy maturation, and promotes EC proliferation. Type H ECs express higher levels of PDGFA and PDGFB, TGFβ1, TGFβ3, and FGF1 relative to type L ECs, which are secreted growth factors to promote osteoprogenitor survival and proliferation. Adapted from [132].*

In response, endothelial cells produce factors that modulate bone formation, such as Notch, BMPs, PDGF and VEGF (Fig. 13B) [122].

PDGF-BB is critical in promoting migration, proliferation and differentiation of several mesenchymal cell types, like endothelial progenitors and MSCs. It has been shown that PDGF-BB, in the bone marrow, is mainly produced by immature precursors of resorptive osteoclasts, and promotes the migration and differentiation of MSCs and endothelial progenitors via binding to PDGFRβ [133]. Recently Böhm et al. found that PDGF-PDGFRβ signaling is functionally required to drive the expansion, recruitment, and blood vessels affinity of skeletal progenitor cells (SSPCs) during bone repair [134]. PDGFRβ positive SSPCs are recruited by PDGF released by blood vessels, and they interact via VCAM-1 that binds to VLA-4 (α4β1 integrin) on the endothelium. As a result of the signaling the SSPCs produce more MMP-9, mediating tissue remodeling required for the osteo-angiogenic co-invasion [134].

SLIT3, a well-known axonal guidance molecule, has been recently described to promote formation of type H vessels and bone formation. Genetic deletion of Slit3 in osteoblast lineage cells results in a reduction of type H capillaries, reduced osteoblast activity, bone formation and fracture repair. Additionally, administration of SLIT3 promotes fracture healing and prevents bone loss by augmentation of type H vessel formation [135].

Activation of Notch signaling in bone endothelial cells was found to promote local angiogenesis and osteogenesis. This involves the Notch-controlled secretion of noggin, an antagonist of the BMP pathway, by endothelial cells, which was found to promote the formation of hypertrophic, VEGF-producing chondrocytes in the adjacent growth plate. Endothelial specific Notch loss-of function mutants, mice lacking the Notch ligand DLL4, exhibited reduced angiogenesis, loss of type H vessels and bone formation defects [127].

Therefore, the cross-talk between the endothelium and other cell types ensures the coupling of angiogenesis and bone formation in the skeletal system.

4.3 Coupling of angiogenesis and osteogenesis by VEGF

VEGF is one of the most important regulators of angiogenesis and it is critical for both bone development and regeneration. In these processes VEGF has a dual role, acting both on endothelial cells to promote their migration and proliferation, and stimulating osteogenesis through the regulation of osteogenic growth factors [136]. VEGF is required for endochondral bone formation, where it promotes vessel invasion and recruitment of osteoclasts into hypertrophic cartilage, enabling the replacement of the cartilaginous template by bony callus [85, 137, 138], but also for intramembranous ossification [126, 139-141]. Angiogenesis and osteogenesis are, therefore, intimately connected and they must be tightly coupled for physiological bone function. In fact, alterations in vascular growth can compromise physiological bone healing, e.g., leading to osteonecrosis, osteoporosis, and non-union fractures [142-146]. On the other hand, VEGF has also been described to inhibit osteoblast differentiation and to compete with PDGF-BB for binding to PDGFRs, impairing pericyte function, leading to the formation of immature blood vessels and to the interruption of the coupling of angiogenesis and osteogenesis [147-149]. Moreover, VEGF overexpression may also cause bone resorption due to excessive osteoclast recruitment [111]. These data suggest that VEGF can have opposite effects on osteogenesis under different circumstances, but the underlying mechanisms through which VEGF regulates bone homeostasis are not yet fully understood, posing a challenge to the design of rational therapies to promote angiogenesis.

4.3.1 Roles of VEGF during bone development

VEGF is essential for coupling angiogenesis and osteogenesis during endochondral ossification. In mice, $VEGF_{164}$ and $VEGF_{188}$ are crucial for a proper bone formation, since a complete loss of both isoforms leads to impaired bone vascularization, growth plate morphogenesis and non-physiological endochondral ossification. These effects are caused by an impairment of differentiation and function of hypertrophic chondrocytes, osteoblasts, endothelial cells and osteoclasts [150]. $VEGF_{164}$ activates the PI3K/AKT pathway in osteoblasts and induces stabilization and signal transduction by the main component of the Wnt signaling pathway, β-catenin. Overexpression of $VEGF_{164}$ leads to hypervascularization and excessive osteoblasts differentiation, resulting in bone overgrowth and altered bone morphology [124]. During mesenchymal cell condensation and cartilage template formation, VEGF is critical. Expression of VEGF by mesenchymal cells and chondrocytes occurs in response to increased protein levels of hypoxia-induced factor 1α (HIF-1α) and Sox9 [151]. Later, hypertrophic chondrocytes increase expression of VEGF inducing osteoblast precursor to migrate into the primary ossification center together with blood vessels, osteoclasts and haemopoietic cells [106, 152] (Fig. 12A).

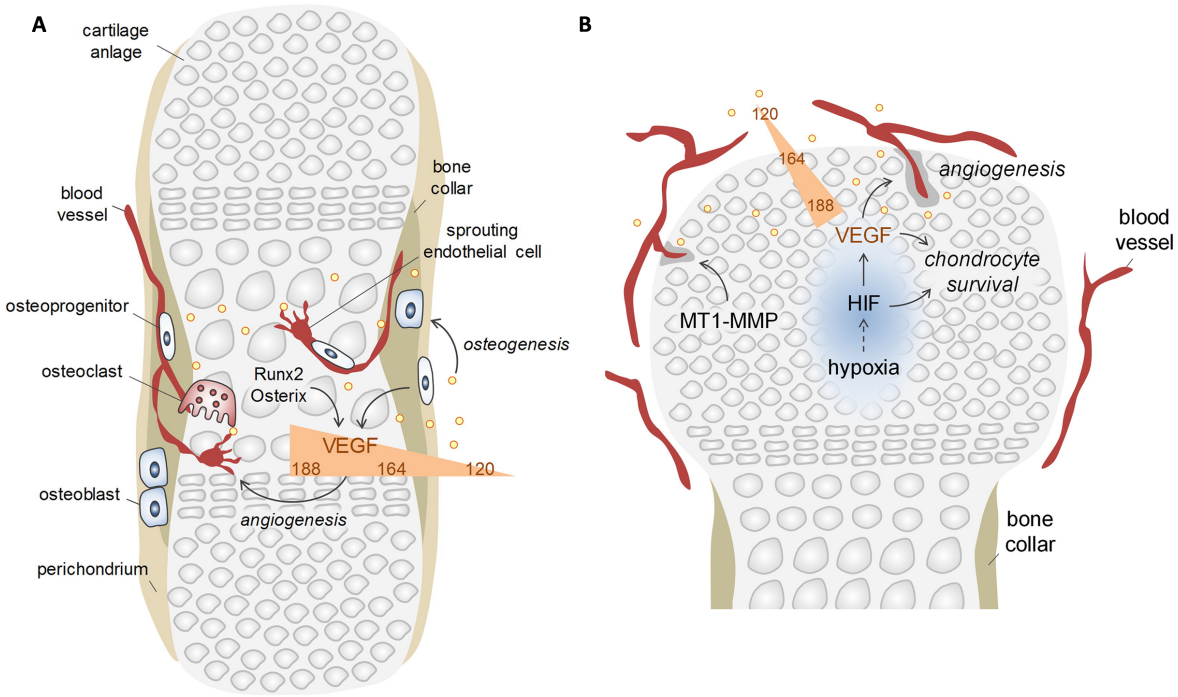

Figure 12. *Angiogenesis and roles of VEGF during bone development. (A) VEGF expression is induced by transcription factor, as Runx2 and Osterix, produced by osteoprogenitors and hypertrophic chondrocytes. The combined secretion of three VEGF isoforms ($VEGF_{120}$, $VEGF_{164}$ and $VEGF_{188}$) results in a VEGF gradient that controls guided sprouting angiogenesis; (B) Hypoxia in the epiphyseal growth plate results in HIF stabilization and VEGF release that triggers vascular ingrowth and chondrocytes survival. MMPs released by blood vessels contribute in cartilage degradation. Adapted from [153].*

The importance of VEGF produced by osteogenic lineage cells has been shown in several different works. Mice with deletion of Vegfa in Col2-expressing cells exhibit a delay in osteoclast and blood vessel invasion into the primary ossification center and cartilage removal [106, 154]. Osterix expressed by osteoblastic precursor cells in the perichondrium and hypertrophic chondrocytes, is essential for osteoblast differentiation and positively regulates VEGF expression by binding to VEGF promoters [155, 156]. Mice with deletion of Vegfa in Osx^{+} osteolineage cells show decreased numbers of blood vessels in perichondrium and impaired differentiation of osteoblast precursors during development of long bones [157]. Hypoxia is a major driver of VEGF expression (Fig. 12B). The protein levels of HIF-1α are greatly elevated under low oxygen stress in osteoblasts, and this promotes transcription of

various angiogenic factors, including VEGF. In mice with HIF-1α deficiency, chondrocyte apoptosis in central epiphyseal regions of developing cartilage is highly increased. Overexpression of VEGF in mice lacking HIF-1α partially rescues chondrocyte apoptosis, suggesting that VEGF is a critical downstream effector of HIF-1α in the support of chondrocyte survival [158]. Not only secreted diffusible VEGF, but also VEGF sequestered in the growth plate matrix contributes to optimal blood vessel growth, as evidenced by the phenotype of mice deficient in matrix metalloproteinase 9 (Mmp9). This enzyme mediates localized proteolytic degradation of the cartilage and bone matrix. Bones from $Mmp9^{-/-}$ mice show decreased metaphyseal vascularization [159], a phenotype that was largely rescued by administration of exogenous VEGF [160] (Fig. 12B).

VEGF has also important roles during intramembranous ossification. VEGF is highly expressed during craniofacial development and cranial neural crest cells-derived VEGF regulates proliferation, vascularization and ossification in membranous bones. Mice lacking $VEGF_{164}$ display multiple craniofacial defects, such as unfused cranial sutures and shorter jaws [161]. Recently, it has been shown that VEGF functions in an autocrine manner in Osx^{+} precursors as it regulates the specification and expansion of mesenchymal cells in the jaw [162].

4.3.2 Roles of VEGF in bone healing and fracture repair

VEGF plays crucial roles during the hematoma formation after trauma and in the subsequent inflammatory phase that initiate bone repair [85]. VEGF concentrations in the hematoma have been reported to increased significantly and to be 15-fold higher than in the plasma. As previously mentioned, hypoxia is one the main driven factor that induces VEGF expression in bone cells. The hypoxia in the hematoma induces VEGF expression and recruits

inflammatory cells to the injury site. VEGF released by cells, bone matrix, platelets and recruited immune cells can bind to the heparin associated with the fibrin clot and be sequestered in the fibrin matrix creating a reservoir. After injury, neutrophils are recruited and contribute removing bone debris and microbial pathogens. VEGF has been reported to induce neutrophil chemotaxis and increase sinusoid permeability in the bone marrow [163]. Release of neutrophils from the bone marrow into the circulation is reduced in mice with specific Vegfa osteoblast deletion, suggesting that osteoblast-derived VEGF facilitates the entry of neutrophils into the circulation in the acute inflammation stage [164]. Following neutrophil infiltration, macrophages and other inflammatory cells are recruited to the injury sites. This results in a release of cytokines, such as Tumor necrosis factor alpha (TNF-α), IL-1α, and IL-1β. These cytokines activate endothelial cells and promote revascularization at the injury sites by inducing VEGF expression in inflammatory and osteoblastic cells. Importantly, VEGF stimulate macrophage/monocytes recruitment during the resolution phase (3-7 days after fracture). Macrophages are responsible for the up-taking of aging and dying neutrophils, they release angiogenic factors, such as VEGF. Uptake of apoptotic neutrophils causes macrophages to change the phenotype from activated M1 to reparative M2 states, and release of mediators, such TGF-β1, suppress the proinflammatory response and initiate the repair process [165]. There is a strong association between the density of macrophages and blood vessels during the inflammation phase of bone repair [164], but what comes first is not entirely clear. In fact, it is likely that angiogenesis and macrophage recruitment are coupled processes. Newly formed blood vessels may recruit macrophages, and these in turn may produce angiogenic factors, including VEGF, to further promote angiogenesis [104].

A specific population of monocytes co-expressing CD11b and NRP1, named neuropilin-expressing monocytes (NEMs), promote smooth muscle cell recruitment and arteriogenesis

by TGF-β1 and PDGF-BB secretion during VEGF-induced angiogenesis [166], and also accelerate vascular stabilization, i.e., the ability of newly induced vessels to persist independently of further VEGF stimulation [167]. It has been recently shown that Sema3A is specifically responsible for NEM recruitment and that VEGF dose dependently inhibits vessel stabilization by impairing both endothelial Sema3A expression and NEM recruitment, leading to decreased TGF-β1 and endothelial SMAD2/3 activation[167]. Given the importance of Sema3A in bone homeostasis [44], these data suggest the possibility Sema3A and NEMs could be important during bone healing and that VEGF might modulate Sema3A expression [122] (Fig 13C).

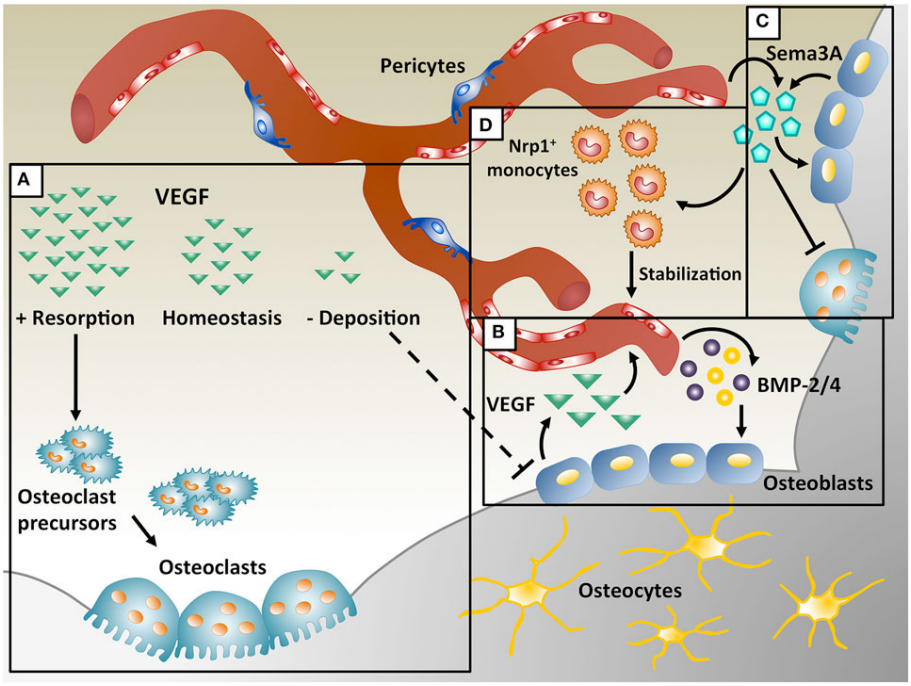

Figure 13. *Coupling of angiogenesis and osteogenesis during intramembranous ossification. (A) Physiological levels of vascular endothelial growth factor (VEGF) maintain bone homeostasis, whereas too little VEGF interrupts osteoblast differentiation and too much VEGF increases osteoclast recruitment, leading to bone resorption. (B) During bone repair, VEGF is produced by osteoblasts and promotes migration and proliferation of endothelial cells. In turn, endothelial cells secrete osteogenic factors, like bone morphogenetic protein (BMP)-2 and BMP-4, which support osteoblast differentiation. (C) VEGF dose dependently regulates Sema3A expression in endothelial cells and Sema3A from different sources suppresses osteoclast differentiation and stimulates bone deposition. (D) Sema3A is also responsible for the recruitment of neuropilin 1-expressing (Nrp1⁺) monocytes (NEM), which promote vessel stabilization. Reproduced from [122]*

Both endochondral and intramembranous ossification occur in bone repair, depending on the stability of the fracture, blood vessel supply, and the location of bone formation. Stable fractures heal primarily by intramembranous ossification, but moderate amounts of cartilage may form in the injured periosteum. Endochondral ossification predominates in unstable fractures and large amounts of cartilage may be formed, facilitated by lack of blood supply [168]. The endochondral ossification repair process recapitulates the stages in developmental endochondral bone formation: cartilage formation, vascular and osteoclast invasion, cartilage resorption and replacement by bone. As during endochondral ossification, VEGF is crucial also in this phase of bone repair. Inhibition of VEGF signaling in skeletal progenitor cells facilitates cartilage formation at the expense of bone formation [71]. Knockdown of Vegf in hypertrophic chondrocytes and osteoblastic precursors causes strong induction of chondrogenesis in the injured periosteum of mice with induced cortical bone defect, consistent with the conclusion that VEGF stimulates differentiation of periosteal progenitor cells to osteoblasts [164]. VEGF induces vessels invasion and osteoclast recruitment to the periosteal callus during the healing of a cortical defect. Inhibition of VEGF signaling, by soluble VEGFR1, delays cartilage turnovers, disrupts conversion of the soft cartilaginous callus to a hard-bony callus, and impairs healing in mice with femoral fractures [140].

The importance of VEGF in recruiting osteoclasts during cartilage remodeling and to the injury sites as been shown in several works [169]. VEGF can substitute for M-CSF in osteoclast recruitment and differentiation [170]. Recently, it has been shown that VEGF recruits osteoclast progenitors in arthritic joints through VEGFR1 and subsequent phosphorylation of focal adhesion kinase [110]. VEGF can also directly stimulate osteoclastic bone resorption and survival of mature osteoclasts via VEGFR2 [171, 172]. Furthermore, VEGF overexpression by genetically modified bone marrow-derived MSC caused excessive osteoclast recruitment and

bone resorption in tissue-engineered osteogenic constructs [111] (Fig. 13A). The potential influence of osteoclast mediated bone resorption should be considered when using VEGF as a therapeutic target to promote bone repair and regeneration.

During intramembranous bone regeneration, exposure to hypoxia in the initial inflammatory phase stimulates osteoblasts to release several factors, including VEGF, via the HIF-1α pathway, inducing endothelial migration and proliferation and vessel permeability [173]. The new vessels increase the supply of nutrients, oxygen and minerals necessary for osteogenesis and may recruit osteoprogenitors to the injury site. Furthermore, endothelial cells also produce osteogenic factors (e.g., BMP-2 and BMP-4) that promote osteoblast differentiation, while differentiating osteoblasts secrete angiogenic factors (e.g., PDGF-BB and VEGF) to further support angiogenesis by a positive feedback loop [157, 162]. Administration of neutralizing antibodies against VEGF receptors to mice, undergoing distraction osteogenesis following a cut across the tibial diaphysis, significantly decreases the amount of blood vessel formation and intramembranous bone formation in the distraction gap [139]. Overexpression of HIF-1α in osteoblasts of the same mice model results in a VEGF-dependent increase in blood vessels and mineralized bone in the distraction gap [141]. In addition to the indirect effects on bone formation by means of stimulation angiogenesis, osteoblast-derived VEGF has been recently described to control transcriptional regulation and cell survival also through intracrine signaling [109, 174]. Osteoblast-specific and conditional VEGF knockout mice exhibited an osteoporosis-like phenotype, with decreased bone mass and increased bone marrow fat [109]. Here VEGF acted as a regulator of stem cell fate: it stimulated osteoblastic and blocked adipogenic differentiation by an intracellular mechanism involving the transcription factors RUNX2 and PPARy2, rather than by paracrine

signaling [18, 109]. However, the precise mechanisms by which intracrine VEGF regulates osteoprogenitor fate are not yet fully understood.

5. Semaphorin 3A family, receptors and signaling

Semaphorin 3A (Sema3A), also known as C-Collapsin-1, H-Sema III, M-SemD, R-Sema III, Sema-Z1a is a membrane-associated secreted protein originally identified as a diffusible axonal chemorepellent that modulates axon guidance and growth in the neurosystem [175-177]. Sema3A is secreted from target tissue, it forms gradients and causes inhibition of axonal outgrowth and cell migration in a concentration-dependent manner. It is fundamental for neural development, indeed $Sema3a^{-/-}$ mice have several neuronal defects in the cerebral cortex, olfactory system and axon projections of dorsal root ganglia neurons [175, 178, 179]. Semaphorins are involved in several other biological processes, including bone biology, angiogenesis, cancer progression, and immune disorders [175, 180-183]. On the other hand, recent studies have shown the importance of Sema3A in the regulation of bone homeostasis. Hayashi et al. showed that Sema3A has an osteoprotective effect by both suppressing osteoclast bone resorption and increasing osteoblastic bone formation, as evidenced by the severe osteopenic phenotype of Sema3A knock-out mice [44, 184].

5.1 Semaphorin family

The semaphorin superfamily contains three protein families: semaphorins, plexins, and the MET and RON receptor tyrosine kinases (RTKs), with central roles in cell signalling. Semaphorins and plexins are present in both vertebrate and invertebrate organisms, whereas MET and RON are vertebrate-specific proteins [185]. The semaphorin family includes 30 proteins divided into 8 classes (Fig. 14). Class 1 and 2 samaphorins are found only

in invertebrates, while class 3-7 can be found only in vertebrates. Among those, class 5 is encoded by viruses. Class 1, 4, 5 and 6 members are type I transmembrane proteins, class 2,3 and 5 members are secreted, and class 7 members are glycosylphosphatidylinositol (GPI) linked. All semaphorins contain a conserved ~400 amino-acid 'Sema' domain. The Sema domain is present as single copy at the N-terminus of Sema proteins and it is essential for signaling. Interestingly, sema domains are also found in plexins and in many receptor tyrosine kinases that are included in the Sema superfamily.

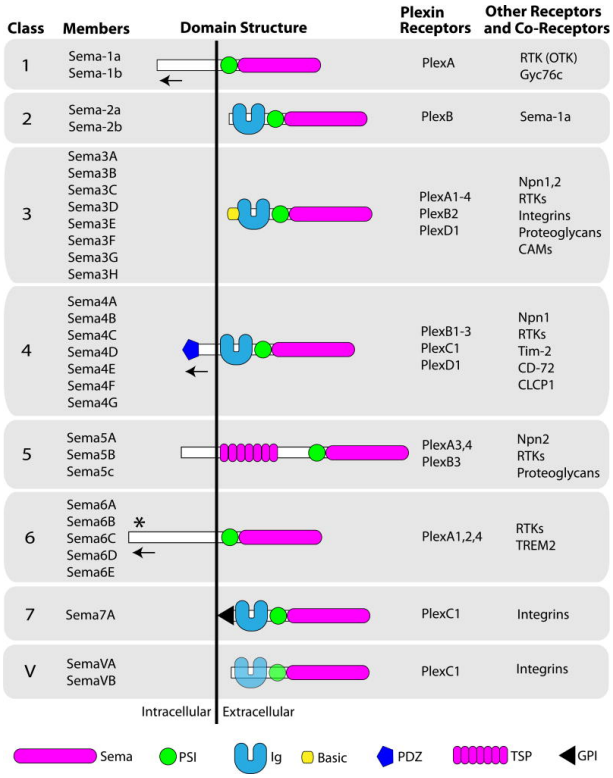

Figure 14. *The semaphorin protein family. Semaphorins are grouped into 8 classes based on their domain structure. All classes of proteins contain a Sema (in pink) domain at N-terminus and it is essential for signalling. Reproduced from* [186]

Consisting with diverse functional studies, different structural studies have indicated that the Sema domain mediates homophilic dimerization, suggesting that dimerization is important for the function of these proteins [185-189].

5.2 Semaphorin receptors

Two group of proteins, neuropilins (NRPs) and plexins, have been identified as the primary semaphorin receptors.

Plexins: most Sema signaling is mediated by plexin receptors and members of all classes of Sema have been shown to interact with plexins. Plexins are canonical semaphorin receptors that have large cytoplasmic domains. In the nervous system, plexin-mediated signals have been shown to exert diverse neural functions by regulating GTPase activities and cytoplasmic/receptor-type protein kinases. These signals are also involved in integrin-mediated attachment [176]. Plexins are grouped into four categories (A-D) based on overall homology. They can function as both ligand-binding receptors and as signaling receptors for semaphorins. Most plexin–semaphorin interactions are mediated through the Sema domains of both proteins, except for class 3 semaphorins, which, with the exception Sema3E, require Neuropilins as essential semaphorin-binding co-receptors to signal through class A plexins [190, 191].

Neuropilins are single-transmembrane-spanning cell-surface glycoproteins that have a large extracellular domain, a single transmembrane domain, and a short cytoplasmic tail. The extracellular domain comprises two N-terminal CUB motifs (domain a1 and a2), two coagulation factor V/VIII homology domains (domain b1 and b2) and a membrane-proximal MAM domain (domain c). Domain b1 is involved in the interaction with VEGF and the basic carboxy terminus of Sema3A [192]. There are two forms of neuropilins, NRP-1 and NRP-2, and they bind to class 3 semaphorins. They have very short intracellular domains that are not required, in some context, for transduction of Sema signaling. Neuropilins work in association

with different signal transducing receptors, including plexins and cell adhesion molecules (CAMs) such as Nr-CAM [193] and L1 CAM [194].

5.3 Semaphorin 3A in bone homeostasis and repair

Sema3A is the first semaphorin identified in vertebrates and acts to induce the retraction and collapse of the structure on axonal growth cone. In 199*6* Behar et al. have shown that Sema3A-deficient mice displayed fusion of cervical bones, partial duplication of ribs, and poor alignment of the rib-sternum junctions, indicating an important role for Sema3A in bone development and bone homeostasis [175]. More recently, different studies have suggested that Sema3A regulates bone resorption and bone deposition synchronously, by suppressing osteoclast differentiation and promoting osteoblastic differentiation [44, 175, 184]. Additionally, Gomez et al. reported that Sema3A expression precede or coincide with the invasion of bone by blood vessels and nerve fibers, not only in the temporal but also at the spatial level. Sema3A and its receptors were identified in the pre-hypertrophic and hypertrophic chondrocytes in ossification centers, around the periosteum, with the onset of endochondral ossification and vascular invasion [195].

5.3.1 Sema3A in osteoclastogenesis

The first indication that Sema3A was involved in osteoclast regulation derives from the observation that Sema3A present in conditioned medium of OPG-deficient mouse calvaria cells could inhibit osteoclast formation *in vitro* and that Sema3A-deficient mice showed a severe osteopenic phenotype, which was caused by a decrease in the osteoblastic bone formation and an increase in osteoclastic bone resorption. Moreover, Hayashi et al. also showed that, mice mutant for Nrp1, which lacked the Sema-binding ability, exhibited a similar

phenotype to Sema3A-deficient mice [44]. Osteoclast precursors express c-Fms (M-CSF receptor) and RANK (RANKL receptor) and they differentiate into osteoclasts in the presence of M-CSF and RANKL, that can be produced by osteoblast and stromal cells [196]. M-CSF can induce the activation of the RhoA and Rac GTPases that are key regulator of osteoclast differentiation and activation. Sema3A has been shown to have repulsive effect on M-CSF induced osteoclast precursor migration and to impair M-CSF induced osteoclast differentiation by inhibiting the activation of RhoA, rather than Rac. Sema3A inhibits RANKL-induced tyrosine phosphorylation of phospholipase Cγ2 (PLCγ2) and calcium oscillation through immune-receptor tyrosine-based activation motif (ITAM) signaling pathway [44]. Osteoclastogenesis induced by RANKL is dependent on the co-stimulatory receptor signaling through ITAMs, including Fc receptor common γ (FcRγ) and DNAX-activating protein (DAP12). RANK and ITAM signaling cooperated to induce NFATc1, which is the transcription of osteoclast-specific genes. FcRγ and DAP12 are associated with osteoclast-associated receptor (OSCAR) and triggering receptor expressed on myeloid cells 2 (TREM2). PlexinA1 promotes osteoclast differentiation by activating the ITAM signal through the formation of the PlexinA1–TREM2–DAP12 complex in response to ligands such as Sema6D. However, Haiyashi et al. showed that NRP1 forms a receptor complex with PlexinA1 in pre-osteoclast once activated by Sema3A. With the increasing expression of NRP1, the amount of PlexinA1 binding to NRP1 increased and PlexinA1 binding to TREM2 decreased. RANKL induced the formation of the PlexinA1-TREM2-DAP12 complex by the downregulation of NRP1, thereby releasing PlexinA1 from the PlexinA1–NRP1 complex. Treatment with Sema3A inhibited RANKL-induced formation of the PlexinA1-TREM2-DAP12 complex by inhibiting NRP1 downregulation and maintaining the PlexinA1-NRP1 complex [44]. As such, the Sema3A-NRP1

axis inhibited the osteoclast differentiation, which separated the PlexinA1 from the PlexinA1-TREM2-DAP12 complex. This further suppressed the ITAM signaling [192]. (Fig 15).

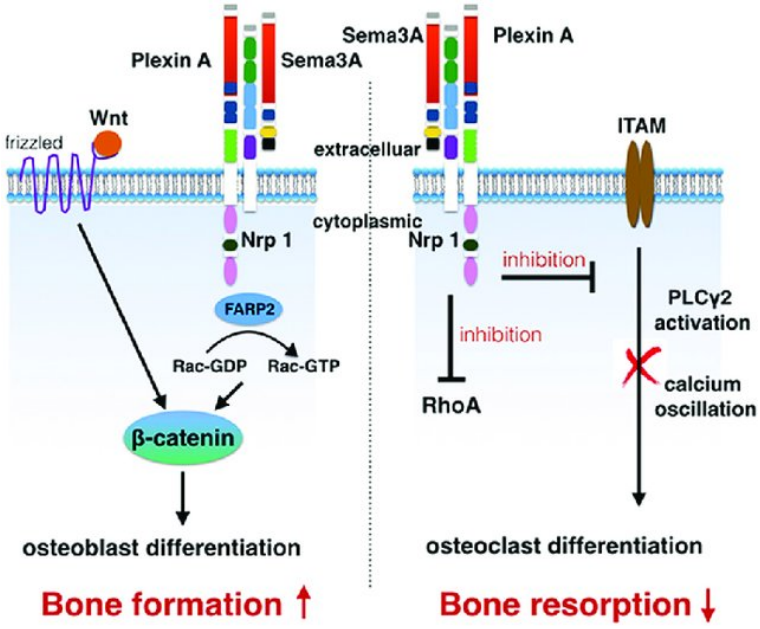

Figure 15. *Sema3A signaling in bone remodeling. Sema3A increases bone mass by the stimulation of osteoblast differentiation and inhibition of osteoclast differentiation. Same3A regulates osteoblasts through Wnt/b-catenin pathway. Sema3A inhibits osteoclast differentiation through the arresting of PLCγ activation and calcium oscillation. Additionally, the inhibition of RhoA suppresses the migration of osteoclast precursors that are bone marrow-derived monocyte/macrophage precursor cells. Reproduced from [192]*

5.3.2 Sema3A in osteoblastogenesis

It has been shown that Sema3A-deficient and Nrp^{Sema-} (mutant with NRP1 lacking Sema binding site) mice display a decreased osteoblast number, a reduced bone forming rate, and an increased adipocyte number. Additionally, calvaria-derived cells isolated from $Sema3a^{-/-}$ and Nrp^{Sema-} mice cultured in osteogenic medium without Sema3A showed a significant decrease in APL activity, bone nodule formation, osteogenic differentiation markers (Runx2, Sp7, Alp and Bglap) and they differentiated toward the adipocyte lineage. Sema3A treatment rescued osteoblast differentiation in $Sema3a^{-/-}$ but not in Nrp^{Sema-} mice. Hayashi et al. concluded that Sema3A activated osteoblast differentiation and inhibited adipocyte

differentiation through NRP1 [44]. The molecular mechanism through which Sema3A modulates osteoblast differentiation it has also been elucidated in the same work, and it involved the canonical Wnt pathway signaling. Canonical Wnt signaling is well-known to regulate the differentiation of osteoblasts and adipocytes. Rac1 activation can promote nuclear accumulation of β-catenin in response to Wnt signaling. Interestingly, in Sema3A deficient calvaria cells, the activation of Rac1 in response to Wnt3a treatment was suppressed and both the mRNA expression of most of the transcriptional targets of β-catenin and the Wnt3a-induced nuclear accumulation of β-catenin were suppressed in Sema3a deficient cells. When cells were treated with Sema3A, instead, nuclear translocation of β-catenin and Rac1 activation were restored. Moreover, Sema3A stimulates the activation of Rac1 through FARP2 [44] (Fig. 15). Recent studies confirmed the involvement of Sema3A in bone homeostasis and Sema3A therapeutic potential has been started to be investigated [197-202]. It has also been reported that Sema3A works as an autocrine factor for neuronal development and neuron-derived Sema3A contributes to normal nervous system development. Neuron-specific Sema3A deficient mice, like $Sema3a^{-/-}$ had a phenotype of a low bone mass, which was due to the decreased bone formation and increased bone resorption. It has been hypothesized that neuronal cell-derived Sema3A regulates bone mass by modifying embryonic sensory innervation and that osteoblast-derived Sema3A plays a less important role [184]. This was mainly based on the observation in mice lacking Sema3A from the neonatal stage, which have a defect in innervation into the bone. However, it has been later proved that Sema3A derived from the mesenchymal cells regulated bone mass in adults in an innervation-independent manner. Indeed, post-natal global deletion of Sema3A resulted in higher bone resorption and lower bone deposition. Moreover, this phenotype was recapitulated in mice in which Sema3A expression was deleted in the limb mesenchyme [198]. In this work, the authors also showed

that, Sema3A deletion in osteoblast lineage cells (Sp7-tTA-tetO-Cre^{+} Sema3a$^{flox/\Delta}$ mice) after 8 weeks of age, resulted in a significant reduction in trabecular bone volume, reduced osteoblast differentiation and enhanced bone resorption.

6. The need for vascularization in bone tissue engineering

Bone tissue engineering (BTE) aims at developing bone substitutes to replace bone tissue losses due several clinical situations, such as trauma, unhealed fractures, osteonecrosis and tumor resection. The capacity for the normal process of fracture healing to repair skeletal defects and restore load-bearing function to the injured bone is often insufficient. In fact, lack of blood supply, infection of the bone or the surrounding tissues and systemic diseases can negatively influence bone healing, resulting in delayed unions or non-unions fractures [203]. Critical-size bone defects do not heal spontaneously and autologous bone transplantation (autograft) is still considered the "gold standard" in clinical treatment [4]. However, autografts are associated with several limitations and disadvantages, such as chronic pain and donor site morbidity, neurovascular injuries, shortage of tissue available and unpredictable biologic behavior upon in vivo implantation [204]. The biologic behavior of a graft includes its ability to integrate with the surrounding bone tissue, resist infection, and tolerate mechanical load. The characteristics of any osseous graft are largely related to the survival of the loaded osteoprogenitors after transplantation. To overcome these issues, BTE combines osteoprogenitors cells, isolated from suitable sources (e.g. BM), with biocompatible scaffolds that mimics the bone ECM, and growth factors to generate osteogenic grafts to replace and heal bone tissue losses. Moreover, to ensure cell survival, the early onset of vascular invasion should be promoted.

The scaffold itself must fulfil primary functions to ensure successful treatment of bone defects. It must provide the correct anatomic geometry to define and maintain the space for tissue regeneration. Importantly, the scaffold must provide temporary mechanical load bearing within the tissue defect and it should enhance the regenerative capability of the chosen factors. After implantation, bone biomaterials modulate the interaction of bone implants with the surrounding cells and tissues. Therefore, the selection of the biomaterials is a key step in the preparation of ideal bone grafts. Ideal materials should be osteoinductive (capable of promoting osteogenic differentiation), osteoconductive (support bone and vascular ingrowth from surrounding native bone) and should promote osteointegration [205]. In addition, bone biomaterials play crucial roles in bone repair by providing the necessary substrate for cell adhesion, proliferation, and differentiation and by modulating cell activity and function. Cells, including stem and progenitor cells, interact with their microenvironment and can sense extracellular signals, which regulate their behavior. Cell adhesion to ECM and biomaterials is mediated by the binding of ligands, such as elastic fibers, collagen, proteoglycans, glycosaminoglycans and adhesive glycoproteins to integrin receptors [206]. As organic materials, biodegradable polymers can act as an ECM for cell attachment, and adhesion is promoted by combining the polymer with ligands. Natural polymers, such as albumin, alginate, amylose/amylopectin, chitosan, collagen, elastin, fibrin, fibronectin, hyaluronic acid, keratin, and silk, are largely used and can promote cell adhesion [207]. Although a variety of well characterized osteoinductive biomaterials have been studied, the precise mechanism through which they promote cell differentiation and bone formation is still unclear [207, 208].

For load-bearing purposes, achieving stiffness and strength equivalent to bone tissue requires minimally porous scaffolds. Conversely, delivery of growth factors requires more

highly connected porous scaffolds to allow cell migration, vascularization and connective tissue formation within scaffolds [82].

However, upon implantation *in vivo*, a major challenge for clinically relevant large-size grafts is the maintenance of cell viability in the core of the scaffold, which critically depends on the rapid invasion by host blood vessels. Vascularization of large bone grafts is one the main problems that held back the clinical translation of engineered bone grafts in the last decades. As discuss previously, the vascular system is crucial to maintain the bone tissue healthy, since it continuously provides oxygen, nutrients, osteoprogenitor cells and angiocrine factors that are necessary for skeletal growth and remodeling. Upon graft implantation, the formation of new blood vessels from pre-existing ones occurs spontaneously in response to inflammation and it is part of the wound-healing process generated by the host as a response to the ischemia-reperfusion injury formed during surgery [209]. The induced vascularization in response to the inflammatory phase is a transient process and new blood vessels regress within a week [210]. In addition to the capillary networks formed during wound healing, neovascularization of the scaffold occurs. However, the slow rate of infiltration of blood vessels into the scaffold makes it an insufficient process to vascularize tissues of clinically relevant size, leading to hypoxia and necrosis in the core. Another problem associated with the lack of vascularization is the removal of degradation products from biodegradable scaffolds. In the absence of a functional vasculature the capacity of the surrounding tissue to eliminate the degradation products derived from the implant material is very low and can trigger inflammatory responses [211]. Physiologically, blood vessels are distributed in within 100-300µm of distance to supply sufficient levels of oxygen and nutrients, as well as to remove metabolic waste [212]. Indeed, when the distance between cells and capillaries increases above this range, the diffusion of nutrients and oxygen

is impaired, and cell viability and proliferation decrease. Insufficient blood circulation in the implanted bone material results in a lack of integration with the host environment, and inner graft necrosis [213]. To date limited success has been achieved in clinical translation of BTE approaches because of these limitations. In particular blood vessels growth and vascular integration must be achieved at multiple levels: larger blood vessels are needed for restoration of blood flow into the site of injury, while smaller microvascular networks are required to provide blood across the entire scaffold volume, sustaining osteogenesis and cell survival until bone function is restored.

7. Strategy to improve vascularization in osteogenic grafts

Several approaches to improve vascularization, through enhanced vasculogenesis and angiogenesis, of the implanted grafts are currently being investigated. The classical vascularization strategies focus on the stimulation of vascular ingrowth into the implanted grafts from the surrounding host tissue by optimizing the material properties of scaffolds, by incorporation of growth factor delivery systems and by endothelial progenitor cells seeding. Hydroxyapatite (HA) and collagen are the main components in natural bone. An ideal scaffold for bone tissue engineering should incorporate the same biological characteristics of these components to help promote vascularized bone formation. Commonly used scaffold materials include bioactive materials with good biocompatibility but poor mechanical properties, such as natural collagen and fibrin gel, and bone cement. In addition, bioactive glass and other artificial materials such as polylactic acid have been investigated as scaffold materials, being degradable but with poor hydrophilicity and histocompatibility [214]. The chemical composition of scaffold materials has been shown to influence the angiogenic process at the implantation site. For example, poly (lactic-co-glycolic acid) (PLGA), HA and

dentin scaffolds induce a slight inflammatory response that results in an increase angiogenic response and a good vascularization of the grafts [215]. Differently, collagen-chitosan-HA hydrogel scaffolds induce severe inflammation that leads to cell death within the surrounding tissue and to a complete lack of vascular ingrowth [215]. Despite extensive research on various materials for the development of bone tissue, a single scaffolding material may not fully meet all the requirements, especially in terms of angiogenesis. Therefore, different combinations of biomaterials might be required for the design of vascularized bone grafts according to the clinical application.

Pre-vascularization of osteogenic grafts, before implantation, is one of the strategies that are extensively investigated in BTE. For example, a two-step *in vivo* pre-vascularization strategy involves the initial implantation of tissue-engineered grafts within well-vascularized sites, such as muscle, for complete vascularization prior to subsequent implantation at the defect site [216]. This approach has the advantage that fully functional blood vessels are formed in the implants without the need of complex cell isolation, seeding and cultivation procedures. This approach allows for instantaneous reperfusion by surgical anastomosis, thereby ensuring its therapeutic efficacy. However, it requires multiple surgeries for transferring the graft from the pre-vascularization to the injury site [217].

Another interesting approach concerns the use of co-culture system with endothelial cells and other cell types to achieve in *vitro* pre-vascularization and generate vascularization within the graft. While endothelial cells cultured alone showed limited potential for vascular growth, studies have shown that their combination with osteoblasts or MSCs as well as with biomolecules involved in osteogenesis enhanced their vascularization capacity [218]. The choice of endothelial cell type is a crucial point for pre-vascularized grafts. Proangiogenic cells, such as endothelial cells, endothelial progenitor cells, and mural cells (pericytes and smooth

muscle cells), are widely used as cell source. Other cell sources including adult stem cells, MSC from adipose tissue and induced pluripotent stem cells are also suggested as suitable sources for this purpose [219]. However, limitations of cell-based pre-vascularization approaches are that these approaches usually need complex and time-consuming cell isolation and cultivation procedures. Besides, their safety and success are highly sensitive to the quality of the cell isolates, the applied seeding strategy, and the number of cells seeded. A promising cell source that might be exploited in tissue engineering is the stromal vascular fraction (SVF) of human adipose tissue. SVF contains heterogeneous cell population, which include multipotent stem cells and progenitor cells, including endothelial cells, adipose derived mesenchymal stem cells (ASCs), pericytes, preadipocytes, and hematopoietic cells. SVF also contains macrophages, which secrete a multitude of vascular growth factors and cytokines. SVF is an interesting source for intraoperative procedures for bone repair [220]. However, compared with bone marrow MSCs, ASCs have been reported to have a lower osteogenic potency. Consequently, additional processing steps are required to promote osteogenic differentiation [221].

Recently, bioprinting has emerged as powerful new tool to develop tissue constructs with precise size, shape and characteristic. For example it has been recently reported that a 3D printed bone constructs implemented in a rat calvaria bone defect, showed newly formed vascularized bone tissue throughout the implants, including the central portion, with no sign of necrosis [222].

Despite the many advances in the previous discussed strategies, one of the most promising and widely investigated approach to improve vascularization in osteogenic grafts is the stimulation of the angiogenic host tissue response by incorporating angiogenic growth-factors. To this end, VEGF, FGF-2, PDGF and angiogenin are the most studied and used.

Growth-factors provide signals that allow progenitors cells to differentiate, migrate and initiate the healing process, moreover, they are also important for the recruitment of inflammatory cells. One of the major challenges for growth factors in clinical use is the development of appropriate delivery systems. Direct injection into the injury sites, systemic injection or local supplementation have been proven to be ineffective and resulted in low availability of growth-factors due to their rapid degradation *in vivo*, instability, short half-life and deactivation by enzymes [223]. To overcome this, delivery of supraphysiologic doses have been investigated, but it resulted in the increase adverse effects. For example, several large-scale studies confirmed a high frequency of adverse effects associated with the clinical use of BMP-2 to treat bone defects. The supraphysiologic dosing requirements have been shown to lead to ectopic bone formation, osteolysis, inflammation, cancer and other severe complications [224]. VEGF, despite promising preclinical data, is also known for adverse effects: delivery of VEGF to adult tissues increases vessel permeability causing severe edema and loss of limbs in animals [225-227]. It was also shown that uncontrolled VEGF expression induces the growth of vascular tumors (hemangiomas) in skeletal muscle [228], myocardium, and other tissues. Physiological VEGF concentrations are tightly controlled and preclinical data also showed a surprisingly narrow therapeutic window for VEGF gene delivery, such that low vector doses are safe but not sufficiently effective to yield a therapeutic benefit, whereas only slightly higher doses rapidly become unsafe [100]. Recent evidences show that VEGF doesn't not have an intrinsically steep dose-response curve in vivo, but rather that the dose delivered must be controlled at the microenvironmental level. Due to the ECM-binding of VEGF, few "hotspots" of excessive VEGF expression can cause toxic effect even in case of a relative low total dose [112]. Therefore, the same total dose of VEGF can have different effects, therapeutic or toxic, depending on whether it is distributed homogeneously in the

tissue or not. Indeed, when the VEGF dose is homogeneously distributed in tissue, a wide range of microenvironmental VEGF doses are capable of inducing exclusively physiological microvascular networks, until a threshold level is reached, above which aberrant angiogenesis is initiated [229]. Moreover, we previously showed the uncontrolled VEGF delivery also cause adverse effects in osteogenic grafts. Indeed, uncontrolled and continuous overexpression of VEGF in BMSC was effective in improving vascularization but caused a global reduction in bone quantity and quality, by strongly increasing osteoclast recruitment into the graft. This suggests that in order to couple angiogenesis and osteogenesis VEGF dose must be tightly controlled [111].

VEGF effects in bone regeneration are not yet fully understood and different in vivo models and delivery platforms have shown different outcomes. First studies showed that treatment of mice with a soluble, neutralizing VEGF receptor decreased angiogenesis, bone formation, and callus mineralization in femoral fractures; on the other hand, treatment with exogenous VEGF enhanced vascularization and ossification in the same model [140]. However, one of the drawbacks with this study, was the supraphysiological doses of VEGF required to induce bone regeneration as high microenvironmental concentrations of VEGF results in the formation of aberrant and leaky vasculature. On the other hand, VEGF has also been described to inhibit osteoblast differentiation and to compete with PDGF-BB for binding to PDGF-Rs, impairing pericyte function, leading to the formation of immature blood vessels and to the interruption of the coupling of angiogenesis and osteogenesis [122]. Interestingly, many reports utilizing VEGF in bone defects showed no difference between scaffolds with and without VEGF, but they showed synergistic effects of VEGF with other proteins, such as BMPs [230].

Current strategies aim at mimicking ECM embedding to reproduce physiological presentation of angiogenic signals within the bone defects. For example, a highly tunable fibrin-based platform has been recently optimized to precisely control the dose and duration of VEGF protein delivery in tissues [231]. In this model growth factors are engineered to contain an octapeptide sequence derived from alpha-2-plasmin inhibitor (NQEQVSPL), which is a substrate for the transglutaminase factor XIIIa and allows the engineered factors to be covalently cross-linked to the fibrin during the polymerization process. Here VEGF could be released only by enzymatic cleavage by invading cells in vivo and optimized delivery ensured normal, stable, and functional angiogenesis over a 500-fold dose range and improved perfusion of ischemic tissues. In a conceptually different strategy, a recombinant fibronectin fragment was engineered to contain the natural binding sites for fibrin, integrins, and growth factors [232]. Delivery of this fragment within a fibrin construct together with BMP-2 and PDGF-BB significantly increased bone healing in a rat calvaria defect at very low and otherwise ineffective doses, thanks to their presentation in the physiological matrix context. Along similar lines, but with a reverse approach, engineering with a short domain of placenta growth factor-2 endowed any growth factor with super affinity for ECM proteins [233]. Such engineering of VEGF, PDGF-BB, and BMP-2 greatly improved both angiogenesis and bone formation in a calvaria defect. Therefore, biomaterials can be more than just carriers and can be engineered to reproduce an ECM-like environment decorated with growth factors, through either covalent or affinity-based interactions, that present physiological signals to endogenous promoters and promote bone healing.

8. References

[1] R. Florencio-Silva, G.R. Sasso, E. Sasso-Cerri, M.J. Simoes, P.S. Cerri, Biology of Bone Tissue: Structure, Function, and Factors That Influence Bone Cells, Biomed Res Int 2015 (2015) 421746.

[2] B. Clarke, Normal bone anatomy and physiology, Clin J Am Soc Nephrol 3 Suppl 3 (2008) S131-9.

[3] M. Unal, A. Creecy, J.S. Nyman, The Role of Matrix Composition in the Mechanical Behavior of Bone, Curr Osteoporos Rep 16(3) (2018) 205-215.

[4] D. Lopes, C. Martins-Cruz, M.B. Oliveira, J.F. Mano, Bone physiology as inspiration for tissue regenerative therapies, Biomaterials 185 (2018) 240-275.

[5] L.J. Raggatt, N.C. Partridge, Cellular and molecular mechanisms of bone remodeling, J Biol Chem 285(33) (2010) 25103-8.

[6] A.D. Kolb, K.M. Bussard, The Bone Extracellular Matrix as an Ideal Milieu for Cancer Cell Metastases, Cancers (Basel) 11(7) (2019).

[7] J.P. Gorski, Biomineralization of bone: a fresh view of the roles of non-collagenous proteins, Front Biosci (Landmark Ed) 16 (2011) 2598-621.

[8] E. Bonucci, Bone mineralization, Front Biosci (Landmark Ed) 17 (2012) 100-28.

[9] A.I. Al-Qtaitat, S.M. Aldalaen, A review of non-collagenous proteins; their role in bone, American Journal of Life Sciences (2014) 351-355.

[10] E. Solheim, Growth factors in bone, Int Orthop 22(6) (1998) 410-6.

[11] T.A. Linkhart, S. Mohan, D.J. Baylink, Growth factors for bone growth and repair: IGF, TGF beta and BMP, Bone 19(1 Suppl) (1996) 1S-12S.

[12] V. Devescovi, E. Leonardi, G. Ciapetti, E. Cenni, Growth factors in bone repair, Chir Organi Mov 92(3) (2008) 161-8.

[13] S. Weiner, H.D. Wagner, THE MATERIAL BONE: Structure-Mechanical Function Relations, Annual Review of Materials Science 28 (1998) 271-298.

[14] S.R. Stock, The Mineral-Collagen Interface in Bone, Calcif Tissue Int 97(3) (2015) 262-80.

[15] A. Rutkovskiy, K.O. Stenslokken, I.J. Vaage, Osteoblast Differentiation at a Glance, Med Sci Monit Basic Res 22 (2016) 95-106.

[16] B. Kaltschmidt, C. Kaltschmidt, D. Widera, Adult craniofacial stem cells: sources and relation to the neural crest, Stem Cell Rev Rep 8(3) (2012) 658-71.

[17] B.K. Hall, T. Miyake, The membranous skeleton: the role of cell condensations in vertebrate skeletogenesis, Anat Embryol (Berl) 186(2) (1992) 107-24.

[18] A.D. Berendsen, B.R. Olsen, Bone development, Bone 80 (2015) 14-18.

[19] L. Yang, K.Y. Tsang, H.C. Tang, D. Chan, K.S. Cheah, Hypertrophic chondrocytes can become osteoblasts and osteocytes in endochondral bone formation, Proc Natl Acad Sci U S A 111(33) (2014) 12097-102.

[20] N. Ono, W. Ono, T. Nagasawa, H.M. Kronenberg, A subset of chondrogenic cells provides early mesenchymal progenitors in growing bones, Nat Cell Biol 16(12) (2014) 1157-67.

[21] F. Descalzi Cancedda, C. Gentili, P. Manduca, R. Cancedda, Hypertrophic chondrocytes undergo further differentiation in culture, J Cell Biol 117(2) (1992) 427-35.

[22] R.S. Tare, J.C. Babister, J. Kanczler, R.O. Oreffo, Skeletal stem cells: phenotype, biology and environmental niches informing tissue regeneration, Mol Cell Endocrinol 288(1-2) (2008) 11-21.

[23] T. Komori, H. Yagi, S. Nomura, A. Yamaguchi, K. Sasaki, K. Deguchi, Y. Shimizu, R.T. Bronson, Y.H. Gao, M. Inada, M. Sato, R. Okamoto, Y. Kitamura, S. Yoshiki, T. Kishimoto, Targeted disruption of Cbfa1 results in a complete lack of bone formation owing to maturational arrest of osteoblasts, Cell 89(5) (1997) 755-64.

[24] T. Komori, Roles of Runx2 in Skeletal Development, Adv Exp Med Biol 962 (2017) 83-93.

[25] N. Dirckx, M. Van Hul, C. Maes, Osteoblast recruitment to sites of bone formation in skeletal development, homeostasis, and regeneration, Birth Defects Res C Embryo Today 99(3) (2013) 170-91.

[26] T.A. Franz-Odendaal, B.K. Hall, P.E. Witten, Buried alive: how osteoblasts become osteocytes, Dev Dyn 235(1) (2006) 176-90.

[27] K. Tanaka-Kamioka, H. Kamioka, H. Ris, S.S. Lim, Osteocyte shape is dependent on actin filaments and osteocyte processes are unique actin-rich projections, J Bone Miner Res 13(10) (1998) 1555-68.

[28] M. Capulli, R. Paone, N. Rucci, Osteoblast and osteocyte: games without frontiers, Arch Biochem Biophys 561 (2014) 3-12.

[29] J.P. Stains, R. Civitelli, Connexins in the skeleton, Semin Cell Dev Biol 50 (2016) 31-9.

[30] M.B. Schaffler, W.Y. Cheung, R. Majeska, O. Kennedy, Osteocytes: master orchestrators of bone, Calcif Tissue Int 94(1) (2014) 5-24.

[31] W.J. Boyle, W.S. Simonet, D.L. Lacey, Osteoclast differentiation and activation, Nature 423(6937) (2003) 337-42.

[32] T. Miyamoto, T. Suda, Differentiation and function of osteoclasts, Keio J Med 52(1) (2003) 1-7.

[33] S.L. Teitelbaum, Bone resorption by osteoclasts, Science 289(5484) (2000) 1504-8.

[34] N. Ono, H.M. Kronenberg, Bone repair and stem cells, Curr Opin Genet Dev 40 (2016) 103-107.

[35] T. Kobayashi, H.M. Kronenberg, Overview of skeletal development, Methods Mol Biol 1130 (2014) 3-12.

[36] V.S. Salazar, L.W. Gamer, V. Rosen, BMP signalling in skeletal development, disease and repair, Nat Rev Endocrinol 12(4) (2016) 203-21.

[37] A. Kawanami, T. Matsushita, Y.Y. Chan, S. Murakami, Mice expressing GFP and CreER in osteochondro progenitor cells in the periosteum, Biochem Biophys Res Commun 386(3) (2009) 477-82.

[38] Y. Yuan, Y. Chai, Regulatory mechanisms of jaw bone and tooth development, Curr Top Dev Biol 133 (2019) 91-118.

[39] K.K. Sivaraj, R.H. Adams, Blood vessel formation and function in bone, Development 143(15) (2016) 2706-15.

[40] B.K. Hall, T. Miyake, All for one and one for all: condensations and the initiation of skeletal development, Bioessays 22(2) (2000) 138-47.

[41] S.W. Jin, K.B. Sim, S.D. Kim, Development and Growth of the Normal Cranial Vault : An Embryologic Review, J Korean Neurosurg Soc 59(3) (2016) 192-6.

[42] T. Takarada, R. Nakazato, A. Tsuchikane, K. Fujikawa, T. Iezaki, Y. Yoneda, E. Hinoi, Genetic analysis of Runx2 function during intramembranous ossification, Development 143(2) (2016) 211-8.

[43] T. Negishi-Koga, M. Shinohara, N. Komatsu, H. Bito, T. Kodama, R.H. Friedel, H. Takayanagi, Suppression of bone formation by osteoclastic expression of semaphorin 4D, Nat Med 17(11) (2011) 1473-80.

[44] M. Hayashi, T. Nakashima, M. Taniguchi, T. Kodama, A. Kumanogoh, H. Takayanagi, Osteoprotection by semaphorin 3A, Nature 485(7396) (2012) 69-74.

[45] T. Negishi-Koga, H. Takayanagi, Bone cell communication factors and Semaphorins, Bonekey Rep 1 (2012) 183.

[46] C. Zhao, N. Irie, Y. Takada, K. Shimoda, T. Miyamoto, T. Nishiwaki, T. Suda, K. Matsuo, Bidirectional ephrinB2-EphB4 signaling controls bone homeostasis, Cell Metab 4(2) (2006) 111-21.

[47] T. Bellido, Osteocyte-driven bone remodeling, Calcif Tissue Int 94(1) (2014) 25-34.

[48] M. Acar, K.S. Kocherlakota, M.M. Murphy, J.G. Peyer, H. Oguro, C.N. Inra, C. Jaiyeola, Z. Zhao, K. Luby-Phelps, S.J. Morrison, Deep imaging of bone marrow shows non-dividing stem cells are mainly perisinusoidal, Nature 526(7571) (2015) 126-30.

[49] Y. Kunisaki, I. Bruns, C. Scheiermann, J. Ahmed, S. Pinho, D. Zhang, T. Mizoguchi, Q. Wei, D. Lucas, K. Ito, J.C. Mar, A. Bergman, P.S. Frenette, Arteriolar niches maintain haematopoietic stem cell quiescence, Nature 502(7473) (2013) 637-43.

[50] A.P. Kusumbe, S.K. Ramasamy, T. Itkin, M.A. Mae, U.H. Langen, C. Betsholtz, T. Lapidot, R.H. Adams, Age-dependent modulation of vascular niches for haematopoietic stem cells, Nature 532(7599) (2016) 380-4.

[51] K. Szade, G.S. Gulati, C.K.F. Chan, K.S. Kao, M. Miyanishi, K.D. Marjon, R. Sinha, B.M. George, J.Y. Chen, I.L. Weissman, Where Hematopoietic Stem Cells Live: The Bone Marrow Niche, Antioxid Redox Signal 29(2) (2018) 191-204.

[52] S.J. Morrison, D.T. Scadden, The bone marrow niche for haematopoietic stem cells, Nature 505(7483) (2014) 327-34.

[53] P. Bianco, "Mesenchymal" stem cells, Annu Rev Cell Dev Biol 30 (2014) 677-704.

[54] M. Crisan, S. Yap, L. Casteilla, C.W. Chen, M. Corselli, T.S. Park, G. Andriolo, B. Sun, B. Zheng, L. Zhang, C. Norotte, P.N. Teng, J. Traas, R. Schugar, B.M. Deasy, S. Badylak, H.J. Buhring, J.P. Giacobino, L. Lazzari, J. Huard, B. Peault, A perivascular origin for mesenchymal stem cells in multiple human organs, Cell Stem Cell 3(3) (2008) 301-13.

[55] B. Sacchetti, A. Funari, S. Michienzi, S. Di Cesare, S. Piersanti, I. Saggio, E. Tagliafico, S. Ferrari, P.G. Robey, M. Riminucci, P. Bianco, Self-renewing osteoprogenitors in bone marrow sinusoids can organize a hematopoietic microenvironment, Cell 131(2) (2007) 324-36.

[56] P. Bianco, X. Cao, P.S. Frenette, J.J. Mao, P.G. Robey, P.J. Simmons, C.Y. Wang, The meaning, the sense and the significance: translating the science of mesenchymal stem cells into medicine, Nat Med 19(1) (2013) 35-42.

[57] P. Bianco, P.G. Robey, Skeletal stem cells, Development 142(6) (2015) 1023-7.

[58] A.I. Caplan, Mesenchymal stem cells, J Orthop Res 9(5) (1991) 641-50.

[59] M. Tavassoli, W.H. Crosby, Transplantation of marrow to extramedullary sites, Science 161(3836) (1968) 54-6.

[60] A.J. Friedenstein, R.K. Chailakhjan, K.S. Lalykina, The development of fibroblast colonies in monolayer cultures of guinea-pig bone marrow and spleen cells, Cell Tissue Kinet 3(4) (1970) 393-403.

[61] A.J. Friedenstein, A.A. Ivanov-Smolenski, R.K. Chajlakjan, U.F. Gorskaya, A.I. Kuralesova, N.W. Latzinik, U.W. Gerasimow, Origin of bone marrow stromal mechanocytes in radiochimeras and heterotopic transplants, Exp Hematol 6(5) (1978) 440-4.

[62] S. Mendez-Ferrer, T.V. Michurina, F. Ferraro, A.R. Mazloom, B.D. Macarthur, S.A. Lira, D.T. Scadden, A. Ma'ayan, G.N. Enikolopov, P.S. Frenette, Mesenchymal and haematopoietic stem cells form a unique bone marrow niche, Nature 466(7308) (2010) 829-34.

[63] M. Dominici, K. Le Blanc, I. Mueller, I. Slaper-Cortenbach, F. Marini, D. Krause, R. Deans, A. Keating, D. Prockop, E. Horwitz, Minimal criteria for defining multipotent mesenchymal stromal cells. The International Society for Cellular Therapy position statement, Cytotherapy 8(4) (2006) 315-7.

[64] E.M. Horwitz, K. Le Blanc, M. Dominici, I. Mueller, I. Slaper-Cortenbach, F.C. Marini, R.J. Deans, D.S. Krause, A. Keating, T. International Society for Cellular, Clarification of the nomenclature for MSC: The International Society for Cellular Therapy position statement, Cytotherapy 7(5) (2005) 393-5.

[65] A.I. Caplan, D. Correa, The MSC: an injury drugstore, Cell Stem Cell 9(1) (2011) 11-5.

[66] A.I. Caplan, Mesenchymal Stem Cells: Time to Change the Name!, Stem Cells Transl Med 6(6) (2017) 1445-1451.

[67] C.K.F. Chan, G.S. Gulati, R. Sinha, J.V. Tompkins, M. Lopez, A.C. Carter, R.C. Ransom, A. Reinisch, T. Wearda, M. Murphy, R.E. Brewer, L.S. Koepke, O. Marecic, A. Manjunath, E.Y. Seo, T. Leavitt, W.J. Lu, A. Nguyen, S.D. Conley, A. Salhotra, T.H. Ambrosi, M.R. Borrelli, T. Siebel, K. Chan, K. Schallmoser, J. Seita, D. Sahoo, H. Goodnough, J. Bishop, M. Gardner, R. Majeti, D.C. Wan, S. Goodman, I.L. Weissman, H.Y. Chang, M.T. Longaker, Identification of the Human Skeletal Stem Cell, Cell 175(1) (2018) 43-56 e21.

[68] M. Maleki, F. Ghanbarvand, M. Reza Behvarz, M. Ejtemaei, E. Ghadirkhomi, Comparison of mesenchymal stem cell markers in multiple human adult stem cells, Int J Stem Cells 7(2) (2014) 118-26.

[69] B. Sacchetti, A. Funari, C. Remoli, G. Giannicola, G. Kogler, S. Liedtke, G. Cossu, M. Serafini, M. Sampaolesi, E. Tagliafico, E. Tenedini, I. Saggio, P.G. Robey, M. Riminucci, P. Bianco, No Identical "Mesenchymal Stem Cells" at Different Times and Sites: Human Committed Progenitors of Distinct Origin and Differentiation Potential Are Incorporated as Adventitial Cells in Microvessels, Stem Cell Reports 6(6) (2016) 897-913.

[70] A.I. Caplan, All MSCs are pericytes?, Cell Stem Cell 3(3) (2008) 229-30.

[71] C.K. Chan, E.Y. Seo, J.Y. Chen, D. Lo, A. McArdle, R. Sinha, R. Tevlin, J. Seita, J. Vincent-Tompkins, T. Wearda, W.J. Lu, K. Senarath-Yapa, M.T. Chung, O. Marecic, M. Tran, K.S. Yan, R. Upton, G.G. Walmsley, A.S. Lee, D. Sahoo, C.J. Kuo, I.L. Weissman, M.T. Longaker, Identification and specification of the mouse skeletal stem cell, Cell 160(1-2) (2015) 285-98.

[72] T.H. Ambrosi, M.T. Longaker, C.K.F. Chan, A Revised Perspective of Skeletal Stem Cell Biology, Front Cell Dev Biol 7 (2019) 189.

[73] I. Martin, A. Muraglia, G. Campanile, R. Cancedda, R. Quarto, Fibroblast growth factor-2 supports ex vivo expansion and maintenance of osteogenic precursors from human bone marrow, Endocrinology 138(10) (1997) 4456-62.

[74] G. Bianchi, A. Banfi, M. Mastrogiacomo, R. Notaro, L. Luzzatto, R. Cancedda, R. Quarto, Ex vivo enrichment of mesenchymal cell progenitors by fibroblast growth factor 2, Exp Cell Res 287(1) (2003) 98-105.

[75] M.N. Knight, K.D. Hankenson, Mesenchymal Stem Cells in Bone Regeneration, Adv Wound Care (New Rochelle) 2(6) (2013) 306-316.

[76] O. Hayashi, Y. Katsube, M. Hirose, H. Ohgushi, H. Ito, Comparison of osteogenic ability of rat mesenchymal stem cells from bone marrow, periosteum, and adipose tissue, Calcif Tissue Int 82(3) (2008) 238-47.

[77] S.C. Pitchford, R.C. Furze, C.P. Jones, A.M. Wengner, S.M. Rankin, Differential mobilization of subsets of progenitor cells from the bone marrow, Cell Stem Cell 4(1) (2009) 62-72.

[78] T. Kitaori, H. Ito, E.M. Schwarz, R. Tsutsumi, H. Yoshitomi, S. Oishi, M. Nakano, N. Fujii, T. Nagasawa, T. Nakamura, Stromal cell-derived factor 1/CXCR4 signaling is critical for the recruitment of mesenchymal stem cells to the fracture site during skeletal repair in a mouse model, Arthritis Rheum 60(3) (2009) 813-23.

[79] R. Tasso, M. Gaetani, E. Molino, A. Cattaneo, M. Monticone, A. Bachi, R. Cancedda, The role of bFGF on the ability of MSC to activate endogenous regenerative mechanisms in an ectopic bone formation model, Biomaterials 33(7) (2012) 2086-96.

[80] C. Lo Sicco, D. Reverberi, C. Balbi, V. Ulivi, E. Principi, L. Pascucci, P. Becherini, M.C. Bosco, L. Varesio, C. Franzin, M. Pozzobon, R. Cancedda, R. Tasso, Mesenchymal Stem Cell-Derived Extracellular Vesicles as Mediators of Anti-Inflammatory Effects: Endorsement of Macrophage Polarization, Stem Cells Transl Med 6(3) (2017) 1018-1028.

[81] J. Shao, W. Zhang, T. Yang, Using mesenchymal stem cells as a therapy for bone regeneration and repairing, Biol Res 48 (2015) 62.

[82] K. Arvidson, B.M. Abdallah, L.A. Applegate, N. Baldini, E. Cenni, E. Gomez-Barrena, D. Granchi, M. Kassem, Y.T. Konttinen, K. Mustafa, D.P. Pioletti, T. Sillat, A. Finne-Wistrand, Bone regeneration and stem cells, J Cell Mol Med 15(4) (2011) 718-46.

[83] R. Marsell, T.A. Einhorn, The biology of fracture healing, Injury 42(6) (2011) 551-5.

[84] Z. Thompson, T. Miclau, D. Hu, J.A. Helms, A model for intramembranous ossification during fracture healing, J Orthop Res 20(5) (2002) 1091-8.

[85] K. Hu, B.R. Olsen, The roles of vascular endothelial growth factor in bone repair and regeneration, Bone 91 (2016) 30-8.

[86] S. Stegen, N. van Gastel, G. Carmeliet, Bringing new life to damaged bone: the importance of angiogenesis in bone repair and regeneration, Bone 70 (2015) 19-27.

[87] L.C. Gerstenfeld, D.M. Cullinane, G.L. Barnes, D.T. Graves, T.A. Einhorn, Fracture healing as a post-natal developmental process: molecular, spatial, and temporal aspects of its regulation, J Cell Biochem 88(5) (2003) 873-84.

[88] R.C. Riddle, T.L. Clemens, Bone Cell Bioenergetics and Skeletal Energy Homeostasis, Physiol Rev 97(2) (2017) 667-698.

[89] C. Colnot, Skeletal cell fate decisions within periosteum and bone marrow during bone regeneration, J Bone Miner Res 24(2) (2009) 274-82.

[90] N. Ferrara, H.P. Gerber, J. LeCouter, The biology of VEGF and its receptors, Nat Med 9(6) (2003) 669-76.

[91] K. Rauniyar, S.K. Jha, M. Jeltsch, Biology of Vascular Endothelial Growth Factor C in the Morphogenesis of Lymphatic Vessels, Front Bioeng Biotechnol 6 (2018) 7.

[92] T.T. Rissanen, J.E. Markkanen, M. Gruchala, T. Heikura, A. Puranen, M.I. Kettunen, I. Kholova, R.A. Kauppinen, M.G. Achen, S.A. Stacker, K. Alitalo, S. Yla-Herttuala, VEGF-D is the strongest angiogenic and lymphangiogenic effector among VEGFs delivered into skeletal muscle via adenoviruses, Circ Res 92(10) (2003) 1098-106.

[93] M. Bry, R. Kivela, V.M. Leppanen, K. Alitalo, Vascular endothelial growth factor-B in physiology and disease, Physiol Rev 94(3) (2014) 779-94.

[94] M. Shibuya, Vascular Endothelial Growth Factor (VEGF) and Its Receptor (VEGFR) Signaling in Angiogenesis: A Crucial Target for Anti- and Pro-Angiogenic Therapies, Genes Cancer 2(12) (2011) 1097-105.

[95] S. Ogawa, A. Oku, A. Sawano, S. Yamaguchi, Y. Yazaki, M. Shibuya, A novel type of vascular endothelial growth factor, VEGF-E (NZ-7 VEGF), preferentially utilizes KDR/Flk-1 receptor and carries a potent mitotic activity without heparin-binding domain, J Biol Chem 273(47) (1998) 31273-82.

[96] G. Fearnley, G. Smith, M. Harrison, S. Wheatcroft, D. Tomlinson, S. Ponnambalam, Vascular endothelial growth factor-A regulation of blood vessel sprouting in health and disease, OA Biochemistry (2013).

[97] J.E. Park, G.A. Keller, N. Ferrara, The vascular endothelial growth factor (VEGF) isoforms: differential deposition into the subepithelial extracellular matrix and bioactivity of extracellular matrix-bound VEGF, Mol Biol Cell 4(12) (1993) 1317-26.

[98] M.M. Martino, S. Brkic, E. Bovo, M. Burger, D.J. Schaefer, T. Wolff, L. Gurke, P.S. Briquez, H.M. Larsson, R. Gianni-Barrera, J.A. Hubbell, A. Banfi, Extracellular matrix and growth factor engineering for controlled angiogenesis in regenerative medicine, Front Bioeng Biotechnol 3 (2015) 45.

[99] S. Koch, L. Claesson-Welsh, Signal transduction by vascular endothelial growth factor receptors, Cold Spring Harb Perspect Med 2(7) (2012) a006502.

[100] A. Uccelli, T. Wolff, P. Valente, N. Di Maggio, M. Pellegrino, L. Gurke, A. Banfi, R. Gianni-Barrera, Vascular endothelial growth factor biology for regenerative angiogenesis, Swiss Med Wkly 149 (2019) w20011.

[101] M. Simons, E. Gordon, L. Claesson-Welsh, Mechanisms and regulation of endothelial VEGF receptor signalling, Nat Rev Mol Cell Biol 17(10) (2016) 611-25.

[102] S. Koch, S. Tugues, X. Li, L. Gualandi, L. Claesson-Welsh, Signal transduction by vascular endothelial growth factor receptors, Biochem J 437(2) (2011) 169-83.

[103] R.S. Kerbel, Tumor angiogenesis, N Engl J Med 358(19) (2008) 2039-49.

[104] K. Hu, B.R. Olsen, Vascular endothelial growth factor control mechanisms in skeletal growth and repair, Dev Dyn 246(4) (2017) 227-234.

[105] M.M. Deckers, M. Karperien, C. van der Bent, T. Yamashita, S.E. Papapoulos, C.W. Lowik, Expression of vascular endothelial growth factors and their receptors during osteoblast differentiation, Endocrinology 141(5) (2000) 1667-74.

[106] E. Zelzer, W. McLean, Y.S. Ng, N. Fukai, A.M. Reginato, S. Lovejoy, P.A. D'Amore, B.R. Olsen, Skeletal defects in VEGF(120/120) mice reveal multiple roles for VEGF in skeletogenesis, Development 129(8) (2002) 1893-904.

[107] U. Mayr-Wohlfart, J. Waltenberger, H. Hausser, S. Kessler, K.P. Gunther, C. Dehio, W. Puhl, R.E. Brenner, Vascular endothelial growth factor stimulates chemotactic migration of primary human osteoblasts, Bone 30(3) (2002) 472-7.

[108] M.J. Jaasma, W.M. Jackson, R.Y. Tang, T.M. Keaveny, Adaptation of cellular mechanical behavior to mechanical loading for osteoblastic cells, J Biomech 40(9) (2007) 1938-45.

[109] Y. Liu, A.D. Berendsen, S. Jia, S. Lotinun, R. Baron, N. Ferrara, B.R. Olsen, Intracellular VEGF regulates the balance between osteoblast and adipocyte differentiation, J Clin Invest 122(9) (2012) 3101-13.

[110] Y. Matsumoto, K. Tanaka, G. Hirata, M. Hanada, S. Matsuda, T. Shuto, Y. Iwamoto, Possible involvement of the vascular endothelial growth factor-Flt-1-focal adhesion kinase pathway in chemotaxis and the cell proliferation of osteoclast precursor cells in arthritic joints, J Immunol 168(11) (2002) 5824-31.

[111] U. Helmrich, N. Di Maggio, S. Guven, E. Groppa, L. Melly, R.D. Largo, M. Heberer, I. Martin, A. Scherberich, A. Banfi, Osteogenic graft vascularization and bone resorption by VEGF-expressing human mesenchymal progenitors, Biomaterials 34(21) (2013) 5025-35.

[112] A. Banfi, G. von Degenfeld, H.M. Blau, Critical role of microenvironmental factors in angiogenesis, Curr Atheroscler Rep 7(3) (2005) 227-34.

[113] W. De Spiegelaere, C. Casteleyn, W. Van den Broeck, J. Plendl, M. Bahramsoltani, P. Simoens, V. Djonov, P. Cornillie, Intussusceptive angiogenesis: a biologically relevant form of angiogenesis, J Vasc Res 49(5) (2012) 390-404.

[114] R. Gianni-Barrera, M. Bartolomeo, B. Vollmar, V. Djonov, A. Banfi, Split for the cure: VEGF, PDGF-BB and intussusception in therapeutic angiogenesis, Biochem Soc Trans 42(6) (2014) 1637-42.

[115] H.M. Eilken, R.H. Adams, Dynamics of endothelial cell behavior in sprouting angiogenesis, Curr Opin Cell Biol 22(5) (2010) 617-25.

[116] M. Hellstrom, L.K. Phng, J.J. Hofmann, E. Wallgard, L. Coultas, P. Lindblom, J. Alva, A.K. Nilsson, L. Karlsson, N. Gaiano, K. Yoon, J. Rossant, M.L. Iruela-Arispe, M. Kalen, H. Gerhardt, C. Betsholtz, Dll4 signalling through Notch1 regulates formation of tip cells during angiogenesis, Nature 445(7129) (2007) 776-80.

[117] R. Gianni-Barrera, N. Di Maggio, L. Melly, M.G. Burger, E. Mujagic, L. Gurke, D.J. Schaefer, A. Banfi, Therapeutic vascularization in regenerative medicine, Stem Cells Transl Med 9(4) (2020) 433-444.

[118] R. Gianni-Barrera, M. Trani, C. Fontanellaz, M. Heberer, V. Djonov, R. Hlushchuk, A. Banfi, VEGF over-expression in skeletal muscle induces angiogenesis by intussusception rather than sprouting, Angiogenesis 16(1) (2013) 123-36.

[119] K.D. Hankenson, M. Dishowitz, C. Gray, M. Schenker, Angiogenesis in bone regeneration, Injury 42(6) (2011) 556-61.

[120] S. Rafii, J.M. Butler, B.S. Ding, Angiocrine functions of organ-specific endothelial cells, Nature 529(7586) (2016) 316-25.

[121] S.K. Ramasamy, A.P. Kusumbe, T. Itkin, S. Gur-Cohen, T. Lapidot, R.H. Adams, Regulation of Hematopoiesis and Osteogenesis by Blood Vessel-Derived Signals, Annu Rev Cell Dev Biol 32 (2016) 649-675.

[122] A. Grosso, M.G. Burger, A. Lunger, D.J. Schaefer, A. Banfi, N. Di Maggio, It Takes Two to Tango: Coupling of Angiogenesis and Osteogenesis for Bone Regeneration, Front Bioeng Biotechnol 5 (2017) 68.

[123] S.K. Ramasamy, Structure and Functions of Blood Vessels and Vascular Niches in Bone, Stem Cells Int 2017 (2017) 5046953.

[124] C. Maes, S. Goossens, S. Bartunkova, B. Drogat, L. Coenegrachts, I. Stockmans, K. Moermans, O. Nyabi, K. Haigh, M. Naessens, L. Haenebalcke, J.P. Tuckermann, M. Tjwa, P. Carmeliet, V. Mandic, J.P. David, A. Behrens, A. Nagy, G. Carmeliet, J.J. Haigh, Increased skeletal VEGF enhances beta-catenin activity and results in excessively ossified bones, EMBO J 29(2) (2010) 424-41.

[125] A.P. Kusumbe, S.K. Ramasamy, R.H. Adams, Coupling of angiogenesis and osteogenesis by a specific vessel subtype in bone, Nature 507(7492) (2014) 323-328.

[126] C.J. Percival, J.T. Richtsmeier, Angiogenesis and intramembranous osteogenesis, Dev Dyn 242(8) (2013) 909-22.

[127] S.K. Ramasamy, A.P. Kusumbe, L. Wang, R.H. Adams, Endothelial Notch activity promotes angiogenesis and osteogenesis in bone, Nature 507(7492) (2014) 376-380.

[128] U.H. Langen, M.E. Pitulescu, J.M. Kim, R. Enriquez-Gasca, K.K. Sivaraj, A.P. Kusumbe, A. Singh, J. Di Russo, M.G. Bixel, B. Zhou, L. Sorokin, J.M. Vaquerizas, R.H. Adams, Cell-matrix signals specify bone endothelial cells during developmental osteogenesis, Nat Cell Biol 19(3) (2017) 189-201.

[129] A. Mendelson, P.S. Frenette, Hematopoietic stem cell niche maintenance during homeostasis and regeneration, Nat Med 20(8) (2014) 833-46.

[130] B.O. Zhou, R. Yue, M.M. Murphy, J.G. Peyer, S.J. Morrison, Leptin-receptor-expressing mesenchymal stromal cells represent the main source of bone formed by adult bone marrow, Cell Stem Cell 15(2) (2014) 154-68.

[131] S.G. Romeo, K.M. Alawi, J. Rodrigues, A. Singh, A.P. Kusumbe, S.K. Ramasamy, Endothelial proteolytic activity and interaction with non-resorbing osteoclasts mediate bone elongation, Nat Cell Biol 21(4) (2019) 430-441.

[132] Y. Peng, S. Wu, Y. Li, J.L. Crane, Type H blood vessels in bone modeling and remodeling, Theranostics 10(1) (2020) 426-436.

[133] H. Xie, Z. Cui, L. Wang, Z. Xia, Y. Hu, L. Xian, C. Li, L. Xie, J. Crane, M. Wan, G. Zhen, Q. Bian, B. Yu, W. Chang, T. Qiu, M. Pickarski, L.T. Duong, J.J. Windle, X. Luo, E. Liao, X. Cao, PDGF-BB secreted by preosteoclasts induces angiogenesis during coupling with osteogenesis, Nat Med 20(11) (2014) 1270-8.

[134] A.M. Bohm, N. Dirckx, R.J. Tower, N. Peredo, S. Vanuytven, K. Theunis, E. Nefyodova, R. Cardoen, V. Lindner, T. Voet, M. Van Hul, C. Maes, Activation of Skeletal Stem and Progenitor Cells for Bone Regeneration Is Driven by PDGFRbeta Signaling, Dev Cell 51(2) (2019) 236-254 e12.

[135] R. Xu, A. Yallowitz, A. Qin, Z. Wu, D.Y. Shin, J.M. Kim, S. Debnath, G. Ji, M.P. Bostrom, X. Yang, C. Zhang, H. Dong, P. Kermani, S. Lalani, N. Li, Y. Liu, M.G. Poulos, A. Wach, Y. Zhang, K. Inoue, A. Di Lorenzo, B. Zhao, J.M. Butler, J.H. Shim, L.H. Glimcher, M.B. Greenblatt, Targeting skeletal endothelium to ameliorate bone loss, Nat Med 24(6) (2018) 823-833.

[136] E. Schipani, C. Maes, G. Carmeliet, G.L. Semenza, Regulation of osteogenesis-angiogenesis coupling by HIFs and VEGF, J Bone Miner Res 24(8) (2009) 1347-53.

[137] M.F. Carlevaro, S. Cermelli, R. Cancedda, F. Descalzi Cancedda, Vascular endothelial growth factor (VEGF) in cartilage neovascularization and chondrocyte differentiation: auto-paracrine role during endochondral bone formation, J Cell Sci 113 (Pt 1) (2000) 59-69.

[138] H.P. Gerber, T.H. Vu, A.M. Ryan, J. Kowalski, Z. Werb, N. Ferrara, VEGF couples hypertrophic cartilage remodeling, ossification and angiogenesis during endochondral bone formation, Nat Med 5(6) (1999) 623-8.

[139] R.S. Carvalho, T.A. Einhorn, W. Lehmann, C. Edgar, A. Al-Yamani, A. Apazidis, D. Pacicca, T.L. Clemens, L.C. Gerstenfeld, The role of angiogenesis in a murine tibial model of distraction osteogenesis, Bone 34(5) (2004) 849-61.

[140] J. Street, M. Bao, L. deGuzman, S. Bunting, F.V. Peale, Jr., N. Ferrara, H. Steinmetz, J. Hoeffel, J.L. Cleland, A. Daugherty, N. van Bruggen, H.P. Redmond, R.A. Carano, E.H. Filvaroff, Vascular endothelial growth factor stimulates bone repair by promoting angiogenesis and bone turnover, Proc Natl Acad Sci U S A 99(15) (2002) 9656-61.

[141] C. Wan, S.R. Gilbert, Y. Wang, X. Cao, X. Shen, G. Ramaswamy, K.A. Jacobsen, Z.S. Alaql, A.W. Eberhardt, L.C. Gerstenfeld, T.A. Einhorn, L. Deng, T.L. Clemens, Activation of the hypoxia-inducible factor-1alpha pathway accelerates bone regeneration, Proc Natl Acad Sci U S A 105(2) (2008) 686-91.

[142] K. Dickson, S. Katzman, E. Delgado, D. Contreras, Delayed unions and nonunions of open tibial fractures. Correlation with arteriography results, Clin Orthop Relat Res (302) (1994) 189-93.

[143] M. Fassbender, C. Strobel, J.S. Rauhe, C. Bergmann, G. Schmidmaier, B. Wildemann, Local inhibition of angiogenesis results in an atrophic non-union in a rat osteotomy model, Eur Cell Mater 22 (2011) 1-11.

[144] Y. Feng, S.H. Yang, B.J. Xiao, W.H. Xu, S.N. Ye, T. Xia, D. Zheng, X.Z. Liu, Y.F. Liao, Decreased in the number and function of circulation endothelial progenitor cells in patients with avascular necrosis of the femoral head, Bone 46(1) (2010) 32-40.

[145] A.P. Kaushik, A. Das, Q. Cui, Osteonecrosis of the femoral head: An update in year 2012, World J Orthop 3(5) (2012) 49-57.

[146] Q. Zhao, X. Shen, W. Zhang, G. Zhu, J. Qi, L. Deng, Mice with increased angiogenesis and osteogenesis due to conditional activation of HIF pathway in osteoblasts are protected from ovariectomy induced bone loss, Bone 50(3) (2012) 763-70.

[147] J.I. Greenberg, D.J. Shields, S.G. Barillas, L.M. Acevedo, E. Murphy, J. Huang, L. Scheppke, C. Stockmann, R.S. Johnson, N. Angle, D.A. Cheresh, A role for VEGF as a negative regulator of pericyte function and vessel maturation, Nature 456(7223) (2008) 809-13.

[148] B.H. Schonmeyr, M. Soares, T. Avraham, N.W. Clavin, F. Gewalli, B.J. Mehrara, Vascular endothelial growth factor inhibits bone morphogenetic protein 2 expression in rat mesenchymal stem cells, Tissue Eng Part A 16(2) (2010) 653-62.

[149] X. Song, S. Liu, X. Qu, Y. Hu, X. Zhang, T. Wang, F. Wei, BMP2 and VEGF promote angiogenesis but retard terminal differentiation of osteoblasts in bone regeneration by up-regulating Id1, Acta Biochim Biophys Sin (Shanghai) 43(10) (2011) 796-804.

[150] C. Maes, P. Carmeliet, K. Moermans, I. Stockmans, N. Smets, D. Collen, R. Bouillon, G. Carmeliet, Impaired angiogenesis and endochondral bone formation in mice lacking the vascular endothelial growth factor isoforms VEGF164 and VEGF188, Mech Dev 111(1-2) (2002) 61-73.

[151] R. Amarilio, S.V. Viukov, A. Sharir, I. Eshkar-Oren, R.S. Johnson, E. Zelzer, HIF1alpha regulation of Sox9 is necessary to maintain differentiation of hypoxic prechondrogenic cells during early skeletogenesis, Development 134(21) (2007) 3917-28.

[152] C. Maes, T. Kobayashi, M.K. Selig, S. Torrekens, S.I. Roth, S. Mackem, G. Carmeliet, H.M. Kronenberg, Osteoblast precursors, but not mature osteoblasts, move into developing and fractured bones along with invading blood vessels, Dev Cell 19(2) (2010) 329-44.

[153] S. Stegen, G. Carmeliet, The skeletal vascular system - Breathing life into bone tissue, Bone 115 (2018) 50-58.

[154] J.J. Haigh, H.P. Gerber, N. Ferrara, E.F. Wagner, Conditional inactivation of VEGF-A in areas of collagen2a1 expression results in embryonic lethality in the heterozygous state, Development 127(7) (2000) 1445-53.

[155] K. Nakashima, X. Zhou, G. Kunkel, Z. Zhang, J.M. Deng, R.R. Behringer, B. de Crombrugghe, The novel zinc finger-containing transcription factor osterix is required for osteoblast differentiation and bone formation, Cell 108(1) (2002) 17-29.

[156] W. Tang, F. Yang, Y. Li, B. de Crombrugghe, H. Jiao, G. Xiao, C. Zhang, Transcriptional regulation of Vascular Endothelial Growth Factor (VEGF) by osteoblast-specific transcription factor Osterix (Osx) in osteoblasts, J Biol Chem 287(3) (2012) 1671-8.

[157] X. Duan, Y. Murata, Y. Liu, C. Nicolae, B.R. Olsen, A.D. Berendsen, Vegfa regulates perichondrial vascularity and osteoblast differentiation in bone development, Development 142(11) (2015) 1984-91.

[158] C. Maes, E. Araldi, K. Haigh, R. Khatri, R. Van Looveren, A.J. Giaccia, J.J. Haigh, G. Carmeliet, E. Schipani, VEGF-independent cell-autonomous functions of HIF-1alpha regulating oxygen consumption in fetal cartilage are critical for chondrocyte survival, J Bone Miner Res 27(3) (2012) 596-609.

[159] T.H. Vu, J.M. Shipley, G. Bergers, J.E. Berger, J.A. Helms, D. Hanahan, S.D. Shapiro, R.M. Senior, Z. Werb, MMP-9/gelatinase B is a key regulator of growth plate angiogenesis and apoptosis of hypertrophic chondrocytes, Cell 93(3) (1998) 411-22.

[160] N. Ortega, K. Wang, N. Ferrara, Z. Werb, T.H. Vu, Complementary interplay between matrix metalloproteinase-9, vascular endothelial growth factor and osteoclast function drives endochondral bone formation, Dis Model Mech 3(3-4) (2010) 224-35.

[161] I. Stalmans, D. Lambrechts, F. De Smet, S. Jansen, J. Wang, S. Maity, P. Kneer, M. von der Ohe, A. Swillen, C. Maes, M. Gewillig, D.G. Molin, P. Hellings, T. Boetel, M. Haardt, V. Compernolle, M. Dewerchin, S. Plaisance, R. Vlietinck, B. Emanuel, A.C. Gittenberger-de Groot, P. Scambler, B. Morrow, D.A. Driscol, L. Moons, C.V. Esguerra, G. Carmeliet, A. Behn-Krappa, K. Devriendt, D. Collen, S.J. Conway, P. Carmeliet, VEGF: a modifier of the del22q11 (DiGeorge) syndrome?, Nat Med 9(2) (2003) 173-82.

[162] X. Duan, S.R. Bradbury, B.R. Olsen, A.D. Berendsen, VEGF stimulates intramembranous bone formation during craniofacial skeletal development, Matrix Biol 52-54 (2016) 127-140.

[163] M. Ancelin, S. Chollet-Martin, M.A. Herve, C. Legrand, J. El Benna, M. Perrot-Applanat, Vascular endothelial growth factor VEGF189 induces human neutrophil chemotaxis in extravascular tissue via an autocrine amplification mechanism, Lab Invest 84(4) (2004) 502-12.

[164] K. Hu, B.R. Olsen, Osteoblast-derived VEGF regulates osteoblast differentiation and bone formation during bone repair, J Clin Invest 126(2) (2016) 509-26.

[165] S.K. Brancato, J.E. Albina, Wound macrophages as key regulators of repair: origin, phenotype, and function, Am J Pathol 178(1) (2011) 19-25.

[166] S. Zacchigna, L. Pattarini, L. Zentilin, S. Moimas, A. Carrer, M. Sinigaglia, N. Arsic, S. Tafuro, G. Sinagra, M. Giacca, Bone marrow cells recruited through the neuropilin-1 receptor promote arterial formation at the sites of adult neoangiogenesis in mice, J Clin Invest 118(6) (2008) 2062-75.

[167] E. Groppa, S. Brkic, E. Bovo, S. Reginato, V. Sacchi, N. Di Maggio, M.G. Muraro, D. Calabrese, M. Heberer, R. Gianni-Barrera, A. Banfi, VEGF dose regulates vascular stabilization through Semaphorin3A and the Neuropilin-1+ monocyte/TGF-beta1 paracrine axis, EMBO Mol Med 7(10) (2015) 1366-84.

[168] R. Dimitriou, E. Tsiridis, P.V. Giannoudis, Current concepts of molecular aspects of bone healing, Injury 36(12) (2005) 1392-404.

[169] H.B. Kristensen, T.L. Andersen, N. Marcussen, L. Rolighed, J.M. Delaisse, Increased presence of capillaries next to remodeling sites in adult human cancellous bone, J Bone Miner Res 28(3) (2013) 574-85.

[170] S. Niida, M. Kaku, H. Amano, H. Yoshida, H. Kataoka, S. Nishikawa, K. Tanne, N. Maeda, S. Nishikawa, H. Kodama, Vascular endothelial growth factor can substitute for macrophage colony-stimulating factor in the support of osteoclastic bone resorption, J Exp Med 190(2) (1999) 293-8.

[171] M. Nakagawa, T. Kaneda, T. Arakawa, S. Morita, T. Sato, T. Yomada, K. Hanada, M. Kumegawa, Y. Hakeda, Vascular endothelial growth factor (VEGF) directly enhances osteoclastic bone resorption and survival of mature osteoclasts, FEBS Lett 473(2) (2000) 161-4.

[172] Q. Yang, K.P. McHugh, S. Patntirapong, X. Gu, L. Wunderlich, P.V. Hauschka, VEGF enhancement of osteoclast survival and bone resorption involves VEGF receptor-2 signaling and beta3-integrin, Matrix Biol 27(7) (2008) 589-99.

[173] Y. Wang, C. Wan, L. Deng, X. Liu, X. Cao, S.R. Gilbert, M.L. Bouxsein, M.C. Faugere, R.E. Guldberg, L.C. Gerstenfeld, V.H. Haase, R.S. Johnson, E. Schipani, T.L. Clemens, The hypoxia-inducible factor alpha pathway couples angiogenesis to osteogenesis during skeletal development, J Clin Invest 117(6) (2007) 1616-26.

[174] Y. Liu, B.R. Olsen, Distinct VEGF functions during bone development and homeostasis, Arch Immunol Ther Exp (Warsz) 62(5) (2014) 363-8.

[175] O. Behar, J.A. Golden, H. Mashimo, F.J. Schoen, M.C. Fishman, Semaphorin III is needed for normal patterning and growth of nerves, bones and heart, Nature 383(6600) (1996) 525-8.

[176] R.P. Kruger, J. Aurandt, K.L. Guan, Semaphorins command cells to move, Nat Rev Mol Cell Biol 6(10) (2005) 789-800.

[177] R.J. Pasterkamp, A.L. Kolodkin, Semaphorin junction: making tracks toward neural connectivity, Curr Opin Neurobiol 13(1) (2003) 79-89.

[178] F. Nakamura, K. Ugajin, N. Yamashita, T. Okada, Y. Uchida, M. Taniguchi, T. Ohshima, Y. Goshima, Increased proximal bifurcation of CA1 pyramidal apical dendrites in sema3A mutant mice, J Comp Neurol 516(5) (2009) 360-75.

[179] L. Tian, H. Rauvala, C.G. Gahmberg, Neuronal regulation of immune responses in the central nervous system, Trends Immunol 30(2) (2009) 91-9.

[180] B. Chaudhary, Y.S. Khaled, B.J. Ammori, E. Elkord, Neuropilin 1: function and therapeutic potential in cancer, Cancer Immunol Immunother 63(2) (2014) 81-99.

[181] C.C. McKenna, A.F. Ojeda, J. Spurlin, 3rd, S. Kwiatkowski, P.Y. Lwigale, Sema3A maintains corneal avascularity during development by inhibiting Vegf induced angioblast migration, Dev Biol 391(2) (2014) 241-50.

[182] H.Q. Miao, S. Soker, L. Feiner, J.L. Alonso, J.A. Raper, M. Klagsbrun, Neuropilin-1 mediates collapsin-1/semaphorin III inhibition of endothelial cell motility: functional competition of collapsin-1 and vascular endothelial growth factor-165, J Cell Biol 146(1) (1999) 233-42.

[183] L. Roth, E. Koncina, S. Satkauskas, G. Cremel, D. Aunis, D. Bagnard, The many faces of semaphorins: from development to pathology, Cell Mol Life Sci 66(4) (2009) 649-66.

[184] T. Fukuda, S. Takeda, R. Xu, H. Ochi, S. Sunamura, T. Sato, S. Shibata, Y. Yoshida, Z. Gu, A. Kimura, C. Ma, C. Xu, W. Bando, K. Fujita, K. Shinomiya, T. Hirai, Y. Asou, M. Enomoto, H. Okano, A. Okawa, H. Itoh, Sema3A regulates bone-mass accrual through sensory innervations, Nature 497(7450) (2013) 490-3.

[185] E. Gherardi, C.A. Love, R.M. Esnouf, E.Y. Jones, The sema domain, Curr Opin Struct Biol 14(6) (2004) 669-78.

[186] L.T. Alto, J.R. Terman, Semaphorins and their Signaling Mechanisms, Methods Mol Biol 1493 (2017) 1-25.

[187] A. Antipenko, J.P. Himanen, K. van Leyen, V. Nardi-Dei, J. Lesniak, W.A. Barton, K.R. Rajashankar, M. Lu, C. Hoemme, A.W. Puschel, D.B. Nikolov, Structure of the semaphorin-3A receptor binding module, Neuron 39(4) (2003) 589-98.

[188] B.J. Janssen, R.A. Robinson, F. Perez-Branguli, C.H. Bell, K.J. Mitchell, C. Siebold, E.Y. Jones, Structural basis of semaphorin-plexin signalling, Nature 467(7319) (2010) 1118-22.

[189] T. Nogi, N. Yasui, E. Mihara, Y. Matsunaga, M. Noda, N. Yamashita, T. Toyofuku, S. Uchiyama, Y. Goshima, A. Kumanogoh, J. Takagi, Structural basis for semaphorin signalling through the plexin receptor, Nature 467(7319) (2010) 1123-7.

[190] A.L. Kolodkin, D.V. Levengood, E.G. Rowe, Y.T. Tai, R.J. Giger, D.D. Ginty, Neuropilin is a semaphorin III receptor, Cell 90(4) (1997) 753-62.

[191] T. Takahashi, A. Fournier, F. Nakamura, L.H. Wang, Y. Murakami, R.G. Kalb, H. Fujisawa, S.M. Strittmatter, Plexin-neuropilin-1 complexes form functional semaphorin-3A receptors, Cell 99(1) (1999) 59-69.

[192] Z. Li, J. Hao, X. Duan, N. Wu, Z. Zhou, F. Yang, J. Li, Z. Zhao, S. Huang, The Role of Semaphorin 3A in Bone Remodeling, Front Cell Neurosci 11 (2017) 40.

[193] J. Falk, A. Bechara, R. Fiore, H. Nawabi, H. Zhou, C. Hoyo-Becerra, M. Bozon, G. Rougon, M. Grumet, A.W. Puschel, J.R. Sanes, V. Castellani, Dual functional activity of semaphorin 3B is required for positioning the anterior commissure, Neuron 48(1) (2005) 63-75.

[194] V. Castellani, J. Falk, G. Rougon, Semaphorin3A-induced receptor endocytosis during axon guidance responses is mediated by L1 CAM, Mol Cell Neurosci 26(1) (2004) 89-100.

[195] C. Gomez, B. Burt-Pichat, F. Mallein-Gerin, B. Merle, P.D. Delmas, T.M. Skerry, L. Vico, L. Malaval, C. Chenu, Expression of Semaphorin-3A and its receptors in endochondral ossification: potential role in skeletal development and innervation, Dev Dyn 234(2) (2005) 393-403.

[196] T. Yamashita, N. Takahashi, N. Udagawa, New roles of osteoblasts involved in osteoclast differentiation, World J Orthop 3(11) (2012) 175-81.

[197] D. de Ridder, S. Marino, R.T. Bishop, N. Renema, C. Chenu, D. Heymann, A.I. Idris, Bidirectional regulation of bone formation by exogenous and osteosarcoma-derived Sema3A, Sci Rep 8(1) (2018) 6877.

[198] M. Hayashi, T. Nakashima, N. Yoshimura, K. Okamoto, S. Tanaka, H. Takayanagi, Autoregulation of Osteocyte Sema3A Orchestrates Estrogen Action and Counteracts Bone Aging, Cell Metab 29(3) (2019) 627-637 e5.

[199] Y. Li, L. Yang, S. He, J. Hu, The effect of semaphorin 3A on fracture healing in osteoporotic rats, J Orthop Sci 20(6) (2015) 1114-21.

[200] X. Xu, K. Fang, L. Wang, X. Liu, Y. Zhou, Y. Song, Local Application of Semaphorin 3A Combined with Adipose-Derived Stem Cell Sheet and Anorganic Bovine Bone Granules Enhances Bone Regeneration in Type 2 Diabetes Mellitus Rats, Stem Cells Int 2019 (2019) 2506463.

[201] K. Yang, R.J. Miron, Z. Bian, Y.F. Zhang, A bone-targeting drug-delivery system based on Semaphorin 3A gene therapy ameliorates bone loss in osteoporotic ovariectomized mice, Bone 114 (2018) 40-49.

[202] L. Zhang, L. Zheng, C. Li, Z. Wang, S. Li, L. Xu, Sema3a as a Novel Therapeutic Option for High Glucose-Suppressed Osteogenic Differentiation in Diabetic Osteopathy, Front Endocrinol (Lausanne) 10 (2019) 562.

[203] D.S. Elliott, K.J. Newman, D.P. Forward, D.M. Hahn, B. Ollivere, K. Kojima, R. Handley, N.D. Rossiter, J.J. Wixted, R.M. Smith, C.G. Moran, A unified theory of bone healing and nonunion: BHN theory, Bone Joint J 98-B(7) (2016) 884-91.

[204] G.F. Rogers, A.K. Greene, Autogenous bone graft: basic science and clinical implications, J Craniofac Surg 23(1) (2012) 323-7.

[205] M.M. Stevens, Biomaterials for bone tissue engineering, Materials Today 11(5) (2008) 18-25.

[206] H.T. Aiyelabegan, E. Sadroddiny, Fundamentals of protein and cell interactions in biomaterials, Biomed Pharmacother 88 (2017) 956-970.

[207] C. Gao, S. Peng, P. Feng, C. Shuai, Bone biomaterials and interactions with stem cells, Bone Res 5 (2017) 17059.

[208] A.M. Barradas, H. Yuan, C.A. van Blitterswijk, P. Habibovic, Osteoinductive biomaterials: current knowledge of properties, experimental models and biological mechanisms, Eur Cell Mater 21 (2011) 407-29; discussion 429.

[209] O.C. Cassell, S.O. Hofer, W.A. Morrison, K.R. Knight, Vascularisation of tissue-engineered grafts: the regulation of angiogenesis in reconstructive surgery and in disease states, Br J Plast Surg 55(8) (2002) 603-10.

[210] A. Szade, A. Grochot-Przeczek, U. Florczyk, A. Jozkowicz, J. Dulak, Cellular and molecular mechanisms of inflammation-induced angiogenesis, IUBMB Life 67(3) (2015) 145-59.

[211] M.I. Santos, R.L. Reis, Vascularization in bone tissue engineering: physiology, current strategies, major hurdles and future challenges, Macromol Biosci 10(1) (2010) 12-27.

[212] M.W. Laschke, Y. Harder, M. Amon, I. Martin, J. Farhadi, A. Ring, N. Torio-Padron, R. Schramm, M. Rucker, D. Junker, J.M. Haufel, C. Carvalho, M. Heberer, G. Germann, B. Vollmar, M.D. Menger, Angiogenesis in tissue engineering: breathing life into constructed tissue substitutes, Tissue Eng 12(8) (2006) 2093-104.

[213] A.E. Mercado-Pagan, A.M. Stahl, Y. Shanjani, Y. Yang, Vascularization in bone tissue engineering constructs, Ann Biomed Eng 43(3) (2015) 718-29.

[214] S. Yin, W. Zhang, Z. Zhang, X. Jiang, Recent Advances in Scaffold Design and Material for Vascularized Tissue-Engineered Bone Regeneration, Adv Healthc Mater 8(10) (2019) e1801433.

[215] M. Rucker, M.W. Laschke, D. Junker, C. Carvalho, A. Schramm, R. Mulhaupt, N.C. Gellrich, M.D. Menger, Angiogenic and inflammatory response to biodegradable scaffolds in dorsal skinfold chambers of mice, Biomaterials 27(29) (2006) 5027-38.

[216] A. Kaempfen, A. Todorov, S. Guven, R.D. Largo, C. Jaquiery, A. Scherberich, I. Martin, D.J. Schaefer, Engraftment of Prevascularized, Tissue Engineered Constructs in a Novel Rabbit Segmental Bone Defect Model, Int J Mol Sci 16(6) (2015) 12616-30.

[217] M.W. Laschke, M.D. Menger, Vascularization in tissue engineering: angiogenesis versus inosculation, Eur Surg Res 48(2) (2012) 85-92.

[218] Y. Liu, J.K. Chan, S.H. Teoh, Review of vascularised bone tissue-engineering strategies with a focus on co-culture systems, J Tissue Eng Regen Med 9(2) (2015) 85-105.

[219] V. Wu, M.N. Helder, N. Bravenboer, C.M. Ten Bruggenkate, J. Jin, J. Klein-Nulend, E. Schulten, Bone Tissue Regeneration in the Oral and Maxillofacial Region: A Review on the Application of Stem Cells and New Strategies to Improve Vascularization, Stem Cells Int 2019 (2019) 6279721.

[220] A.M. Muller, A. Mehrkens, D.J. Schafer, C. Jaquiery, S. Guven, M. Lehmicke, R. Martinetti, I. Farhadi, M. Jakob, A. Scherberich, I. Martin, Towards an intraoperative engineering of osteogenic and vasculogenic grafts from the stromal vascular fraction of human adipose tissue, Eur Cell Mater 19 (2010) 127-35.

[221] J.B. Mitchell, K. McIntosh, S. Zvonic, S. Garrett, Z.E. Floyd, A. Kloster, Y. Di Halvorsen, R.W. Storms, B. Goh, G. Kilroy, X. Wu, J.M. Gimble, Immunophenotype of human adipose-derived cells: temporal changes in stromal-associated and stem cell-associated markers, Stem Cells 24(2) (2006) 376-85.

[222] H.W. Kang, S.J. Lee, I.K. Ko, C. Kengla, J.J. Yoo, A. Atala, A 3D bioprinting system to produce human-scale tissue constructs with structural integrity, Nat Biotechnol 34(3) (2016) 312-9.

[223] A.C. Mitchell, P.S. Briquez, J.A. Hubbell, J.R. Cochran, Engineering growth factors for regenerative medicine applications, Acta Biomater 30 (2016) 1-12.

[224] A.W. James, G. LaChaud, J. Shen, G. Asatrian, V. Nguyen, X. Zhang, K. Ting, C. Soo, A Review of the Clinical Side Effects of Bone Morphogenetic Protein-2, Tissue Eng Part B Rev 22(4) (2016) 284-97.

[225] D.O. Bates, Vascular endothelial growth factors and vascular permeability, Cardiovasc Res 87(2) (2010) 262-71.

[226] I. Masaki, Y. Yonemitsu, A. Yamashita, S. Sata, M. Tanii, K. Komori, K. Nakagawa, X. Hou, Y. Nagai, M. Hasegawa, K. Sugimachi, K. Sueishi, Angiogenic gene therapy for experimental critical limb ischemia: acceleration of limb loss by overexpression of vascular endothelial growth factor 165 but not of fibroblast growth factor-2, Circ Res 90(9) (2002) 966-73.

[227] S.M. Weis, D.A. Cheresh, Pathophysiological consequences of VEGF-induced vascular permeability, Nature 437(7058) (2005) 497-504.

[228] M.L. Springer, A.S. Chen, P.E. Kraft, M. Bednarski, H.M. Blau, VEGF gene delivery to muscle: potential role for vasculogenesis in adults, Mol Cell 2(5) (1998) 549-58.

[229] C.R. Ozawa, A. Banfi, N.L. Glazer, G. Thurston, M.L. Springer, P.E. Kraft, D.M. McDonald, H.M. Blau, Microenvironmental VEGF concentration, not total dose, determines a threshold between normal and aberrant angiogenesis, J Clin Invest 113(4) (2004) 516-27.

[230] R.E. Geuze, L.F. Theyse, D.H. Kempen, H.A. Hazewinkel, H.Y. Kraak, F.C. Oner, W.J. Dhert, J. Alblas, A differential effect of bone morphogenetic protein-2 and vascular endothelial growth factor release timing on osteogenesis at ectopic and orthotopic sites in a large-animal model, Tissue Eng Part A 18(19-20) (2012) 2052-62.

[231] V. Sacchi, R. Mittermayr, J. Hartinger, M.M. Martino, K.M. Lorentz, S. Wolbank, A. Hofmann, R.A. Largo, J.S. Marschall, E. Groppa, R. Gianni-Barrera, M. Ehrbar, J.A. Hubbell, H. Redl, A. Banfi, Long-lasting fibrin matrices ensure stable and functional angiogenesis by highly tunable, sustained delivery of recombinant VEGF164, Proc Natl Acad Sci U S A 111(19) (2014) 6952-7.

[232] M.M. Martino, F. Tortelli, M. Mochizuki, S. Traub, D. Ben-David, G.A. Kuhn, R. Muller, E. Livne, S.A. Eming, J.A. Hubbell, Engineering the growth factor microenvironment with fibronectin domains to promote wound and bone tissue healing, Sci Transl Med 3(100) (2011) 100ra89.

[233] M.M. Martino, P.S. Briquez, E. Guc, F. Tortelli, W.W. Kilarski, S. Metzger, J.J. Rice, G.A. Kuhn, R. Muller, M.A. Swartz, J.A. Hubbell, Growth factors engineered for super-affinity to the extracellular matrix enhance tissue healing, Science 343(6173) (2014) 885-8.

9. Aims of the thesis

After blood transfusion, bone is the second most transplanted tissue, with over two million bone grafting procedures performed annually worldwide [1]. In fact, non-healing bone fractures and defects are a significant source of patient morbidity and a relevant economic load for the healthcare system of Western countries [2, 3]. Autologous bone transplantation is still the gold standard approach for the treatment of large bone defects. However, the shortage of tissue supply and post-surgery complications, especially donor-site morbidity, highlight the need for new and more effective therapeutic strategies.

Bone tissue engineering is a promising alternative to autologous grafts and it aims at developing bone substitutes based on the combination of tailor-made biomaterials, osteogenic progenitor cells and growth factors to fulfill this as yet unmet medical need. Despite intensive research, the clinical translation of this approach has not been widespread so far. One of the major challenges limiting the clinical success, in particular for large critical-size osteogenic graft, is the rapid and efficient vascularization upon implantation *in vivo*, which is required for tissue integration and engrafting, the maintenance of cell viability and for the robust formation of healthy bone tissue [4]. To add further complexity to the endeavor, the biological processes of osteogenesis and angiogenesis are intimately coupled. In fact, blood vessels do not simply provide metabolic exchange and minerals, but they also serve as structural templates for bone development [5], and even help regulating bone homeostasis and regeneration through angiocrine signaling [6].

The growth factor VEGF is the master regulator of vascular growth both in normal and pathological angiogenesis and therefore its delivery, in combination with suitable biomaterials and osteogenic progenitor cells, is an attractive strategy to generate vascularized

bone grafts. However, the biology of VEGF is complex and the simple addition of the factor to an osteogenic graft does not suffice to achieve a therapeutic benefit, showing the need for careful regulation of its dose and spatio-temporal distribution [7].

For example, we have previously showed that sustained over-expression of VEGF by transduced BMSC can efficiently improve the vascularization of ectopic osteogenic constructs [8] and blood perfusion in critical-size grafts, as well as their mineralization. However, these studies also showed that paradoxically the amount of bone tissue formed by the implanted BMSCs was severely reduced, due to excessive osteoclast recruitment and increased bone resorption [8]. Furthermore, it has been shown that VEGF distribution in tissue needs to be finely controlled both at the spatial and temporal levels in order to ensure functional assembly and persistence of new vascular structures: the physiological interaction of VEGF with extracellular matrix plays a key role in determining these requirements [9].

A better understanding of the molecular crosstalk between VEGF, angiogenesis and osteogenesis is clearly needed. Therefore, the overarching aim of this thesis is to elucidate the role of VEGF in controlling both vascularization and bone formation, in order to provide rational bases for novel, safe and effective therapeutical strategies for the repair of bone tissue and the generation of vascularized osteogenic grafts. To this end, three aspects have been investigated experimentally and the results are presented in the form of three scientific manuscripts:

- In Chapter 2 we addressed the role of duration of exposure to VEGF signaling and the therapeutic potential of transient delivery of recombinant VEGF from factor-decorated fibrin matrices both in an ectopic and in a critical-size orthotopic models of bone formation.
- In Chapter 3 we rigorously investigated the dose-dependent effects of VEGF on osteogenesis and angiogenesis. In particular, we sought to identify a VEGF dosing therapeutic window

that could enable both rapid vascularization and efficient bone formation. We also studied the cellular mechanisms through which VEGF dose regulates bone homeostasis during ossification by human BMSC in osteogenic grafts.

- In Chapter 4 we investigated the molecular mechanisms underlying the coupling of angiogenesis and osteogenesis by VEGF, and in particular the role of Sema3A signaling. In fact, it has been shown that Sema3A regulates both bone resorption and deposition during bone development and repair [10, 11], while we found that VEGF dose-dependently and directly inhibits endothelial Sema3A expression in skeletal muscle [12]. We have also studied the requirement for Sema3A during intramembranous bone formation and its therapeutic potential in coupling angiogenesis and osteogenesis in tissue-engineered bone grafts.

9.1 References

[1] V. Campana, G. Milano, E. Pagano, M. Barba, C. Cicione, G. Salonna, W. Lattanzi, G. Logroscino, Bone substitutes in orthopaedic surgery: from basic science to clinical practice, J Mater Sci Mater Med 25(10) (2014) 2445-61.

[2] H. Lohmann, G. Grass, C. Rangger, G. Mathiak, Economic impact of cancellous bone grafting in trauma surgery, Arch Orthop Trauma Surg 127(5) (2007) 345-8.

[3] K.A. Smith, G.S. Russo, A.R. Vaccaro, P.M. Arnold, Scientific, Clinical, Regulatory, and Economic Aspects of Choosing Bone Graft/Biological Options in Spine Surgery, Neurosurgery 84(4) (2019) 827-835.

[4] O. Scheufler, D.J. Schaefer, C. Jaquiery, A. Braccini, D.J. Wendt, J.A. Gasser, R. Galli, G. Pierer, M. Heberer, I. Martin, Spatial and temporal patterns of bone formation in ectopically pre-fabricated, autologous cell-based engineered bone flaps in rabbits, J Cell Mol Med 12(4) (2008) 1238-49.

[5] K.D. Hankenson, M. Dishowitz, C. Gray, M. Schenker, Angiogenesis in bone regeneration, Injury 42(6) (2011) 556-61.

[6] S.K. Ramasamy, A.P. Kusumbe, T. Itkin, S. Gur-Cohen, T. Lapidot, R.H. Adams, Regulation of Hematopoiesis and Osteogenesis by Blood Vessel-Derived Signals, Annu Rev Cell Dev Biol 32 (2016) 649-675.

[7] A. Grosso, M.G. Burger, A. Lunger, D.J. Schaefer, A. Banfi, N. Di Maggio, It Takes Two to Tango: Coupling of Angiogenesis and Osteogenesis for Bone Regeneration, Front Bioeng Biotechnol 5 (2017) 68.

[8] U. Helmrich, N. Di Maggio, S. Guven, E. Groppa, L. Melly, R.D. Largo, M. Heberer, I. Martin, A. Scherberich, A. Banfi, Osteogenic graft vascularization and bone resorption by VEGF-expressing human mesenchymal progenitors, Biomaterials 34(21) (2013) 5025-35.

[9] R. Gianni-Barrera, N. Di Maggio, L. Melly, M.G. Burger, E. Mujagic, L. Gurke, D.J. Schaefer, A. Banfi, Therapeutic vascularization in regenerative medicine, Stem Cells Transl Med 9(4) (2020) 433-444.

[10] M. Hayashi, T. Nakashima, M. Taniguchi, T. Kodama, A. Kumanogoh, H. Takayanagi, Osteoprotection by semaphorin 3A, Nature 485(7396) (2012) 69-74.

[11] M. Hayashi, T. Nakashima, N. Yoshimura, K. Okamoto, S. Tanaka, H. Takayanagi, Autoregulation of Osteocyte Sema3A Orchestrates Estrogen Action and Counteracts Bone Aging, Cell Metab 29(3) (2019) 627-637 e5.

[12] E. Groppa, S. Brkic, E. Bovo, S. Reginato, V. Sacchi, N. Di Maggio, M.G. Muraro, D. Calabrese, M. Heberer, R. Gianni-Barrera, A. Banfi, VEGF dose regulates vascular stabilization through Semaphorin3A and the Neuropilin-1+ monocyte/TGF-beta1 paracrine axis, EMBO Mol Med 7(10) (2015) 1366-84.

Chapter 2

Robust coupling of angiogenesis and osteogenesis by VEGF-decorated matrices improves critical bone defect healing

Maximilian G. Burger[1,2*], Andrea Grosso[1*], Priscilla S. Briquez[3], Gordian M. E. Born[4], Alexander Lunger[1,2], Flavio Schrenk[1], Atanas Todorov[2,4], Veronica Sacchi[1,5], Jeffrey A. Hubbell[3], Dirk J. Schaefer[1,2], Andrea Banfi[1,2*], Nunzia Di Maggio[1*]

[1]Cell and Gene Therapy, Department of Biomedicine, Basel University Hospital and University of Basel, Basel, Switzerland;

[2] Department of Plastic, Reconstructive, Aesthetic and Hand Surgery, Basel University Hospital, Switzerland;

[3]Pritzker School for Molecular Engineering, University of Chicago, Chicago IL, USA

[4]Tissue Engineering, Department of Biomedicine, Basel University Hospital, Basel, Switzerland;

[5]Present address: Genomic Institute of the Novartis Research Foundation, San Diego, CA, US

**These authors contributed equally*

Introduction

Bone tissue loss due to trauma, surgical resection or degenerative diseases, for which physiological endogenous bone repair is not sufficient, poses a significant clinical need. Autologous bone transplantation (autograft) is the current gold-standard approach used in clinic, but its efficacy is limited by significant issues related to chronic pain at the harvest site, neurovascular injury, structural weakness and the limited amount of autologous bone available [1, 2]. Bone tissue engineering aims at developing bone substitutes, combining osteogenic progenitors and suitable biomaterials, and is an attractive solution to the unmet clinical need of bone replacement.

A major challenge for clinically relevant large-size grafts is the maintenance of cell viability in the core of the scaffold upon implantation *in vivo*, which critically depends on the rapid invasion of the constructs by host blood vessels from the surrounding vascular beds. In fact, a functional vasculature is fundamental to provide oxygen and nutrients, as well as to remove metabolic waste [3, 4], and spontaneous vascular growth is too slow to avoid progenitor death in the central core of the implants. Therefore, under normal conditions bone tissue formation is limited to the outer 1-2 millimeters of osteogenic grafts with clinically relevant size [5].

An attractive strategy to accelerate the vascularization of osteogenic grafts is the stimulation of the endogenous response by supplying specific signals that regulate physiological angiogenesis. Vascular Endothelial Growth Factor (VEGF) is the master regulator of vascular growth both in normal tissue growth and regeneration and in pathological conditions [6]. Therefore, VEGF is the most attractive and well-characterized factor for inducing the therapeutic growth of new blood vessels [7].

For example, we previously showed that sustained VEGF over-expression by genetically modified osteoprogenitors was effective both to increase the vascularization of small-size osteogenic constructs [8], and also to accelerate early blood perfusion and improve progenitor survival, tissue formation and mineralization in clinically relevant large grafts [9]. However, sustained production of VEGF by transduced cells also significantly increased osteoclast recruitment and bone resorption, paradoxically reducing the net efficiency of bone formation [8]. These observations suggest that prolonged exposure to VEGF also has the potential to disrupt bone homeostasis towards excessive resorption, posing a challenge to its clinical application.

Although the biological processes of vascular growth and bone formation are functionally connected, they develop with fundamentally different kinetics. In fact, vascular morphogenesis takes place rapidly within 1 week, followed by functional remodeling of the formed networks, and within 3-4 weeks newly formed vessels are stabilized and persist indefinitely without the need for further VEGF stimulation [10, 11]. On the other hand, new bone tissue in osteogenic grafts starts appearing about 4 weeks after in vivo implantation, fully developing in quantity and quality until 8-12 weeks. Also during development and repair of native bone vascular ingrowth precedes bone matrix deposition [12, 13]. This suggests that, in order to improve vascularization in osteogenic grafts, prolonged VEGF expression, as well as causing adverse effects, might actually be unnecessary.

The duration of therapeutic protein delivery *in vivo* can be precisely controlled by decoration of fibrin matrices with engineered factors [14]. As factors are engineered with an octapeptide sequence derived from alpha-2-plasmin inhibitor (NQEQVSPL), which is a substrate for the transglutaminase factor XIIIa (TG-factors), they can be covalently cross-linked to the fibrin during its polymerization and released only upon enzymatic cleavage. The

rate of release and its duration can then be controlled by tuning the rate of degradation of the hydrogel with different concentrations of the fibrinolysis inhibitor aprotinin, which is also covalently cross-linked into the hydrogel by the TG-hook (TG-aprotinin) [15].

Here we hypothesized that short-term controlled delivery of recombinant TG-VEGF, limited to less than 4 weeks after *in vivo* implantation, may efficiently couple angiogenesis and bone formation in osteogenic grafts, ensuring increased and rapid vascularization and avoiding excessive osteoclast recruitment.

Materials and methods

BMSC isolation and culture

Human primary MSC were isolated from bone marrow aspirates (BMSC). The aspirates were obtained from the iliac crest of 3 healthy donors during routine orthopaedic surgical procedures according to established protocols, after informed consent by the patients and following protocol approval by the local ethical committee (EKBB, Ref. 78/07). Cells were isolated and cultured as previously described [8, 16]. Briefly, after centrifugation the pellet was washed in PBS (Gibco^{TM}, Thermo Fisher Scientific, Waltham, Massachusetts, USA). Cells were resuspended in α-MEM medium (Gibco^{TM}, Thermo Fisher Scientific, Waltham, Massachusetts, USA) supplemented with 10% bovine fetal serum (HyClone, South Logan, Utah, USA), 1mM Sodium Pyruvate (Gibco^{TM}, Thermo Fisher Scientific, Waltham, Massachusetts, USA), 10mM HEPES (Gibco^{TM}, Thermo Fisher Scientific, Waltham, Massachusetts, USA) and 5 ng/mL FGF-2 (R&D System Minneapolis, Minnesota, USA), plated at a density of 10^5 nucleated cells/cm^2 and cultured in 5% CO_2 at 37°C.

Generation of VEGF-expressing BMSC

Primary human BMSC were transduced according to a high-efficiency protocol [17]. Briefly, starting on day 6 after plating, cells were transduced twice a day for a total of 4 rounds with bicistronic retroviral vectors carrying either the gene for mouse $VEGF_{164}$ ($mVEGF_{164}$) linked to a truncated version of mouse CD8a (trCD8a) by an internal ribosomal entry site (IRES) sequence (VICD8), or trCD8a alone as a control (ICD8). For this purpose, BMSC were cultured in 60-mm dishes, incubated with retroviral vector supernatants supplemented with 8 mg/ml polybrene (Sigma Aldrich, St. Louis, Missouri, USA) for 5 min at 37°C. The dishes were then

centrifuged at 1100g for 30 min at room temperature and supernatants were replaced with fresh medium. All experiments were performed with freshly prepared viral supernatants.

Assessment of transduction efficiency

Transduction efficiency was assessed by flow cytometry staining of transduced BMSC with an antibody against mouse CD8a (clone 53-6.7; BD Pharmingen, San Jose, California, USA) at 1:20. Data were acquired with a FACSCalibur flow cytometer (BD Biosciences, San Jose, California, USA) and analysed using FlowJo™ software (FlowJo LLC, Ashland, Oregon, USA).

mVEGF$_{164}$ ELISA measurements

mVEGF$_{164}$ production by VEGF-expressing VICD8 cells was quantified in cell culture supernatants using a Quantikine mouse VEGF immunoassay ELISA kit (R&D Systems Europe, Abingdon, UK). 1 ml of medium was harvested from VICD8 cells in one 60-mm dish, following a 4h incubation at 37°C, filtered and analysed in duplicate. Results were normalized by the number of cells in the dish and time of exposure to medium. Two dishes of cells were assayed per donor (3 independent donors, n = 6).

Recombinant α2PI1–8-VEGF164 production and purification

The cDNA for mouse VEGF-A$_{164}$ was amplified by PCR using primers designed to allow for fusion of the transglutaminase substrate sequence NQEQVSPL, comprising the 8 N-terminal residues of α2-plasmin inhibitor (α2PI$_{1–8}$), onto the N-terminus of the amplified cDNA before insertion into the expression vector pRSET (Invitrogen, Carlsbad, California, USA). The fusion protein was expressed in Escherichia coli strain BL21 (Dϵ3) pLys (Novagen, Merck, Darmstadt, Germany). The recombinant α_2PI$_{1–8}$-VEGF-A$_{164}$ was isolated from inclusion bodies, processed, and refolded using a slightly modified version of a previously published protocol [18]. Briefly, the inclusion bodies were collected from the bacterial lysate by centrifuging, washed with

Triton X114 to remove membrane proteins and endotoxins, and extracted with urea buffer overnight at 4°C under magnetic stirring. Further dimerization of α_2PI_{1-8}-VEGF-A_{164} was done with a redox system (0.5 mM oxidized glutathione, 5 mM reduced glutathione) added into the protein solution after the 2 M urea dialysis, and α_2PI_{1-8}-VEGF-A_{164} was dimerized under stirring for 48 h at 4°C. Then, glutathione and urea were removed by three sequential dialyses of 24 h against Tris buffers. Proteins were then concentrated using a 10-kDa Amicon tube (Millipore, Merck, Darmstadt, Germany) and further filtered through a 0.22-µm filter. α_2PI_{1-8}-VEGF-A_{164} monomers and dimers were separated using size exclusion with a HiLoad 16/60 Superdex 75-pg column (GE healthcare, Chicago, Illinois, USA). Fractions corresponding to α_2PI_{1-8}-VEGF dimers were pooled together, concentrated with Amicon tubes, and filtered through a 0.22-µm filter. α_2PI_{1-8}-VEGF dimers were verified to be >99% pure by SDS/PAGE and MALDI-TOF analysis. Endotoxin level was verified to be under 0.05 EU/mg of protein using the LAL assay (GenScript, Piscataway, New Jersey, USA).

Generation and in vivo subcutaneous implantation of osteogenic constructs

60 mm^3 of silicate-substituted apatite granules of 1-2mm size (Actifuse®; Apatech-Baxter, Elstree, UK) where mixed with $1x10^6$ BMSC and embedded in a fibrin gel prepared by mixing 25 mg/ml human fibrinogen (plasminogen-, von Willebrand Factor-, and fibronectin-depleted; Milan Analytica AG, Rheinfelden, Switzerland), 3 U/mL factor XIIIa (CSL Behring, King of Prussia, Pennsylvania, USA), and 6 U/ml thrombin (Sigma-Aldrich, St. Louis, Missouri, USA) with 2.5 mM Ca^{2+} in 4-(2-hydroxyethyl)-1- piperazineethanesulfonic acid (Hepes, Lonza, Basel, Switzerland). Fibrin gels decorated with 51 µg/ml of aprotinin-$\alpha2PI_{1-8}$ and 1 µg/ml of $\alpha2PI_{1-8}$-VEGF-A_{164} were obtained by adding the engineered proteins to the cross-linking enzymes solution before mixing with fibrinogen. Osteogenic grafts were allowed to

polymerize at 37°C for 10 min after mixing before *in vivo* implantation. The resulting constructs were implanted subcutaneously in nude mice (CD1-*Foxn1*^{nu}, Charles-River, Sulzfeld, Germany). Six constructs were implanted for each condition (n=6 samples/group), generated with cells from 3 independent donors (2 replicates/donor). After 1, 4 and 8 weeks, mice were sacrificed by inhalation of CO_2 and constructs were explanted.

Critical-size calvaria bone defects

Critical-size bilateral bone defects of 6 mm were created in both parietal bones of immune-deficient nude NIH-*Foxn1*^{rnu} rats (Charles-River, Sulzfeld, Germany), lateral to the midsagittal suture, using a trephine bur (ACE Dental Implant System, Brockton, Massachusetts, USA) and a piezoelectric tool (Mectron, Flexident AG, Stansstad, Switzerland) under low-speed drilling with continuous cool saline irrigation. Rats were under inhalation anesthesia (isoflurane) throughout the surgical procedure. Round osteogenic constructs of 6-mm diameter and 3-mm thickness were generated in the same way as described above with cells from 2 independent donor (n=4 samples/group, 2 replicates/donor) and implanted in the defects. After 1 and 4 weeks, rats were anesthetized with ketamine (100 mg/kg) and xylazine (10 mg/kg), and sacrificed by total-body vascular perfusion of 1% paraformaldehyde in PBS pH 7.4 for 3 min under 120 mm/Hg of pressure, followed by 2 h of post-fixation in 0.5% paraformaldehyde in PBS and kept in PBS at 4°C until micro-CT analysis was performed. After micro-CT analysis, constructs were processed for histological analysis as described below. Animals were treated in agreement with Swiss legislation and according to a protocol approved by the Veterinary Office of Canton Basel-Stadt (permission #1797).

Micro-CT

Micro-computed tomography (µCT) data were acquired using a Phoenix Nanotom M scanner (General Electric, Fairfield, CT, http://www.ge.com) with 0.5 mm aluminum-filtered X-rays (applied voltage 70 kV; current 260 µA). Transmission images were done during a 360° rotational scan with an incremental rotation step size of 0.25°. Reconstruction was made using a modified Feldkamp algorithm at an isotropic voxel size of 2.5 µm. For quantification of bone mineral density and bone volume, all data were normalized to the volume of each constructs. Threshold-based segmentation, 3D measurement analyses (mineral density and volume) and 3D rendering of the structures was performed using VGStudio MAX 2.2 software (Volume Graphics, Heidelberg, Germany, http://www.volumegraphics.com/en/).

Histological processing

Explanted constructs were washed with PBS and fixed over night at 4°C with freshly prepared 1% paraformaldehyde (Sigma Aldrich, St. Louis, Missouri, USA) in PBS. Subsequently, the samples were decalcified in a PBS-based solution containing 7% w/v EDTA (Sigma-Aldrich, St. Louis, Missouri, USA) and 10% w/v sucrose (Sigma-Aldrich, St. Louis, Missouri, USA) and incubated at 37°C on an orbital shaker. The solution was renewed daily for 20 days, until the samples were fully decalcified, as estimated by the degree of sample stiffness. Finally, the samples were embedded in OCT compound (CellPath Ltd, Newtown, UK) frozen in freezing 2-methylbutane (Sigma Aldrich, St. Louis, Missouri, USA) and 10 µm-thick sections were obtained with a cryostat.

Immunofluorescence tissue staining

Immunofluorescence staining was performed on 10 µm-thick frozen sections. The following primary antibodies and dilutions were used: rat anti-mouse CD31 (clone MEC 13.3,

BD Bioscience, San Jose, California, USA) at 1:100; mouse anti-rat CD31 (clone TLD-3A12, BD Bioscience, San Jose, California, USA); mouse anti-Human nuclei (clone 235-1, Merk Millipore, Darmstadt, Germany) at 1:200; polyclonal rabbit anti-Ki67 (Abcam, Cambridge, UK) at 1:100; polyclonal rabbit anti-Cleaved Caspase 3 (Asp175) (Cell Signaling Technology, Danvers, Massachusetts, USA) at 1:200; mouse anti-human BSPII (Clone LFMb-24, Santa Cruz Biotechnology, California, USA) at 1:50. Fluorescently labelled secondary antibodies (Invitrogen, Thermo Fisher Scientific, Waltham, Massachusset, USA) were used at 1:200.

Images were acquired with an Olympus BX63 microscope (Olympus, Münster, Germany) and a Nikon Ti2 Eclipse microscope (Nikon, Tokyo, Japan). All image measurements were performed with CellSens software (Olympus, Münster, Germany), NIS-Elements (Nikon, Tokyo, Japan) and FIJI software (ImageJ, http://fiji.sc/Fiji).

Angiogenesis

Vascularization in the ectopic bone grafts was assessed by immunofluorescent CD31 staining. At least 5 representative images were acquired per sample (n=6 samples/group) and vessel length density (VLD) was measured by tracing the total length of vessels in the fields and by normalizing it to the tissue area in each field. The quantification of the vascular invasion and the VLD in the rat calvaria defects was performed on cryosections stained for rat CD31 (n=4 samples/group). Briefly, complete images of the whole samples were acquired, the areas of tissue invaded by blood vessels were manually measured and normalized by the total tissue area of the defect. VLD was measured within the areas of invasion in at least 5 different fields per sample, as described above.

Bone formation and maturation

Bone tissue was detected by Hematoxylin and Eosin (H&E) staining. In addition, the presence of mature bone matrix was examined with Masson trichrome staining (Réactifs RAL, Martillac, France), performed according to manufacturer's instructions. Ten whole-section reconstructions per sample (n=6 samples/group) were acquired with transmitted light and bone tissue was quantified by tracing the area occupied by mineralized matrix and normalizing it by the total area of the section. In addition, the presence of mature bone matrix (red staining in Masson's trichrome staining) was measured and normalized by the total amount of bone.

Osteoclast recruitment

In order to detect osteoclasts, sections were stained for tartrate-resistant acid phosphatase (TRAP) activity. Briefly, after rising with water, slides were incubated for 20 minutes with 0.1M Acetate Buffer (0.2M Sodium Acetate, 0.2M Acetic Acid, 50mM Sodium L-tartrate dibasic dihydrate, pH 5.0) and then stained with a solution of 1 mg/ml Fast Red LB salt (Sigma-Aldrich, St. Louis, Missouri, USA) and 1 mg/ml naphthol AS-MX phosphate (Sigma-Aldrich, St. Louis, Missouri, USA) in 0.1M acetate buffer for 1 hour at 37°C. After TRAP staining, nuclear counter staining was performed with Haematoxylin for 1 min at room temperature. TRAP-positive cells were quantified on 15 random fields per construct in 6 constructs/condition (n=6 samples/group). Multinucleated TRAP+ cells in the fields were counted manually and the total number was normalized by the tissue area.

Human progenitor engraftment

The presence of human cells was assessed by staining with a specific anti-human nuclei antibody. In the ectopic bone grafts, human cells were counted automatically in at least 15 random fields (n=6 samples/group) by using ImageJ software. Quantification of the number of human cells in the rat calvaria defects was performed on complete images of the whole samples longitudinally divided in 5 standardized segments, in order to distinguish border, intermediate and center areas (Fig. 8B). Human cells were manually counted in each area and the number was normalized by the tissue area (n=4 samples/group). Proliferation and apoptosis of implanted human progenitor cells were assessed after 1 week *in vivo* by immunostaining for Ki67 and Cleaved-Caspase3 (Cas3), respectively, together with the anti-human nuclei antibody. 15-20 random fields per sample (n=6 samples/group) were analyzed by manually counting the number of human cells that were also Ki67+ or Cas3+ in the field and normalizing it by the total number of human cells. Osteogenic differentiation of human progenitors was assessed in rat calvaria defects 4 weeks after *in vivo* implantation by immunostaining for human-specific Bone Sialoprotein (BSP).

Statistics

Results are expressed as the mean ± standard error of the mean (SEM). The significance of differences was assessed with the GraphPad Prism 7.03 software (GraphPad Software, San Diego, California, USA). The normal distribution of all data sets was tested by D'Agostino and Pearson or Shapiro–Wilk tests and, depending on the results, the significance of differences was determined with the parametric 1-way analysis of variance (ANOVA) followed by the Bonferroni test for multiple comparisons, or with the non-parametric Kruskal–Wallis test followed by Dunn's post-test. $P<0.05$ was considered statistically significant.

Results

TG-VEGF induces rapid and stable angiogenesis in osteogenic grafts

In order to compare sustained and transient VEGF signaling, the factor was provided in osteogenic grafts at functionally equivalent doses, either as stable transgene expression from retrovirally transduced BMSC, or as recombinant protein cross-linked into the fibrin matrix (TG-VEGF). Human BMSC from 3 independent bone marrow donors were retrovirally transduced to express mouse VEGF linked to a truncated form of murine CD8a as a FACS-detectable cell surface marker (VICD8-BMSC), as previously described [17] with >90% transduction efficiency. Production of mouse VEGF protein was quantified *in vitro* by ELISA and found to be 68.0±18.7 ng/10^6cells/day by transduced cells, whereas it was absent in naïve BMSC (0.7±0.3 ng/10^6cells/day). Based on previous studies of the dose-dependent outcomes of VEGF delivery in skeletal muscle by cell-based gene transfer [11, 19] and by fibrin-based protein delivery [15], it was determined that expression levels of about 60 ng/10^6 cells/day by transduced cells induce similarly normal and functional angiogenesis as a concentration of 1 µg/ml of fibrin-bound TG-VEGF.

Ectopic osteogenic grafts were therefore generated with naïve human BMSC embedded in fibrin hydrogels decorated with 1 µg/ml TG-VEGF or with VICD8 BMSC embedded in empty fibrin. Naïve BMSC were also combined with empty fibrin matrices as control. The mineral phase was provided by silicate-substituted hydroxy-apatite (HA) granules of 1-2mm size in all conditions (Fig. 1)

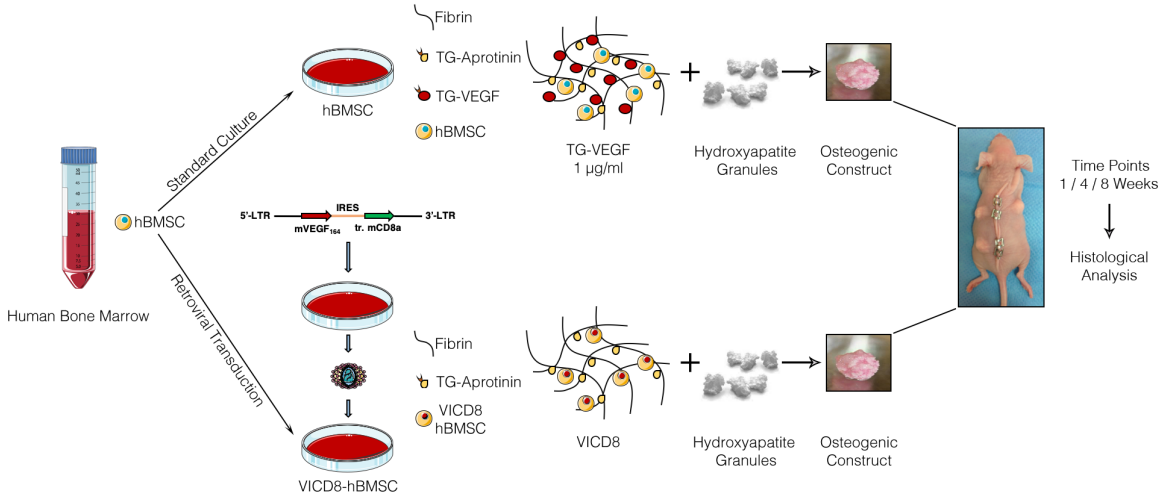

Figure 1. *Study design for the ectopic model of bone formation.*

Graft vascularization was assessed by immunostaining for CD31 after 1, 4 and 8 weeks *in vivo*. After 1 week, blood vessels were only present in the periphery of the grafts in all conditions, whereas by 4 weeks the constructs were homogeneously vascularized. As shown in Fig. 2, both TG-VEGF and VICD8 cells increased graft vascularization at all time points compared to the controls. Quantification of vessel length density (VLD), i.e. the total vessel length per tissue area, showed that the increased vascular density induced by both VEGF conditions was stable over time and, after a further increase between 1 and 4 weeks, persisted essentially unchanged after 8 weeks (Fig. 2B-D).

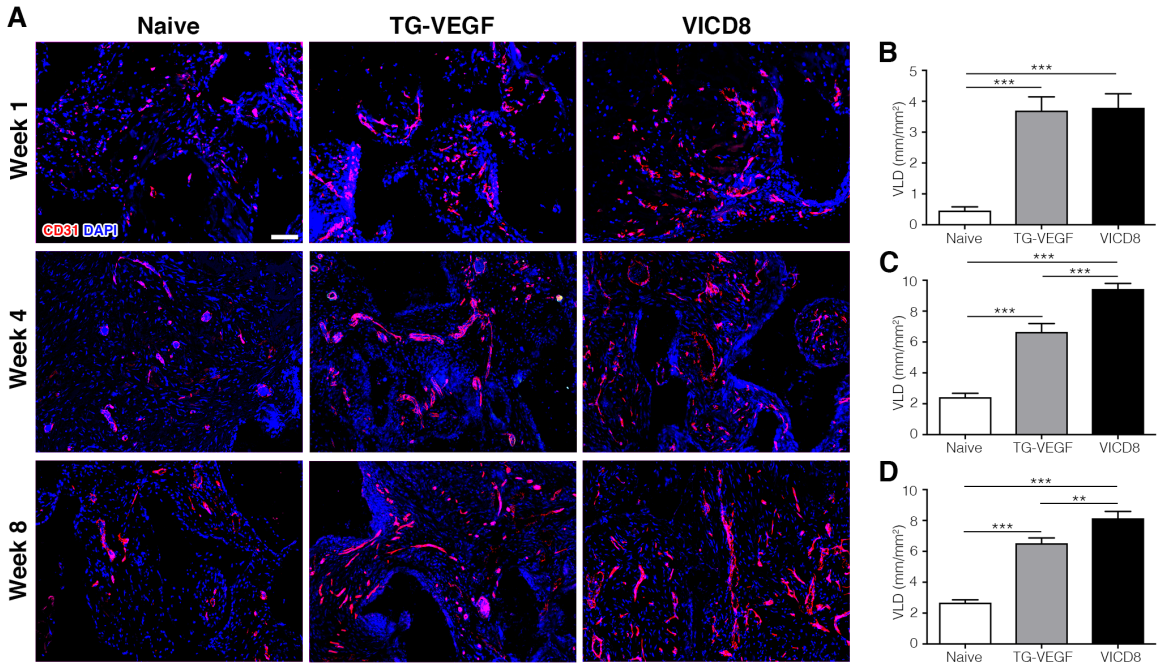

Figure 2. *(A) Immunostaining of endothelium (CD31, in red) and nuclei (DAPI, in blue) of constructs after 1, 4 and 8 weeks of in vivo implantation; (B-D) Quantification of induced angiogenesis. VLD = vessel length density, expressed as millimeters of vessel length per square millimeter of tissue area (mm/mm^2), in constructs after 1 (B), 4 (C) and 8 (D) weeks of in vivo implantation (**=p<0.01, ***=p<0.001). Scale bar = 100 µm.*

TG-VEGF prevents bone tissue loss and enables mature bone tissue formation

Bone formation was assessed by H&E staining. After 1 week *in vivo* (Fig. 3A, upper panels), fibrin was still abundantly present in the constructs of all conditions (F=Fibrin), with embedded cells (black arrows), and no bone tissue was present in any graft. After 4 weeks (Fig. 3A, middle panels), fibrin was essentially completely degraded and initial formation of dense collagenous matrix (DM=Dense Matrix) could be observed at the interface with HA granules (G=Granules) in the naïve and TG-VEGF conditions, but not in the constructs with VEGF-expressing BMSC. After 8 weeks (Fig. 3A bottom panels), frank bone tissue, characterized by a dense collagenous matrix with organized collagen fibers and the presence of osteocyte lacunae (B=Bone), could again be detected only with Naïve BMSC and TG-VEGF, but not in the VICD8 condition. Quantification of the area occupied by osteogenic matrix

showed that bone formation in the presence of TG-VEGF was as efficient as with Naïve BMSC alone, but was almost completely abolished with VEGF-expressing BMSC both after 4 weeks (Fig. 3B; Naïve=1.89±0.3%, TG-VEGF=1.30±0.2%, VICD8=0.14±0.04%, $p<0.001$ and $p<0.05$ vs VICD8) and after 8 weeks (Fig. 3C; Naïve=6.83±0.84%, TG-VEGF=4.91±0.85%, VICD8=0.46±0.15%, $p<0.001$ vs VICD8).

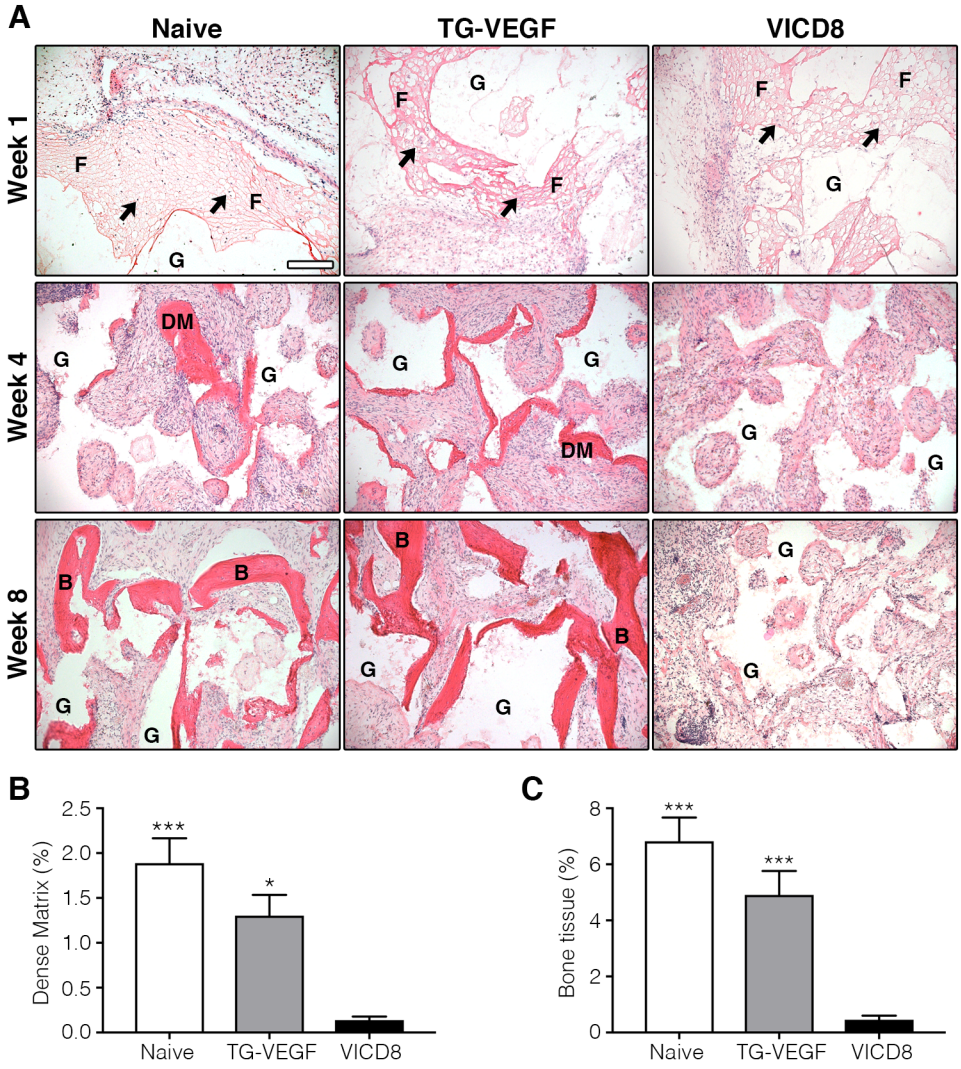

Figure 3. *(A) H&E staining of constructs harvested 1, 4 and 8 weeks after in vivo implantation. (B-C) Quantification of areas occupied by osteogenic matrix (expressed as % of construct area) after 4 (B) and 8 weeks (C). *=p<0.05, ***=p<0.001. Black arrows = embedded cells; F=Fibrin; G=Granules; DM=Dense Matrix; B=Bone. Scale bar = 100 µm.*

The degree of bone maturation after 8 weeks was evaluated by Masson's trichrome staining, as defined by the presence of elastic fibers (Fig. 4A, in red). Quantification of the areas occupied by elastic fibers (Fig. 4B) showed a similar amount of mature bone in the Naive and TG-VEGF conditions (Naïve=1.88±0.4%, TG-VEGF=2.64±0.4%; p=n.s.), whereas the little amount of bone detectable in the VICD8 constructs was completely immature (VICD8=0.08±0.01%, p<0.001 vs. Naive and TG-VEGF).

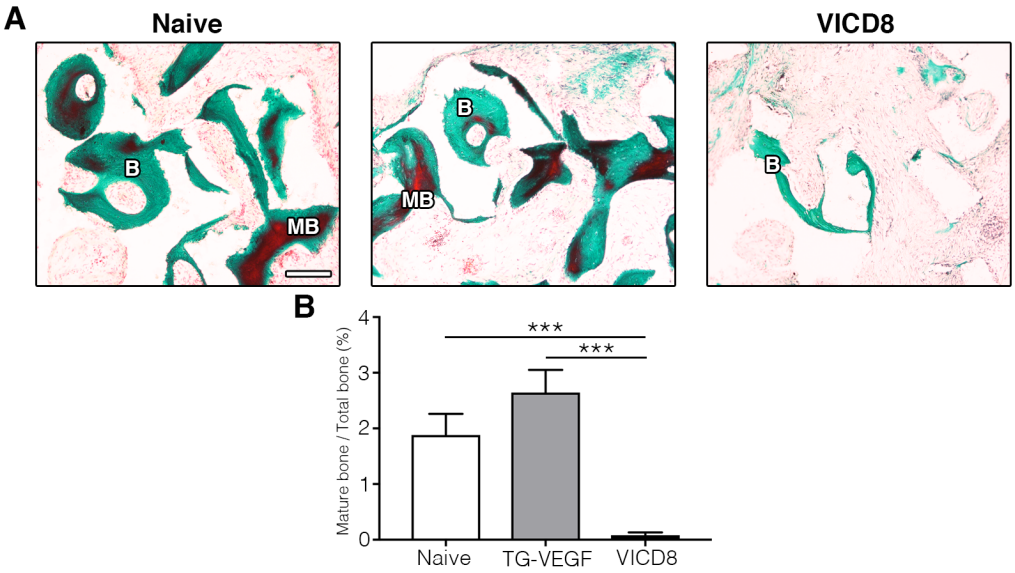

Figure 4. *(A) Masson's trichrome staining of constructs 8 weeks after in vivo implantation (B=Bone tissue, in green; MB=Mature Bone with elastic fibers, in red). (B) Quantification of areas occupied by mature bone (expressed as % of total bone tissue; ***=p<0.001). Scale bar = 100 µm.*

TG-VEGF prevents excessive osteoclasts recruitment

We previously shown that a mechanism by which sustained expression of VEGF by genetically modified BMSCs causes loss of bone tissue in osteogenic grafts is a significant increase in bone resorption by osteoclasts [8]. Therefore, osteoclast activity was evaluated by tartrate-resistant acid phosphatase (TRAP) staining. After 4 and 8 weeks, both naïve and TG-VEGF constructs contained very few TRAP-positive cells (Fig. 5A, in red), which were visible in close proximity to the bone matrix or at the interface with the HA granules. In contrast, grafts

with VEGF-expressing BMSC contained a high density of TRAP-positive cells, usually in contact with the HA granules (Fig. 5A, right panels).

Quantification of the density of multinucleated TRAP-positive cells (Fig 5B-C) showed that VEGF-expressing BMSC increased osteoclast recruitment by 2- to 3-fold compared to the naïve and TG-VEGF conditions, both after 4 and 8 weeks (4 weeks: Naïve=24.53±2.1, TG-VEGF=36.34±2.0, VICD8=73.35±11.6 $TRAP^+$ MNC/mm^2, $p<0.001$; and 8 weeks: Naïve=23.44±1.9, TG-VEGF=37.73±1.9, VICD8=68.94±9.3 $TRAP^+$ MNC/mm^2, $p<0.001$).

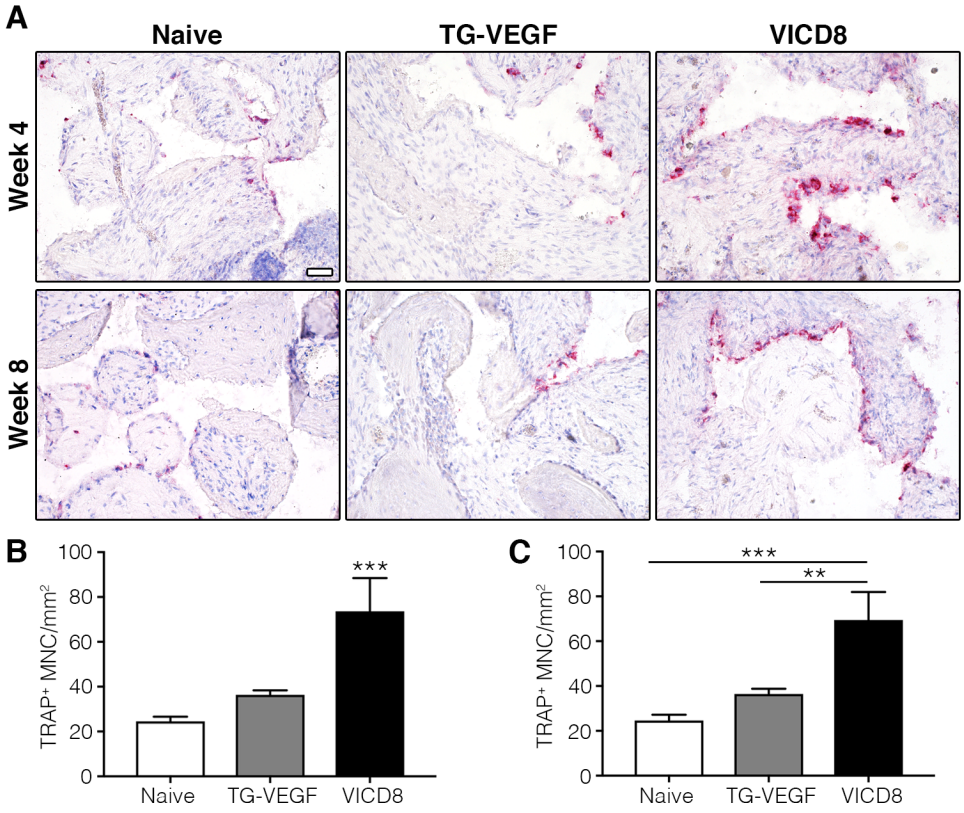

Figure 5. *(A) Histochemical stain for TRAP activity (red) and nuclear counterstaining with hematoxylin (blue) of constructs harvested 4 and 8 weeks after in vivo implantation. (B-C) Quantification of TRAP+ multinucleated cells ($TRAP^+$ MNC) after 4 (B) and 8 weeks (C), expressed as number of $TRAP^+$ MNC/mm^2 of tissue (**=p<0.01, ***=p<0.001). Scale bar = 100 µm.*

TG-VEGF preserves in vivo expansion of human progenitors

Since bone formation depends on the balance between matrix deposition by progenitor-derived osteoblasts and resorption by osteoclasts, we investigated the engraftment of the implanted human osteo-progenitors. Human cells were quantified both after 1 and 4 weeks by staining for a human-specific nuclear antigen (HuNu, red nuclei in Fig. 6A). After 1 week human cells were homogenously distributed within the graft and their density was similar in all conditions (Fig. 6B; Naïve=92.00±7.2 cells/field, TG-VEGF=91.15±7.6 cells/field, VICD8=94.84±17.3 cells/field; p=n.s.). After 4 weeks human cells had significantly expanded by about 3-fold in both the naïve and TG-VEGF conditions (Fig. 6C; Naïve=260.10±38.5 cells/field, TG-VEGF=325.7±51.5 cells/field; p=n.s.), but did not increase in the constructs containing VEGF-expressing cells (VICD8=110.04±15.6 cells/field; $p<0.05$ vs Naïve and $p<0.01$ vs TG-VEGF). Furthermore, human progenitors in the naïve and TG-VEGF constructs were found embedded within the dense matrix areas (Fig. 6A; DM) deposited at the surface of HA granules (G) and as bone lining cells (white arrows), whereas in the VICD8 grafts they appeared sparse and did not form a compact bone-depositing front.

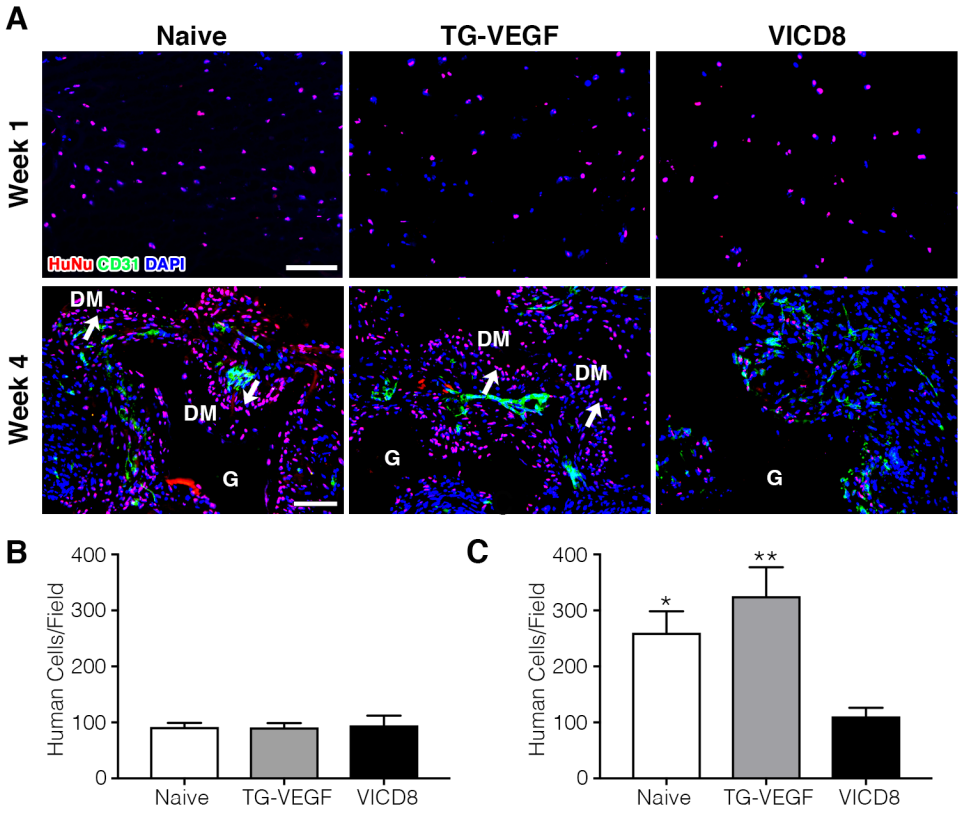

Figure 6. *(A) Immunostaining of human nuclei (HuNu, red), blood vessels (CD31, green), and nuclei (DAPI, blue) 1 and 4 weeks after in vivo implantation; (B, C) quantification of human nuclei per microscopic field of view (*=p<0.05, **=p< 0.01). DM = Dense Matrix; G = Granules; White arrows = bone-lining cells. Scale bar = 200 µm*

Next, we asked whether the lack of human progenitor expansion in the VEGF-expressing constructs was due to decreased proliferation or increased cell death 1 week after implantation (Fig. 7). Human cells were specifically stained with an anti-human nuclei antibody (HuNu, in red), in combination with a proliferation marker (Ki67, in cyan in Fig. 7A) or with the apoptosis marker cleaved-Caspase3 (Cas3, in green in Fig. 7C). No significant difference in human progenitor proliferation was found between all conditions (Fig. 7B; Naïve=2.7±0.3%, TG-VEGF=3.6±0.2%, VICD=2.4±0.5%, p=n.s.). However, apoptosis was significantly increased in the VICD8 condition compared to both Naïve and TG-VEGF constructs (Fig. 7D; Naïve=3.7±0.6%, TG-VEGF=5.0±0.7%, VICD8=7.51.2%; p<0.05 vs both Naïve and TG-VEGF).

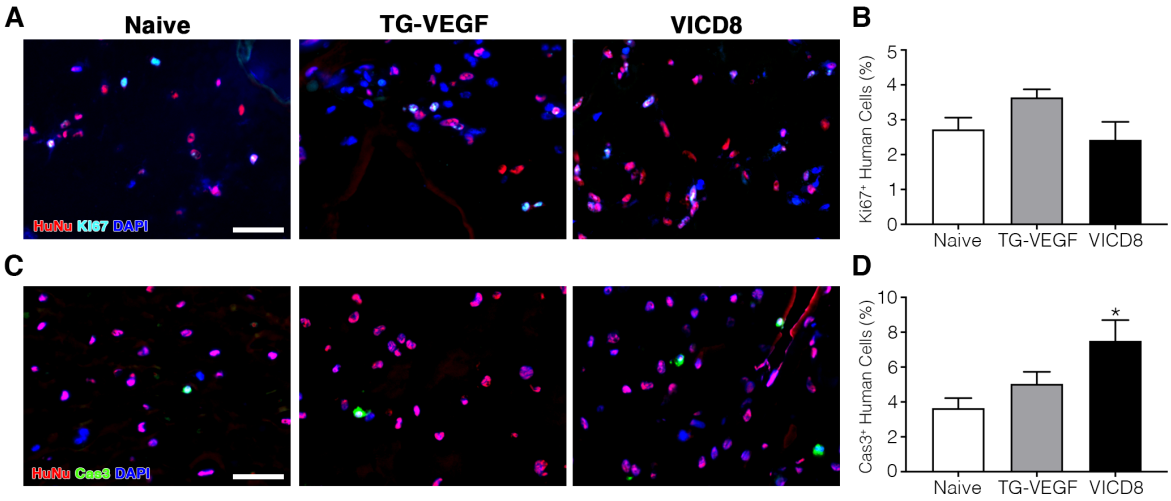

Figure 7. *Quantification of human cell proliferation and apoptosis 1 week after in vivo implantation. (A) Immunostaining for human nuclei (HuNu, red), proliferating cells (KI67, cyan) and nuclei (DAPI, blue); (B) Quantification of proliferating human cells (%) (*=p<0.05); (C) Immunostaining for human nuclei (HuNu, red), apoptotic cells (Cas3, green) and nuclei (DAPI, blue); (D) Quantification of apoptotic human cells (%). Scale bar = 50 µm*

TG-VEGF promotes rapid vascularization and repair of critical bone defects

We next investigated whether the ability of VEGF-decorated fibrin matrices to effectively couple angiogenesis and osteogenesis, shown above in an established small-size model of ectopic bone formation, could translate to improved repair of critical-size bone defects in an orthotopic setting, where insufficiently rapid vascularization of the central area of the defect is a key limitation to its repair. Therefore, osteogenic constructs incorporating human BMSC alone or in combination with 1 µg/ml TG-VEGF or VEGF-expressing BMSC were implanted into 6-mm critical-size defects in rat calvaria (Fig. 8A). Vascularization of the constructs was assessed along the whole length of the defects, on sections of the central part corresponding to the largest diameter, as shown graphically on a representative H&E image in Fig. 8B. Immunostaining for rat CD31 showed that after 1 week *in vivo* initial spontaneous vascularization of the constructs was limited and started independently from the sides of the defect (surrounding bone) and from the overlying skin at the center of the defect, but not

from the underlying meningeal layer (Fig. 8C, Naïve condition, white dotted areas). However, both VEGF conditions significantly accelerated vascular invasion of the constructs, more than doubling the vascularized area (Fig 8C-D; Naive=27.3±8.3% vs TG-VEGF=62.0±9.9% and VICD8=65.8±9.6%; $p<0.05$ for both vs Naive). Quantification of vessels length density (VLD) within the areas of vascular invasion showed that both VEGF conditions also similarly increased vascular density by about 3-fold compared to spontaneous vascular growth in Naïve conditions (Fig. 8C and 8E; Naive=2.4±0.5 mm/mm^2 vs TG-VEGF=6.9±0.8 mm/mm^2 and VICD8=6.4±1.0 mm/mm^2; $p<0.05$ for both vs Naïve).

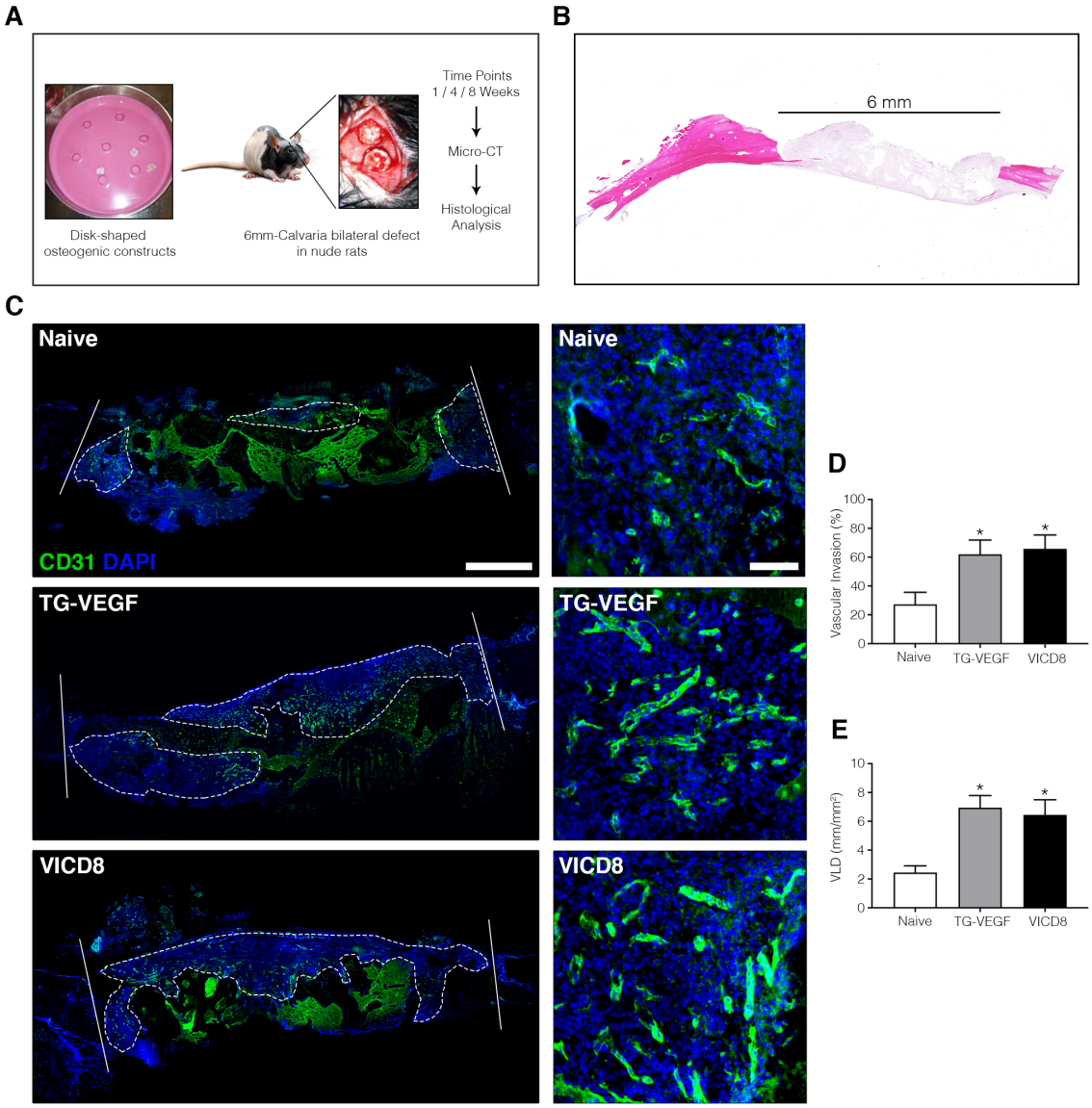

Figure 8. *(A) Study design for the orthotopic model of critical-size defect repair; (B) Representative H&E image across the larges diameter of a rat calvaria defect with the quantified 6-mm region of interest containing the implanted constructs; (C) Immunostaining of endothelium (CD31, in green) and nuclei (DAPI, in blue) in osteogenic constructs 1 week after in vivo implantation. The left panels show overviews of the whole defects, with areas invaded by vascular structures indicated by white dotted lines. Homogeneous green staining outside of these areas is caused by autofluorescence of the remaining fibrin; (D) Quantification of areas of vascular invasion 1 week after in vivo implantation, expressed as a percentage of the total construct area (%); (E) Quantification of vascular density (VLD = vessel length density) within the areas of invasion 1 week after in vivo implantation, expressed as millimeters of vessel length per square millimeter of tissue area (mm/mm^2); *=p<0.05. Scale bars = 1 mm (left panels in C) and 100 µm (right panels in C).*

The survival of seeded human BMSC was assessed by immunofluorescent staining 1 and 4 weeks after implantation in 3 different standardized regions of interest along the defect, in order to distinguish a border, an intermediate and center part, as show in Fig. 9A. After 1 week, the presence of TG-VEGF cross-linked into the fibrin greatly increased human cell survival throughout the defect compared with the naïve condition, between 2.6-fold (in the center) and 6.5-fold (at the border) whereas VEGF expression by the cells (VICD8) was less effective (Fig. 9B-C; Border: Naïve=36.5±17.2 human cells/mm^2, TG-VEGF=237.4±26.1, VICD8=145.0±46.8, $p<0.05$ TG-VEGF vs Naïve; Intermediate: Naïve=69.9±16.8 human cells/mm^2, TG-VEGF=284.2±18.4, VICD8=206.0±32.8, $p<0.01$ TG-VEGF vs Naïve and $p<0.05$ VICD8 vs Naïve; Center: Naïve=94.9±26.1 human cells/mm^2, TG-VEGF=252.0±45.2, VICD8=160.7±8.3, $p<0.05$ TG-VEGF vs Naïve). Interestingly, after 4 weeks human cells were essentially lost in the VICD8 condition, whereas they could still be found in both the naïve and TG-VEGF constructs (Fig. 9D). The human BMSC still present in both these conditions had undergone proper osteogenic differentiation, as demonstrated by their expression of human bone sialo-protein (hBSP; Fig. 9E).

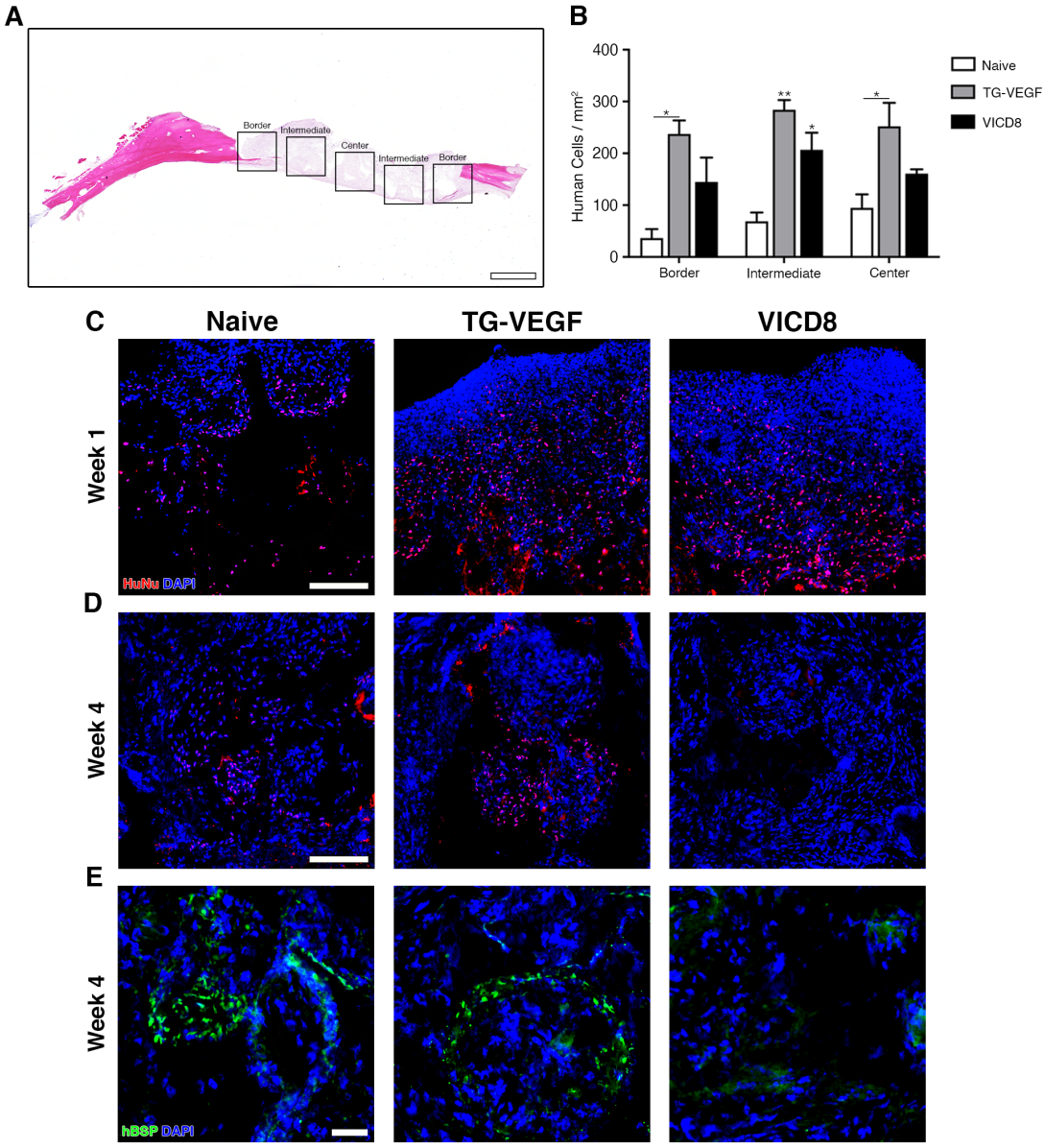

Figure 9. *(A) Representative H&E image across the larges diameter of a rat calvaria defect with the implanted constructs, showing the standardized areas (2x border, 2x intermediate and 1x center) that were separately quantified; (B) Quantification of human cell survival 1 week after in vivo implantation, expressed as number of human cells per square millimeter (human cells/mm²) of tissue area (*=p<0.05, **=p<0.01); (C, D) Immunostaining of human cells (HuNu, in red) and nuclei (DAPI, in blue) 1 (C) and 4 weeks (D) after in vivo implantation; (E) Immunostaining for human-Bone Sialoprotein (hBSP, green) and nuclei (DAPI, blue) 4 weeks after in vivo implantation. Scale bars: (C, D) = 200 µm, (E) = 50 µm.*

Lastly, the efficiency of bone formation in the treated defects was assessed by micro-computerized tomography of explanted calvaria after 4 weeks (micro-CT; Fig. 10A). Quantification of the calcified tissue inside the defects showed that transient provision of matrix-bound recombinant TG-VEGF significantly improved bone formation by about 2-fold compared to naïve BMSC alone, both in the center part of the defect and in the outer part in contact with the native calvaria (Fig. 10B). In contrast, sustained VEGF gene expression by VICD8 cells failed to improve bone formation despite the effective promotion of vascularization. The presence of actual bone tissue was confirmed by histological analysis with Masson-Trichrome staining (Fig. 10C-D).

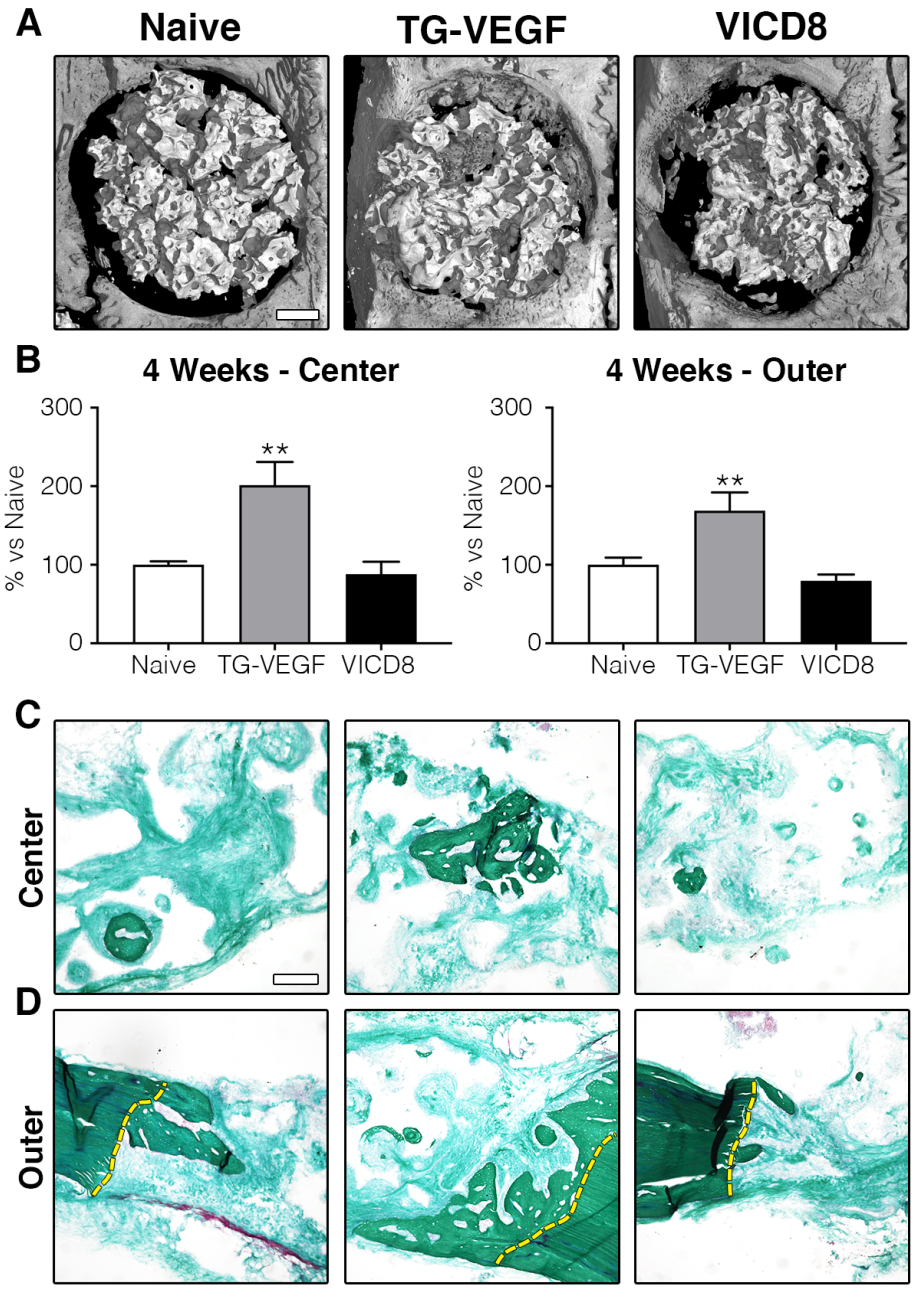

Figure 10. *(A) Micro-CT representative images of osteogenic grafts after 4 weeks of in vivo implantation in a rat calvaria defect. Gray areas = new bone tissue, white areas = HA granules; (B) Quantification of bone volume in the defects 4 weeks after in vivo implantation, measured by micro-CT and normalized by the naïve condition (% vs Naïve; *=p<0.05); (C-D) Masson's trichrome staining showing bone tissue (green) in the central area of the grafts (C) and in the outer area in contact with the native calvaria (D) 4 weeks after in vivo implantation. Yellow dashed lines indicate the edge of the defects. Scale bars: (A) = 1 mm; (C, D) = 200 µm.*

Discussion

Angiogenesis and osteogenesis are physiologically coupled processes that need to be coordinated for therapeutic regeneration of vascularized bone. VEGF is the master regulator of angiogenesis during bone development, but it also has the potential to paradoxically impair net bone formation when delivered therapeutically. Here we found that the timing of VEGF supply is key to its therapeutic potential. In fact, transient delivery of VEGF protein for less than 4 weeks, controlled through a highly tunable fibrin-based platform, was able to effectively stimulate vascularization of human BMSC osteogenic grafts without interfering with bone formation, whereas prolonged sustained expression led to bone loss. Efficient coupling of angiogenesis and osteogenesis by transient VEGF protein delivery translated into accelerated vascular invasion and significantly improved bone formation in the repair of critical-size calvaria defects.

Rapid vascular ingrowth is a fundamental requirement to ensure cells survival in the core of a critical-size scaffold and the subsequent formation of healthy bone tissue. Upon VEGF stimulation, the process of blood vessels formation can be divided in two functional stages: 1) vascular morphogenesis, i.e. the initial growth of new vessels from pre-existing ones, which is a rapid process and requires only a few days; and 2) vessel stabilization, which takes 3-4 weeks and during which the newly formed vascular structures become independent of continued VEGF stimulation [7]. Therefore, VEGF signaling is only necessary for a duration of up to 4 weeks, beyond which newly formed vasculature persists indefinitely in the absence of further angiogenic stimulus [10, 11]. Consistently with these biological features, here we found that both TG-VEGF and VEGF-expressing cells effectively promoted the morphogenesis of new vessels within 1 week *in vivo* compared to the naïve conditions. Further, vessel density

remained stable between 4 and 8 weeks with TG-VEGF, despite the fact that fibrin and its associated recombinant VEGF had completely degraded by 4 weeks, showing that the newly induced vascularization had successfully stabilized and could persist indefinitely.

It should also be considered that vessels invading osteogenic grafts may actually stabilize faster than in other tissues. In fact, vascular stabilization is mediated by endothelial association with support cells called pericytes and the establishment of a paracrine molecular cross-talk [7]. Multiple lines of evidence indicate that MSC share functional features of vascular pericytes, as MSC are found in the perivascular niche of virtually every organ, share common markers with pericytes (e.g. CD146) and can be activated upon injury to support tissue regeneration [20, 21]. Therefore, it is reasonable to speculate that the BMSC in the constructs, beyond providing the population of osteoprogenitors for bone formation, may also accelerate the stabilization of newly induced blood vessels, further reducing the period of time over which VEGF signaling needs to be sustained. Testing this hypothesis will require further experimental work, e.g. by reducing the concentration of TG-aprotinin, or omitting it altogether, in order to accelerate fibrin degradation and so further reduce the duration of VEGF stimulation.

Osteogenesis, on the other hand, takes place with significantly slower kinetics than angiogenesis [12, 22]. In fact, vascular invasion precedes the initiation of osteogenic differentiation of progenitors and, as confirmed by the data reported here, while significant blood vessel in-growth took place within the first week of implantation, no signs of bone tissue formation could be detected at the same time. Only after 4 weeks, when angiogenesis is complete and new vessels have already stabilized and achieved VEGF-independence, an initial template of dense collagenous matrix was deposited on the surface of the hydroxyapatite granules by MSC-derived osteoblasts. This immature osteoid matrix required

several more weeks to develop into mature bone tissue by 8 weeks, characterized by the presence of organized lamellar structures, osteocytes embedded in their lacunae and elastic fibers. The clear difference in the kinetics of blood vessels growth and bone tissue formation in osteogenic grafts underlies the notion that the timing and duration of angiogenic stimulation by VEGF delivery carries significant therapeutic implications.

If prolonged VEGF delivery is not necessary for efficient vascularization, it can actually have detrimental effects on bone tissue formation. In fact, we have previously found that continuous expression of VEGF by genetically modified human BMSCs can impair bone formation in osteogenic grafts by promoting osteoclast recruitment and unbalancing bone homeostasis towards excessive bone resorption [8]. VEGF signaling is crucial and required during bone development both in endochondral and in intramembranous ossification [13] and VEGF-receptors are expressed by various cells involved in the osteogenic process, such as osteoprogenitors, osteoblasts and osteoclasts [23, 24]. Therefore, the detrimental effects of sustained VEGF delivery on net bone formation may not be limited to increasing resorption and affect also bone anabolism. However, both previous evidence and the data reported here do not suggest a direct toxicity to the implanted osteoprogenitors by VEGF. In fact, VEGF transgene expression did not impair either BMSCs proliferation nor their osteogenic differentiation potential *in vitro* [17], and here we found that in small-size ectopic implants human BMSCs engraftment was not impaired after 1 week of *in vivo* implantation and exposure to VEGF, regardless of its delivery method (Fig. 6B).

On the other hand, sustained VEGF expression impaired osteoprogenitor expansion by 4 weeks, while transient delivery did not (Fig. 6C). This suggests an indirect effect, requiring longer time to develop, and in fact it has been found to correlate with the VEGF-induced stimulation of osteoclast recruitment, which is not sustained in the conditions of transient

VEGF (Fig. 5). It has been described that osteoclast differentiation requires a combination of paracrine signals and cell-to cell contacts with stromal cells, osteoblasts and osteocytes at the site of bone remodeling [25]. During active bone resorption, osteoclasts produce coupling signals, which temporarily impair osteoblasts differentiation [26]. After osteoclasts erode the matrix they normally undergo apoptosis, and osteoblasts are recruited and can deposit new bone matrix [27]. On the other hand, the majority of osteoblasts assembled at the remodeling site also die, while only a small percentage becomes quiescent as bone lining cells or remains entrapped within the mineralized matrix as osteocytes [28]. Our data suggest that, in conditions of prolonged VEGF overexpression, osteoclast recruitment is uncoupled from its physiological regulation and driven to sustained activity. This provides a likely mechanism for the observed drop in human osteoprogenitors in small ectopic grafts between 1 and 4 weeks after *in vivo* implantation specifically in the sustained VEGF condition, through unregulated osteoclast activity both impairing further bone deposition and driving MSC-derived osteoblasts towards apoptosis (Fig. 7B). Transient delivery of VEGF protein, instead, avoids sustained perturbation of osteoclast activity and allows the establishment of the physiological coupling between osteoblast and osteoclast activity after the first few weeks.

Results in the small-size ectopic model show that increased vascularization by VEGF protein delivery did not further improve progenitor survival and expansion compared to naive conditions. In contrast, in the critical-size calvaria defects human cells survival was already compromised after 1 week when VEGF was not provided (Fig. 9B). This difference highlights the importance of early vascularization in clinically relevant conditions. In fact, small-size ectopic models allow the study of the intrinsic bone-forming potential of the implanted cells, but do not provide critical vascularization conditions for progenitor survival and engraftment [29].

In summary, these results show that the therapeutic effects of VEGF delivery for the regeneration of vascularized bone are time-dependent: 1) VEGF is beneficial over the first 3-4 weeks to accelerate early vascular ingrowth in osteogenic grafts, improving both progenitor survival and bone formation in critical-size defects; but 2) is detrimental if sustained beyond this duration, through excessive osteoclast activation leading to both progenitor death and bone loss.

These findings bear translational relevance for the design of effective therapeutic strategies to generate vascularized osteogenic grafts. In particular we showed that by controlling the kinetics of VEGF delivery it is possible to maintain the physiological coupling of angiogenesis and osteogenesis that is required for effective bone regeneration, by first stimulating rapid vascular ingrowth and osteogenic progenitor survival, and then avoiding detrimental VEGF effects on excessive bone resorption. From this perspective, fibrin matrices decorated with engineered VEGF protein provide a highly tunable and readily translatable platform to generate a controlled regenerative environment, which can mimic the ECM proprieties, present growth factors in a physiological manner and improve tissue regeneration [14].

References

[1] R. Dimitriou, E. Jones, D. McGonagle, P.V. Giannoudis, Bone regeneration: current concepts and future directions, BMC Med 9 (2011) 66.

[2] A.M. Giladi, J.R. Rinkinen, J.P. Higgins, M.L. Iorio, Donor-Site Morbidity of Vascularized Bone Flaps from the Distal Femur: A Systematic Review, Plast Reconstr Surg 142(3) (2018) 363e-372e.

[3] A.E. Mercado-Pagan, A.M. Stahl, Y. Shanjani, Y. Yang, Vascularization in bone tissue engineering constructs, Ann Biomed Eng 43(3) (2015) 718-29.

[4] T. Rademakers, J.M. Horvath, C.A. van Blitterswijk, V.L.S. LaPointe, Oxygen and nutrient delivery in tissue engineering: Approaches to graft vascularization, J Tissue Eng Regen Med 13(10) (2019) 1815-1829.

[5] O. Scheufler, D.J. Schaefer, C. Jaquiery, A. Braccini, D.J. Wendt, J.A. Gasser, R. Galli, G. Pierer, M. Heberer, I. Martin, Spatial and temporal patterns of bone formation in ectopically pre-fabricated, autologous cell-based engineered bone flaps in rabbits, J Cell Mol Med 12(4) (2008) 1238-49.

[6] G. Eelen, L. Treps, X. Li, P. Carmeliet, Basic and Therapeutic Aspects of Angiogenesis Updated, Circ Res 127(2) (2020) 310-329.

[7] R. Gianni-Barrera, N. Di Maggio, L. Melly, M.G. Burger, E. Mujagic, L. Gurke, D.J. Schaefer, A. Banfi, Therapeutic vascularization in regenerative medicine, Stem Cells Transl Med 9(4) (2020) 433-444.

[8] U. Helmrich, N. Di Maggio, S. Guven, E. Groppa, L. Melly, R.D. Largo, M. Heberer, I. Martin, A. Scherberich, A. Banfi, Osteogenic graft vascularization and bone resorption by VEGF-expressing human mesenchymal progenitors, Biomaterials 34(21) (2013) 5025-35.

[9] R.D. Largo, M.G. Burger, O. Harschnitz, C.F. Waschkies, A. Grosso, C. Scotti, A. Kaempfen, S. Gueven, G. Jundt, A. Scherberich, D.J. Schaefer, A. Banfi, N. Di Maggio, VEGF Over-Expression by Engineered BMSC Accelerates Functional Perfusion, Improving Tissue Density and In-Growth in Clinical-Size Osteogenic Grafts, Front Bioeng Biotechnol 8 (2020) 755.

[10] E. Groppa, S. Brkic, E. Bovo, S. Reginato, V. Sacchi, N. Di Maggio, M.G. Muraro, D. Calabrese, M. Heberer, R. Gianni-Barrera, A. Banfi, VEGF dose regulates vascular stabilization through Semaphorin3A and the Neuropilin-1+ monocyte/TGF-beta1 paracrine axis, EMBO Mol Med 7(10) (2015) 1366-84.

[11] C.R. Ozawa, A. Banfi, N.L. Glazer, G. Thurston, M.L. Springer, P.E. Kraft, D.M. McDonald, H.M. Blau, Microenvironmental VEGF concentration, not total dose, determines a threshold between normal and aberrant angiogenesis, J Clin Invest 113(4) (2004) 516-27.

[12] J. Filipowska, K.A. Tomaszewski, L. Niedzwiedzki, J.A. Walocha, T. Niedzwiedzki, The role of vasculature in bone development, regeneration and proper systemic functioning, Angiogenesis 20(3) (2017) 291-302.

[13] K. Hu, B.R. Olsen, The roles of vascular endothelial growth factor in bone repair and regeneration, Bone 91 (2016) 30-8.

[14] M.M. Martino, S. Brkic, E. Bovo, M. Burger, D.J. Schaefer, T. Wolff, L. Gurke, P.S. Briquez, H.M. Larsson, R. Gianni-Barrera, J.A. Hubbell, A. Banfi, Extracellular matrix and growth factor engineering for controlled angiogenesis in regenerative medicine, Front Bioeng Biotechnol 3 (2015) 45.

[15] V. Sacchi, R. Mittermayr, J. Hartinger, M.M. Martino, K.M. Lorentz, S. Wolbank, A. Hofmann, R.A. Largo, J.S. Marschall, E. Groppa, R. Gianni-Barrera, M. Ehrbar, J.A. Hubbell, H. Redl, A. Banfi, Long-lasting fibrin matrices ensure stable and functional angiogenesis by highly tunable, sustained delivery of recombinant VEGF164, Proc Natl Acad Sci U S A 111(19) (2014) 6952-7.

[16] I. Martin, A. Muraglia, G. Campanile, R. Cancedda, R. Quarto, Fibroblast growth factor-2 supports ex vivo expansion and maintenance of osteogenic precursors from human bone marrow, Endocrinology 138(10) (1997) 4456-62.

[17] U. Helmrich, A. Marsano, L. Melly, T. Wolff, L. Christ, M. Heberer, A. Scherberich, I. Martin, A. Banfi, Generation of human adult mesenchymal stromal/stem cells expressing defined xenogenic vascular endothelial growth factor levels by optimized transduction and flow cytometry purification, Tissue Eng Part C Methods 18(4) (2012) 283-92.

[18] A.H. Zisch, U. Schenk, J.C. Schense, S.E. Sakiyama-Elbert, J.A. Hubbell, Covalently conjugated VEGF--fibrin matrices for endothelialization, J Control Release 72(1-3) (2001) 101-13.

[19] G. von Degenfeld, A. Banfi, M.L. Springer, R.A. Wagner, J. Jacobi, C.R. Ozawa, M.J. Merchant, J.P. Cooke, H.M. Blau, Microenvironmental VEGF distribution is critical for stable and functional vessel growth in ischemia, FASEB J 20(14) (2006) 2657-9.

[20] M. Crisan, S. Yap, L. Casteilla, C.W. Chen, M. Corselli, T.S. Park, G. Andriolo, B. Sun, B. Zheng, L. Zhang, C. Norotte, P.N. Teng, J. Traas, R. Schugar, B.M. Deasy, S. Badylak, H.J. Buhring, J.P. Giacobino, L. Lazzari, J. Huard, B. Peault, A perivascular origin for mesenchymal stem cells in multiple human organs, Cell Stem Cell 3(3) (2008) 301-13.

[21] L.E. de Souza, T.M. Malta, S. Kashima Haddad, D.T. Covas, Mesenchymal Stem Cells and Pericytes: To What Extent Are They Related?, Stem Cells Dev 25(24) (2016) 1843-1852.

[22] K.K. Sivaraj, R.H. Adams, Blood vessel formation and function in bone, Development 143(15) (2016) 2706-15.

[23] N. Dirckx, M. Van Hul, C. Maes, Osteoblast recruitment to sites of bone formation in skeletal development, homeostasis, and regeneration, Birth Defects Res C Embryo Today 99(3) (2013) 170-91.

[24] H.B. Kristensen, T.L. Andersen, N. Marcussen, L. Rolighed, J.M. Delaisse, Increased presence of capillaries next to remodeling sites in adult human cancellous bone, J Bone Miner Res 28(3) (2013) 574-85.

[25] S.L. Teitelbaum, Bone resorption by osteoclasts, Science 289(5484) (2000) 1504-8.

[26] T. Negishi-Koga, H. Takayanagi, Bone cell communication factors and Semaphorins, Bonekey Rep 1 (2012) 183.

[27] N.S. Soysa, N. Alles, Positive and negative regulators of osteoclast apoptosis, Bone Rep 11 (2019) 100225.

[28] S.C. Manolagas, Birth and death of bone cells: basic regulatory mechanisms and implications for the pathogenesis and treatment of osteoporosis, Endocr Rev 21(2) (2000) 115-37.

[29] M.A. Scott, B. Levi, A. Askarinam, A. Nguyen, T. Rackohn, K. Ting, C. Soo, A.W. James, Brief review of models of ectopic bone formation, Stem Cells Dev 21(5) (2012) 655-67.

Chapter 3

VEGF dose controls the coupling of angiogenesis and osteogenesis in engineered bone

Andrea Grosso[1], Maximilian G. Burger[1,2], Alexander Lunger[1,2], Francesca Mai[1], Priscilla S. Briquez[3], Jeffrey A. Hubbell[3], Dirk J. Schaefer[1,2], Andrea Banfi[1,2*], Nunzia Di Maggio[1*]

[1]Cell and Gene Therapy, Department of Biomedicine, Basel University Hospital and University of Basel, Basel, Switzerland;

[2]Department of Plastic, Reconstructive, Aesthetic and Hand Surgery, Basel University Hospital, Switzerland;

[3]Pritzker School for Molecular Engineering, University of Chicago, Chicago IL, USA

**These authors contributed equally*

Introduction

Bone has the intrinsic capacity to heal in response to injury, as well as during skeletal development or remodeling in adult life. In physiological conditions, bone repair is a rapid, well-orchestrated and an efficient process that involves endogenous regenerative potentials to restore the pre-exiting characteristics and function. However, this process can be compromised and may not be sufficient to repair large tissue losses due to trauma, surgery or other clinical conditions [1], and the treatment of these large bone defects is still a significant challenge in clinical practice. Autologous bone transplantation is the current "gold standard" approach to treat critical-size bone defects, but it is associated with several limitations, including chronic pain at the harvest site, neurovascular injury, structural weakness and limited amount of autologous bone available [2].

Tissue-engineered bone grafts are a promising strategy for the treatment of critical-size bone defects. However, the success of these constructs critically depends on rapid vascularization by host blood vessels. In fact, lack of a functional vasculature exposes cells to hypoxia and insufficient nutrients supply and full blood vessels ingrowth may require weeks, until it is achieved. This can lead to loss of cell functionality, impairment of differentiation and also to cell death [3]. Furthermore, the processes of osteogenesis and angiogenesis are biologically coupled: blood vessels provide nutrients, minerals and allow the recruitment of endogenous osteoprogenitors and immune cells, and also serve as structural templates for bone development [4]. Due to their angiocrine functions, blood vessels also provide paracrine signals that coordinate bone development and regeneration, as well as osteoprogenitor differentiation and behaviour [5].

An attractive strategy to drive vascular growth into osteogenic grafts is the supply of specific signals that regulate physiological angiogenesis. Vascular Endothelial Growth Factor (VEGF) is the master regulator of vascular growth both in normal and pathological angiogenesis and is therefore the key target for inducing the therapeutic growth of new blood vessels [6].

Several lines of evidence indicate that VEGF levels of expression must be carefully regulated during osteogenesis *in vivo*. In fact, while physiological levels are required to maintain bone homeostasis, too little VEGF can impair osteoblast differentiation and bone deposition, whereas too much can stimulate excessive bone resorption and likewise lead to bone loss (reviewed in [7]). Therefore, it is of great interest to understand the dose-dependent effects of VEGF delivery on both angiogenesis and osteogenesis for the therapeutic regeneration of vascularized bone. However, this line of investigation is challenging because of the difficulty of precisely controlling the amount of VEGF available in developing osteogenic grafts (reviewed in [8]). Genetic modification of progenitors leads to sustained and uncontrolled overexpression of heterogenous levels within the cell populations. On the other hand, the recombinant VEGF protein has a very short half-life *in vivo* and, while different biomaterial-based approaches have been developed to allow sustained release of angiogenic factors, the kinetics of release are uneven over time and their application to an osteogenic environment remains challenging. Furthermore, the physiological presentation of VEGF to its target cells requires the interaction with extracellular matrix, which orchestrates its activity by regulating its local concentration, bioavailability and signalling [9].

Therefore, here we employed a protein engineering approach to decorate fibrin matrices with homogeneous concentrations of VEGF, in order to both control its dose and recapitulate

its physiological matrix-bound presentation in osteogenic grafts. An engineered version of mouse $VEGF_{164}$ was fused to the octapeptide substrate sequence for the transglutaminase coagulation Factor XIII (TG-VEGF), whereby upon cross-linking of fibrinogen monomers into a fibrin hydrogel, TG-VEGF is covalently linked to the fibrin network. The degradation rate of the fibrin matrix *in vivo* is further controlled by also incorporating a TG-version of the plasmin inhibitor aprotinin. This optimized platform is highly tunable and allows precise control over the dose of VEGF presented to endothelial cells invading the fibrin matrix, while ensuring a duration of about 4 weeks *in vivo* [10].

Taking advantage of this unique platform to engineer a specific signalling microenvironment within osteogenic grafts, we investigated the role of VEGF dose in regulating the effective coupling of angiogenesis and osteogenesis for the therapeutic regeneration of vascularized bone.

Materials and methods

BMSC isolation and culture

Human primary bone marrow mesenchymal stromal cells (BMSC) were isolated from marrow aspirates. The aspirates were obtained from the iliac crest of healthy donors during routine orthopaedic surgical procedures according to established protocols, after informed consent by the patients and following protocol approval by the local ethical committee (EKBB, Ref. 78/07). Cells were isolated and cultured as described [11, 12]. Briefly, after centrifugation, the cell pellet was washed in PBS (Gibco^{TM}, Thermo Fisher Scientific, Waltham, Massachusetts, USA), resuspended in α-MEM medium (Gibco^{TM}, Thermo Fisher Scientific, Waltham, Massachusetts, USA) containing 10% bovine serum (HyClone, South Logan, Utah, USA), 1mM Sodium Pyruvate (Gibco^{TM}, Thermo Fisher Scientific, Waltham, Massachusetts, USA), 10mM HEPES Buffer Solution (Gibco^{TM}, Thermo Fisher Scientific, Waltham, Massachusetts, USA) and 5 ng/ml FGF-2 (R&D System Minneapolis, Minnesota, USA) and plated at a density of 10^5 nucleated cells/cm^2. BMSC were cultured in 5% CO^2 at 37°C.

Generation and in vivo implantation of osteogenic constructs

Osteogenic constructs were prepared as described above in Chapter 2 (Burger and Grosso et al., manuscript submitted). Briefly, fibrin matrices were decorated with recombinant VEGF engineered with a transglutaminase substrate sequence (TG-VEGF) to allow cross-linking into fibrin hydrogels. Fibrin gels were prepared by mixing 25 mg/ml human fibrinogen (plasminogen, von Willebrand Factor-, and fibronectin-depleted; Milan Analytica AG, Rehinfelden, Switzerland), 3 U/mL factor XIIIa (CSL Behring, King of Prussia, Pennsylvania, USA), and 6 U/ml thrombin (Sigma-Aldrich, St. Louis, Missouri, USA) with 2.5 mM Ca2+ in 4-(2-hydroxyethyl)-1- piperazineethanesulfonic acid (Hepes, Lonza, Basel, Switzerland). To

control fibrin degradation *in vivo* a TG-version of the plasminogen inhibitor Aprotinin (TG-Aprotinin) was also incorporated at 51 μg/ml.

Osteogenic grafts were prepared with $1x10^6$ human BMSC and hydroxyapatite granules in a fibrin hydrogel containing different doses of TG-VEGF (0.1, 1 and 100 μg/ml) and implanted subcutaneously in nude mice (CD1-*Foxn1*^{nu}, Charles-River, Sulzfeld, Germany). Animals were treated in agreement with Swiss legislation and according to a protocol approved by the Veterinary Office of Canton Basel-Stadt (permission #1797). Naïve BMSCs were also combined with fibrin matrices with no TG-VEGF as controls. Six constructs were implanted for each condition (n=6-9 samples/group), generated with cells from 3 independent donors (2-3 replicates/donor). After 1, 4 and 8 weeks, mice were sacrificed by inhalation of CO_2 and constructs were explanted.

Histological processing and immunofluorescence tissue staining

Explanted constructs were washed with PBS and fixed overnight at +4°C with freshly prepared 1% paraformaldehyde (Sigma-Aldrich, St. Louis, Missouri, USA) in PBS. Subsequently, the samples were decalcified in a PBS-based solution containing 7% w/v EDTA (0.5M, pH 8, Sigma-Aldrich, St. Louis, Missouri, USA) and 10% w/v sucrose (Sigma-Aldrich, St. Louis, Missouri, USA) and incubated at 37°C on an orbital shaker. The solution was renewed daily for about 20 days, until the samples were fully decalcified, as estimated by the degree of sample stiffness. Finally, the samples were embedded in OCT compound (CellPath LTD, Newtown, UK), frozen in freezing 2-methylbutane (isopentane) (Sigma-Aldrich, St. Louis, Missouri, USA) and 10 μm-thick sections were obtained with a cryostat.

Immunofluorescence staining was performed with the following primary antibodies and dilutions: rat anti-mouse CD31 (clone MEC 13.3, BD Bioscience, San Jose, California, USA) at

1:100; mouse anti-Human nuclei (clone 235-1, Merk Millipore, Darmstadt, Germany) at 1:200; rabbit anti-Ki67 (abcam, Cambridge, UK) at 1:100; rabbit anti-Cleaved Caspase 3 (Asp175; Cell Signaling Technology, Danvers, Massachusetts, USA) at 1:200; mouse anti-human BSPII (Clone LFMb-24, Santa Cruz Biotechnology, California, USA) at 1:50; rabbit anti-mouse BSPII (Clone M-154, Santa Cruz Biotechnology, California, USA) at 1:50. Fluorescently labeled secondary antibodies (Invitrogen, Thermo Fisher Scientific, Waltham, Massachusset, USA) were used at 1:200. Mouse-on-mouse (M.O.M) kit (Vector Laboratories, Inc., Burlingame, California, USA) was used when primary mouse antibodies were applied.

Fluorescence images were acquired with an Olympus BX63 microscope (Olympus, Münster, Germany), a Nikon Ti2 Eclipse (Nikon, Tokyo, Japan) and with 40x objectives on a Carl Zeiss LSM710 3-laser scanning confocal microscope (Carl Zeiss, Oberkochen, Germany). All image measurements were performed with cellSens software (Olympus, Münster, Germany), NIS-Elements (Nikon, Tokyo, Japan) and FIJI software (ImageJ, http://fiji.sc/Fiji).

Angiogenesis

Invasion of osteogenic constructs by blood vessels, as well as vascular density were assessed after 1 week *in vivo* by immunostaining for CD31. Complete images of whole sections from the central part of each sample were acquired (n=6 samples/group) and the area of invasion was measured by tracing the area occupied by blood vessels ($CD31^+$ structures) and expressed as percentage of the total graft area. To quantify vessel density at week 1, at least 15 images were acquired per sample within the invaded areas (n=6 samples/group) and vessel length density (VLD) was measured tracing the total length of vessels in the fields and by normalizing it to the field area (mm/mm^2). Total vessels length (mm) was obtained multiplying the measured VLD by the area invaded by blood vessels. VLD at 4 and 8 weeks

was quantified on 15 randomly acquired images, covering all the area of the tissue section, since constructs were completely invaded by these time-points.

Proliferation and apoptosis

Proliferation and apoptosis of implanted human progenitor cells were quantified after 1 week *in vivo* by immunostaining for Ki67 or Cleaved-Caspase3, respectively, together with anti-Human nuclei. Images of whole sections for each condition (n=6 samples/group) were divided in three concentric layers, each spanning a depth of 500 µm from the external surface, and the remaining central part was considered the core (Fig. 3A). $Ki67^+$ or $Caspase3^+$ human cells were manually counted in 6-8 fields of 300 μm^2-area within each layer and expressed as percentage of the total number of human cells in the field.

Bone formation

Bone tissue was detected by Masson's trichrome staining (Réactifs RAL, Martillac, France), performed according to manufacturer's instructions. Ten whole-section reconstructions per sample (n=6 samples/group) were acquired with transmitted light and bone tissue was quantified tracing the area occupied by mineralized matrix (dark green staining) and normalizing it by the total area of the section. In addition, the presence of mature bone (red staining) matrix was measured and normalized by the total amount of bone.

Osteoclast detection

In order to detect osteoclasts, sections were stained for tartrate-resistant acid phosphatase (TRAP) activity. Briefly, after rinsing with water, slides were incubated for 20 minutes with 0.1M Acetate Buffer (0.2M Sodium Acetate, 0.2M Acetic Acid, 50mM Sodium L-tartrate dibasic dihydrate, pH 5.0) and then stained with 1 mg/ml of Fast Red LB salt (Sigma-Aldrich, St. Louis, Missouri, USA) and 1 mg/ml of naphtol AS-MX phosphate (Sigma-Aldrich,

St. Louis, Missouri, USA) dissolved in 0.1M acetate buffer for 1 hour at 37°C. After TRAP staining, nuclear counter staining was performed with Haematoxylin for 1 min at room temperature. TRAP-positive cells were quantified on 15 randomly-chosen fields per construct in 6 constructs/condition (n=6 samples/group). Multinucleated TRAP+ cells in the fields were counted manually and the total number was normalized by the field area.

Quantification of bone sialoprotein II (BSPII)

To quantify the amount of human BSP, immunofluorescence staining was performed and 5-7 random fields (n=6 samples/group) were acquired per each condition. The amount of human BSP was quantified using a custom-made macro in FIJI software. Briefly, a region of interest (ROI) was traced, thresholding was applied to the human BSP channel and the number of pixels above the threshold was normalized by the total number of the pixels of the ROI. The number of human cells (detected by immunofluorescence staining for an anti-human nuclei antibody) was quantified automatically on a whole section per each sample (n=6 samples/group) using FIJI software and normalized by the tissue area.

Quantitative real-time PCR

For RNA extraction from osteogenic grafts, constructs were immediately frozen in liquid nitrogen after harvesting (n=8-10 samples/group). Tissues were disrupted and homogenized using a Qiagen Tissue Lyser (Qiagen, Basel, Switzerland) in 1 ml TRIzol Reagent (Thermo Fisher Scientific, Waltham, Massachusetts, USA) for every 100 mg of tissue. Total RNA from lysed tissues was isolated with a RiboPure RNA purification kit (Thermo Fisher Scientific, Waltham, Massachusetts, USA) according to manufacturer's instruction. Total RNA from *in vitro*-cultured human BMSC (n=6, from 3 independent donor) was isolated with a Quick-RNA

Miniprep plus kit (Zymo Research Europe GbmH, Freiburg im Breisgau, Germany) according to manufacturer's instruction.

RNA from tissues and human BMSC was reverse-transcribed into cDNA with the SuperScript III Reverse Transcriptase (Thermo Fisher Scientific, Waltham, Massachusetts, USA). Quantitative Real-Time PCR (qRT-PCR) was performed on an ABI 7300 Real-Time PCR system (Applied Biosystems, Foster City, California, USA). Expression of genes of interest was determined using the following human-specific TaqMan gene expression assays (Thermo Fisher Scientific, Waltham, Massachusetts, USA): Runx2 (Hs01047973_m1); SP7/Osterix (Hs01866874_s1); BSP (Hs00913377_m1); BGLAP/Osteocalcin (Hs01587814_g1). Reactions were performed in duplicate for each template, and normalized to expression of the GAPDH housekeeping gene (Hs02786624_g1).

Statistics

Data are presented as mean ± standard error of the mean (SEM). The significance of differences was assessed with the GraphPad Prism 8 software (GraphPad Software, San Diego, California, USA). The normal distribution of all data sets was tested and, depending on the results, multiple comparisons were performed with the parametric one-way analysis of variance (ANOVA) followed by the Bonferroni test, or with the nonparametric Kruskal–Wallis test followed by Dunn's post-test. Percentage of proliferating and dying human cells were first normalized by log2-transformation and then analyzed by one-way ANOVA followed by Bonferroni test for multiple comparisons. Differences were considered statistically significant if $p<0.05$.

Results

Increasing VEGF doses impair rapid vascular invasion and determine the distribution of vascular growth

Vascularization of the constructs by host blood vessels needs to occur rapidly within the first week after *in vivo* implantation to ensure survival of the implanted progenitor cells. Therefore, osteogenic constructs were harvested after 1 week *in vivo* and tissue sections were immunostained for CD31 to assess vascular invasion. Reconstructions of whole construct sections were acquired under fluorescent light (Fig. 1A) and areas invaded by blood vessels were traced according to the presence of CD31 staining (in yellow in Fig. 1A) and quantified. As expected, blood vessel growth started from the surrounding tissue and remained confined at the periphery of the control constructs (Naïve), while significantly larger areas of the grafts containing 0.1 μg/ml of TG-VEGF were already invaded by blood vessels. Surprisingly, higher doses of TG-VEGF not only did not further increase vascular invasion, but actually prevented it, as invaded areas were similar to the control condition with no VEGF at all (Fig. 1A). In fact, quantifications showed that while 0.1 μg/ml of TG-VEGF dose accelerated vascular invasion to reach about 30% of the total graft area in the first week (Fig. 1B; TG-VEGF 0.1=24.9±4.8% vs Naïve=9.5±1.9%, $p<0.05$), increasing TG-VEGF doses did not improve vascular invasion compared to the Naïve condition (TG-VEGF 1=10.1±2.7%, TG-VEGF 10=10.5±3.1%, TG-VEGF 100=8.2±2.6%; p=n.s.).

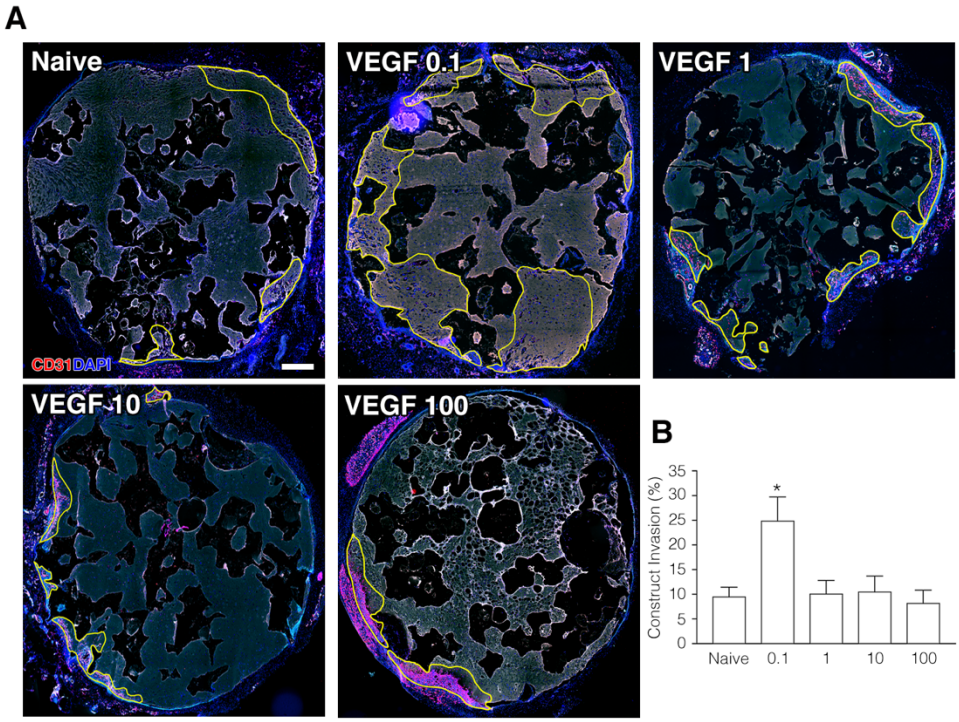

Figure 1. *(A) Reconstruction of graft sections under fluorescent light to evidence the areas of blood vessel growth (in yellow); (B) Quantification of the areas invaded by blood vessels. (*=p<0.05). Scale bar = 500 µm.*

In order to determine whether increasing TG-VEGF doses actually impaired vascular growth or just vessel migration into the constructs, vascular density was assessed within the invaded areas after immunostaining for CD31 (Fig. 2A) by quantification of vessel length density (VLD), defined as millimeters of vessel length per square millimeter of tissue area (Fig. 2B). Interestingly, 0.1 µg/ml of TG-VEGF did not increase VLD compared to controls, whereas higher doses progressively increased vascular density within the invaded areas (Naïve=8.2±0.9 mm/mm^2, TG-VEGF 0.1=7.8±0.6 mm/mm^2, TG-VEGF 1=11.5±2.6 mm/mm^2, TG-VEGF 10=23.2±3.9 mm/mm^2, TG-VEGF 100=35.2±7.2 mm/mm^2). Since the area of vascular invasion and the vessel density within those areas appeared to be inversely regulated by TG-VEGF dose, the total amount of vascular growth was measured by quantifying the total vessel length in each construct, i.e. VLD in each area of invasion multiplied by the surface of the area itself. This quantification showed that all TG-VEGF doses stimulated vascular growth within

the constructs without significant differences (Fig. 2C) (Naïve=13.0±2.5 mm, TG-VEGF 0.1=25.0±3.7 mm, TG-VEGF 1=17.7±2.9 mm, TG-VEGF 10=37.4±10.1 mm, TG-VEGF 100=30.7±6.3 mm; p=n.s.). Therefore, these results suggest that VEGF dose determined how the induced vascular growth distributes within the construct, with a low dose favoring rapid ingrowth while maintaining density similar to controls, and higher doses slowing effective ingrowth, thereby increasing vessel density in the periphery.

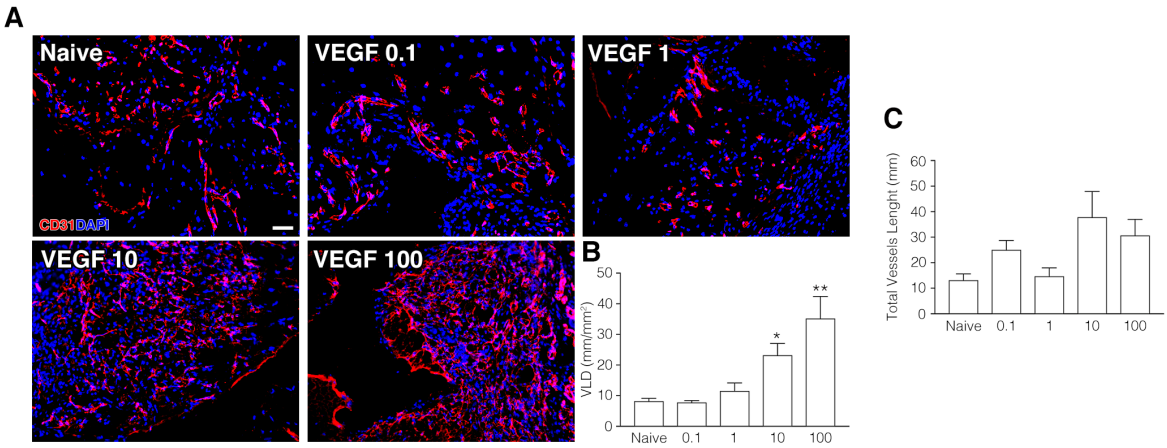

Figure 2. *(A) Immunostaining of endothelium (CD31, in red) and nuclei (DAPI, in blue) of areas invaded by blood vessels after 1 week of in vivo implantation; (B) quantification of induced angiogenesis, after 1 week in vivo, expressed as VLD (vessel length density), calculated as millimeters of vessel length per square millimeter of tissue area (mm/mm^2); (C) quantification of total vessel length within the invaded areas, expressed as mm. (*=p<0.05, **=p<0.01). Scale bar = 100 µm.*

Only a low TG-VEGF dose promotes human progenitor proliferation and survival down to the core

To investigate the functional effects of the rapid vascular invasion provided by a low dose (0.1 µg/ml) of TG-VEGF, proliferation and apoptosis of the implanted human cells were analyzed at different levels of depth inside the graft, by arbitrarily designing four concentric areas: 3 layers each spanning a depth of 500 µm and a the central core of about 1 mm radius (Fig. 3A). Tissue sections were immunostained with an antibody that specifically recognizes

human cell nuclei (HuNu), in combination with a marker for proliferation (Ki67) or apoptosis (Cleaved-Caspase3, Cas3), as exemplified in Figure 3B and 3C, and human cells positive for either marker were counted in each layer for every condition. A clear trend of decreasing proliferation was observed at increasing depths towards the centre of the graft in each condition, with the notable exception of the 0.1 ug/ml dose of TG-VEGF, which significantly increased the proportion of proliferating human progenitors in each layer compared to all other conditions (Fig. 3D). Interestingly, even deep inside the core, grafts containing 0.1 μg/ml of TG-VEGF enabled human progenitors to proliferate similarly to the middle layer of all other conditions (TG-VEGF 0.1 = 2.0±0.4% $Ki67^+$ human cells vs 1-2% for all other conditions in the middle layer), despite being about 1 mm deeper (Core depth = 1.5-2.5 mm; Middle layer depth = 0.5-1 mm).

Conversely, quantification of $Cas3^+$ human cells showed a clear trend of increasing apoptosis, for each condition, from the surface towards the core of the graft (Fig. 3E). While no significant difference between the conditions was observed in the outer layer of the grafts, only 0.1 μg/ml of TG-VEGF significantly promoted human cells survival in all deeper layers down to the core, never exceeding the frequency of apoptotic cells of the outer layer (TG-VEGF 0.1 Core = 3.8±0.7% $Cas3^+$ human cells vs 2-3% for all other conditions in the outer layer).

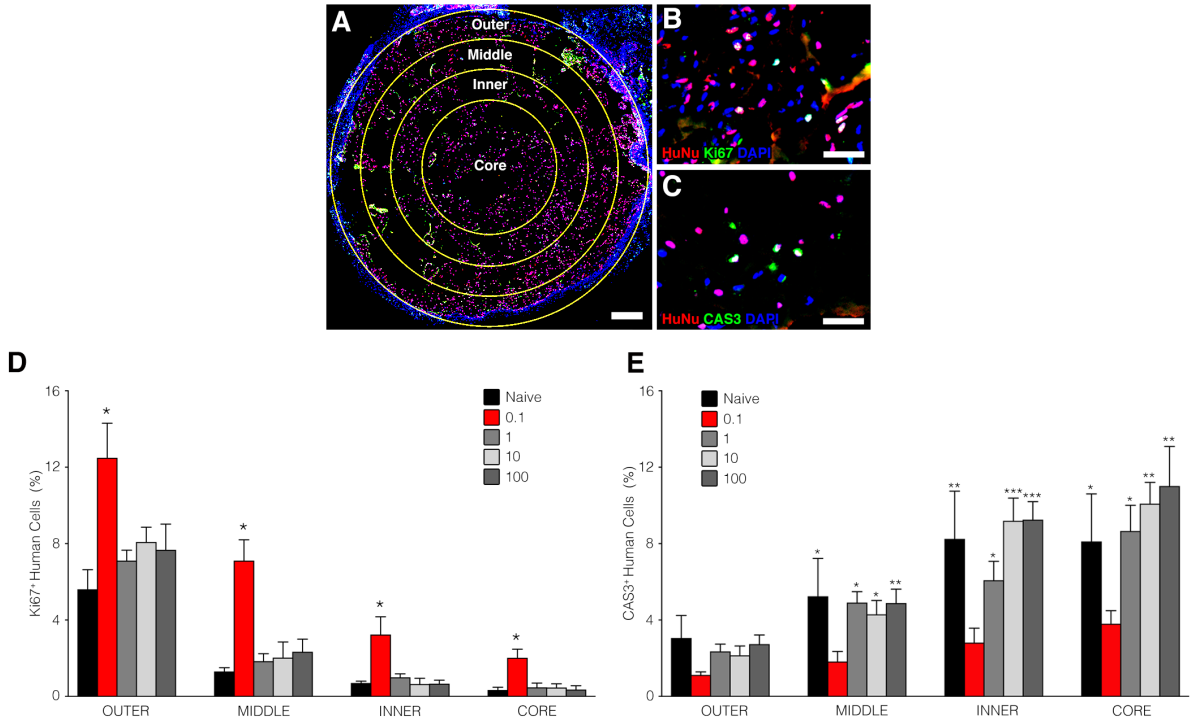

Figure 3. *(A) Reconstruction of graft sections under fluorescent light (layer subdivision in yellow); (B) Example of immunostaining of human nuclei (HuNu, in red), proliferating cells (Ki67, also in the nucleus, in green) and all nuclei (DAPI, in blue) of constructs (representative picture of the outer layer of TG-VEGF 0.1 condition) after 1 week of in vivo implantation; (C) Immunostaining of human nuclei (HuNu, in red), dying cells (CAS3, also in the nucleus, in green) and all nuclei (DAPI, in blue) of constructs (representative picture of the middle layer of TG-VEGF 10 condition) after 1 week of in vivo implantation (D) Quantification of proliferating human cells (%) in each layer (*=p<0.05). (E) Quantification of dying human cells (%) in each layer (*=p<0.05, **=p<0.01, ***=p<0.001). (A) Scale bar = 500 µm; (B, C) Scale bar = 50 µm.*

TG-VEGF dose-dependently increases steady-state vascular density

Four weeks after *in vivo* implantation constructs were completely invaded by blood vessels in all conditions. Vascularization was still increased by increasing TG-VEGF doses as shown by the presence of more $CD31^+$ structures (Fig. 4A) compared to the constructs containing only Naïve cells. Quantification of vessel length density (Fig. 4A-B), showed that global vascular density was progressively increased by increasing TG-VEGF doses starting from 1 µg/ml compared to the Naïve condition (Naïve =1.3±0.1 mm/mm^2, TG-VEGF 0.1=1.9±0.1 mm/mm^2, TG-VEGF 1=2.2±0.1 mm/mm^2 p<0.001; TG-VEGF 10=3.7±0.2 mm/mm^2 p<0.001;

TG- VEGF 100=5.8±0.3 mm/mm^2 p<0.001). After 8 weeks, vascular density remained similar to what was observed at the 4 week time-point (Fig. 4C-D; Naïve=1.63±0.1 mm/mm^2, TG-VEGF 0.1=1.6±0.1 mm/mm^2, TG-VEGF 1=2.5±0.1 mm/mm^2 p<0.001; TG-VEGF 10=2.5±0.1 mm/mm^2 p<0.001; TG-VEGF 100=5.0±0.3 mm/mm^2 p<0.001). These results show that the steady-state had been reached by 4 weeks and the induced vasculature was stable.

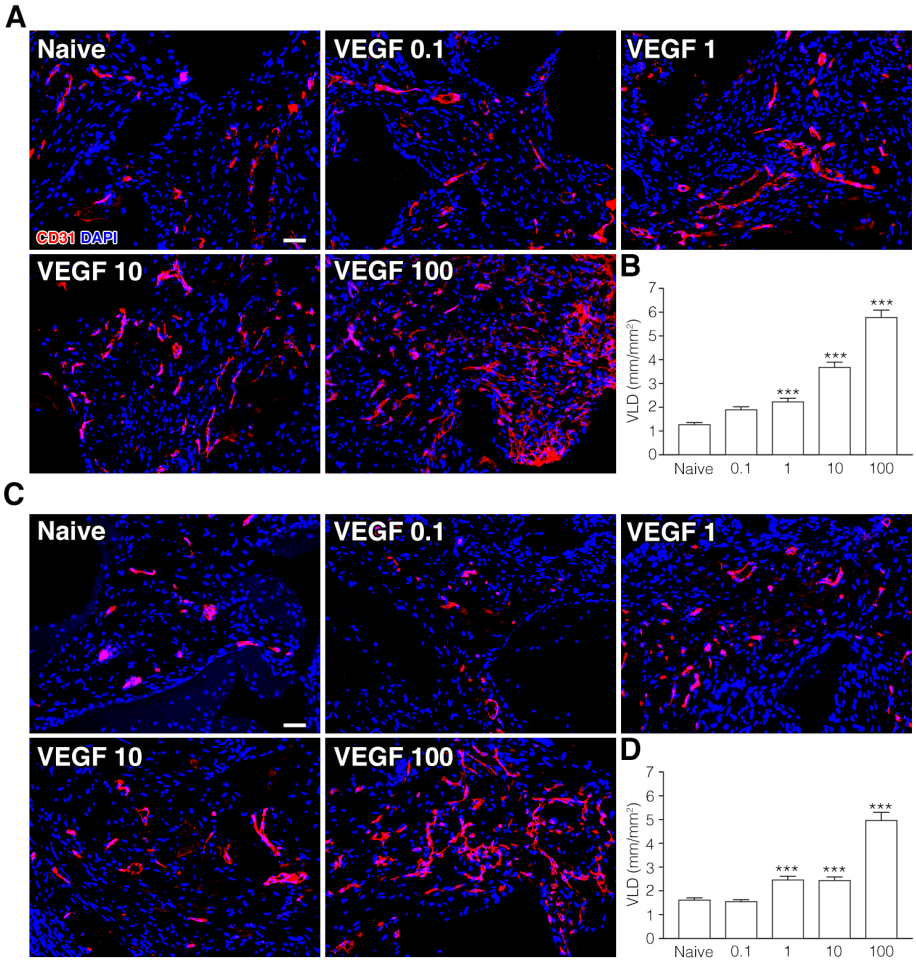

Figure 4. *Immunostaining of endothelium (CD31, in red) and nuclei (DAPI, in blue) of constructs after 4 (A) and 8 (C) weeks of in vivo implantation; Quantification of vessel length density (VLD), expressed as millimeters of vessel length per square millimeter of tissue area (mm/mm^2) after 4 (B) and 8 (D) weeks of in vivo implantation (***=p<0.001). Scale bar = 100 µm.*

TG-VEGF dose-dependently impairs bone tissue formation

Bone matrix deposition was assessed with Masson's trichrome staining, which shows the presence of compact collagen fibers in green and of elastic fibers in red [11]. After 4 weeks in vivo, fibrin was almost completely degraded and initial formation of a dense collagenous matrix could be observed at the interface with the hydroxyapatite granules (dark green stain in Fig. 5A). However, grafts with TG-VEGF doses higher than 1 µg/ml contained almost only fibrous tissue. Quantification of the areas occupied by dense collagenous matrix (Fig. 5B) showed that only 0.1 µg/ml TG-VEGF dose supported matrix deposition as efficiently as in the Naïve condition (Naïve=1.2±0.2% and TG-VEGF 0.1=1.0±0.2%; p=n.s.). In constructs containing higher TG-VEGF doses, instead, dense matrix deposition was progressively impaired (TG-VEGF 1=0.6±0.1 %, TG-VEGF 10=0.1±0.1%, TG-VEGF 100=0.04±0.0%; p<0.05 vs Naïve and TG-VEGF 0.1).

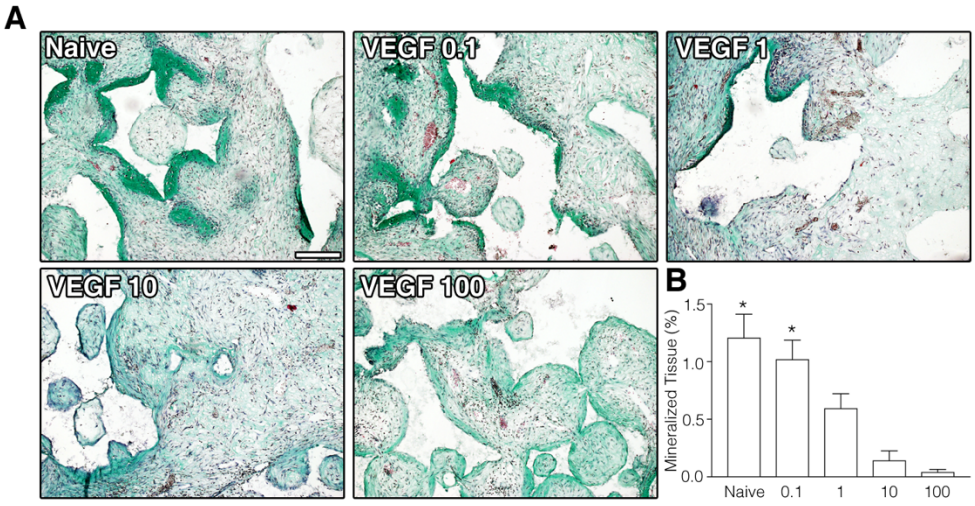

Figure 5. *(A) Representative images of Masson's trichrome staining of constructs 4 weeks after in vivo implantation (dense collagenous tissue in green). (B) Quantification of areas occupied by dense collagenous matrix (expressed as % of construct area; *=p<0.05). Scale bar = 200 µm.*

After 8 weeks, frank bone tissue formation could be observed, characterized by dense collagenous matrix with organized collagen fibers and the presence of osteocyte lacunae

(Fig. 6A). Quantification of bone matrix showed that bone formation was severely and dose-dependently impaired by TG-VEGF doses higher that 1 µg/ml, whereas the 0.1 µg/ml dose supported bone tissue formation as efficiently as in the Naïve condition (Fig. 6B: Naïve=8.1±0.6%, TG-VEGF 0.1=8.5±0.8%, TG-VEGF 1=3.3±0.3%, TG-VEGF 10=1.7±0.4%, TG VEGF 100=0.3±0.1%; $p<0.001$ for Naïve and TG-VEGF 0.1 vs all other conditions).

Masson's trichrome staining also allows the evaluation of the degree of maturation of bone tissue, characterized by the deposition of elastic fibers and detected by a red staining. Mature bone tissue was mainly found in constructs containing Naïve MSC alone or in combination with 0.1 µg/ml of TG-VEGF (Fig. 6A). Interestingly, quantification of the areas occupied by elastic fibers (Fig. 6C, expressed as percentage of total bone tissue formed) showed that that the 0.1 µg/ml TG-VEGF dose could significantly increase the amount of mature bone tissue compared to all other conditions (TG-VEGF 0.1=5.4±1.4% vs Naïve=2.5±1.1%, TG-VEGF 1=1.4±0.5%, TG-VEGF 10=1.3±0.9%, TG-VEGF 100=0.7±0.4%; $p<0.05$).

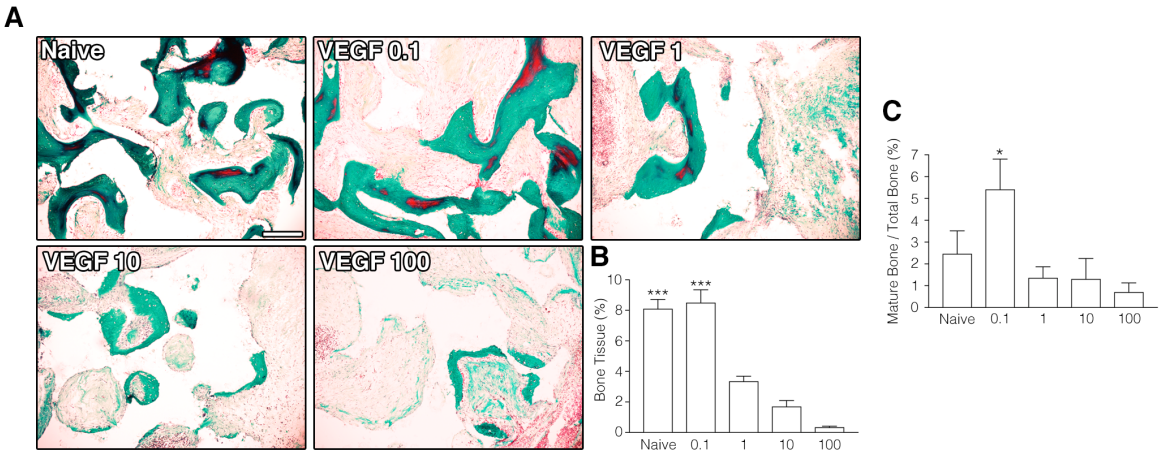

Figure 6. *(A) Representative pictures of Masson's trichrome staining of constructs 8 weeks after in vivo implantation (bone tissue in green, elastic fibers in red); (B) Quantification of areas occupied by bone tissue (expressed as % of construct area); ***=p<0.001; (C) Quantification of areas occupied by mature bone (expressed as % of total bone tissue); *=p<0.05. Scale bar = 200 µm.*

TG-VEGF dose-dependently stimulates bone resorption

The amount of bone tissue depends on the balance between deposition by osteoblasts and resorption by osteoclasts. Therefore, osteoclast recruitment was assessed by staining for the osteoclast-specific enzyme tartrate-resistant acid phosphatase (TRAP). Few TRAP-positive cells were detected in the constructs with Naïve BMSC alone or in combination with 0.1 µg/ml TG-VEGF, in close proximity to the bone matrix or at the interface with the hydroxyapatite granules, both at 4 and 8 weeks (Fig. 7A and 7C). However, constructs containing higher TG-VEGF doses showed a greater density of TRAP-positive cells at both time-points. Quantification of the number of $TRAP^+$ multinucleated cells per tissue area ($TRAP^+$ MNC/mm^2) in the different conditions showed that TG-VEGF doses of 1 µg/ml or higher significantly increased osteoclast recruitment compared to the Naïve conditions at both time points (Fig. 7B and 7D; 4 weeks: Naïve=15.3±1.6 $TRAP^+$ MNC/mm^2, TG-VEGF 1=30.0±2.7, TG- VEGF 10=37.4±2.5, TG-VEGF 100=41.0±4.6; 8 weeks: Naïve=23.4±1.7 $TRAP^+$ MNC/mm^2, TG-VEGF 1=40.0±2.7, TG-VEGF 10=37.4±3.2, TG-VEGF 100=44.6±3.8). Constructs containing 0.1 µg/ml of TG-VEGF, instead, did not increase osteoclast recruitment compared to BMSC alone (TG-VEGF 0.1=17.1±2.0 at 4 weeks and 24.2±1.9 at 8 weeks, p=n.s. vs Naive).

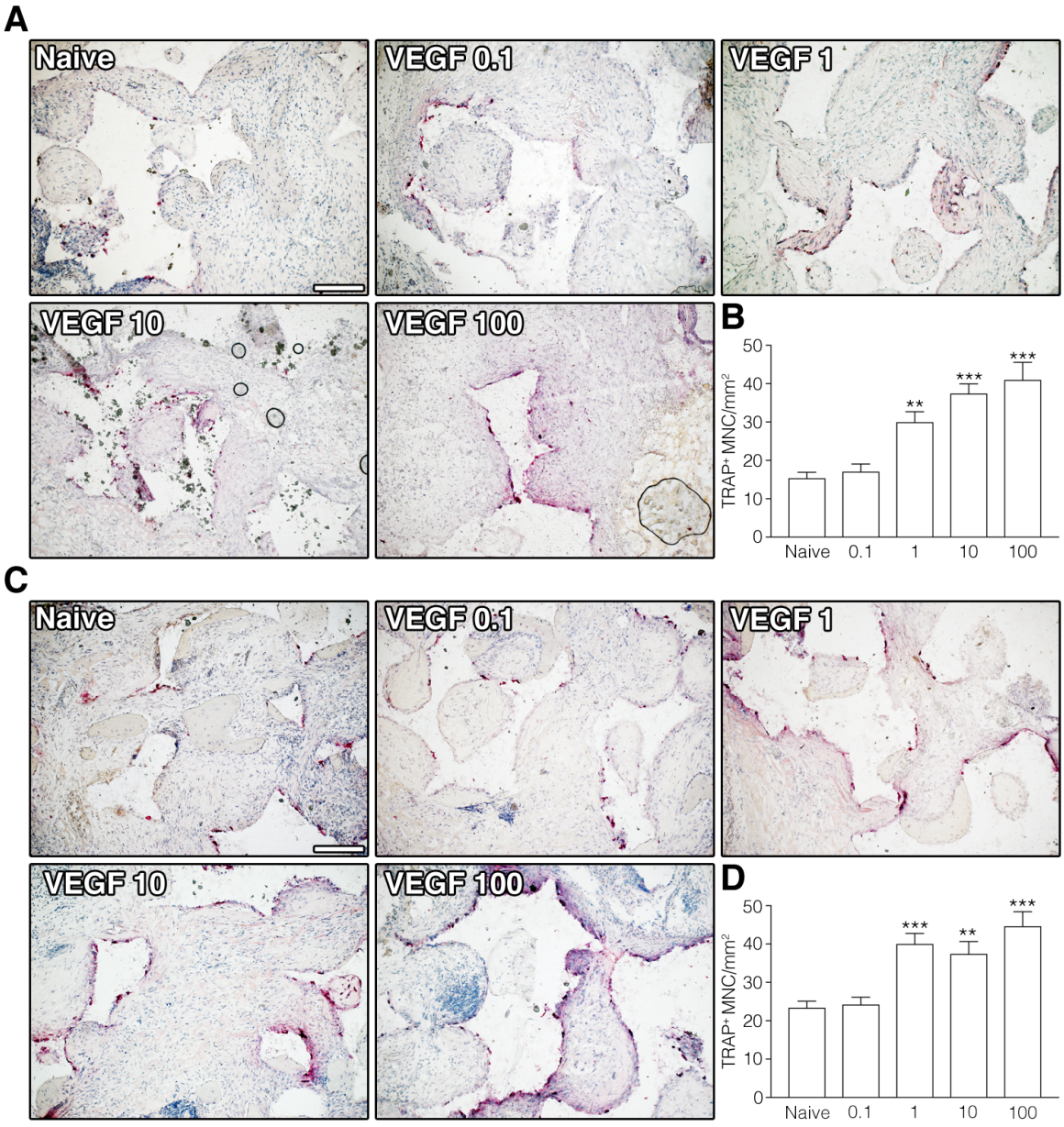

Figure 7. *(A, C) Histochemical stain for TRAP activity (red) and nuclear counterstaining with hematoxylin (blue) of constructs 4 (A) and 8 (C) weeks after in vivo implantation; (B, D) Quantification of Trap⁺ multinucleated cells (MNC) per tissue area (mm²) after 4 (C) and 8 (D) weeks; **=p<0.01, ***=p<0.001. Scale bar = 200 µm*

TG-VEGF dose-dependently impairs osteogenic differentiation of human progenitors in vivo

In order to evaluate the VEGF dose-dependent effects on bone homeostasis, we also investigated its influence on osteogenic differentiation of the implanted human BMSC. Since bone differentiation is a dynamic process and the first appearance of bony matrix *in vivo* takes about 4 weeks, expression of human-specific osteogenic genes was measured on samples harvested 1 and 4 weeks after *in vivo* implantation and compared to their expression in the undifferentiated BMSCs cultered *in vitro*, right before implantation. As shown in Fig. 8A, after 1 week (black dots), the expression of human Runx2, Osterix (OSX), Bone sialoprotein (BSP) and Osteocalcin (OCN) in all conditions was similar to that of undifferentiated cells *in vitro* (dotted line, gray area), indicating that ostegenic differentiation had not started yet. After 4 weeks (red dots), all osteogenic genes were strongly upregulated in constructs containg BMSC alone as well as 0.1 µg/ml of TG-VEGF, indicating robust differentiation. However, in constructs containing 100 µg/ml of TG-VEGF, which displayed reduced bone mass, the upregulation of osteogenic gene expression was significantly impaired compared to the other conditions and barely greater than the undifferentiated controls. Gene expression data were confirmed by immunostaining for human bone sialoprotein protein (hBSP, in red Fig. 8B and 8E) on tissue sections. These showed a significant loss of human BSP protein in the presence of high TG-VEGF both after 4 and 8 weeks, whereas BSP production by human cells was preserved with the low TG-VEGF dose of 0.1 µg/ml in comparison with the Naïve condition.

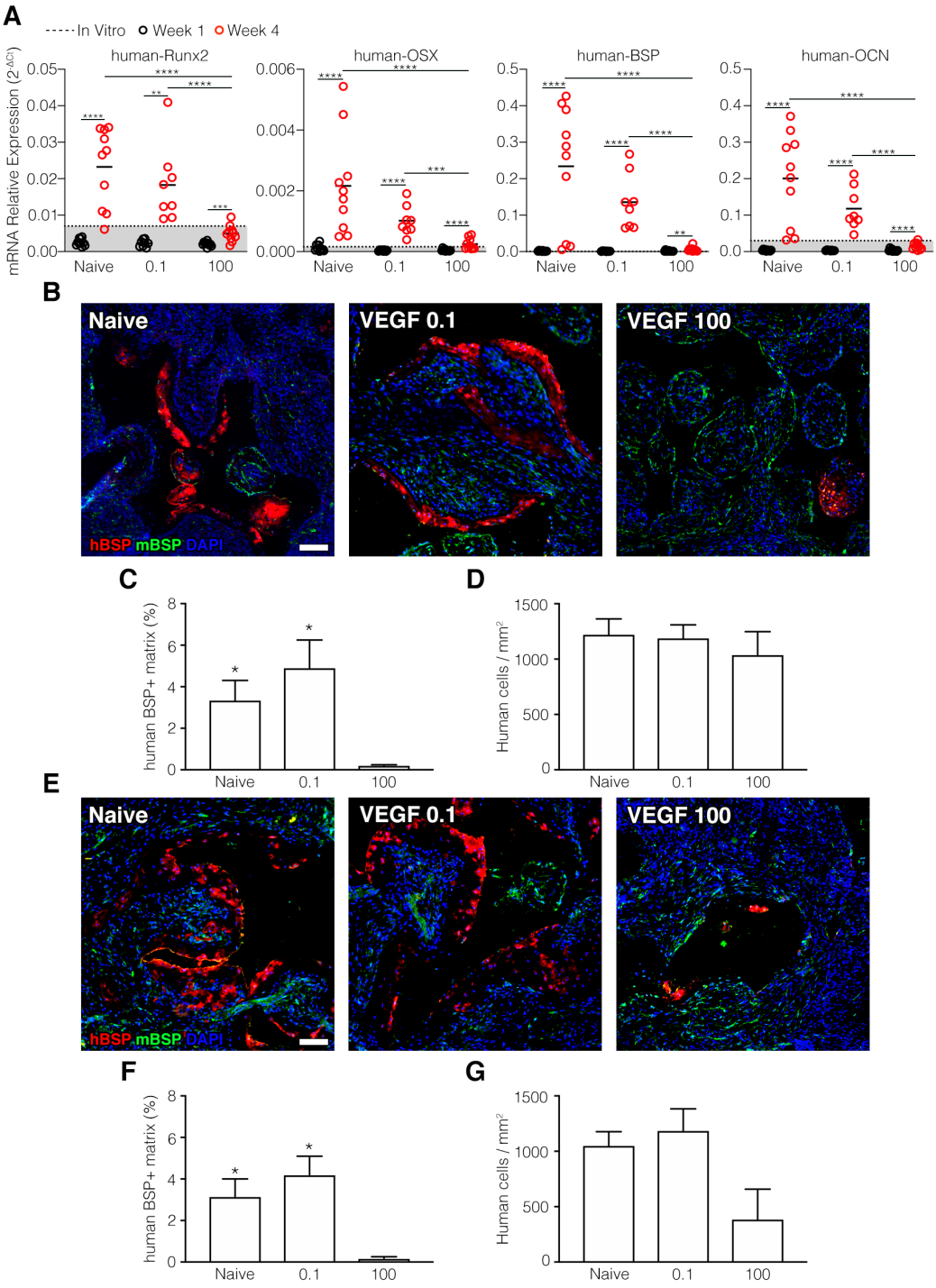

Figure 8. *(A) Gene expression of human Runx2, OSX, BSP and OCN was quantified by qRT-PCR and expressed as relative expression to human GAPDH ($2^{-\Delta Ct}$). Data represent the values of individual samples (colored dots) and the mean (black bar; n= 8-10); **=p<0.01, ***=p<0.001, ****=p<0.0001. Dotted line and grey area = expression range of undifferentiated hBMSC in vitro; black dots = 1 week; red dots = 4 weeks. (B, E) Immunostaining of osteogenic constructs 4 (B) and 8 (E) weeks after in vivo implantation for human BSP (hBSP, red), mouse BSP (mBSP, green) and nuclei (DAPI, blue). (C, F) Quantification of human BSP positive matrix after 4 (C) and 8 (F) weeks expressed as percentage of total tissue area. (D, G) Quantification of the number of human cells per tissue area (mm^2) after 4 (D) and 8 (G) weeks; *p<0.05; Scale bar = 100 µm.*

In order to determine whether the loss of human-derived osteogenic matrix was due to a specific impairement of human BMSC-derived osteoblast differentiation or their loss, the amount of human BSP-positive matrix was quantified and correlated to the number of human cells present in each condition. The number of human cells was similar among all conditions after 4 weeks (Fig. 8D; Naïve=1220±143.6 cells/mm^2, TG-VEGF 0.1=1186±123.7 cells/mm^2, TG-VEGF 100=1036±212.5 cells/mm^2; p = n.s.), showing that initial osteoprogenitor survival and engraftment was not affected by VEGF at any dose. However, the amount of human BSP positive matrix was significantly reduced in the presence of 100 µg/ml of TG-VEGF compared to BMSC alone, but not with 0.1 µg/ml of TG-VEGF (Fig. 8C; Naïve=3.33±0.97%, TG- VEGF 0.1=4.66±1.17%, TG-VEGF 100=0.19±0.06%; $p<0.05$). These data strongly suggest that high VEGF doses specifically impair differentiation of the implanted human BMSC, without affecting their initial engraftment. After 8 weeks (Fig. 8E), human BSP protein abundance was stable compared to 4 weeks and significantly reduced in the presence of 100 µg/ml of TG-VEGF, but not with 0.1 µg/ml (Fig. 8F; Naïve=3.13±0.97%, TG- VEGF 0.1=4.18±0.91%, TG-VEGF 100=0.15±0.11%; $p<0.05$). However, by this later time-point the frequency of human cells appeared also reduced in grafts containing 100 µg/ml of TG-VEGF, although the difference was not statistically significant (Fig. 8G; Naïve=1048±128.8 cells/mm^2, TG-VEGF 0.1=1183±200.3 cells/mm^2, TG-VEGF 100=382.9±275.1 cells/mm^2). Interestingly, BSP of murine origin (stained in green) could be found both at 4 (Fig. 8B) and 8 weeks (Fig. 8E), but in different locations compared to human BSP, mainly within the matrix in between the granules, and it was similarly expressed in all conditions (data not shown).

Discussion

In this study we found that VEGF dose-dependently controls both the kinetics of vascular in-growth and the efficiency of bone formation in osteogenic grafts. Effective and optimal coupling of the two processes requires a low VEGF dose in the graft microenvironment (0.1 μg/ml) and both are progressively disrupted by higher doses. The underlying mechanism is complex and comprises distinct and opposing effects on vessel migration inside the constructs, bone resorption through osteoclast recruitment and bone formation through osteoprogenitor differentiation. The balance between these processes is directed towards robust formation of vascularized bone at low VEGF doses, but is skewed towards net bone catabolism and failure of osteogenesis with increasing VEGF signaling.

In order to ensure the survival of the osteoprogenitor cells seeded into the initially avascular osteogenic grafts, blood vessels in-growth has to be stimulated from the surrounding pre-existing vascular network. In fact, it has become clear that improving vascularization is fundamental for the design and the clinical application of bone grafts [13]. However, most of the studies mainly focused on inducing a greater amount of blood vessels within the implant, without taking in consideration the kinetics of growth. As we have shown here, progenitors survival depends on the extent of vascular invasion rapidly achieved within 1 week rather than on its density. In fact, the vascular density induced spontaneously, in the grafts containing only BMSC, but not VEGF, was sufficient to support osteogenesis. Moreover, it can be noted how after 4 weeks the steady-state vascular density was significantly reduced by 5 to 10 times compared to the initial growth after 1 week at all VEGF doses and it remained stable at 8 weeks. This observation further reinforces the notion that the spontaneously

occurring vascular density is more than sufficient to support physiological tissue formation, while the speed of vascular invasion is a more important therapeutic target.

The observation that higher VEGF doses impaired active vascular migration inside the graft and rather promoted vessel expansion at the graft surface, leading to high vascular densities in limited areas, is remarkable. Considering the different mechanisms, by which new vessels grow, may suggest an explanation for this phenomenon. In fact, rapid invasion of an avascular tissue, such as an implanted graft, takes place by the process of vascular sprouting [14]. Sprouting angiogenesis is guided by the formation of VEGF concentration gradients, which determine the specialization of activated endothelial cells into two functionally distinct phenotypes: tip and stalk. Tip cells respond to the gradient distribution by migrating toward its source, while stalk cells proliferate behind and form the new vessel lumen [15]. Therefore, coordinated endothelial migration and proliferation are required for new vascular structures to enter avascular tissue and be guided towards the source of VEGF production, i.e. the hypoxic areas in need of blood supply. However, vascular growth can also take place by the alternative mechanism of intussusception, or splitting angiogenesis. In this case, endothelial cells proliferate without migrating, leading to circumferential enlargement of pre-existing vessels, which subsequently split longitudinally to form new structures [16]. This mode of vascular growth is highly efficient to expand pre-existing networks, but does not have an intrinsic directional component, leading rather to increases in vessel density than to invasion. Recent unpublished findings suggest that splitting angiogenesis may result from higher doses of VEGF, which saturate the extracellular matrix of the vessel microenvironment and therefore present endothelial cells with a flat concentration profile rather than a gradient (Gianni-Barrera, R.; Banfi, A. et al. manuscript in preparation). Preferential activation of splitting angiogenesis by higher VEGF doses, and its associated inhibition of endothelial

migration, could explain the observed delay in vascular invasion of grafts decorated with concentrations greater than 1 μg/ml of TG-VEGF. In fact, TG-VEGF is released from the fibrin hydrogel upon enzymatic cleavage and becomes available both for signaling and for binding to the extracellular matrix: if its concentration is sufficient to saturate the microenvironment surrounding the graft, the lack of a gradient would direct endothelium to proliferate without migration, leading to enlargement and splitting rather than sprouting towards the core of the graft. On the other hand, the release of lower VEGF concentrations may allow the formation of a gradient suitable for endothelial sprouting and effective migration inside the graft. The dichotomy between vascular expansion and in-growth determined by increasing VEGF doses carries functional implications for human osteoprogenitors survival, which was directly proportional to the extent of blood vessels invasion and not to their density.

The initial discrepancy in vascular invasion was a transient phenomenon, as all grafts were fully vascularized with all VEGF doses after 4 weeks. A likely explanation is related to the transient nature of the fibrin-bound delivery of VEGF: as fibrin degrades over this time-frame, the “barrier” of high VEGF concentration also is lost and the endothelium is again exposed to moderate VEGF concentrations and microenvironmental gradients conducive to migration inside the tissue. Therefore, high VEGF doses do not stably prevent vascular invasion, but rather delay it over the crucial initial time window of 1 week, increasing progenitor apoptosis and decreasing their proliferation.

On the other hand, VEGF is also known to play key roles in bone development, both in intramembranous and endochondral ossification, as well as during bone repair. Its loss causes skeletal deficits and malformities [17, 18]. Both osteoprogenitors and osterix-positive osteoblasts express VEGF receptors (especially VEGF-R2) and VEGF can directly regulate their differentiation and activity maintaining bone homeostasis, through paracrine and intracrine

mechanisms [19]. Here we found that VEGF signaling controls several processes at the crossroads of angiogenesis and osteogenesis in a dose-dependent manner, with clear implications for the therapeutic development of osteogenic grafts. In fact, while a low dose of 0.1 µg/ml improves both the speed of vascular ingrowth and the early survival of seeded osteoprogenitors, higher doses not only delay optimal angiogenesis, but also significantly impaired bone tissue formation. Beyond confirming the previously found effect on stimulating excessive osteoclast recruitment and bone resorption [11], here we uncovered a specific impairment of osteoprogenitors differentiation by increasing VEGF doses. In fact, while 0.1 µg/ml of VEGF ensured the activation of osteogenic differentiation genes (Runx2, OSX, BSP, OCN) in human cells, 100 µg/ml of VEGF dramatically impaired their upregulation. The impairment of osteoblast development was not accompanied by any loss of implanted human osteoprogenitors, which engrafted similarly in all conditions, showing a specific effect on the cell fate decision of osteogenic commitment. Therefore, VEGF dose-dependently impairs bone formation through 2 parallel mechanisms, i.e. by both increasing osteoclast recruitment and impairing osteoblast differentiation, which in combination lead to greatly decreased net bone mass already after 4 weeks of *in vivo* implantation.

Despite the acceleration of vascular invasion and the improvement of osteoprogenitor survival over the first week afforded by the optimal VEGF dose of 0.1 µg/ml, the amount of bone tissue formed was not increased compared to the Naïve condition, although the amount of mature bone was improved. This was expected, since the model we used was not critical, meaning that the small size of the subcutaneous grafts enables efficient formation of bone throughout the constructs without the need to stimulate vascular invasion. Based on the results obtained in this standardized and medium-throughput model, the optimal VEGF dose will need to be tested in a critical-size bone repair model, such as in rat calvaria defects, in

which spontaneous angiogenesis does not suffice for complete repair and a faster and deeper vascularization would be expected to translate into improved progenitor survival and bone tissue regeneration.

Hu and Olsen [20] also reported that excessive VEGF delivery can impair endogenous bone repair. In fact, it was found that 1 μg of VEGF (at a concentration of 1'000 μg/ml) loaded in collagen sponges inhibits intramembranous bone formation in a tibial cortical defect when the endogenous levels of VEGF are normal. This was ascribed mainly to reduced collagen I accumulation and BSP expression in the area of the defect, suggesting a possible impairment of endogenous osteoprogenitors differentiation. In agreement with the results reported here, a lower dose of VEGF (0.1 μg total, at a concentration of 100 μg/ml) did not impair, but also did not increase bone repair at the defect site. In contrast, delivering of 0.1 μg of VEGF increased formation of mineralized bone in the injury region in $Vegfa^{fl/fl}$ Osx-Cre, in which VEGF was specifically deleted in the osteoblast lineage cells, compared to the control group. The authors suggested that local delivery of optimal amounts of VEGF may enhance bone repair when VEGF levels are low (or depleted) at the repair site, but that exogenous VEGF treatment may fail at improving regeneration when endogenous VEGF levels are physiological. These observations are generally in agreement with the data reported here and support the importance of VEGF dose in regulating osteogenesis. However, key differences in the experimental design prevent a detailed comparison. In fact, 1) exogenous human osteoprogenitors were not used in the mouse bone defect model, limiting the significance of the findings in the context of therapeutic bone tissue engineering; 2) VEGF concentrations were much higher compared to the ones used in this study; and 3) VEGF was passively released very rapidly from the collagen sponges within 3 days of implantation. Therefore, the collagen-based delivery platform could not provide a sufficiently sustained VEGF release to

investigate the steady-state consequences of different VEGF doses on either angiogenesis, osteogenesis or osteoclastogenesis, which require several weeks to complete.

Taking advantage of a unique delivery platform based on factor-decorated fibrin matrix, in the present study we could rigorously investigate the dose-dependent effects of VEGF on both osteogenesis and angiogenesis, during intramembranous bone generation within human BMSC-based tissue-engineered grafts. In particular, we found that a low VEGF dose of 0.1 μg/ml is required for efficient coupling of angiogenesis and osteogenesis, which are instead disrupted by higher doses. These results carry translational relevance for the therapeutic generation of functionally vascularized bone grafts. In fact, the factor-decorated fibrin matrix that was used for these investigations provides also a readily applicable platform for a clinical application, with several attractive features: 1) no need for genetic modifications of progenitors; 2) homogeneous and easily tunable factor dosing and 3) limited and controllable duration of factor delivery over the physiologically required time-window of 4 weeks. However, it is still unclear whether VEGF affects bone formation by human BMSCs in a direct way or by modulating the expression of other osteogenic molecules, for example angiocrine factors by endothelial cells [5]. Elucidating the underlying mechanisms through which VEGF dose controls osteogenic differentiation might identify further molecular targets for bone tissue repair.

References

[1] E. Gomez-Barrena, P. Rosset, D. Lozano, J. Stanovici, C. Ermthaller, F. Gerbhard, Bone fracture healing: cell therapy in delayed unions and nonunions, Bone 70 (2015) 93-101.

[2] R. Dimitriou, E. Jones, D. McGonagle, P.V. Giannoudis, Bone regeneration: current concepts and future directions, BMC Med 9 (2011) 66.

[3] B.M.J.Y.C.a.J.P.F. Guang Yang Vascularization in tissue engineering: fundamentals

and state-of-art, Progress in Biomedical Engineering 2 (2020).

[4] K.D. Hankenson, M. Dishowitz, C. Gray, M. Schenker, Angiogenesis in bone regeneration, Injury 42(6) (2011) 556-61.

[5] S.K. Ramasamy, A.P. Kusumbe, T. Itkin, S. Gur-Cohen, T. Lapidot, R.H. Adams, Regulation of Hematopoiesis and Osteogenesis by Blood Vessel-Derived Signals, Annu Rev Cell Dev Biol 32 (2016) 649-675.

[6] M. Giacca, S. Zacchigna, VEGF gene therapy: therapeutic angiogenesis in the clinic and beyond, Gene Ther 19(6) (2012) 622-9.

[7] A. Grosso, M.G. Burger, A. Lunger, D.J. Schaefer, A. Banfi, N. Di Maggio, It Takes Two to Tango: Coupling of Angiogenesis and Osteogenesis for Bone Regeneration, Front Bioeng Biotechnol 5 (2017) 68.

[8] M.M. Martino, S. Brkic, E. Bovo, M. Burger, D.J. Schaefer, T. Wolff, L. Gurke, P.S. Briquez, H.M. Larsson, R. Gianni-Barrera, J.A. Hubbell, A. Banfi, Extracellular matrix and growth factor engineering for controlled angiogenesis in regenerative medicine, Front Bioeng Biotechnol 3 (2015) 45.

[9] R.O. Hynes, The extracellular matrix: not just pretty fibrils, Science 326(5957) (2009) 1216-9.

[10] V. Sacchi, R. Mittermayr, J. Hartinger, M.M. Martino, K.M. Lorentz, S. Wolbank, A. Hofmann, R.A. Largo, J.S. Marschall, E. Groppa, R. Gianni-Barrera, M. Ehrbar, J.A. Hubbell, H. Redl, A. Banfi, Long-lasting fibrin matrices ensure stable and functional angiogenesis by highly tunable, sustained delivery of recombinant VEGF164, Proc Natl Acad Sci U S A 111(19) (2014) 6952-7.

[11] U. Helmrich, N. Di Maggio, S. Guven, E. Groppa, L. Melly, R.D. Largo, M. Heberer, I. Martin, A. Scherberich, A. Banfi, Osteogenic graft vascularization and bone resorption by VEGF-expressing human mesenchymal progenitors, Biomaterials 34(21) (2013) 5025-35.

[12] I. Martin, A. Muraglia, G. Campanile, R. Cancedda, R. Quarto, Fibroblast growth factor-2 supports ex vivo expansion and maintenance of osteogenic precursors from human bone marrow, Endocrinology 138(10) (1997) 4456-62.

[13] A.E. Mercado-Pagan, A.M. Stahl, Y. Shanjani, Y. Yang, Vascularization in bone tissue engineering constructs, Ann Biomed Eng 43(3) (2015) 718-29.

[14] E.M. Conway, D. Collen, P. Carmeliet, Molecular mechanisms of blood vessel growth, Cardiovasc Res 49(3) (2001) 507-21.

[15] R. Blanco, H. Gerhardt, VEGF and Notch in tip and stalk cell selection, Cold Spring Harb Perspect Med 3(1) (2013) a006569.

[16] R. Gianni-Barrera, N. Di Maggio, L. Melly, M.G. Burger, E. Mujagic, L. Gurke, D.J. Schaefer, A. Banfi, Therapeutic vascularization in regenerative medicine, Stem Cells Transl Med 9(4) (2020) 433-444.

[17] K. Hu, B.R. Olsen, The roles of vascular endothelial growth factor in bone repair and regeneration, Bone 91 (2016) 30-8.

[18] C. Maes, G. Carmeliet, Vascular and Nonvascular Roles of VEGF in Bone Development, VEGF in Development, Springer New York, New York, NY, 2008, pp. 79-90.

[19] Y. Liu, B.R. Olsen, Distinct VEGF functions during bone development and homeostasis, Arch Immunol Ther Exp (Warsz) 62(5) (2014) 363-8.

[20] K. Hu, B.R. Olsen, Osteoblast-derived VEGF regulates osteoblast differentiation and bone formation during bone repair, J Clin Invest 126(2) (2016) 509-26.

Chapter 4

Semaphorin3A couples osteogenesis and angiogenesis in tissue-engineered osteogenic grafts

Andrea Grosso[1], Priscilla S. Briquez[3], Dirk J. Schaefer[1,2], Jeffrey A. Hubbell[3], Andrea Banfi[1,2*], Nunzia Di Maggio[1*]

[1]Cell and Gene Therapy, Department of Biomedicine, Basel University Hospital and University of Basel, Basel, Switzerland

[2]Department of Plastic, Reconstructive, Aesthetic and Hand Surgery, Basel University Hospital, Switzerland

[3]Pritzker School of Molecular Engineering, University of Chicago, IL, USA

**These authors contributed equally*

Introduction

Therapeutic bone regeneration requires rapid and effective vascularization of engineered osteogenic grafts [1]. However, the processes of angiogenesis and osteogenesis are biologically coupled and the therapeutic control of both is complex [2-4]. In order to identify rational molecular targets to induce vascularized bone regeneration, it is crucial to understand the cross-talk between angiogenesis and osteogenesis.

Spontaneous angiogenesis is insufficient to support the survival and differentiation of engineered osteogenic grafts sufficiently large to repair clinical-size defects and it is necessary to provide a therapeutic stimulation. Vascular Endothelial Growth Factor (VEGF) is the master regulator of blood vessel growth and has been widely investigated to stimulate angiogenesis in tissue engineering [5-8]. However, VEGF delivery for therapeutic vascularization of osteogenic grafts remains challenging. In fact, VEGF can also promote osteoclast activity and excessive bone resorption [5]. We have previously found that the effective coupling of angiogenesis and osteogenesis in tissue-engineered osteogenic grafts crucially depends on VEGF dose (Grosso et al., manuscript in preparation; see Chapter 3). Transient delivery of a low dose of 0.1 μg/ml of recombinant VEGF protein, cross-linked into fibrin matrix, both improved rapid vascular ingrowth and ensured efficient bone formation, whereas increasing doses delayed vascular invasion and progressively impaired bone formation, by increasing bone resorption and inhibiting osteogenic differentiation. While it is clear that VEGF dose-dependently regulates both angiogenesis and osteogenesis, the underlying mechanism is not known.

Semaphorins have been described to be involved in several biological processes, including bone and cardiac development, cancer progression, inflammation and angiogenesis [9-12]. In

particular, Semaphorin3A (Sema3A) has gained increasing interest for its role in bone development, homeostasis and repair [13-16]. In particular, it has been reported that Sema3A binding to the Neuropilin-1 (NP1)/Plexin A1 complex receptor enhances bone formation by both inducing osteoblasts differentiation and inhibiting osteoclast differentiation [14] $Sema3a^{-/-}$ and $NP1^{Sema-}$ mice (in which NP1 lacks the Sema3A-binding site) displayed severe osteopenia, characterized by increase osteoclast number and decrease osteoblastic bone formation [14]. Mechanistically, Sema3A activates the canonical Wnt/β-catenin pathway in the process of osteoblast differentiation and suppresses macrophage-colony-stimulating factor (M-CSF)-induced osteoclast differentiation through the Rho A signaling pathway [14].

On the other hand, Sema3A has also been described to regulate sprouting angiogenesis, inhibiting endothelial cell migration [12] and increasing vascular permeability [17]. Interestingly, we have previously found that Sema3A is required to stabilize newly formed blood vessels, but VEGF dose-dependently inhibits endothelial Sema3A expression in skeletal muscle, causing vascular instability and regression [18].

Therefore, here we hypothesized that VEGF dose might couple bone formation and vascularization by regulating Sema3A expression. In particular, we investigated whether, in tissue-engineered osteogenic grafts: a) high VEGF doses impair bone formation by inhibiting endogenous Sema3A expression; b) Sema3A/NP1 signaling is required for intramembranous bone formation; c) Sema3A treatment can improve both bone formation and vascularization.

Material and methods

BMSC isolation and culture

Human primary MSC were isolated from bone marrow aspirates (BMSC). The aspirates were obtained from the iliac crest of 3 healthy donors during routine orthopaedic surgical procedures according to established protocols, after informed consent by the patients and following protocol approval by the local ethical committee (EKBB, Ref. 78/07). Cells were isolated and cultured as previously described [5, 19]. After centrifugation the pellet was washed in PBS (Gibco^{TM}, Thermo Fisher Scientific, Waltham, Massachusetts, USA). Cells were resuspended in α-MEM medium (Gibco^{TM}, Thermo Fisher Scientific, Waltham, Massachusetts, USA) supplemented with 10% bovine fetal serum (HyClone, South Logan, Utah, USA), 1mM Sodium Pyruvate (Gibco^{TM}, Thermo Fisher Scientific, Waltham, Massachusetts, USA), 10mM HEPES (Gibco^{TM}, Thermo Fisher Scientific, Waltham, Massachusetts, USA) and 5 ng/mL FGF-2 (R&D System Minneapolis, Minnesota, USA), plated at a density of 10^5 nucleated cells/cm^2 and cultured in 5% CO_2 at 37°C.

Generation and in vivo subcutaneous implantation of osteogenic constructs

60 mm^3 of silicate-substituted apatite granules of 1-2mm size (Actifuse®; Apatech-Baxter, Elstree, UK) where mixed with 1x10^6 BMSC and embedded in a fibrin gel prepared by mixing 25 mg/ml human fibrinogen (plasminogen-, von Willebrand Factor-, and fibronectin-depleted; Milan Analytica AG, Rheinfelden, Switzerland), 3 U/mL factor XIIIa (CSL Behring, King of Prussia, Pennsylvania, USA), and 6 U/ml thrombin (Sigma-Aldrich, St. Louis, Missouri, USA) with 2.5 mM Ca^{2+} in 4-(2-hydroxyethyl)-1- piperazineethanesulfonic acid (Hepes, Lonza, Basel, Switzerland). Recombinant α_2PI_{1-8}-$VEGF_{164}$, α_2PI_{1-8}-Sema3a and α_2PI_{1-8}-aprotinin were produced as previously described (Chapter 2). Fibrin gels were decorated with $\alpha2PI_{1-8}$-VEGF-

A_{164} at 0.1, 1, 10 or 100 µg/ml, α_2PI_{1-8}-Sema3A at 0.1, or 10 µg/ml, or with both mixed at ratio 1:1 or 1:10. 51 µg/ml of aprotinin-$\alpha 2PI_{1-8}$ were also incorporated into the hydrogel to control its degradation time. The engineered proteins were mixed to the cross-linking enzymes solution before mixing with fibrinogen. Osteogenic grafts were allowed to polymerize at 37°C for 10 min after mixing before *in vivo* implantation. The resulting constructs were implanted subcutaneously in nude mice (CD1-*Foxn1*^{nu}, Charles-River, Sulzfeld, Germany). Animals were treated in agreement with Swiss legislation and according to a protocol approved by the Veterinary Office of Canton Basel-Stadt (permission #1797). Three to nine constructs were implanted for each condition (n=3-10 samples/group), generated with cells from 3 independent donors. After 1, 4 and 10 weeks, mice were sacrificed by inhalation of CO_2 and constructs were explanted.

Anti-NRP1^A antibody treatment

Animals were treated systemically by i.p. injection of the blocking antibody anti-NP1^A (YW64.3, Genentech Inc., South San Francisco, California, USA) [20] in PBS with 0.5% BSA (10 mg/kg) at the time of constructs implantation (day 0) and every 3 days, according to the previously published treatment schedule [21]. IgG2a antibody (10 mg/kg in PBS with 0.5% BSA; Lubio Science, Lucerne, Switzerland) was given i.p. as isotype control.

Histological processing and immunofluorescence tissue staining

Explanted constructs were washed with PBS and fixed over night at +4°C with freshly prepared 1% paraformaldehyde (Sigma-Aldrich, St. Louis, Missouri, USA) in PBS. Subsequently, the samples were decalcified. Constructs were transferred into a PBS-based solution containing 7% w/v EDTA (0.5M, pH 8, Sigma-Aldrich, St. Louis, Missouri, USA) and 10% w/v sucrose (Sigma-Aldrich, St. Louis, Missouri, USA) and incubated at 37°C on an orbital

shaker. The solution was renewed daily for about 20 days, until the samples were fully decalcified, as estimated by the degree of sample stiffness. Finally, the samples were embedded in OCT compound (CellPath LTD, Newtown, UK), frozen in freezing 2-methylbutane (isopentane) (Sigma-Aldrich, St. Louis, Missouri, USA) and 10 µm thick sections were obtained with a cryostat.

Immunofluorescence staining was performed on 10 µm-thick frozen sections. The following primary antibodies and dilutions were used: rat anti-mouse CD31 (clone MEC 13.3, BD Bioscience, San Jose, California, USA) at 1:100; mouse anti-Human nuclei (clone 235-1, Merk Millipore, Darmstadt, Germany) at 1:200; rabbit anti-Sema3A (Abcam, Cambridge, UK) at 1:100; rat anti-CD11b (Thermo Fisher Scientific, Waltham, Massachusset, USA) at 1:200; rabbit anti-Neuropiln 1 (Abcam, Cambridge, UK) at 1:200. Fluorescently labeled secondary antibodies (Thermo Fisher Scientific, Waltham, Massachusset, USA) were used at 1:200.

For pSMAD2/3 staining, tissue sections were permeabilized with ice-cold methanol for 10 min and blocked with 5% goat serum and 2% BSA in PBS with 0.3% Triton X for 1h at RT. Rabbit anti-pSMAD 2/3 (Santa Cruz Biotechnology, California, USA) was used at 1:100.

Fluorescence images were acquired with an Olympus BX63 microscope (Olympus, Münster, Germany), a Nikon Ti2 Eclipse (Nikon, Tokyo, Japan) and with 40x objectives on a Carl Zeiss LSM710 3-laser scanning confocal microscope (Carl Zeiss, Oberkochen, Germany). All image measurements were performed with cellSens software (Olympus, Münster, Germany), NIS-Elements (Nikon, Tokyo, Japan) and FIJI software (ImageJ, http://fiji.sc/Fiji).

Quantification of Sema3A expression

The quantification of Sema3A$^+$ human cells was performed on frozen sections after immunostaining for human nuclei (HuNu), endothelium (CD31) and Sema3A. The number of Sema3A$^+$ cells was counted either in the core or within the vascularized areas of the graft, and normalized by the total number of human cells. At least 7 random fields in each sample were acquired with a confocal microscope for both the core and invaded areas.

The immunofluorescent staining for Sema3A was quantified on complete images of whole samples using a custom-made macro in FIJI software. Briefly, the region of interest (ROI) was traced and thresholding was applied to the Sema3A channel and the number of pixels above the threshold was normalized by the total number of the pixels of the ROI. All conditions were stained with the same batch of antibodies and at the same time. Pictures were acquired with a Nikon-Ti2 Eclipse microscope during the same session.

Quantification of SMAD2/3 activation

The quantification of nuclei positive for pSMAD2/3 was performed on cryosections after immunostaining for human nuclei (HuNu), endothelium (CD31) and pSMAD2/3. Human or mouse endothelial nuclei, positive for pSMAD2/3 were manually counted in at least 7 randomly acquired fields in each sample.

Quantification of Neuropilin-Expressing Monocytes (NEM)

The quantification of CD11b$^+$/NP1$^+$ NEM was performed on frozen sections after immunostaining for monocytes (CD11b) and NP1, counting all the CD11b$^+$/NP1$^+$ cells found in all the sections of each histological sample preparation. Quantification was expressed as the absolute number of NEM per sample.

Analysis of angiogenesis

Invasion of osteogenic constructs by blood vessels was assessed after 1 week *in vivo* by immunofluorescence for CD31 (n=3-6 samples/group). Briefly, complete images of the whole samples were acquired, the areas of tissue invaded by blood vessels were manually measured and normalized by the total tissue area. Vessel length density (VLD, mm/mm^2) was quantified tracing the total length of vessels within the invaded areas and dividing it by the area of invasion. Total vessels length (mm) was obtained multiplying the quantified VLD within the area of invasions by the area invaded by blood vessels.

Vascularization at 4 weeks was assessed on at least 15 random fields which were acquired per sample (n=3-6 samples/group). VLD was measured by tracing the total length of vessels in the fields and by normalizing it to the tissue area in each field.

Analysis of bone formation

Bone tissue was detected by Masson's trichrome staining (Réactifs RAL, Martillac, France), performed according to manufacturer's instructions. Twenty section reconstructions per sample (n=3-6 samples/group) were acquired with transmitted light and bone tissue was quantified by tracing the area occupied by dense collagenous matrix (dark green staining) and normalizing it by the total area of the section.

Osteoclast detection

In order to detect osteoclasts, histological sections were stained for tartrate-resistant acid phosphatase (TRAP) activity. Briefly, after rising with water, slides were incubated for 20 minutes with 0.1M Acetate Buffer (0.2M Sodium Acetate, 0.2M Acetic Acid, 50mM Sodium L-tartrate dibasic dihydrate, pH 5.0) and then stained with a solution of 1 mg/ml Fast Red LB salt (Sigma-Aldrich, St. Louis, Missouri, USA) and 1 mg/ml naphthol AS-MX phosphate (Sigma-

Aldrich, St. Louis, Missouri, USA) in 0.1M acetate buffer for 1 hour at 37°C. After TRAP staining, nuclear counter staining was performed with Haematoxylin for 1 min at room temperature. TRAP-positive cells were quantified on 15 random fields per construct in 6 constructs/condition (n=3-6 samples/group). Multinucleated TRAP+ cells in the fields were counted manually and the total number was normalized by the tissue area.

Human progenitor engraftment

The presence of human cells was assessed by staining with a specific anti-human nuclei antibody. Human cells were counted automatically in at least 15 random fields/sample (n=6 samples/group) by using ImageJ software.

Quantitative real-time PCR

For RNA extraction from osteogenic grafts, constructs were immediately frozen in liquid nitrogen after harvesting (n=8-10 samples/group). Tissues were disrupted and homogenized using a Qiagen Tissue Lyser (Qiagen, Hilden, Germany) in 1 ml TRIzol Reagent (Thermo Fisher Scientific, Waltham, Massachusetts, USA) for 100 mg of tissue. Total RNA was isolated from lysed tissues with a RiboPure RNA purification kit (Thermo Fisher Scientific, Waltham, Massachusetts, USA) according to manufacturer's instruction.

RNA from tissues was reverse-transcribed into cDNA with the SuperScript III Reverse Transcriptase (Thermo Fisher Scientific, Waltham, Massachusetts, USA). Quantitative Real-Time PCR (qRT-PCR) was performed on an ABI 7300 Real-Time PCR system (Applied Biosystems, Foster City, California, USA).

Expression of genes of interest was determined using the following TaqMan gene expression assays: (Thermo Fisher Scientific, Waltham, Massachusetts, USA): human- *Sema3a* (Hs00173810_m1), mouse- *Sema3a* (Mm00436469_m1). Reactions were performed in

duplicate for each template, and normalized to expression of the species-specific *Gapdh* housekeeping gene (human: Hs02786624_g1; mouse: Mm99999915_g1).

Statistics

Results are expressed as the mean ± standard error of the mean (SEM). The significance of differences was assessed with the GraphPad Prism 8 software (GraphPad Software, San Diego, California, USA). The normal distribution of all data sets was tested by D'Agostino and Pearson or Shapiro–Wilk tests and, depending on the results, the significance of differences was determined with the parametric 1-way analysis of variance (ANOVA) followed by the Bonferroni test for multiple comparisons, or with the non-parametric Kruskal–Wallis test followed by Dunn's post-test. $p<0.05$ was considered statistically significant.

Results

High VEGF dose impairs Sema3A production in osteogenic grafts

To investigate whether Sema3A expression is affected by different VEGF doses after *in vivo* implantation, grafts were decorated with a low (0.1 μg/ml) and a high (100 μg/ml) dose of TG-VEGF, which were previously shown to preserve and impair bone formation, respectively (see Chapter 3 above). Histological sections of constructs explanted after 1 and 4 weeks were immunostained for Sema3A. After 1 week, Sema3A was detected around human progenitor cells present both in the core of the constructs and in the area invaded by blood vessels (Fig. 1A and 1C). However, constructs containing a high dose of VEGF (100 μg/ml) displayed a significantly reduced percentage of human progenitors expressing Sema3A compared to constructs loaded with a low dose of VEGF (0.1 μg/ml) and to control grafts (Fig. 1B and 1C).

Interestingly, while in the core of the grafts the number of $Sema3A^+$ cells was only slightly reduced by high VEGF (Fig. 1B; Naïve = 41.6±3.8%, TG-VEGF 0.1 = 42.6±2.4% vs TG-VEGF 100 = 29.9±2.0%; $p<0.05$), the angiogenic areas displayed a much greater reduction (Fig. 1C; Naïve = 37.7±2.9%, TG-VEGF 0.1 = 38.3±4.8% vs TG-VEGF 100 = 8.9±0.9%; $p<0.001$).

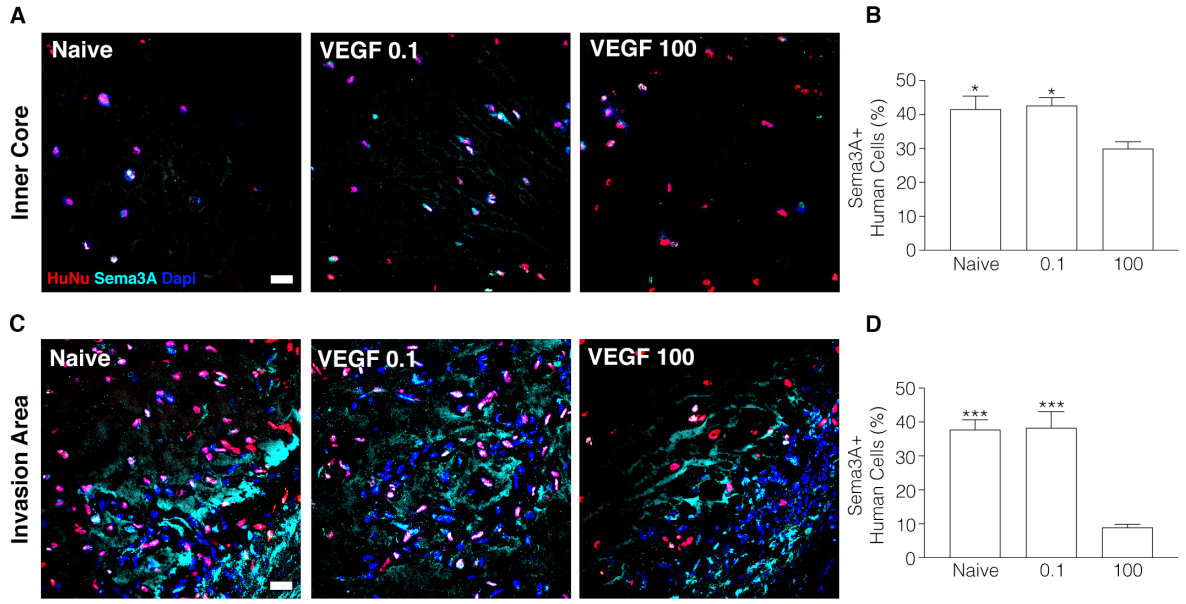

Figure 1. *Immunostaining of human cells (HuNu, red), Sema3A (cyan) and nuclei (DAPI, blue) of osteogenic grafts after 1 week of in vivo implantation, in the core (A) and in the invaded areas (C); quantification of the percentage of human cells expressing Sema3A in the core (B) and in the invaded areas (D); *=p<0.05, ***=p<0.001; scale bar = 30 µm.*

After 4 weeks Sema3A abundance was increased from 1 week and it could be detected in close proximity to endothelial cells, bone lineage cells (osteoblasts and osteocytes) and embedded within the extracellular matrix (in green in Fig. 2A). Constructs loaded with 0.1 µg/ml of TG-VEGF and Naïve cells contained similarly high amounts of Sema3A, whereas in grafts with 100 µg/ml of TG-VEGF, Sema3A presence was significantly reduced (Fig. 2A-B; Naïve=10.3±1.2%, TG-VEGF 0.1=11.9±1.9% vs TG-VEGF 100=4.2.9±0.6%; p<0.05).

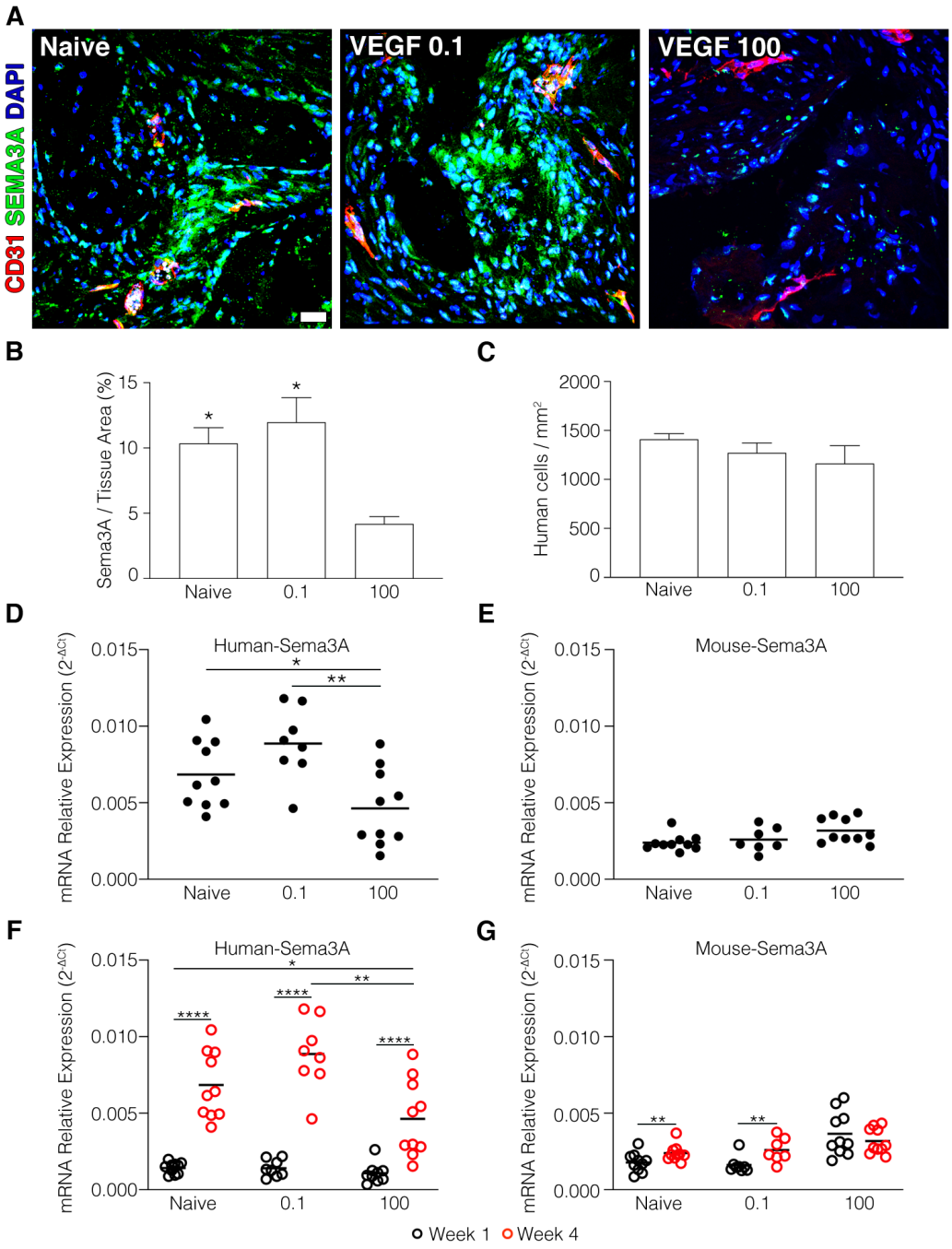

Figure 2. *(A) Immunostaining of endothelium (CD31, red), Sema3A (green) and nuclei (DAPI, blue) of osteogenic constructs after 4 weeks of in vivo implantation. Scale bar=30 µm; (B) Quantification of Sema3A⁺ pixels (expressed as % of the total number of pixels; (C) Quantification of the density human cells within the tissue (human cells/mm²); (D-G) Gene expression of human- and mouse- Sema3A was quantified by qRT-PCR and expressed as relative expression to human and mouse GAPDH respectively ($2^{-\Delta Ct}$); (D,E) Gene expression of human- and mouse- Sema3A after 4 weeks of in vivo implantation; (F, G) Comparison of the gene expression of human- and mouse- Sema3A at 1 and 4 weeks after in vivo implantation. Data represent the values of individual samples (colored dots) and the mean (black bar; n=8-10); *=p<0.05, **=p<0.01, ****=p<0.0001. Black dots = 1 week; red dots = 4 weeks.*

Quantification of human progenitors, which are a source of Sema3A (Fig. 1) showed similar persistence in all conditions (Fig. 2C; Naïve=1409.0±1.2 human cells/mm^2, TG- VEGF 0.1=1272.0±100.6, TG-VEGF 100=1161.0±181.8; p=n.s.), suggesting that Sema3a protein may be reduced through downregulation of its expression rather than loss of producing cells.

Gene expression analysis further confirmed that Sema3A gene expression was downregulated in human cells with high VEGF (Fig. 2D). As it has been shown that endothelial cells can also be a source of Sema3A [18] and the endothelium invading the constructs is derived from the host, we also quantified the expression of murine Sema3A and found that its expression level was not appreciably affected by VEGF at any dose (Fig. 2E).

By comparing expression levels between 1 and 4 weeks it was found that human Sema3A was significantly upregulated over this time frame (Fig. 2F), whereas mouse Sema3a remained much less expressed (Fig. 2G). Taken together, these data suggest that human osteoprogenitors are the principal source of Sema3a in osteogenic grafts and VEGF can dose-dependently downregulate its expression, consensually with its effect on impairing bone formation.

Early Sema3A expression by human progenitors is not impaired by Neuropilin-1 blockage

To determine the role of Sema3A/Neuropilin-1 (NP1) signaling on the vascularization and the intramembranous bone formation of tissue-engineered osteogenic grafts, we performed a loss of function experiment by systemic treatment with a specific antibody that recognizes the CUB domain (a1a2) of NP1 and prevents its binding with Sema3A, but does not affect the interaction with VEGF with a different domain (anti-NP1^A, YW64.3) [21].

It has been shown that Sema3A/NP1 signaling starts a positive feedback loop sustaining Sema3A production itself in skeletal muscle endothelium [18]. Therefore, constructs were stained for Sema3A 1 week after *in vivo* implantation. Sema3A protein was detected with similar frequency in all conditions, in association with human progenitor cells present both in the core of the construct and in the areas invaded by blood vessels (Fig. 3; Inner Core: Naïve Ctrl=75.6±4.3%, Naïve α-NP1^{A}=70.4±9.1%, TG-VEGF 0.1 Ctrl=80.1±3.8%; TG-VEGF 0.1 α-NP1^{A}=72.7±7.2%, p=n.s.; Invasion Area: Naïve Ctrl=62.9±1.6%, Naïve α-NP1^{A}=68.7±4.3%, TG-VEGF 0.1 Ctrl=70.4±0.9%; TG-VEGF 0.1 α-NP1^{A}=60.6±10.1%, p=n.s.). These results suggest that Sema3A expression by human osteoprogenitor cells in the early stage of engraftment does not depend on NP1 activation.

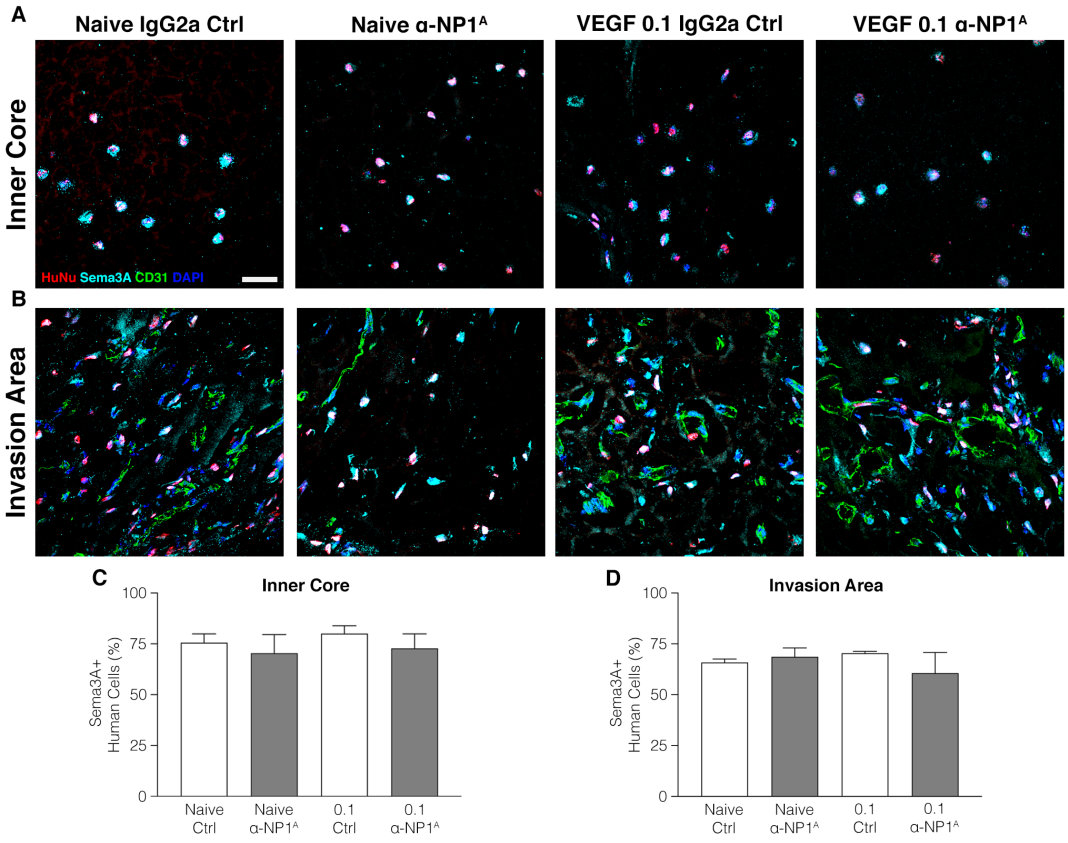

Figure 3. *Immunostaining of human cells (HuNu, red), Sema3A (cyan), endothelium (CD31, green) and nuclei (DAPI, blue) of osteogenic grafts after 1 week of in vivo implantation, in the core (A) and in the invaded areas (B); quantification of the percentage of human cells expressing Sema3A in the core (C) and in the invaded areas (D); scale bar=30 µm.*

Neuropilin-1 blockade impairs vascularization of osteogenic grafts

Sema3A is a multifunctional factor, with roles in processes as diverse as neural guidance and angiogenesis, as well as in bone homeostasis, and its functions are often context-dependent. Further, we previously found that VEGF directly and dose-dependently regulates the amplitude of blood vessels invasion into osteogenic grafts (Chapter 3). While endothelial cell migration and vascular invasion of the graft are promoted by low VEGF levels (0.1 µg/ml), they are delayed by increasing doses. We therefore investigated whether Sema3A/NP1 blockade could affect blood vessels in-growth in the presence and in the absence of VEGF. As expected, graft decoration with 0.1 µg/ml of TG-VEGF promoted vascular invasion compared to Naïve condition (Fig. 4A-B; TG-VEGF 0.1 Ctrl=16.4±1.8% vs Naïve Ctrl=4.9±0.7%, $p<0.001$).

Strikingly, inhibition of Sema3A/NP1 signaling significantly impaired the extent of vascular invasion, especially in the presence of VEGF (Fig. 4A-B; Naïve α-NP1^{A}=2.6±1.5%, TG-VEGF 0.1 α-NP1^{A}=8.2±1.3%, $p<0.01$ vs TG-VEGF 0.1 Ctrl).

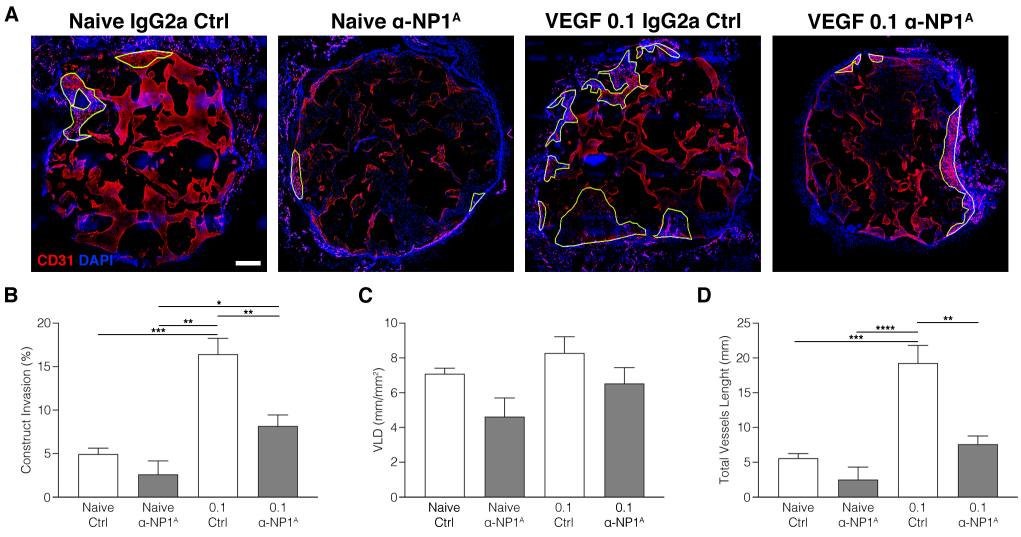

Figure 4. *(A) Reconstruction of graft sections under fluorescent light to evidence the areas of blood vessel growth (in yellow) stained for CD31 (red); (B) Quantification of the areas invaded by blood vessels (expressed as % of total section area). Scale bar = 500 µm. (C) Quantification of induced angiogenesis within the invaded areas, after 1 week in vivo, expressed as VLD (vessel length density), calculated as millimeters of vessel length per square millimeter of tissue area (mm/mm^2); (D) quantification of total vessel length within the invaded areas, expressed as mm. (*=p<0.05, **=p<0.01, ***=p<0.001, ****=p<0.0001)*

Vessel length density (VLD) within the invaded areas was also slightly reduced, although not significantly (Fig. 4C; Naïve Ctrl=7.1±0.3 mm/mm^2, Naïve α-NP1^A=4.6±1.1, TG-VEGF 0.1 Ctrl=8.3±0.9, TG-VEGF 0.1 α-NP1^A=6.5±0.9; p=n.s.), but the total vessel amount within the grafts was significantly reduced compared to the controls (Fig. 4D; TG-VEGF 0.1 Ctrl=19.2±2.5 mm vs Naïve Ctrl=5.6±0.7 mm, Naïve α-NP1^A=2.5±1.9 mm, TG-VEGF 0.1 α-NP1^A=7.6±1.2 mm; p<0.01).

By 4 weeks vascularization was complete throughout all grafts, as expected. However, NP1 blockade significantly decreased vascular density, especially in the presence of VEGF (Fig. 5; Naïve Ctrl=2.6±0.1 mm/mm^2, Naïve α-NP1^A=1.9±0.2, TG-VEGF 0.1 Ctrl=2.9±0.4, TG-VEGF 0.1 α-NP1^A=1.6±0.2; p<0.05 Naïve Ctrl vs TG-VEGF 0.1 α-NP1^A; p<0.01 TG-VEGF 0.1 Ctrl vs TG-VEGF 0.1 α-NP1^A).

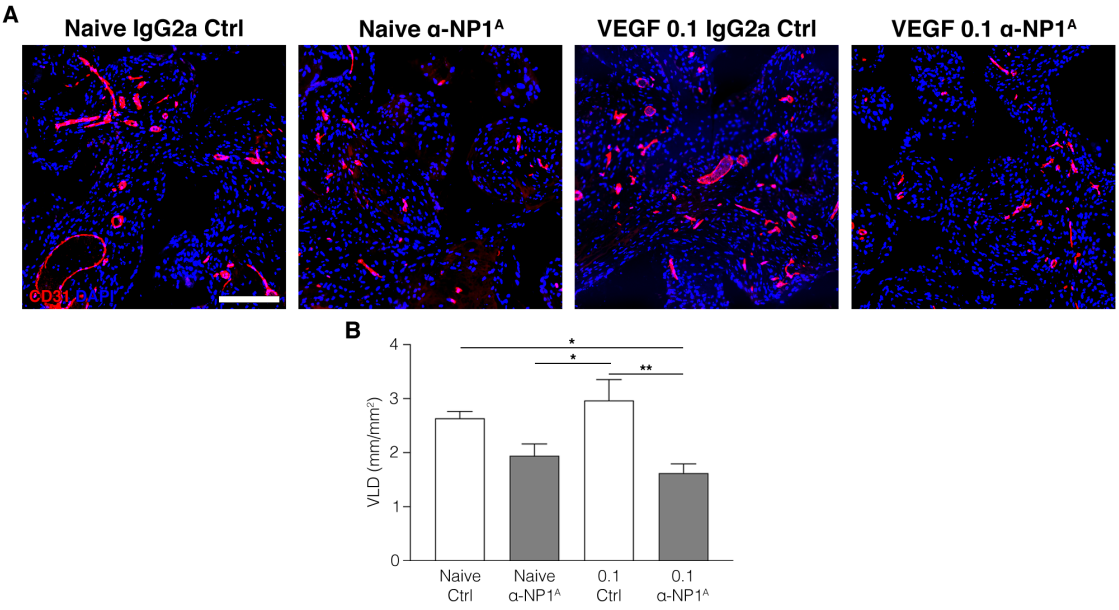

Figure 5. *(A) Immunostaining of endothelium (CD31, in red) and nuclei (DAPI, in blue) of constructs after 4 weeks of in vivo implantation; (B) Quantification of vessels density vessel length density (VLD)) expressed as millimeters of vessel length per square millimeter of tissue area (mm/mm^2) after 4 weeks of in vivo implantation (*= p<0.05, **=p<0.01). Scale bar = 200 µm.*

Neuropilin-1 blockade impairs bone formation and decreases Sema3A expression after 4 weeks

After 4 weeks, bone tissue development was similarly efficient with 0.1 µg/ml of TG-VEGF and with naïve BMSC alone, but treatment with the anti-$NP1^A$ blocking antibody severely impaired bone formation by over 80% in both conditions (Fig. 6A and 6D; Naïve Ctrl=3.4±0.6%, Naïve α-$NP1^A$=0.5±0.2%, TG-VEGF 0.1 Ctrl=2.3±0.3%; TG-VEGF 0.1 α-$NP1^A$=0.6±0.7%).

Sema3A signaling through NP1 regulates the recruitment and differentiation of osteoclasts [14]. As expected, Naïve and low TG-VEGF conditions, which are characterized by efficient bone formation, displayed a low number of osteoclasts (Fig. 6B and 6E; Naïve Ctrl=9.3±1.0 $TRAP^+$ MNC/mm^2, TG-VEGF 0.1 Ctrl=7.7±1.0; p=n.s). Instead, after Sema3A/NP1 inhibition the density of TRAP-positive cells was significantly increased (Fig. 6B and 6E; Naïve α-$NP1^A$=14.6±1.1 $TRAP^+$ MNC/mm^2, TG-VEGF 0.1 α-$NP1^A$=17.3±2.3).

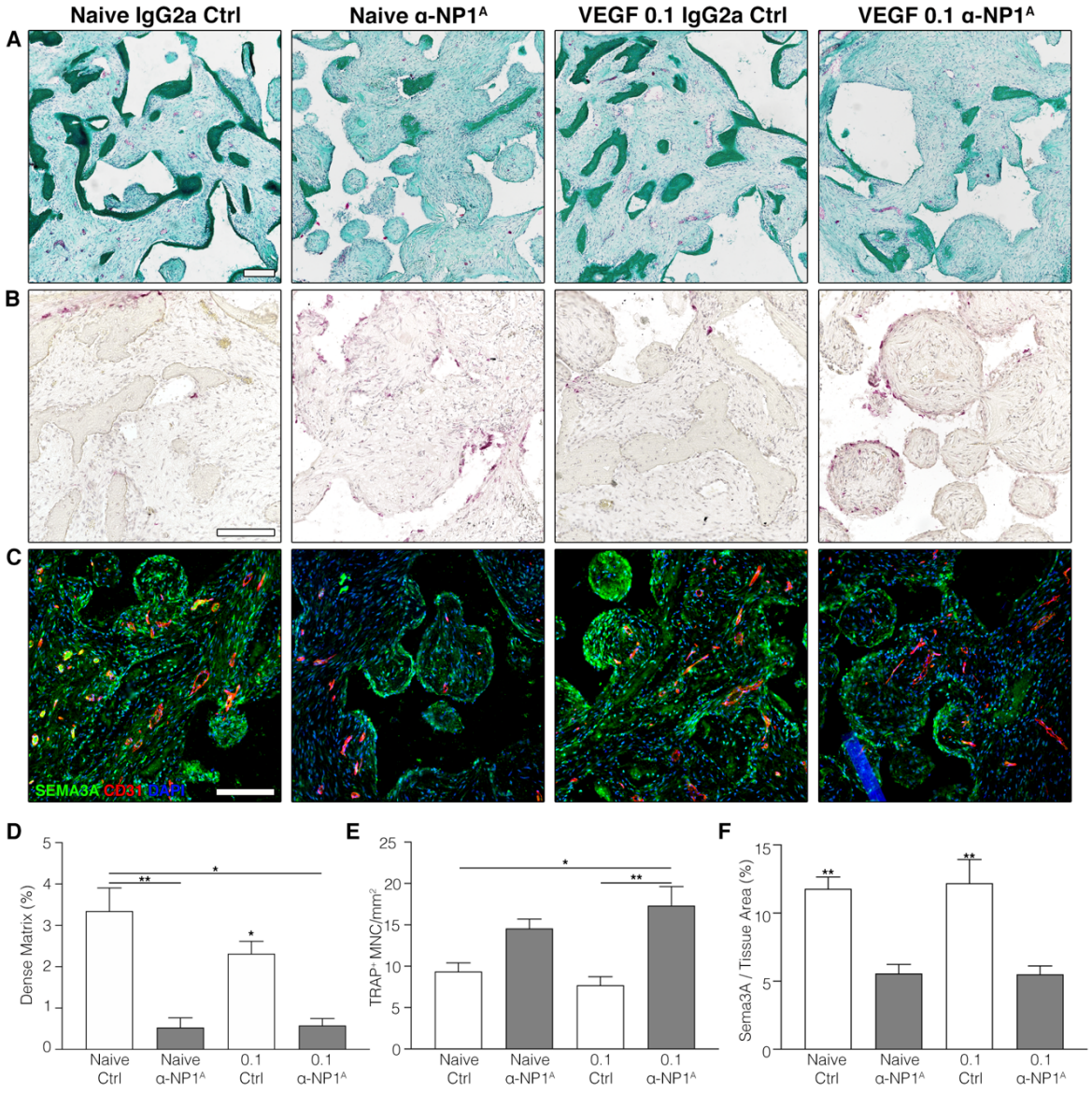

Figure 6. *(A) Representative pictures of Masson's trichrome staining of constructs after 4 weeks of in vivo implantation (mineralized tissue in green); (B) Histochemical stain for TRAP activity (red) and nuclear counterstaining with hematoxylin (blue) of constructs after 4 weeks of in vivo implantation; (C) Immunostaining of endothelium (CD31, red), Sema3A (green) and nuclei (DAPI, blue) of osteogenic constructs after 4 weeks of in vivo implantation; scale bar = 100 µm; (D) Quantification of areas occupied by mineralized tissue (expressed as % of construct area); (D) Quantification of Trap⁺ multinucleated cells (MNC) per tissue area (mm²): (E) Quantification of Sema3A+ pixels (expressed as % of total number of pixels);.*=p<0.05, **=p<0.01. Scale bars = 200 µm.*

Interestingly, the amount of endogenous Sema3A protein, quantified by immunostaining in constructs containing naïve BMSC alone or with low VEGF, was also significantly reduced, but not completely abolished, by the treatment with the blocking antibody (Fig. 6C and 6F; Naïve Ctrl=11.7±0.8%, TG-VEGF 0.1 Ctrl=12.2±1.7% vs Naïve α-NP1^{A}=5.6±0.7%, TG-VEGF 0.1 α-NP1^{A}=5.5±0.6%; $p<0.01$). On the other hand, the engraftment of human progenitors was also significantly impaired by Sema3a/NP1 blockade 4 weeks after *in vivo* implantation, both with and without VEGF (human cells in red, Fig. 7A; Naïve Ctrl=1342.0±79.78 human cells/mm^2, TG-VEGF 0.1 Ctrl=1351.0±116.1 vs Naïve α-NP1^{A}=534.5±148.4, TG-VEGF 0.1 α-NP1^{A}=471.5±105.6; $p<0.001$).

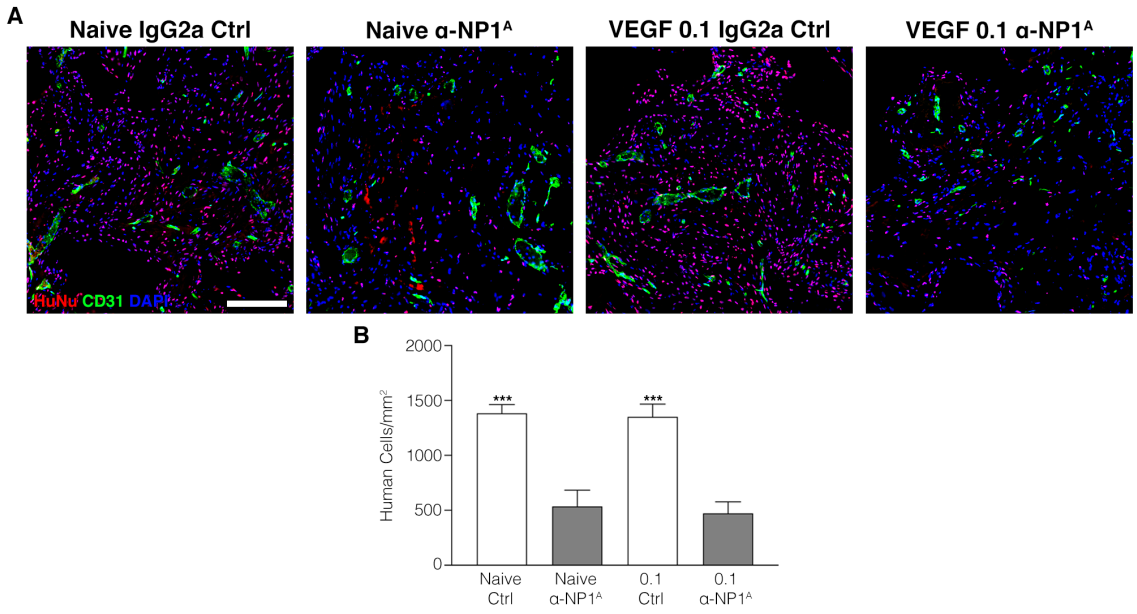

Figure 7. *(A) Immunostaining for human nuclei (Hunu, in red), blood vessels (CD31, In green) nuclei (DAPI, blue) of osteogenic constructs after 4 weeks of in vivo implantation; (B) quantification of the number of human cells per tissue area (mm^2); ***=p<0.001. Scale bar = 200 µm*

These data suggest that Sema3A binding to NP1 is required for bone formation by intramembranous ossification, and that its blockade shifts bone homeostasis towards excessive bone resorption.

NEM recruitment is impaired by high VEGF levels and requires Sema3A

During angiogenesis Sema3A has been shown to recruit a specific population of circulating monocytes expressing NP1 (Neuropilin-Expressing Monocytes, or NEM), which produce several paracrine factors [22]. Among these, TGF-β1 has been found to be important to stabilize newly induced vessels and also to further promote Sema3A production by endothelium [18]. A role for NEM during osteogenesis is unknown.

NEM presence in the osteogenic grafts was quantified by co-staining for the monocyte marker CD11b and NP1. We found that, 1 week after *in vivo* implantation, $CD11b^{+}/NP1^{+}$ NEM were recruited in the areas of active angiogenesis in all the conditions (Fig. 8A). However, NEM recruitment was significantly reduced in constructs decorated with 100 µg/ml of TG-VEGF compared to both Naïve and low-VEGF conditions (Fig. 8B; Naïve=35.0±2.1 NEM/Construct, TG-VEGF 0.1=36.4±4.8 vs TG-VEGF 100=9.2±1.3; p<0.0001), consistently with the loss of Sema3A production with high VEGF.

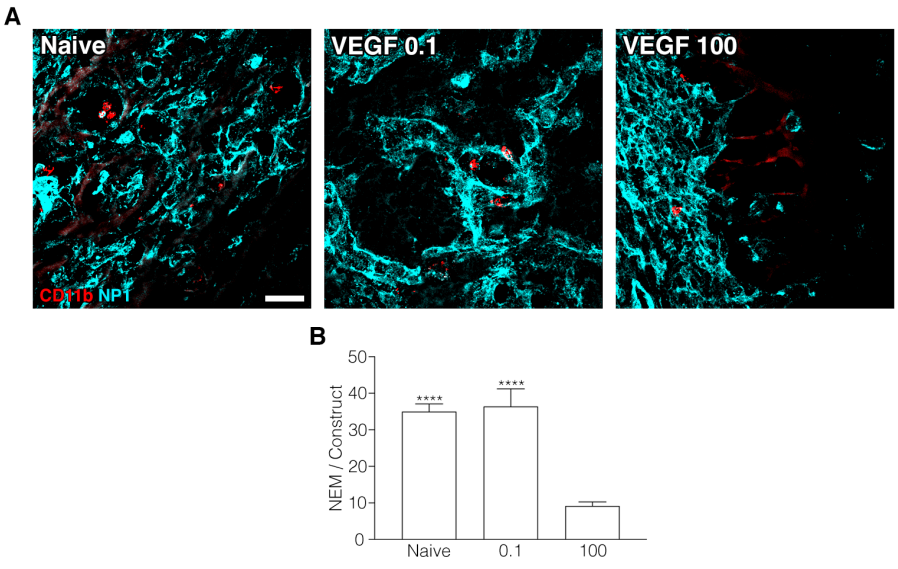

Figure 8. *(A) Immunofluorescence staining for CD11b (in red), and NP1 (in cyan) on frozen section from constructs after 1 week of in vivo implantation. Scale bar=30 µm; (B) Quantification of the number of NEM, expressed as absolute number per sample; ****=p<0.0001.*

Inhibition of Sema3A/NP1 signaling also significantly impaired NEM recruitment into the angiogenic areas of both Naïve and low-VEGF grafts (Fig. 9), showing that Sema3A is required for NEM recruitment during intramembranous osteogenesis in tissue-engineered grafts (Naïve Ctrl=42.5±6.7 NEM/Construct, TG-VEGF 0.1 Ctrl=54.0±8.7 vs Naïve α-NP1^{A}=11.2±2.0, TG-VEGF 0.1 α-NP1^{A}=21.0±3.7; p<0.01).

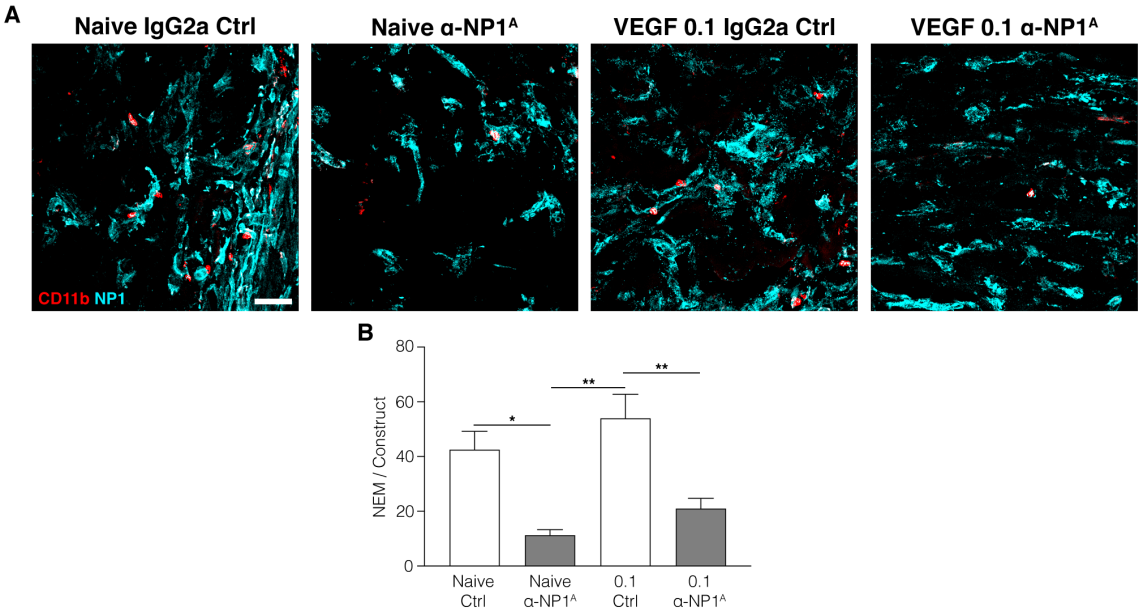

Figure 9. *(A) Immunofluorescence staining for CD11b (in red), and NP1 (in cyan) on frozen section from constructs after 1 week of in vivo implantation. Scale bar=30µm; (B) Quantification of the number of NEM, expressed as absolute number per sample. *=p<0.05, **=p<0.01.*

Neuropilin-1 blockade inhibits SMAD2/3 activation in human progenitor cells and mouse endothelium

We have previously shown that NEM-derived TGF-β1 signaling through SMAD 2/3 phosphorylation plays a key role in sustaining Sema3A expression during VEGF-induced angiogenesis [18]. Therefore, we determined whether the Sema3A/NEM/TGF-β1 axis is active also in the crosstalk between angiogenesis and osteogenesis and investigated if the changes

in Sema3A expression and NEM recruitment translated in alterations of TGF-β1 signaling in osteogenic grafts.

As shown in Fig. 10A, phospho-SMAD2/3 (in cyan) was translocated into the nuclei of both human progenitors (in red) and murine endothelial cells (nuclei within $CD31^{+}$ structures, in green) in all conditions 1 week after *in vivo* implantation. However, quantification of the proportion of positive nuclei showed that SMAD2/3 activation was significantly reduced upon inhibition of Sema3A/NP1 signaling both in human progenitors (Fig. 10B and 10C) and in endothelial cells (Fig. 10D). Interestingly, inhibition of SMAD2/3 phosphorylation in the low-VEGF condition was only mild in the core graft areas, which were not vascularized yet, but much more significant in the areas where blood vessels were already present.

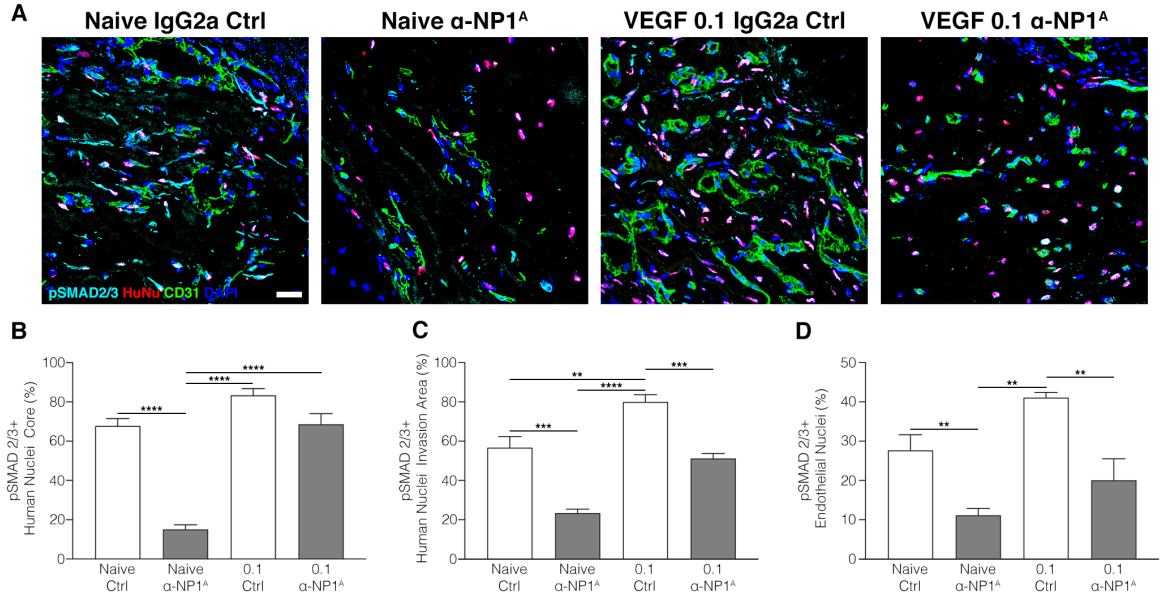

Figure 10. *(A) Immunofluorescence staining for pSMAD2/3 (in cyan), human cells (HuNu, in red) and endothelium (CD31, in green)) on frozen section from constructs after 1 week of in vivo implantation. Scale bar=30µm; (B, C) Quantification of the percentage of human cells nuclei positive for pSMAD2/3 in the core (B) and in the invaded area (C); (D) Quantification of the percentage of endothelium nuclei positive for pSMAD2/3. **=p<0.01. ***=p<0.001, ****=p<0.0001.*

Sema3A delivered as single factor significantly improves both vascularization and bone formation in osteogenic grafts

The previous data show that Sema3A/NP1 signaling is required in osteogenic grafts both for bone tissue formation and early blood vessel ingrowth, even in the presence of an optimal dose of VEGF. Based on these results, we asked whether Sema3A could be exploited as a therapeutic target for the generation of vascularized bone. An engineered version of Sema3A protein (TG-Sema3A) was incorporated into fibrin hydrogels at 0.1 and 10 μg/ml and the generated osteogenic constructs were implanted subcutaneously in nude mice for 1, 4 and 10 weeks. As previously shown in Chapter 3, rapid vascular ingrowth is crucial to promote cell survival in the core of the graft. Conversely from the effects of blocking Sema3A/NP1 signaling in the presence of a low VEGF dose (Fig. 4), when Sema3A was delivered as a single factor, without VEGF, both doses induced significantly larger and deeper areas of blood vessels invasion after 1 week compared to the Naïve condition (Fig. 11A-B; Naïve=4.2±0.1% vs TG-Sema3A 0.1=12.4±2.4%, $p<0.05$; vs TG-Sema3A 10=17.8±1.7%, $p<0.01$).

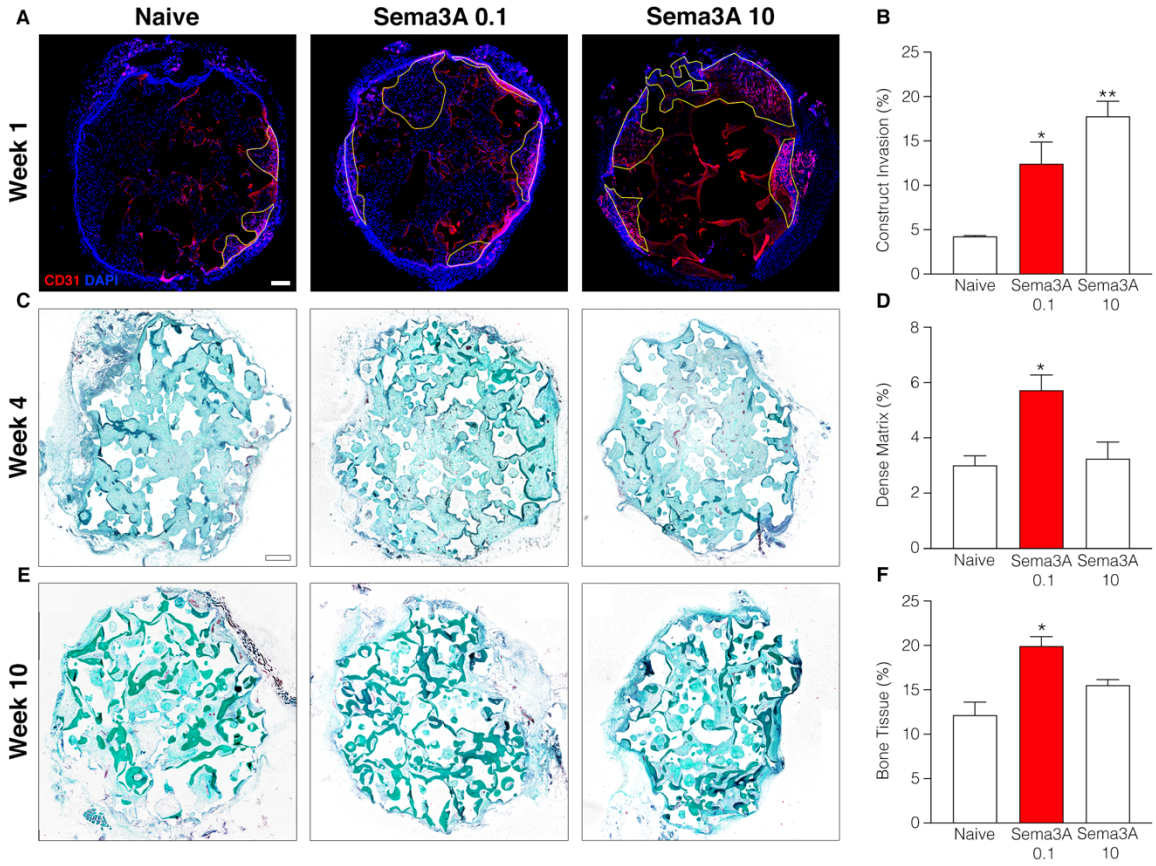

Figure 11. *(A) Reconstruction of graft sections under fluorescent light to evidence the areas of blood vessel growth (in yellow) stained for CD31 (red) after 1 week in vivo); (B) Quantification of the areas invaded by blood vessels (expressed as % of total section area); scale bar= 300µm. Representative pictures of Masson's trichrome staining of constructs after 4 (C) and 8 (E) weeks of in vivo implantation (mineralized tissue in dark green); scale bar = 500µm; quantification of areas occupied by dense collagenous matrix after 4 weeks (D) (expressed as % of construct area, and by bone tissue after 10 weeks (F); *=p<0.05, **=p<0.01.*

After 4 weeks, initial bone formation was visible in all conditions, as shown by dense collagenous matrix in Masson's trichrome staining (Fig. 11C). However, the quantity of dense matrix was increased by about two-fold by 0.1 µg/ml of Sema3A compared to naïve cells alone, but not by the higher Sema3A dose of 10 µg/ml (Fig. 11D; TG-Sema3A 0.1=5.7±0.5% vs Naïve=3.0±0.3% and TG-Sema3A 10=3.2±0.6%, $p<0.05$). After 10 weeks, frank bone tissue had developed, characterized by dense organized collagen fibers and the presence of osteocyte lacunae (Fig. 11E). Again, 0.1 µg/ml of Sema3A (but not 10 µg/ml) significantly increased bone

tissue formation compared to Naïve cells (Fig. 11F; TG-Sema3A 0.1=19.9±1.1% vs Naïve=12.2±1.4% and TG-Sema3A 10=15.5±0.6%, $p<0.05$), even though the fibrin-bound Sema3A was only present for about 4 weeks and was long exhausted by this time-point.

Sema3A co-delivery prevents bone loss induced by high VEGF doses without impairing VEGF-induced vascularization

Taken together, the studies reported here suggest that Sema3A may act downstream of VEGF to couple angiogenesis and osteogenesis, as: 1) its expression in osteoprogenitors is downregulated by increasing VEGF doses (Figs. 1-2); 2) it is required for both vascular invasion (Figs. 4-5) and osteogenesis (Fig. 6); and 3) it can stimulate both vascular invasion and osteogenesis in the absence of exogenous VEGF (Fig. 11). Therefore, we lastly sought to investigate if Sema3A co-delivery may rescue bone loss induced by high VEGF doses. TG-Sema3A and TG-VEGF were combined at a ratio of 1:1 or 1:10 and the osteogenic constructs were analyzed 4 weeks after *in vivo* implantation in nude mice. Constructs containing both 1 and 10 μg/ml of TG-VEGF displayed a significant reduction in dense collagenous matrix deposition compared to control grafts (Fig. 12A and 12D; Naïve=0.5±0.1% vs TG-VEGF 1 =0.1±0.1%, $p<0.05$; vs TG-VEGF 10=0.02±0.01%, $p<0.001$). Instead, co-delivery of Sema3A at both ratios completely prevented bone loss and restored bone formation to the same or even higher level as Naïve cells alone (Fig 12A and 12D; V1/S0.1=0.8±0.1%, V10/S10=0.4±0.1%, p=n.s. vs Naïve).

The prevention of bone loss by Sema3A correlated with a lower recruitment of osteoclasts (Fig. 12B). Quantification of multinucleated $TRAP^+$ cells showed that, while VEGF alone significantly increased the number of osteoclasts compared to control grafts (Fig. 12E; Naïve=19.1±1.4 $TRAP^+$ MNC cells/mm^2 vs TG-VEGF 1=47.3±4.2, $p<0.0001$; vs

TG- VEGF 10=36.2±3.4, p<0.001) co-delivery of Sema3A completely prevented this increase, maintaining osteoclasts recruitment to a similar level as in the naïve condition (Fig. 12E; V1/S0.1=21.4±1.9 TRAP$^+$ MNC cells/mm^2, V10/S10=20.6±2.7, p=n.s. vs Naïve). Steady-state vascular density in the grafts was not affected by Sema3A co-delivery in the presence of VEGF, which was significantly increased compared to the naïve condition (Fig. 12F; Naïve=1.7±0.11 mm/mm^2 vs TG-VEGF 1=3.1±0.2, V1/S0.1=2.6±0.1, TG-VEGF 10=3.6±0.1, V10/S10=3.9±0.2; p<0.01).

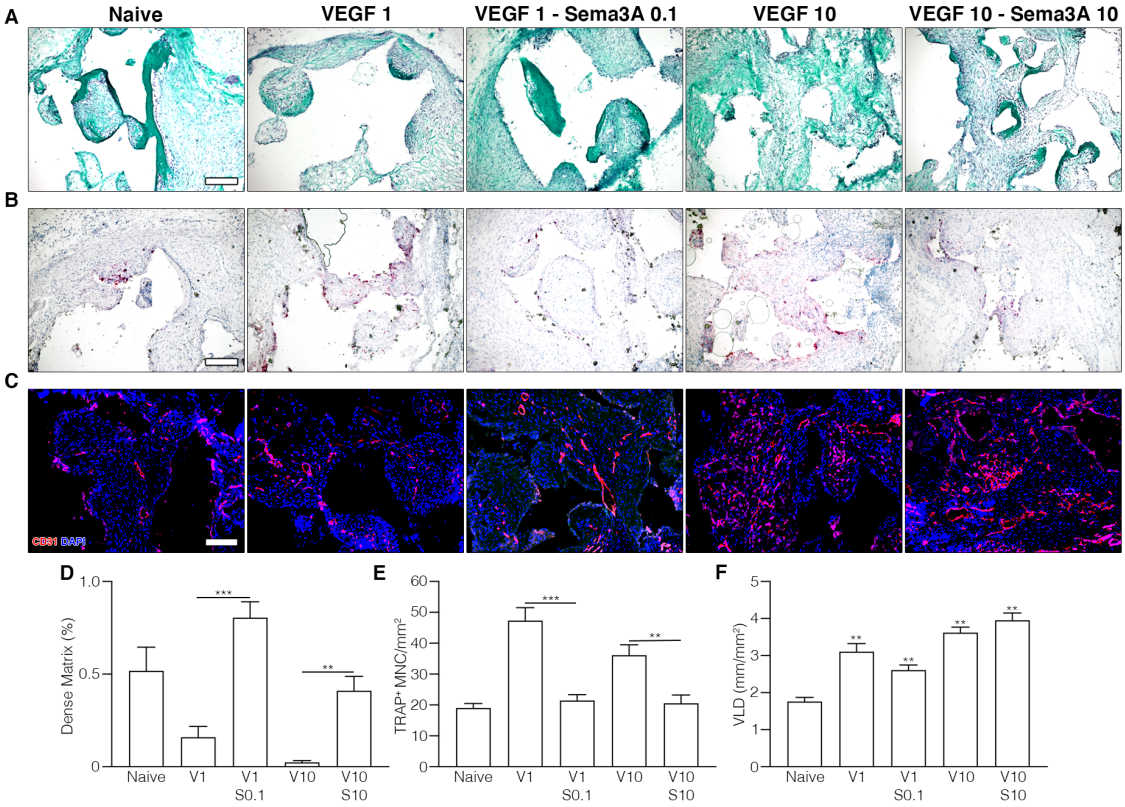

Figure 12. *(A) Representative pictures of Masson's trichrome staining of constructs after 4 weeks of in vivo implantation (mineralized tissue in green); scale bar = 100 µm; (B) Histochemical stain for TRAP activity (red) and nuclear counterstaining with hematoxylin (blue) of constructs after 4 weeks of in vivo implantation; scale bar = 100µm; (C) Immunostaining of endothelium (CD31,red) and nuclei (DAPI, blue) of osteogenic constructs after 4 weeks of in vivo implantation; scale bar = 100 µm; (D) Quantification of areas occupied by mineralized tissue (expressed as % of construct area); (E) Quantification of Trap$^+$ multinucleated cells (MNC) per tissue area (mm^2); (F) Quantification of vessels density vessel length density (VLD) expressed as millimeters of vessel length per square millimeter of tissue area (mm/mm^2); **=p<0.01, ***=p<0.001.*

Discussion

In this study we found that efficient coupling of angiogenesis and osteogenesis in tissue-engineered grafts critically depends on Sema3A signaling downstream from VEGF. Delivery of high VEGF doses induced severe bone loss and caused a significant downregulation of Sema3A expression, while low doses preserved both bone formation and Sema3A expression. Blocking of Sema3A signaling significantly impaired both vascular invasion and bone tissue development, and increased osteoclasts recruitment. On the other hand, Sema3A delivered as a single factor was able to increase both vascular invasion and bone formation.

Sema3A is involved in the physiological regulation of bone development and homeostasis. Already in 1996 Behar et al. have shown that Sema3A-deficient mice are characterized by fusion of cervical bones, partial duplication of ribs, and poor alignment of the rib-sternum junctions [9]. More recently, different studies showed that Sema3A regulates both bone resorption and bone deposition, by suppressing osteoclast differentiation and promoting osteoblastic differentiation [13-15]. Additionally, we have previously shown that, in skeletal muscle, increasing doses of VEGF impair blood vessel stabilization by inhibiting the endothelial Sema3A/Neuropilin-1 expressing monocytes (NEM)/TGF-β1 paracrine axis, thus providing a direct molecular link between VEGF and Sema3A expression in endothelium [18].

Although VEGF is a key molecular target for the generation of vascularized bone grafts, its therapeutic use is limited by its potential to induce aberrant angiogenesis [23], to impair bone formation through the inhibition of osteoprogenitor cells differentiation and the stimulation of osteoclast recruitment (Chapters 2-3). As we have previously shown, osteogenic constructs containing 100 µg/ml of VEGF displayed a severe loss of bone mass after 4 weeks in vivo. This

was due both to excessive osteoclast recruitment and to the downregulation of osteogenic differentiation of the implanted human BMSC (Chapter 3).

Here, we identified Sema3A as a molecular mediator by which VEGF dose-dependently regulates bone formation in tissue-engineered constructs, as well as a key effector of angiogenesis-osteogenesis coupling. Low VEGF levels (0.1 μg/ml) attracted rapid vascular invasion of the grafts while also activating osteoprogenitors differentiation, and maintained robust Sema3A expression, with efficient intramembranous bone formation and balanced bone resorption. Instead, high VEGF levels (100 μg/ml) impaired Sema3A expression. inhibited human BMSC osteogenic differentiation and increased resorption, while also impairing initial vascular ingrowth (Chapter 3). These observations suggested a causal link between the effects of VEGF on Sema3A expression and the coupling of angiogenesis and osteogenesis. The mechanistic link was then proven by complementary loss-of-function and gain-of-function experiments. These results showed that specifically blocking Sema3A/NP1 signaling phenocopied the effects of high VEGF doses on both angiogenesis and osteogenesis even in the presence of low VEGF or just under unstimulated conditions. Conversely, Sema3A delivery stimulated both angiogenesis and osteogenesis both in the presence of high VEGF doses and as a single factor. Since VEGFR2 is known to be expressed by osteoblasts *in* vivo [6, 24] it is likely that VEGF directly regulates Sema3A expression by human implanted progenitors.

In bone tissue, Sema3A expression was observed mainly in osteoblasts, while its receptor NP1 is expressed by osteoblasts and osteoclast precursors [14]. It has been shown that $Sema3a^{-/-}$ and $NP1^{Sema3A-}$ mice, which lack Sema3a and the Sema3A-binding domain of NP1 respectively, display a severe osteopenic phenotype caused by a decrease in osteoblastic bone formation and an increase in osteoclast number during bone development through

endochondral ossification [14]. However, the role of Sema3A in intramembranous ossification within osteogenic grafts has never been investigated. Here we showed for the first time that also in BMSC bone grafts, Sema3A signaling is crucial to maintain efficient bone formation. In fact, inhibition of Sema3A binding to NP1 resulted in decreased bone mass and increased bone resorption (Fig. 6).

Interestingly, the amount of endogenous Sema3A protein was also significantly reduced, although not completely abrogated, when its binding to NP1 was impaired. We also found that, after 4 weeks of treatment, downregulation of Sema3A correlated with a decreased number of human cells within the constructs (Fig. 7). Recently, an autoregulatory loop via Sema3A has been described to sustain osteocytes survival and Sema3A expression through the sGC-PKG pathway [15]. Therefore, this suggests that Sema3A expression might be self-sustained by an autocrine loop, required not only for osteoprogenitor differentiation but also for their survival.

Sema3A has been shown to recruit NEM during VEGF-induced angiogenesis, which release TGF-β1, causing on one hand the stabilization of blood vessels through Smad 2/3 signaling, and on the other sustaining a positive feed-back loop that stimulates further Sema3A expression by endothelium [18]. In agreement with these observations and with the pattern of expression of Sema3A at 1 week, we found that Sema3A regulates NEM recruitment also in osteogenic grafts and that its inhibition by NP1 blockade translates into a reduction in TGF-β signaling, as shown by the significant impairment of SMAD 2/3 phosphorylation and nuclear translocation in both human progenitors and mouse endothelial cells (Fig. 10). However, further investigation is needed to elucidate the role of TGF-β1 and NEM recruitment in intramembranous ossification of osteogenic grafts, e.g. by TGF-β1 blockade experiments.

Sema3A has been described to exert anti-angiogenic functions by inhibiting sprouting angiogenesis. It has been shown that Sema3A impairs endothelial cell migration *in vitro* [12], and regulates tumor-induced angiogenesis in vivo [25]. Acevedo et al. described a role for Sema3A both as a selective inhibitor of VEGF-mediated angiogenesis and as a potent inducer of vascular permeability [17]. Recently it was shown that NP1 is more expressed in tip cells than in stalk cells [26],and that endothelial cell-derived Sema3A specifically exerts repelling functions on tip cell filopodia, via NP1 and probably Plexin-A1 [27]. Surprisingly, we did not observe any anti-angiogenic effects by Sema3A. Rather, blockade of Sema3A signaling, even in the presence of low VEGF levels, led to impaired vascular invasion, while conversely, Sema3A delivery significantly stimulated blood vessels in-growth in the absence of VEGF. The discrepancy between these data and previous findings, both with robust levels of evidence, suggest that Sema3A regulation of vascular growth is more complex than anticipated and may be context-, dose- or tissue-dependent. Further investigations are clearly warranted.

The therapeutic potential of Sema3A in bone regeneration is currently under investigation. It has been shown that local administration of Sema3A into a cortical bone defect accelerates bone repair [14] and that treatment with Sema3A recombinant protein protects against bone loss even in aged and in estrogen-depleted mice [15]. Others showed that Sema3A treatment increases callus volume and density at 4 weeks post-fracture, and promotes ossification and remodeling at 8 weeks post-fracture compared to control [28]. However, to our knowledge, the data reported here show for the first time that Sema3A is a key mediator of angio-osteogenesis coupling downstream of VEGF during intramembranous ossification. A further understanding of the underlying molecular mechanisms is necessary to further elucidate the role of Sema3A in bone angiogenesis. The unforeseen function of Sema3A signaling to

promote both the speed of vascular invasion into grafts and the efficiency of bone formation is very attractive for the therapeutic generation of vascularized bone grafts.

References

[1] A.E. Mercado-Pagan, A.M. Stahl, Y. Shanjani, Y. Yang, Vascularization in bone tissue engineering constructs, Ann Biomed Eng 43(3) (2015) 718-29.

[2] A.P. Kusumbe, S.K. Ramasamy, R.H. Adams, Coupling of angiogenesis and osteogenesis by a specific vessel subtype in bone, Nature 507(7492) (2014) 323-328.

[3] U.H. Langen, M.E. Pitulescu, J.M. Kim, R. Enriquez-Gasca, K.K. Sivaraj, A.P. Kusumbe, A. Singh, J. Di Russo, M.G. Bixel, B. Zhou, L. Sorokin, J.M. Vaquerizas, R.H. Adams, Cell-matrix signals specify bone endothelial cells during developmental osteogenesis, Nat Cell Biol 19(3) (2017) 189-201.

[4] S.K. Ramasamy, A.P. Kusumbe, M. Schiller, D. Zeuschner, M.G. Bixel, C. Milia, J. Gamrekelashvili, A. Limbourg, A. Medvinsky, M.M. Santoro, F.P. Limbourg, R.H. Adams, Blood flow controls bone vascular function and osteogenesis, Nat Commun 7 (2016) 13601.

[5] U. Helmrich, N. Di Maggio, S. Guven, E. Groppa, L. Melly, R.D. Largo, M. Heberer, I. Martin, A. Scherberich, A. Banfi, Osteogenic graft vascularization and bone resorption by VEGF-expressing human mesenchymal progenitors, Biomaterials 34(21) (2013) 5025-35.

[6] K. Hu, B.R. Olsen, Osteoblast-derived VEGF regulates osteoblast differentiation and bone formation during bone repair, J Clin Invest 126(2) (2016) 509-26.

[7] D. Kaigler, E.A. Silva, D.J. Mooney, Guided bone regeneration using injectable vascular endothelial growth factor delivery gel, J Periodontol 84(2) (2013) 230-8.

[8] H. Peng, A. Usas, A. Olshanski, A.M. Ho, B. Gearhart, G.M. Cooper, J. Huard, VEGF improves, whereas sFlt1 inhibits, BMP2-induced bone formation and bone healing through modulation of angiogenesis, J Bone Miner Res 20(11) (2005) 2017-27.

[9] O. Behar, J.A. Golden, H. Mashimo, F.J. Schoen, M.C. Fishman, Semaphorin III is needed for normal patterning and growth of nerves, bones and heart, Nature 383(6600) (1996) 525-8.

[10] B. Chaudhary, Y.S. Khaled, B.J. Ammori, E. Elkord, Neuropilin 1: function and therapeutic potential in cancer, Cancer Immunol Immunother 63(2) (2014) 81-99.

[11] C.C. McKenna, A.F. Ojeda, J. Spurlin, 3rd, S. Kwiatkowski, P.Y. Lwigale, Sema3A maintains corneal avascularity during development by inhibiting Vegf induced angioblast migration, Dev Biol 391(2) (2014) 241-50.

[12] H.Q. Miao, S. Soker, L. Feiner, J.L. Alonso, J.A. Raper, M. Klagsbrun, Neuropilin-1 mediates collapsin-1/semaphorin III inhibition of endothelial cell motility: functional competition of collapsin-1 and vascular endothelial growth factor-165, J Cell Biol 146(1) (1999) 233-42.

[13] T. Fukuda, S. Takeda, R. Xu, H. Ochi, S. Sunamura, T. Sato, S. Shibata, Y. Yoshida, Z. Gu, A. Kimura, C. Ma, C. Xu, W. Bando, K. Fujita, K. Shinomiya, T. Hirai, Y. Asou, M. Enomoto, H. Okano, A. Okawa, H. Itoh, Sema3A regulates bone-mass accrual through sensory innervations, Nature 497(7450) (2013) 490-3.

[14] M. Hayashi, T. Nakashima, M. Taniguchi, T. Kodama, A. Kumanogoh, H. Takayanagi, Osteoprotection by semaphorin 3A, Nature 485(7396) (2012) 69-74.

[15] M. Hayashi, T. Nakashima, N. Yoshimura, K. Okamoto, S. Tanaka, H. Takayanagi, Autoregulation of Osteocyte Sema3A Orchestrates Estrogen Action and Counteracts Bone Aging, Cell Metab 29(3) (2019) 627-637 e5.

[16] Z. Li, J. Hao, X. Duan, N. Wu, Z. Zhou, F. Yang, J. Li, Z. Zhao, S. Huang, The Role of Semaphorin 3A in Bone Remodeling, Front Cell Neurosci 11 (2017) 40.

[17] L.M. Acevedo, S. Barillas, S.M. Weis, J.R. Gothert, D.A. Cheresh, Semaphorin 3A suppresses VEGF-mediated angiogenesis yet acts as a vascular permeability factor, Blood 111(5) (2008) 2674-80.

[18] E. Groppa, S. Brkic, E. Bovo, S. Reginato, V. Sacchi, N. Di Maggio, M.G. Muraro, D. Calabrese, M. Heberer, R. Gianni-Barrera, A. Banfi, VEGF dose regulates vascular stabilization through Semaphorin3A and the Neuropilin-1+ monocyte/TGF-beta1 paracrine axis, EMBO Mol Med 7(10) (2015) 1366-84.

[19] I. Martin, A. Muraglia, G. Campanile, R. Cancedda, R. Quarto, Fibroblast growth factor-2 supports ex vivo expansion and maintenance of osteogenic precursors from human bone marrow, Endocrinology 138(10) (1997) 4456-62.

[20] W.C. Liang, M.S. Dennis, S. Stawicki, Y. Chanthery, Q. Pan, Y. Chen, C. Eigenbrot, J. Yin, A.W. Koch, X. Wu, N. Ferrara, A. Bagri, M. Tessier-Lavigne, R.J. Watts, Y. Wu, Function blocking antibodies to neuropilin-1 generated from a designed human synthetic antibody phage library, J Mol Biol 366(3) (2007) 815-29.

[21] Q. Pan, Y. Chanthery, W.C. Liang, S. Stawicki, J. Mak, N. Rathore, R.K. Tong, J. Kowalski, S.F. Yee, G. Pacheco, S. Ross, Z. Cheng, J. Le Couter, G. Plowman, F. Peale, A.W. Koch, Y. Wu, A. Bagri, M. Tessier-Lavigne, R.J. Watts, Blocking neuropilin-1 function has an additive effect with anti-VEGF to inhibit tumor growth, Cancer Cell 11(1) (2007) 53-67.

[22] S. Zacchigna, L. Pattarini, L. Zentilin, S. Moimas, A. Carrer, M. Sinigaglia, N. Arsic, S. Tafuro, G. Sinagra, M. Giacca, Bone marrow cells recruited through the neuropilin-1 receptor promote arterial formation at the sites of adult neoangiogenesis in mice, J Clin Invest 118(6) (2008) 2062-75.

[23] R. Gianni-Barrera, N. Di Maggio, L. Melly, M.G. Burger, E. Mujagic, L. Gurke, D.J. Schaefer, A. Banfi, Therapeutic vascularization in regenerative medicine, Stem Cells Transl Med 9(4) (2020) 433-444.

[24] M.M. Deckers, M. Karperien, C. van der Bent, T. Yamashita, S.E. Papapoulos, C.W. Lowik, Expression of vascular endothelial growth factors and their receptors during osteoblast differentiation, Endocrinology 141(5) (2000) 1667-74.

[25] F. Maione, F. Molla, C. Meda, R. Latini, L. Zentilin, M. Giacca, G. Seano, G. Serini, F. Bussolino, E. Giraudo, Semaphorin 3A is an endogenous angiogenesis inhibitor that blocks tumor growth and normalizes tumor vasculature in transgenic mouse models, J Clin Invest 119(11) (2009) 3356-72.

[26] A. Fantin, J.M. Vieira, A. Plein, L. Denti, M. Fruttiger, J.W. Pollard, C. Ruhrberg, NRP1 acts cell autonomously in endothelium to promote tip cell function during sprouting angiogenesis, Blood 121(12) (2013) 2352-62.

[27] A.M. Ochsenbein, S. Karaman, S.T. Proulx, M. Berchtold, G. Jurisic, E.T. Stoeckli, M. Detmar, Endothelial cell-derived semaphorin 3A inhibits filopodia formation by blood vascular tip cells, Development 143(4) (2016) 589-94.

[28] Y. Li, L. Yang, S. He, J. Hu, The effect of semaphorin 3A on fracture healing in osteoporotic rats, J Orthop Sci 20(6) (2015) 1114-21.

10. Summary and future perspectives

Angiogenesis and osteogenesis are two intimately connected processes. Bone vasculature is crucial to supply oxygen and nutrients, as well as to provide angiocrine signals, which are required for the maintenance, differentiation and survival of stem and progenitor cells within the bone tissue [1]. Furthermore, a functional vasculature is extremely important during bone development and repair, as blood vessels serve as structural templates, around which bone formation takes place. Moreover, vessels bring together key components for bone regeneration, such as minerals, growth factors, immune cells and osteogenic progenitor cells, which all contribute to a correct bone homeostasis [2, 3].

Large bone tissue losses, caused by diseases or trauma, cannot fully heal and the current medical practice still faces significant challenges for their treatment. Bone tissue-engineering has emerged as a promising alternative to bone transplantation and many different strategies are currently being investigated to fulfil this unmet clinical need. Tissue engineered constructs, delivering progenitor cells and/or growth factors, have been widely tested to bridge large bone defects. However, in most cases lack of sufficient spontaneous vascular perfusion in the bone grafts results in inner necrosis, poor integration with the host tissue and insufficient bone healing. In fact, vascularization is a crucial aspect to consider for the design of tissue-engineering strategies and it is a major hurdle for the regenerative medicine field.

Vascular endothelial growth factor-A (VEGF) is the master regulator of angiogenesis and is also critical for both bone development and regeneration. In these processes VEGF has multiple roles, both acting on endothelial cells to promote their migration and proliferation, and stimulating osteogenesis through the regulation of osteogenic growth factors [4, 5]. VEGF

is therefore a key molecular target for the generation of vascularized bone grafts, but a better understanding of the molecular cross-talk between angiogenesis and osteogenesis is needed in order to fully exploit its therapeutic potential. Therefore, here we have investigated 3 aspects of how VEGF controls the coupling of angiogenesis and osteogenesis in bone generation by BMSC:

1) Duration of VEGF delivery;
2) VEGF dose;
3) The underlying molecular mechanism and in particular the role of Sema3A/NP1 signaling downstream of VEGF.

VEGF protein delivery, in most cases, requires precise control of its release and spatial concentrations, which are critical for the stimulation of physiological angiogenesis and bone formation. Even though the initial growth of new vessels can be quite rapid, sustained VEGF signaling for about 4 weeks is required for their subsequent stabilization and ability to persist indefinitely. In fact, if delivery is too short, newly induced vessels regress promptly upon cessation of the VEGF stimulus [6]. VEGF in its free form has an extremely short half-life *in vivo* and therefore bolus injections and rapid passive release from scaffolds are inadequate to ensure new vessel persistence. However, if from one side a prolonged exposure to VEGF ensures a stable and persistent vasculature, from the other it might also affect important biological processes involved in bone homeostasis, causing for example excessive bone resorption [7]. We therefore hypothesized and showed that one of the key elements to efficiently stimulate both vascularization and osteogenesis is, in fact, the control of the timing of VEGF supply.

As described in Chapter 2, we found that a transient delivery of VEGF protein for about 4 weeks *in vivo*, controlled through a highly tunable fibrin-based platform, is more desirable

and efficient compared to genetic VEGF overexpression. In fact, delivery of 1 μg/ml of fibrin-bound VEGF stimulated the early vascular invasion of the grafts, with improvement of both progenitor survival and bone formation in critical-size bone defects, while avoiding the detrimental effects caused by sustained exposure to the factor.

The temporal control of VEGF delivery is not the only important aspect to be considered for the generation of vascularized bone grafts. We have shown that, depending on its concentration, VEGF has different effects on blood vessel migration into the graft and on the osteogenic differentiation of osteoprogenitors. We found that 0.1 μg/ml of VEGF significantly accelerated vascular invasion of the osteogenic grafts and maintained efficient bone formation. Conversely, increasing doses of VEGF limited vascular ingrowth on one hand, and also progressively impaired net bone formation by both increasing bone resorption and impairing osteoprogenitor differentiation. Taken together, these data indicate that VEGF signaling must be controlled to moderate levels, as prolonged expression and high doses are not only unnecessary for optimal angiogenesis, but also trigger multiple processes that negatively affect osteogenesis.

Despite promoting vascular invasion, low VEGF doses did not increase the amount of bone in ectopic implants. This is due to the small size of these implants, for which spontaneous vascularization is sufficient. In fact, in a critical-size orthotopic defect, in which spontaneous angiogenesis is not sufficiently fast to sustain progenitor survival, the presence of VEGF did promote bone healing. Interestingly, we observed an increased degree of bone maturation in subcutaneous grafts containing a low dose of VEGF. Osteogenesis has a slow kinetics. In fact, the initial template of immature osteoid, which is deposited by BMSCs after about 4 weeks, requires further time to develop into mature bone tissue. A greater amount of organized mature bone at 8 weeks might suggest that, low VEGF could accelerate the deposition of

dense collagenous matrix. Since after 1 week gene expression analysis did not reveal any significant difference in the expression of osteogenic genes among all conditions, to test this hypothesis histological and gene expression analysis at 2 and 3 weeks after *in vivo* implantation should be performed. The formation of mature bone tissue characterized by physiological structural and mechanical properties is desirable for successful clinical outcomes.

Our data indicate that VEGF delivery should be tightly controlled to achieve efficient bone formation, suggesting an explanation for why VEGF has been found to enhance bone healing and regeneration in many studies, but has failed to have positive effects in others [8, 9]. Moreover, the expression of VEGF receptors in BMSCs and osteoblasts is quite variable, making direct effects of VEGF on this cell types complicated to study [4, 10]. For example, in murine osteoblastic MC3T3 cells, VEGF was shown to promote the expression of alkaline phosphatase and osteocalcin [11].However, other studies also showed that primary murine mesenchymal progenitors and osteoblasts failed to respond to exogenous VEGF [12]. The dose-dependent impairment of BMSC osteogenic *in vivo* differentiation that we reported in Chapter 3 (Fig. 8) suggests a possible direct effect of VEGF on osteoprogenitors. In order to test this hypothesis more experimental work is needed, such as *in vitro* stimulation of differentiating human BMSC with increasing VEGF doses.

For clinical efficacy it is crucial to improve both angiogenesis and osteogenesis, i.e. angio-osteogenic coupling. For this reason, different studies have been focusing on possible synergistic effects of VEGF with other growth factors. For example, it has been shown that VEGF and BMP2 within polymer scaffolds enhance bone regeneration in clinical-size defects [13]. In another study a sequential angiogenic and osteogenic growth factor release was beneficial for the enhancement of bone regeneration [14]. However, results were often

controversial: for example, in the case of BMPs high doses of growth factor were associated with excessive amounts of ectopic bone formation and increased inflammation and neuropathies [15], and in the case of VEGF with the development of aberrant and leaky vasculature [16]. Therefore, it is important to control the release and presentation of growth factors, avoiding undesired effects and reducing the costs of therapy.

On the other hand, a better understanding of the complex cross-talk between angiogenesis and osteogenesis could identify novel molecular targets to more precisely and safely stimulate bone formation and vascularization. As it has been extensively discussed in this thesis, osteogenesis requires a balance between bone deposition and bone resorption. Excessive VEGF delivery leads to both increased bone resorption and decreased osteogenic differentiation of progenitor cells. A few years ago, the neural guidance molecule Sema3A has been found to play a crucial role in bone homeostasis, by both inhibiting osteoclast recruitment/maturation and stimulating osteoblast differentiation [17]. On the other hand, we previously found that Sema3A is required for blood vessel stabilization and that VEGF dose-dependently inhibits its expression in muscle endothelium [18]. Therefore, here we hypothesized that Sema3A may mediate VEGF dose-dependent functions in vascularized bone formation. The data reported in Chapter 4 show that indeed Sema3A is fundamental for both efficient vascularization and bone formation in osteogenic grafts. In fact, we found that: 1) high doses of VEGF decreased Sema3A expression, resulting in increased bone resorption and impaired osteogenic differentiation; 2) Sema3A signaling is required for efficient bone formation, as the blockade of its interaction with neuropilin-1 (NP1) led to the same outcomes; and 3) Sema3A delivered as a single factor could promote both vascular invasion and bone formation.

One of the most exciting results of this study is related to the pro-angiogenic properties of Sema3A. The inhibition of Sema3A signaling significantly limited vascular invasion of the osteogenic constructs at 1 week, even in the presence of the optimal dose (0.1 μg/ml) of VEGF. Conversely, when delivered as single factor, Sema3A stimulated blood vessels ingrowth. These two complementary observations show that Sema3A may act as a pro-angiogenic factor, and not only as a crucial osteoprotective molecule.

The role of Sema3A during angiogenesis is still unclear. For example, no vascular alterations were seen in Sema3a$^{-/-}$ embryos [19], or in mice expressing a mutated form of NP1 lacking the Sema-binding domain, but its VEGF-binding ability intact [20]. However, several lines of evidence suggest potent anti-angiogenic functions to Sema3A. It has been shown that Sema3A inhibits endothelial cell migration *in vitro* [21] and regulates tumor-induced angiogenesis in vivo [22]. Others found that, within the cardiovascular system, Sema3A modulates vessel formation by inhibiting integrin activity [23]. Acevedo et al. described a role for Sema3A both as a selective inhibitor of VEGF-mediated angiogenesis and as a potent inducer of vascular permeability [24]. Interestingly, it has been recently shown that NP1 is more strongly expressed in tip cells than in stalk cells [25]. This would open the possibility that Sema3A may specifically have a role in regulating sprouting angiogenesis. Furthermore, Sema3A signaling relies on the interaction of NP1 with co-receptors of the Plexin family [26]. It has been recently shown that endothelial cell-derived Sema3A specifically exerts repelling functions on tip cell filopodia, probably via NP1 and plexin-A1 [27]. The role of Sema3A in angiogenesis is complex and likely context-, dose- and tissue-dependent. The data reported here suggest that also during intramembranous bone formation Sema3A acts as a key angiogenic player. Whether Sema3A-induced angiogenesis is

due to the direct stimulation of endothelial cells sprouting or to other indirect mechanisms, is unclear and has not been investigated here.

Importantly, the delivery of Sema3A improved not only vascularization but also significantly increased bone deposition compared to BMSCs alone. This dual and positive role of Sema3A on angiogenesis and osteogenesis could be clearly beneficial for a clinical translation.

The co-delivery of Sema3A with high doses of VEGF prevented excessive osteoclast recruitment and promoted efficient bone formation, without impairing VEGF-induced vascularization. These observations, together with the evidence that Sema3A was dose-dependently downregulated by VEGF, suggest that Sema3A acts as a downstream mediator of VEGF and therefore it may regulate a feed-back loop similar to the one that we have previously described in skeletal muscle [18]. In this tissue VEGF dose-dependently inhibits endothelial Sema3A expression, thereby impairing recruitment of Neuropilin-1-expressing monocytes (NEM), TGF-β1 production and endothelial SMAD2/3 activation. TGF-β1 further initiates a feedback loop stimulating further endothelial Sema3A expression, thereby amplifying the signaling cascade leading to stabilization of the newly formed blood vessels [18]. Here we have seen that NEM recruitment within the active angiogenic areas takes place also in osteogenic grafts and it is impaired by high doses of VEGF or by inhibition of Sema3A/NP1 signaling. Furthermore, the blocking experiment also showed that SMAD2/3 nuclear translocation was reduced both in endothelial cells and human progenitors, indicating that TGF-β1 signaling was impaired. To more precisely investigate the role of TGF-β1 in this process, blocking of TGF-β1 signaling should be performed, e.g. by treatment with the small molecule inhibitor SB431542 [28]. Based on the hypothesis that TGF-β1 may be part of a positive feedback loop sustaining Sema3A expression, it would be expected that TGF-β1

inhibition would cause a reduction in Sema3A expression and bone loss. It would also be important to test whether Sema3A can rescue the effects of TGF-β1 inhibition. This would prove that the Sema3A/NEM/TGF-β1 axis is active in osteogenic grafts and that it is required for efficient bone formation. Lastly, as it has been established that Sema3A can prevent bone loss induced by high doses of VEGF, future experiments will investigate whether co-delivery of the optimal low dose (0.1 μg/ml) of VEGF together with Sema3A might have synergistic effects and further improve vascular invasion and bone formation when compared to single factor delivery.

As future perspective, development of preclinical proof-of-concept studies of the fibrin-based platform used here is one of the main objectives. We have already seen that 1 μg/ml of TG-VEGF can improve bone healing in a clinical-size bone defect. However, in the subcutaneous grafts, we have later found that lower doses might provide a significant advantage in terms of vascular invasion and bone maturation. Therefore, it will be important to investigate the effect of 0.1 μg/ml of TG-VEGF in a critical-size model.

The choice of the appropriate animal model has also to be carefully evaluated. Different animal models, such as mouse/rat, rabbit, goat, sheep, dog and pig have been applied to test bone substitute biomaterials. Several defect sites have been also explored in order to mimic various clinical situations. Among these calvaria, femur and ulna represent the most used for the generation of non-healing critical defects [29]. In the study reported here, we investigated the effects of VEGF, both delivered as fibrin-bound factor and overexpressed by human-BMSC, in a rat calvaria critical-size bone defect. Despite the promising results, the calvaria environment differs from long bones in regard to mechanical stress, such as load and strain. In fact, mechanical forces are known to modulate stem cell behavior in development and regeneration and they also have to be considered in the design of biomaterials [30, 31].

Therefore, it would be important to consider alternative orthotopic models, to further test the therapeutic potential of this approach.

In bone tissue-engineering, osteoprogenitor cells have been used in combination with biomaterials to recapitulate both endochondral and intramembranous ossification. The potential of stem and progenitor cells has been demonstrated for the repair and regeneration of craniomaxillofacial and long bone defects. However, clinical use of bone tissue engineering protocols has been very limited due to some unsolved or intrinsic hurdles. For example, it has been shown that the osteogenic potential of human-derived MSC is donor-dependent and tends to decrease with age [32]. Cell-based therapies also require time-consuming and costly *in vitro* cell expansion procedures which limit their clinical application [33, 34].

Due to these limitations, in the past few decades research has focused on the stimulation of the intrinsic regenerative abilities of bone tissue [35, 36]. Skeletal stem cell recruitment is a critical step in bone healing and, for instance, failed regeneration has been associated to various clinical situation in which the BMSC pool was reduced [37]. We have also extensively discussed that a lack of vascularization leads to delayed or failed tissue regeneration. This highlights the importance of promoting the physiological occurrence of these two processes for efficient bone regeneration. A better understanding of the underlying molecular mechanisms involved in the homing, maintenance and differentiation of skeletal progenitors will be important for the design of cell-free therapies for enhancing bone healing. In this context, the data reported here provide useful insights regarding VEGF dose-dependent effects on both osteogenic differentiation and angiogenesis. It would be interesting to understand whether cell-free osteogenic constructs composed of fibrin matrices decorated with VEGF and/or Sema3A at optimal doses might stimulate endogenous bone repair.

Unpublished data from our group show evidence that Platelet-Derived Growth Factor-BB (PDGF-BB) can regulate the Sema3A/NEM/TGF-β1 signaling axis in skeletal muscle, which is disrupted by high VEGF levels. In this study, PDGF-BB has been found to restore Sema3A expression despite high concentrations of VEGF. PDGF-BB also has important roles in the proliferation, differentiation and chemoattraction of multiple cells of mesodermal origin, including BMSC [38, 39], as well as in bone regeneration [40, 41]. However, the therapeutic potential of PDGF-BB for bone repair has not yet been fully investigated. As a future perspective, it will be interesting to study the effect of fibrin-bound PDGF-BB on angiogenesis and osteogenesis in bone grafts. In particular we can hypothesize that PDGF-BB delivery might stimulate Sema3A expression thus coupling vascularization and bone formation. This would be relevant as an alternative strategy for the generation of vascularized bone grafts.

In conclusion, here we demonstrated that VEGF promotes vascularization and bone formation in a dose-dependent manner. The coupling of the two processes requires a fine tuning of VEGF delivery, as excessive VEGF concentrations or prolonged stimulation delay early blood vessel ingrowth, progressively increase bone resorption and impair osteogenic differentiation of BMSC. Low VEGF doses, instead, ensure fast vascularization, improve osteoprogenitor survival and promote osteogenesis.

We also described a crucial role of Sema3A in both intramembranous bone formation and vascularization, and found that it provides a direct molecular link with VEGF. In addition, to our knowledge, we described for the first time the angiogenic potential of Sema3A during bone formation.

These results confirm the importance of both VEGF and Sema3A in bone biology and provide the basis for the design of novel rational strategies to generate vascularized bone grafts with the aim to improve the healing of clinical-size bone defects.

10.1 References

[1] J. Chen, M. Hendriks, A. Chatzis, S.K. Ramasamy, A.P. Kusumbe, Bone Vasculature and Bone Marrow Vascular Niches in Health and Disease, J Bone Miner Res 35(11) (2020) 2103-2120.

[2] J. Filipowska, K.A. Tomaszewski, L. Niedzwiedzki, J.A. Walocha, T. Niedzwiedzki, The role of vasculature in bone development, regeneration and proper systemic functioning, Angiogenesis 20(3) (2017) 291-302.

[3] A. Grosso, M.G. Burger, A. Lunger, D.J. Schaefer, A. Banfi, N. Di Maggio, It Takes Two to Tango: Coupling of Angiogenesis and Osteogenesis for Bone Regeneration, Front Bioeng Biotechnol 5 (2017) 68.

[4] K. Hu, B.R. Olsen, The roles of vascular endothelial growth factor in bone repair and regeneration, Bone 91 (2016) 30-8.

[5] E. Schipani, C. Maes, G. Carmeliet, G.L. Semenza, Regulation of osteogenesis-angiogenesis coupling by HIFs and VEGF, J Bone Miner Res 24(8) (2009) 1347-53.

[6] R. Gianni-Barrera, N. Di Maggio, L. Melly, M.G. Burger, E. Mujagic, L. Gurke, D.J. Schaefer, A. Banfi, Therapeutic vascularization in regenerative medicine, Stem Cells Transl Med 9(4) (2020) 433-444.

[7] U. Helmrich, N. Di Maggio, S. Guven, E. Groppa, L. Melly, R.D. Largo, M. Heberer, I. Martin, A. Scherberich, A. Banfi, Osteogenic graft vascularization and bone resorption by VEGF-expressing human mesenchymal progenitors, Biomaterials 34(21) (2013) 5025-35.

[8] J.R. Garcia, A.J. Garcia, Biomaterial-mediated strategies targeting vascularization for bone repair, Drug Deliv Transl Res 6(2) (2016) 77-95.

[9] M. Kaipel, S. Schutzenberger, A. Schultz, J. Ferguson, P. Slezak, T.J. Morton, M. Van Griensven, H. Redl, BMP-2 but not VEGF or PDGF in fibrin matrix supports bone healing in a delayed-union rat model, J Orthop Res 30(10) (2012) 1563-9.

[10] K. Hu, B.R. Olsen, Osteoblast-derived VEGF regulates osteoblast differentiation and bone formation during bone repair, J Clin Invest 126(2) (2016) 509-26.

[11] Y.Y. Tan, Y.Q. Yang, L. Chai, R.W. Wong, A.B. Rabie, Effects of vascular endothelial growth factor (VEGF) on MC3T3-E1, Orthod Craniofac Res 13(4) (2010) 223-8.

[12] Y. Liu, A.D. Berendsen, S. Jia, S. Lotinun, R. Baron, N. Ferrara, B.R. Olsen, Intracellular VEGF regulates the balance between osteoblast and adipocyte differentiation, J Clin Invest 122(9) (2012) 3101-13.

[13] Z.S. Patel, S. Young, Y. Tabata, J.A. Jansen, M.E. Wong, A.G. Mikos, Dual delivery of an angiogenic and an osteogenic growth factor for bone regeneration in a critical size defect model, Bone 43(5) (2008) 931-40.

[14] D.H. Kempen, L. Lu, A. Heijink, T.E. Hefferan, L.B. Creemers, A. Maran, M.J. Yaszemski, W.J. Dhert, Effect of local sequential VEGF and BMP-2 delivery on ectopic and orthotopic bone regeneration, Biomaterials 30(14) (2009) 2816-25.

[15] A.W. James, G. LaChaud, J. Shen, G. Asatrian, V. Nguyen, X. Zhang, K. Ting, C. Soo, A Review of the Clinical Side Effects of Bone Morphogenetic Protein-2, Tissue Eng Part B Rev 22(4) (2016) 284-97.

[16] C.R. Ozawa, A. Banfi, N.L. Glazer, G. Thurston, M.L. Springer, P.E. Kraft, D.M. McDonald, H.M. Blau, Microenvironmental VEGF concentration, not total dose, determines a threshold between normal and aberrant angiogenesis, J Clin Invest 113(4) (2004) 516-27.

[17] M. Hayashi, T. Nakashima, M. Taniguchi, T. Kodama, A. Kumanogoh, H. Takayanagi, Osteoprotection by semaphorin 3A, Nature 485(7396) (2012) 69-74.

[18] E. Groppa, S. Brkic, E. Bovo, S. Reginato, V. Sacchi, N. Di Maggio, M.G. Muraro, D. Calabrese, M. Heberer, R. Gianni-Barrera, A. Banfi, VEGF dose regulates vascular stabilization through Semaphorin3A and the Neuropilin-1+ monocyte/TGF-beta1 paracrine axis, EMBO Mol Med 7(10) (2015) 1366-84.

[19] J.M. Vieira, Q. Schwarz, C. Ruhrberg, Selective requirements for NRP1 ligands during neurovascular patterning, Development 134(10) (2007) 1833-43.

[20] C. Gu, E.R. Rodriguez, D.V. Reimert, T. Shu, B. Fritzsch, L.J. Richards, A.L. Kolodkin, D.D. Ginty, Neuropilin-1 conveys semaphorin and VEGF signaling during neural and cardiovascular development, Dev Cell 5(1) (2003) 45-57.

[21] H.Q. Miao, S. Soker, L. Feiner, J.L. Alonso, J.A. Raper, M. Klagsbrun, Neuropilin-1 mediates collapsin-1/semaphorin III inhibition of endothelial cell motility: functional competition of collapsin-1 and vascular endothelial growth factor-165, J Cell Biol 146(1) (1999) 233-42.

[22] F. Maione, F. Molla, C. Meda, R. Latini, L. Zentilin, M. Giacca, G. Seano, G. Serini, F. Bussolino, E. Giraudo, Semaphorin 3A is an endogenous angiogenesis inhibitor that blocks tumor growth and normalizes tumor vasculature in transgenic mouse models, J Clin Invest 119(11) (2009) 3356-72.

[23] G. Serini, D. Valdembri, S. Zanivan, G. Morterra, C. Burkhardt, F. Caccavari, L. Zammataro, L. Primo, L. Tamagnone, M. Logan, M. Tessier-Lavigne, M. Taniguchi, A.W. Puschel, F. Bussolino, Class 3 semaphorins control vascular morphogenesis by inhibiting integrin function, Nature 424(6947) (2003) 391-7.

[24] L.M. Acevedo, S. Barillas, S.M. Weis, J.R. Gothert, D.A. Cheresh, Semaphorin 3A suppresses VEGF-mediated angiogenesis yet acts as a vascular permeability factor, Blood 111(5) (2008) 2674-80.

[25] A. Fantin, J.M. Vieira, A. Plein, L. Denti, M. Fruttiger, J.W. Pollard, C. Ruhrberg, NRP1 acts cell autonomously in endothelium to promote tip cell function during sprouting angiogenesis, Blood 121(12) (2013) 2352-62.

[26] L.T. Alto, J.R. Terman, Semaphorins and their Signaling Mechanisms, Methods Mol Biol 1493 (2017) 1-25.

[27] A.M. Ochsenbein, S. Karaman, S.T. Proulx, M. Berchtold, G. Jurisic, E.T. Stoeckli, M. Detmar, Endothelial cell-derived semaphorin 3A inhibits filopodia formation by blood vascular tip cells, Development 143(4) (2016) 589-94.

[28] G.J. Inman, F.J. Nicolas, J.F. Callahan, J.D. Harling, L.M. Gaster, A.D. Reith, N.J. Laping, C.S. Hill, SB-431542 is a potent and specific inhibitor of transforming growth factor-beta superfamily type I activin receptor-like kinase (ALK) receptors ALK4, ALK5, and ALK7, Mol Pharmacol 62(1) (2002) 65-74.

[29] Y. Li, S.K. Chen, L. Li, L. Qin, X.L. Wang, Y.X. Lai, Bone defect animal models for testing efficacy of bone substitute biomaterials, J Orthop Translat 3(3) (2015) 95-104.

[30] K.S. Griffin, K.M. Davis, T.O. McKinley, J.O. Anglen, T.-M.G. Chu, J.D. Boerckel, M.A. Kacena, Evolution of Bone Grafting: Bone Grafts and Tissue Engineering Strategies for Vascularized Bone Regeneration, Clinical Reviews in Bone and Mineral Metabolism 13(4) (2015) 232-244.

[31] K.H. Vining, D.J. Mooney, Mechanical forces direct stem cell behaviour in development and regeneration, Nat Rev Mol Cell Biol 18(12) (2017) 728-742.

[32] A. Infante, C.I. Rodriguez, Osteogenesis and aging: lessons from mesenchymal stem cells, Stem Cell Res Ther 9(1) (2018) 244.

[33] C. Ikebe, K. Suzuki, Mesenchymal stem cells for regenerative therapy: optimization of cell preparation protocols, Biomed Res Int 2014 (2014) 951512.

[34] A. Oryan, A. Kamali, A. Moshiri, M. Baghaban Eslaminejad, Role of Mesenchymal Stem Cells in Bone Regenerative Medicine: What Is the Evidence?, Cells Tissues Organs 204(2) (2017) 59-83.

[35] M. Herrmann, S. Verrier, M. Alini, Strategies to Stimulate Mobilization and Homing of Endogenous Stem and Progenitor Cells for Bone Tissue Repair, Front Bioeng Biotechnol 3 (2015) 79.

[36] C. Lo Sicco, R. Tasso, Harnessing Endogenous Cellular Mechanisms for Bone Repair, Front Bioeng Biotechnol 5 (2017) 52.

[37] M. Mathieu, S. Rigutto, A. Ingels, D. Spruyt, N. Stricwant, I. Kharroubi, V. Albarani, M. Jayankura, J. Rasschaert, E. Bastianelli, V. Gangji, Decreased pool of mesenchymal stem cells is associated with altered chemokines serum levels in atrophic nonunion fractures, Bone 53(2) (2013) 391-8.

[38] A.I. Caplan, D. Correa, PDGF in bone formation and regeneration: new insights into a novel mechanism involving MSCs, J Orthop Res 29(12) (2011) 1795-803.

[39] A. Tokunaga, T. Oya, Y. Ishii, H. Motomura, C. Nakamura, S. Ishizawa, T. Fujimori, Y. Nabeshima, A. Umezawa, M. Kanamori, T. Kimura, M. Sasahara, PDGF receptor beta is a potent regulator of mesenchymal stromal cell function, J Bone Miner Res 23(9) (2008) 1519-28.

[40] Y.J. Park, Y.M. Lee, S.N. Park, S.Y. Sheen, C.P. Chung, S.J. Lee, Platelet derived growth factor releasing chitosan sponge for periodontal bone regeneration, Biomaterials 21(2) (2000) 153-9.

[41] M. Zhang, W. Yu, K. Niibe, W. Zhang, H. Egusa, T. Tang, X. Jiang, The Effects of Platelet-Derived Growth Factor-BB on Bone Marrow Stromal Cell-Mediated Vascularized Bone Regeneration, Stem Cells Int 2018 (2018) 3272098.

Acknowledgments

I would like to express all my gratitude to Dr. Andrea Banfi for giving me the opportunity to do my PhD in his lab, for all the scientific discussions and his precious advices. I am really grateful for the time spent in his lab, in which I could really understand the true beauty of science.

I sincerely thank Prof. Dr. Markus Affolter and Prof. Dr. Ivan Martin for their support as members of my PhD Committee.

One of the most important acknowledgements is for Dr. Nunzia di Maggio, for being my supervisor and guide during all these years.

Surviving a PhD would not have been possible without the incredible people I shared this crazy journey. A huge thank is for all the people that have worked with me and have crossed my path in the past 5 years. In particular:

Robbie, for all the help and the laughs we had together.
Andrea, for sharing all these years with me and for all the great moments we had together.
Adelin, my dear Frenchy, for being a great friend and gym buddy.
Simon, Pauline and Daniele, for all the beers and laughs, and in particular for supporting me and helping me going through these last months.
Ludovic, for always supporting me.
Juan, for all the good time.

I would also like to thank all the other people that I have met in the department, in the lab and in Basel in general.
You all have contributed, in one way or another, to help me to get to this point.

All of this would not have been possible and even imaginable without the support of my family.
To my mom and dad, thank you for all the sacrifices that you have made for me and my brothers for your entire life. Thank you for giving me all the opportunities and freedom to do what I wanted, to dream, to fail and to find my own way.
To my beloved brothers, Fabio and Marco, thanks for helping me to become the man that I am today. You have always been an example to me.
To my grandma and my uncle, the kindest people on Earth, thanks for showing me the importance of being kind to others since I was a child.
Thank you all, for your love.

I have been incredibly lucky to have the support of my best friends back in Italy, my second family.
Luca, Nicolas, Riccardo, thank you for making me feel at home and like the time did not past at all every time I came back.
Francesco and Riccardo, my dear friends, thank you for always being close to me.

During these years I realized how many beautiful people I have in my life, and I would like to thank you all again for everything.

"Happiness is only real when shared"